# Supply Temperature Control Concepts in Heat Pump Heating Systems

Von der Fakultät für Maschinenwesen der Rheinisch-Westfälischen Technischen Hochschule Aachen zur Erlangung des akademischen Grades eines Doktors der Ingenieurwissenschaften genehmigte Dissertation

vorgelegt von

Kristian Huchtemann

Berichter: Univ.-Prof. Dr.-Ing. Dirk Müller
Prof. Bjarne W. Olesen, Ph.D.

Tag der mündlichen Prüfung: 22. Mai 2015

Diese Dissertation ist auf den Internetseiten der Universitätsbibliothek online verfügbar.

Kristian Huchtemann

"Supply Temperature Control Concepts in Heat Pump Heating Systems"

**Bibliographische Information der Deutschen Nationalbibliothek**
Die Deutsche Nationalbibliothek verzeichnet diese Publikation in der Deutschen Nationalbibliografie; detaillierte bibliografische Daten sind im Internet über http://dnb-nb.de abrufbar.

D 82 (Diss. RWTH Aachen University, 2015)

Herausgeber:
Univ.-Prof. Dr.ir. Dr.h.c. Rik W. De Doncker
Direktor E.ON Energy Research Center

Univ.-Prof. Dr.-Ing. Dirk Müller
Institut Energy Efficient Buildings and Indoor Climate
E.ON Energy Research Center
Mathieustr. 10
52074 Aachen

E.ON Energy Research Center | 31. Ausgabe der Serie
EBC | Energy Efficient Buildings and Indoor Climate



Printed in Germany

ISBN: 978-3-942789-30-1
1. Auflage 2015

Verlag:
E.ON Energy Research Center, RWTH Aachen University
Mathieustr. 10
52074 Aachen
Internet: www.eonerc.rwth-aachen.de
E-Mail: post_erc@eonerc.rwth-aachen.de

Herstellung:
Druckservice Zillekens
Am Bachpütz 4
52224 Stolberg

# Acknowledgements

The graduation process starting with the first evaluation of field test data till the day of the doctoral examination was only possible with the help of colleagues, friends and family.

I would like to thank my supervisor Univ.-Prof. Dr.-Ing. Dirk Müller for giving me the possibility and freedom to work on this thesis and for his confidence and support. I would like to thank Prof. Bjarne Olesen, Ph.D. for his interest in my research, for reviewing the thesis and for being the co-examiner on my doctoral examination. Univ.-Prof. Dr.-Ing. Schröder and Univ.-Prof. Dr.-Ing. Jeschke were chairmen of the doctoral examination comittee and I would like to thank them for that.

In addition I would like to thank all students who contributed to this thesis for their good work.

Moreover, I would like to thank my colleagues at the Institute for Energy Efficient Buildings and Indoor Climate for their support and encouragement. Especially I would like to thank the colleagues who supported me in the preperation for the doctoral examination for their advice and their time.

I would like to thank the E.ON gGmbH for the financial support and the E.ON S.E. and Fraunhofer Institute for Solar Energy Systems for the preparation of field test data.

Last but not least I give my thanks to my family and friends for supporting me even when having to do without me during the time I wrote this thesis. This includes my wife Marie who I would additionally like to thank for proofreading this thesis.

Aachen, August 2015

*Kristian Huchtemann*

# Abstract

In recent years, electrically driven compression heat pumps have come to be widely used for the heating of buildings. Their efficiency strongly depends on the temperature lift which is influenced by the supply temperature of the heat sink. When used with radiator heating systems it is challenging to operate heat pumps efficiently because high supply temperatures are required. Therefore, in order to efficiently operate heat pumps, this work analyses advanced control concepts for heat pump heating systems that adapt the supply temperature according to the demand. The heat output of radiators is influenced by the mass flow rate and the supply temperature. Today, usually only the outdoor air temperature is used for controlling the supply temperature. However, control strategies exist that consider additional disturbances.

In this work, heat pumps in existing buildings are analyzed on the basis of field test data. The temperature of heat source and heat sink influence the efficiency of the heat pump. But additional influences such as the usage of additional appliances can be found which were studied and documented comprehensively. However, without data on user influences, room temperature and control settings, the potential of the field test cannot be fully realized.

Field test data are used to evaluate models of the heat pump and the buffer storage of the heating system. The heat pump is implemented as a table-based model, the buffer storage is modeled as a stratified fluid volume. The validated models and existing model components make up a model of the overall system. It includes a model of a one-family home with nine heated zones. User influences implemented as different user schedules, the building physics, dimensioning of components and control are analyzed in simulations of heating periods. The usage and insulation standard of the building have a strong influence on the energy demand and thermal comfort.

The system model is also used to analyze different supply temperature control strategies. Three control concepts are modeled: A rule-based one which adapts the set temperature step-wise, a model predictive one which calculates the optimal supply temperature for each heated zone, and a continuously operating controller which uses an integral element controlling the supply temperature according to the room air temperature. The advantages and disadvantages of each strategy are evaluated on the basis of the simulation results. A decrease of the mean supply temperature leads to considerable savings in energy demand. However, an increased thermal discomfort cannot be fully avoided. Attained energy savings crucially depend on the type of building physics and the user influences. Energy savings in real buildings can exceed the ones simulated using ideally parametrized systems.

# Zusammenfassung

Elektrisch angetriebene Kompressionswärmepumpen haben sich in den letzten Jahren als Wärmeerzeuger etabliert. Ihre Effizienz hängt stark vom Temperaturhub ab. Dieser wird auf der Nutzungsseite durch die Vorlauftemperatur des Heizsystems beeinflusst. Der effiziente Betrieb von Wärmepumpen mit Heizkörper-Heizungen ist aufgrund hoher erforderlicher Vorlauftemperaturen schwer zu erreichen. Deshalb werden in dieser Arbeit fortschrittliche Regelungskonzepte für Wärmepumpen-Heizsysteme untersucht, die bedarfsabhängig die Vorlauftemperatur anpassen, um einen effizienten Betrieb der Wärmepumpe zu erreichen. Die Leistungsabgabe von Heizkörpern lässt sich über den Massenstrom und die Vorlauftemperatur regeln. Eine Regelung der Vorlauftemperatur wird heutzutage üblicherweise nur anhand der Außentemperatur realisiert. Es gibt jedoch auch Heizungsregelungen, die weitere Störgrößen in die Regelung der Vorlauftemperatur einbeziehen.

Es erfolgt eine Untersuchung bestehender Wärmepumpen im Gebäudebestand anhand der Daten eines Feldversuchs. Der Einfluss der Wärmequelle und -senke auf die Effizienz der Wärmepumpe wird aufgezeigt. Allerdings wird auch deutlich, dass zahlreiche weitere Einflüsse berücksichtigt werden müssen. Letztere wurden analysiert und dokumentiert. Ohne Daten über die Nutzung, Raumtemperaturen und Reglereinstellungen kann das Potential des Feldversuches nicht voll ausgeschöpft werden.

Modelle für die Wärmepumpe und den zentralen Pufferspeicher des Wärmepumpen-Heizsystems werden mithilfe von Feldversuchsdaten überprüft. Die Wärmepumpe wird als tabellenbasiertes Modell umgesetzt, der Pufferspeicher wird durch ein geschichtetes Fluidvolumen abgebildet. Mit den validierten Modellen und bestehenden Modellkomponenten wird ein Gesamtsystem erstellt. Dieses beinhaltet ein Gebäudemodell eines Einfamilienhauses mit neun beheizten Zonen. Verschiedene Nutzungsprofile werden definiert. Einflüsse der Nutzung, der Gebäudephysik, der Auslegung der Komponenten und der Regelung auf die Effizienz des Heizsystems und auf den thermischen Komfort werden untersucht. Insbesondere die Gebäudenutzung und der Dämmstandard haben einen starken Einfluss sowohl auf den Energiebedarf als auch auf den thermischen Komfort.

Das Systemmodell wird außerdem genutzt um verschiedene Vorlauftemperatur-Regelstrategien zu untersuchen. Drei Regelkonzepte werden untersucht: Ein regelbasiertes, welches schrittweise die Solltemperatur adaptiert, ein modellprädiktives, welches für jede beheizte Zone die optimale Vorlauftemperatur errechnet und ein kontinuierliches Konzept, welches die Vorlauftemperatur über ein integrierendes Glied in Abhängigkeit der Raumtemperaturen regelt. Die Vor- und Nachteile der Regelkonzepte können durch die Simulation über die Dauer einer Heizperiode dargestellt werden.

Über eine Absenkung der mittleren Vorlauftemperatur lassen sich deutliche Energieeinsparungen realisieren. Diese sind aber immer mit Einbußen im errechneten thermischen Komfort verbunden. Die mögliche Energieeinsparung hängt stark von der Gebäudehülle und Nutzereinflüssen ab. In realen Gebäuden sind zusätzliche Einsparungen möglich, die über die mit optimal parametrierten Systemen simulierten Einsparungen hinausgehen.

# Contents

# Nomenclature

**Abbreviations**

| | |
|---|---|
| AFUE | Annual fuel utilization ratio |
| AWHP | Air-to-water heat pump |
| BS | Buffer storage |
| BWHP | Brine-to-water heat pump |
| CoP | Coefficient of Performance |
| DHW | Domestic hot water |
| HC | Heating cycle |
| LC | Loading cycle |
| MPC | Model predictive control |
| PE | Primary energy demand |
| PF | Performance factor |
| PMV | Predicted mean vote |
| PPD | Predicted Percentage Dissatisfied |
| SPF | Seasonal performance factor |

**Greek Symbols**

| | |
|---|---|
| $\bar{\vartheta}$ | Mean temperature, °C |
| $\beta$ | Thermal coefficient of expansion, 1/K |
| $\eta_C$ | Quality grade of heat pump |
| $\kappa$ | von Kármán constant |
| $\lambda$ | Thermal conductivity, W/(mK) |
| $\rho$ | Density, kg/m$^3$ |
| $\tau$ | Mixing time constant, s |
| $\vartheta$ | Temperature, °C |

**Symbols**

| | |
|---|---|
| $\dot{m}$ | Mass flow rate, kg/s |
| $\dot{Q}$ | Heat flow rate, W |
| $c$ | Specific heat capacity, J/(kg K) |
| $E$ | Energy, J |

| | |
|---|---|
| $f$ | Relative error |
| $f_{\mathrm{PE}}$ | Primary energy factor |
| $g$ | Acceleration of gravity, m/s$^2$ |
| $H$ | Heat loss coefficient, W/K |
| $n$ | Radiator index |
| $n_{\mathrm{op}}$ | Number of operating cycles |
| $P$ | Power, W |
| $Q$ | Heat, J |
| $R^2$ | Coefficient of determination |
| $s$ | Height of storage layer, m |
| $T$ | Temperature, K |
| $t$ | Time, s |
| $W$ | Work, J |

**Subscripts**

| | |
|---|---|
| act | actual |
| C | Carnot |
| CC | Condenser cycle |
| d | Daily value |
| DHW | Domestic hot water |
| drop | dropping |
| eff | effective |
| el | electrical |
| evap | Evaporator |
| H | Heating |
| HC | Heating cycle |
| hcu | heating curve |
| hl | Heat load |
| HP | Heat pump |
| hyst | Hysteresis |
| ig | inner gains |
| lay | layer |
| LC | Loading cycle |

| | |
|---|---|
| log | logarithmic |
| low | lower boundary |
| meas | measurement |
| nom | nominal |
| out | outdoor air |
| pump | pump |
| ref | reference system |
| rise | rising |
| room | room |
| set | set value |
| sg | solar gains |
| sim | simulation |
| source | source |
| tot | total |
| up | upper boundary |
| use | usable |

**Codes used for configurations of simulation**

| | |
|---|---|
| B | Bivalent system set-up |
| E | High insulation standard of building (according to EnEV09) |
| EA | Electric valve actuators with PI control |
| H | High occupation of building |
| L | Low occupation of building |
| M | Monovalent system set-up |
| MPC | Model prediction controlled supply temperature control |
| N | No occupation of building |
| PI | PI controlled supply temperature control |
| RB | Rule-based supply temperature control |
| RR | Reference room control |
| var | Variable room set temperature profile |
| W | Low insulation standard of building (according to WSchV84) |

# List of Figures

# List of Tables

# 1 Introduction

The decision to use a heat pump for heating of buildings generally is made for two reasons: Through its application energy savings and cost savings are expected compared with a standard heating system. Additionally, the heat pump is considered environmentally friendly because usually carbon dioxide emissions can be reduced as a result of energy savings.

But today not only energy efficiency is in the focus of homeowners. Users of buildings increasingly request an individual and demand-based control that ensures thermal comfort within the heated room and which also results in energy savings. These requirements can indeed be met by electric valve actuators which additionally allow for a single room temperature control, an easy programmability and remote access. However, energy savings are limited since these actuators are commonly not intelligently linked with the heat generator.

Controlling the temperature of a heated zone according to user requirements provides potential savings compared to a constant temperature level, e.g. when the room temperature is lowered outside the periods of user presence. This means that heat demand is reduced by means of a lower average room temperature. If heat is generated by a heat pump, additional savings can result from higher heat pump efficiency through lower necessary supply temperatures. Especially when considering high temperature radiator heating systems in existing buildings, any reduction of supply temperature can yield substantial savings.

The temperature of the heat sink in standard heat pump heating systems is controlled depending on the outdoor air temperature. Influences on the heat load other than the outdoor air temperature are usually not considered in supply or return temperature control but instead thermostatic valves control the mass flow rate in the heat emitter.

## 1.1 Objectives

The main objective of this work is the analysis of new, advanced supply temperature control concepts for heat pump heating systems. These concepts are supposed to enable a demand-based control of the supply temperature and an increase of heat pump efficiency using single room temperature control.

Therefore, a detailed analysis of heat pumps in existing buildings has to be carried out. The dependency of heat pump efficiency on the temperature lift has to be studied with a focus on the sink temperature. Therefore, comprehensive measurement data of a field test with retrofit heat pumps is available and has to be assessed.

In order to be capable to execute parameter studies on heat pump heating systems and to develop and evaluate control concepts, a model has to be created. It has to be able to calculate multiple heated zones of a building, the proper hydraulic system, the heat generation system and the heat pump source. Additionally, particular attention should be paid to the option of implementing different kinds of control.

## 1.2 Structure of this work

The objectives are attained in six chapters which are indicated in figure 1.1.

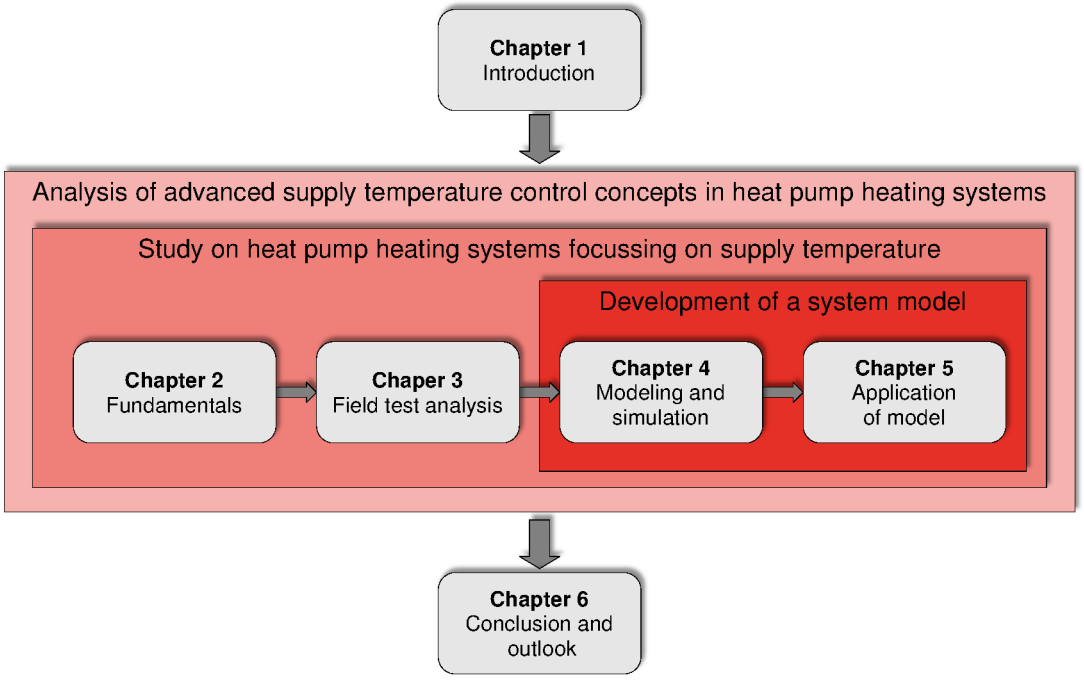


**Figure 1.1:** Overview on objectives and structure of this work.

The basic knowledge and governing equations for the analysis of heat pump systems and the heat sink is discussed in chapter 2. Based on these theoretical elaborations, findings from a field test with heat pumps in existing buildings can be used to study the realistic behavior of heat pumps. The field test is comprehensively analyzed in chapter 3 and provides data for the validation of heat pump systems. In chapter 4 the development of a heat pump model and the model of a buffer storage is discussed. These models and additional components are combined in a model of the total system which is subject to a detailed parameter study.

Finally, chapter 5 discusses the development of different advanced control strategies which are compared regarding energy demand and thermal comfort using the model of the total heat pump system.

## 1.3 Literature review

### 1.3.1 Current usage and potential of heat pumps

Electrically driven compression heat pumps can save primary energy compared to standard heat generators such as gas condensing boilers. The seasonal performance factor (SPF) is used to describe the annual efficiency of a heat pump. Today, a SPF boundary value of 2.3[1] can be set, which means that with higher SPF heat pumps achieve savings in annual primary energy demand compared to gas condensing boilers. With a decreasing primary energy factor for electric energy in the future due to growing shares of renewable energy in electricity grids, heat pumps will become increasingly economically attractive.

According to BDH (2012), since 2007 the market share of heat pumps remains constant at 8 to 10% in Germany (annual data until 2011, prognosis for 2012). In the last decade, the market share of heat pumps in Germany has increased mainly at the expense of oil boilers that had a share of 26% in 2002 and 12% in 2012, whereas the share of gas boilers increased. Heat pumps are independent from local gas grids, thus they are a common substitute for oil boilers.

Additionally, a reason for increasing heat pump market shares are last years' governmental grants for heating systems that use renewable energy sources. The heat extracted from the environment by a heat pump is considered a renewable energy source by the directive of the European Council RES (2009), which serves as a framework for national directives and incentives. Michelsen and Madlener (2012) give a overview on these political instruments in Germany, whereas the "BAFA" funding[2] is mentioned as the most important one for heat pumps in Germany. The funding and its amount depend on the heat pump type and the seasonal performance factor (SPF) which is calculated using the guideline VDI 4650-1 (2009) (BAFA, 2011, 2012).

Ground coupled devices dominated the German market before 2010. Since then increasing sales of air-to-water heat pumps have lead to an inverse market allocation[3]. 59,500 heat pumps for room heating applications have been sold in Germany in 2012 (BWP, 2013). Until 2009, heat pumps were merely used for retrofits, in 2010 the application in new buildings prevails (BWP, 2011). Heat pumps in Germany are mainly used in one (88%) and two family houses (10%) (Platt et al., 2010).

The efficient operation of heat pumps in existing buildings usually requires an adaption of the existing heating system (Brugmann, 2006). Existing buildings make up the majority of the German and European building stock (BPIE, 2014). Especially considering the political will to save energy in buildings[4] new heat generators will be increasingly implemented in existing buildings.

[1] Assuming the German primary energy factor for natural gas of 1.1, cf. (DIN SPEC 4701-10-A1:2012, 2012). For a typical gas condensing boiler with an annual fuel utilization ratio (AFUE) of 0.96, cf. Wolff et al. (2004), related to the lower heating value and a primary energy factor for electricity of 2.6, valid for Germany, in the evaluated years of the field test analyzed within this work, cf. DIN SPEC 4701-10-A1:2012 (2012), the boundary SPF value above that the heat pump achieves savings compared to the boiler, is 2.3.

[2] See BAFA (2012). BAFA: Abbr. for German Federal Office of Economics and Export Control.

[3] The share of air-to-water heat pumps is 62.7% in 2012, cf. BWP (2013).

[4] See e.g. RES (2009).

### 1.3.2 Terminology

Within this work the term "heat pump" is used synonymously for electrically driven compression heat pumps, which is commonly done in literature. The terminology concerning different system parts is defined more precisely: In standardization and other publications (DIN EN 15316, 2008; Bollin, 2009; Song, 1999; Wemhöner and Afjei, 2003) the terms *heat pump system* and *heat pump heating system* are defined as follows: *Heat pump system* defines the heat pump including the hydraulic distribution but without the heat delivery system. A *heat pump heating system* combines the *heat pump system* and the *heating system* and thus includes the heat emitters.

### 1.3.3 Methods of heat pump system evaluation

Literature provides various studies on heat pump systems which are analyzed with different methods, such as field tests simulation or laboratory test benches or combinations of both; in this context, modeling according to field test data or hardware in the loop tests can be mentioned. In the latter test bench measurements are combined with simulations.

#### Field tests

Several field studies have been conducted in recent years. In Germany several field tests have been done by the Fraunhofer Institute for Solar Energy Systems, Freiburg (ISE) (Miara and Günther, 2011), amongst others the one which is analyzed in this work (chapter 3) introduced by Miara et al. (2007). Field tests in other European countries are summarized in Nordman (2012). A very detailed analysis of a field test in the UK is presented in Dunbabin and Wickins (2012). Special requirements for dimensioning of heat pump systems in the UK due to characteristics of the electricity grid are emphasized. A large difference of field test and laboratory heat pump efficiency is detected by Hoogmartens et al. (2011) in a Belgian field test. A field study with a ground coupled heat pump is presented by Montagud et al. (2011) who evaluate heat pump performance after five years of operation. In this study, no decrease of efficiency could be detected.

Boait et al. (2011) analyze a field test in the UK and study temperature set-back periods, which are periods in which the heat pump is turned off because of requirements of the electricity grid. A simple model of building and heat pump is used, which is validated against field test results. Low efficiency of heat pumps in the UK is explained by over-sized aggregates and false control settings such as too high heating curves. The authors propose heat pump control that takes into account outdoor air temperature trend and user presence.

Field test data is used in model tests or transformed into models. Salvalai (2012) models a heat pump for the building modeling platform IDA-ICE[5] and checks it against field test data of a German

[5] See IDA-ICE (2014).

field test conducted by the Fraunhofer ISE. Djuric et al. (2011) use field test data for modeling of heat pumps and reduce uncertainty by a data fusion method. Esen et al. (2008) use measurement data in an artificial neural network for modeling of a ground coupled heat pump.

### Simulation and calculation procedures

A common method for heat pump system evaluation is dynamic simulation, especially for the examination of control strategies. Whereas formerly, specific models where implemented on a very basic level (cf. e.g. Ney (1990)) in the last years system simulation with the modeling environment TRNSYS have become popular[6]. TRNSYS is a software for the simulation of building physics and building engineering systems. There are interfaces or add-ons to TRNSYS as used by Madani et al. (2013) or Seifert et al. (2009).

Another simulation environment for buildings is Energy Plus, which is also used for the simulation of heat pump systems[7]. Simulink[8] is used for building simulation, too, commonly when the focus is on controller development or coupling with other software or with test benches for example as done by Partenay et al. (2010).

Various simulation studies deal with the implementation of ground source heat exchangers and their impact on a system level[9]. The combination of heat pumps and solar collectors is also the subject of simulation studies[10].

The building models used within these simulation studies sometimes are one-zone[11] or two-zone models[12]. Many authors use three or more zone models[13].

Whereas dynamic simulation of heat pump systems is usually used in research[14], for design calculations or prediction of energy demand, static calculation methods are commonly used. A very simple one is presented in VDI 4650-1 (2009). It gives a rough estimation of the seasonal performance factor and only needs few input variables. Wemhöner and Afjei (2003) give an overview on static calculation methods for heat pump heating systems and compare their outcomes; furthermore, a detailed calculation method is proposed. Detailed methods operate with *bins* that represent operating points that are weighted according to their frequency and corrected to account for specific system features. This kind of procedure is described in Eskola et al. (2011) and used in the standard DIN EN 15316 (2008).

[6] See Olympia Zogou (2007); Rad et al. (2009); Seifert et al. (2009); Helpin et al. (2011); Hoogmartens and Helsen (2011); Marx and Spindler (2011); Verhelst (2012); Madani et al. (2013); TRNSYS (2014).
[7] See EnergyPlus (2014); Fisher and Rees (2005); He et al. (2009).
[8] See MathWorks (2012).
[9] See Fisher and Rees (2005); Olympia Zogou (2007); He et al. (2009); Rad et al. (2009); Partenay et al. (2010); Hackel and Pertzborn (2011); Javed (2012); Verhelst (2012).
[10] E.g. see Helpin et al. (2011).
[11] See Verhelst et al. (2012).
[12] See Bianchi (2006); Verhelst (2012).
[13] See Fisher and Rees (2005); Olympia Zogou (2007); Hoogmartens and Helsen (2011).
[14] A literature review on different modeling approaches for heat pumps is given in section 4.1.2.

#### Hardware in the loop

Hardware in the loop (HiL) tests are an additional method for the analysis of heat pumps. Riederer et al. (2009) present a heat pump test bench which is coupled to a Simulink simulation as well as a test and evaluation procedure that allows for the determination of seasonal performance. Chen et al. (2012) present a HiL test bed that allows not only for emulation of the heating system but also the local electricity grid and other home energy systems.

### 1.3.4 Control concepts for heat pump heating systems

Different levels of control in heat pump heating systems can be defined. The *control of the heat pump's working fluid circuit* sets boundaries for the *heat pump system control* which interacts with the *control of the heating system.* These levels and their control is depicted in chapter 2. The next paragraphs give an overview on literature that deals with control in heat pump systems.

#### Heat pump working cycle control

Within heat pump working cycle control, the control of the compressor is crucial. It can be either on/off controlled or speed controlled, the latter meaning a capacity control of the heat pump.

In recent years, compressor capacity control has been studied intensively[15]. Choi et al. (2011) implement a fuzzy control for compressor speed control that performs better than a typical PI control.

On the working fluid level, another control unit is the expansion valve. Either thermostatic or electronically controlled valves are used. By conducting an exergy analysis, Gasser et al. (2008) find that electronically controlled expansion valves improve the working fluid cycle by setting a precise super-heating in the evaporator. A self-adapting control of super-heating is presented by Küpper (2010).

#### Standard heat pump heating system control

Little literature is available on standard heat pump heating system control concepts. This is also stated by Madani et al. (2013) who compare three control concepts: a return temperature control, a "degree-minute" control (this is a supply temperature control with a variable hysteresis which is calculated with the integral of differences between set and actual value) and a return temperature control with a floating hysteresis. Electric energy savings over controllers with a constant hysteresis can be detected by using the variable hysteresis implementation. The room set temperature and its control hysteresis are analyzed in Corberan et al. (2011); this publication deals with a heat pump used for cooling purposes.

[15] See Karlsson (2007); Bugbee and Swift (2013); Adhikari et al. (2011); Safa et al. (2011).

Hoogmartens and Helsen (2011) do a parameter study on a heat pump system changing different control parameters of the heating curve, room thermostats and a reference room compensation. The authors demonstrate savings in electrical energy usage due to different control strategies which, in most cases influence thermal comfort marginally. The parameters of the heating curve, however, have a strong impact on the energy demand as well as comfort.

A common control element in heating systems is the aforementioned heating curve which generates a heating water supply temperature depending on the outdoor air temperature. This is a feed-forward kind of control, whereas other control systems in buildings generally use feedback control (Thomas et al., 2005). Influences on the heat load other than the outdoor air temperature are usually coped with using feed-back controllers such as thermostatic radiator valves or room thermostats that calculate an offset on the heating curve from the temperature in a reference room (Thomas et al., 2005).

### Advanced heating system control

The following control concepts are not restricted to heat pump heating systems but are applied to different kinds of heat generation systems. The advanced control systems found in literature are often adaptive controllers or predictive controllers[16]. The benefits of optimal, predictive and adaptive control methods for heating systems are reviewed by Zaheer-Uddin (1993); the advantages over standard control concepts are pointed out. Model predictive control can also be used to control the interaction of multiple elements in buildings such as the heating system, active shading or ventilation systems as has been investigated by Hube (2004).

In a basic simulation study using transfer functions Thomas et al. (2005) analyse a feed-forward control system for an idealized electric heater. The inner gains of a room are fed forward. It is concluded that the control performance as well as the energy consumption is optimized though such control.

Prívara et al. (2011) compare a MPC controller to a standard heating curve control in a test building; the predictive control successfully saves heating energy over the standard controller while maintaining the room comfort. However, the authors emphasize the importance of a well chosen model and the difficulty of finding the right model.

A predictive control concept is used by Giannakis et al. (2011) using weather prediction. A fine-tuning of proportional controllers is done using a cost function optimization alongside with a process model. The same concept is applied by Constantin et al. (2013).

There are advanced control strategies that adapt the supply temperature according to the load conditions. Their basic principle is described in Rietschel (2005). The algorithm proposed by Kähler and Ohl (2009) works in discrete time steps and load conditions are taken into account by measuring the position of thermostatic valves. A detailed description of this control method is given

[16] See (Zaheer-Uddin, 1993; Prívara et al., 2011; Giannakis et al., 2011).

by Kraft (2002). Another study evaluates these systems, where energy savings through lower heat losses in the heat distribution system are analyzed (Matthes et al., 2007). These heat losses can be reduced, but attention has to be paid to higher mass flow rates leading to higher return temperatures.

In this context, the effect of influencing the efficiency of a heat pump has been studied, too. Seifert et al. (2009) show that an adaptive control of the supply temperature can increase heat pump efficiency. According to their results, in a well-insulated building the SPF can be increased by approximately 0.2. Focusing on cooling applications, Beghi and Cecchinato (2011) present an adaptive supply temperature control. They use the chiller supply and return temperature for load estimation. This estimation is low-pass filtered to avoid unstable control.

### Advanced heat pump heating system control

While standard control concepts are rarely described, literature provides several studies on advanced control concepts in heat pump heating systems. In many of these works controllers are tested within simulation models. Usually, the building model has a reduced number of zones and the room temperature of one reference room is used as the measured variable (Bianchi, 2006; Hube, 2004; Thron, 2001). The problem of multiple heated zones with different characteristics is mentioned by Thron (2001), who, however, does not explore the problem further.

Model predictive control is proposed for heat pump systems and has to be preferred over heating curve control according to Zogg (2000). Bianchi (2006) proposes a predictive heat pump controller that calculates the operating cycles of an on-off controlled heat pump with a pulse-width modulation scheme. The model used for control is a self-parametrizing one-node house model that considers not only the room capacity but also the capacity of the heating fluid. The controller is tested in a simulation environment with a two-zone house model where the room temperature of one room serves as the measured variable.

Verhelst et al. (2012) study different heat pump models and cost function formulations for a model predictive control in an AWHP heating system with floor heating and compare them to a standard heating curve control. The advanced control strategies result in nearly the same energy and comfort as the standard one. However, with variable electricity tariffs being considered, cost savings can be achieved with advanced control.

A multi-agent system control is studied by Mokhtar et al. (2013). The operating hours of a heat pump supplying a floor heating system can be increased compared to a gas boiler that delivers heat to radiators in the same heated zones, if the inertia of the heat emitting system is considered in control.

Many publications dealing with advanced heat pump control address control according to electricity tariffs. By shifting a highest possible load to off-peak periods with low electricity prices,

energy costs are lowered and heat pumps are indirectly used for load management on electricity grid level[17]. Rink et al. (1988) approach this subject by assuming a night-time low price period; applying the maximum principle, optimal operation schedules are found for the heat pump systems for different outdoor air temperature levels. Knapp and Wagner (2012) propose applying predictive control for this kind of load management. Ginsburg (1999) develops a heat pump control using fuzzy control theory involving weather and off-time prediction.

[17] The potential of this kind of load management from an energy grid point of view is studied by Nabe and Seefeldt (2011).

# 2 Fundamentals

## 2.1 Heat pumps

### 2.1.1 General definition and coefficient of performance (CoP)

A heat pump absorbs a heat flow on a low temperature level and extracts a heat flow on a higher temperature level by using an external power $P$. With the high temperature heat flow being the one used for heating $\dot{Q}_{\text{use}}$, also called *heat pump capacity*, the efficiency of a heat pump can generally be expressed by the coefficient of performance CoP:

$$\text{CoP} = \frac{\dot{Q}_{\text{use}}}{P} \tag{2.1}$$

The low temperature heat generally is extracted from the environment, more precisely the ground, outdoor air or ground water. The power driving the process can be either a technical or thermal one. However, thermally driven sorption based processes are underrepresented on the market, the vapor compression cycle clearly dominates, whereas the driving power is usually electricity (Platt et al., 2010). The usable heat flow is transferred directly to the indoor air or to a hydronic heating system.

In this work, electrically driven compression heat pumps are analyzed which use the ground or the outdoor air as heat source and have a hydronic heating system as heat sink. As mentioned before, the term "heat pump" is used synonymously for this kind of heat pump within this work.

### 2.1.2 The working fluid cycle

A typical working fluid cycle of a vapor compression heat pump is shown in figure 2.1 on page 12 and in a $\log(p)$-$h$-diagram in figure 2.2 on page 12. Several variations of this kind of cycle exist that use internal heat exchangers and/or multiple compressors and are optimized for certain operating conditions. However, for the following basic considerations the simple set-up as shown in the figure is studied. It consists of the evaporator, compressor, condenser and the expansion valve. Heat is extracted from a low temperature heat source while the working fluid evaporates on a low pressure level, i.e. a low temperature level in the two phase region. Fully vaporized, the fluid enters the compressor which raises the pressure to the upper pressure level and thus a higher temperature. In the condenser/gas cooler heat is transferred to the heat sink while the working fluid condenses. Passing the expansion valve the working fluid pressure falls to the lower pressure level. In real heat

pump cycles pressure losses occur in the heat exchangers, the working fluid is usually super-heated to avoid liquid in the compressor, the compressor works by producing entropy.

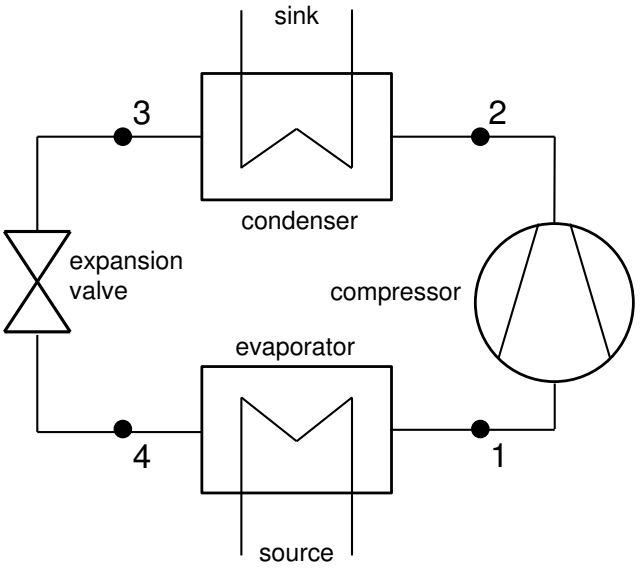


**Figure 2.1:** Basic scheme of heat pump working fluid cycle.

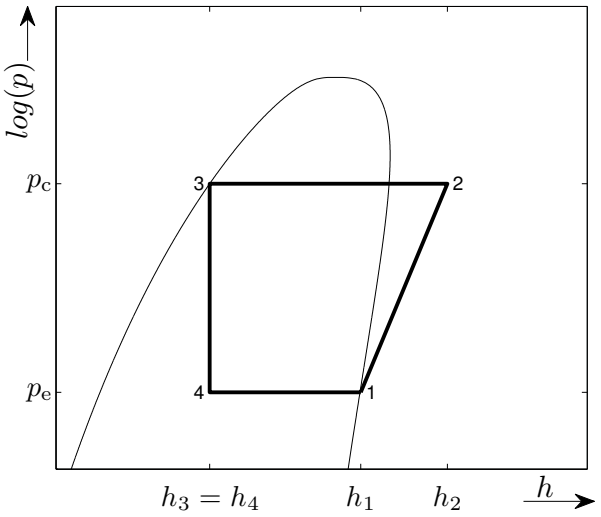


**Figure 2.2:** Basic heat pump cycle in a log($p$)-$h$-diagram. Numbers refer to states marked in figure 2.1.

### The Carnot Cycle

The theoretical, ideal principle of the heat pump process is represented by the reversed Carnot cycle which presumes isentropic pressure changes and isobaric and isothermal heat transfers. Its

CoP is expressed by

$$\mathrm{COP_C} = \frac{T_{\mathrm{use}}}{T_{\mathrm{use}} - T_{\mathrm{source}}} \tag{2.2}$$

where $T_{\mathrm{source}}$ is the temperature of heat gain and $T_{\mathrm{use}}$ is the temperature of heat output. The difference between these two temperatures is the *temperature lift*. Equation 2.2 shows that an increasing temperature lift leads to a lower $\mathrm{COP_C}$. The dependency of the $\mathrm{CoP_C}$ on source and sink temperature is illustrated in figure 2.3.

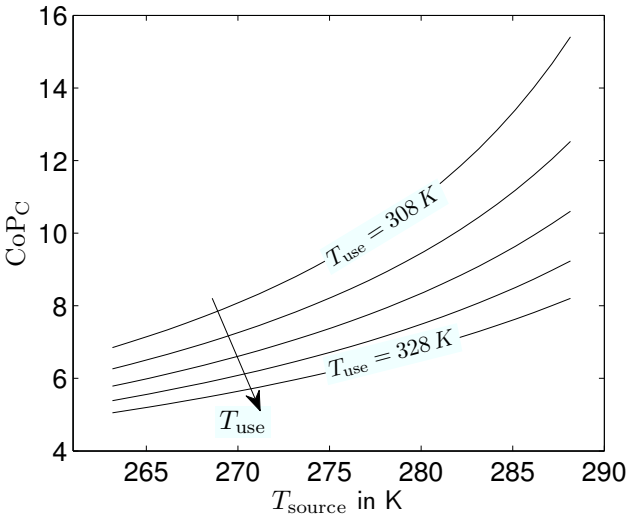


**Figure 2.3:** Dependency of $\mathrm{COP_C}$ on source and use temperature, according to equation 2.2.

In real heat pumps the assumptions of the Carnot cycle are not valid; the internal temperature lift is higher than the used temperature lift because of temperature differences in the heat exchangers. Furthermore, auxiliary appliances are used to operate the heat pump. The source temperature in real heat pumps is the temperature of the source medium entering the evaporator, the sink temperature is the temperature of the sink medium leaving the condenser (here: supply water of the heating system). This leads to a real CoP being distinctly lower than the $\mathrm{COP_C}$. This circumstance is expressed by the quality grade $\eta_{\mathrm{C}}$ which is defined by

$$\eta_{\mathrm{C}} = \frac{\mathrm{CoP}}{\mathrm{CoP_C}} \tag{2.3}$$

and ranges from 0.35 to 0.50 according to Zogg (2009), depending on the type of heat pump and its application.

### 2.1.3 Efficiency measures

On the one hand the aforementioned non-ideal changes of state and the non-ideal heat exchanges are the reason for the quality grade being below one. The real CoP also depends on the control volume that is used for its determination.

#### Coefficient of performance

The total electric power input to the heat pump device includes the power for the electric drive of the compressor (with eventual power electronics) and auxiliary drives on the source and sink side as well as power for internal control appliances. The CoP can thus be expressed as

$$\mathrm{CoP} = \frac{\dot{Q}_{\mathrm{use}}}{P_{\mathrm{el,tot}}} \tag{2.4}$$

with $P_{\mathrm{el,tot}}$ as total electric power input. The European standard EN 14511 (2012) defines the boundary conditions to measure the CoP of electrically driven compression heat pumps. These are inlet and outlet temperatures on source and sink of the heat pump, air humidity and the allowed deviations and measurement time. It includes power for defrosting of air source heat pump evaporators and the share of electricity of source and sink drives that is used to pass the pressure differences of the evaporator respectively condenser. The standard defines conventions for notation of CoP values: The source medium is abbreviated by one letter (e.g. A for air, B for brine) followed by its inlet temperature into the evaporator in degree Celsius. This is followed by one letter for the sink medium (generally W for water) and its outlet temperature from the condenser[1]. This convention is used within this work, too. The former standard EN 255 (1997) should also be mentioned. The main difference between this standard and EN 14511 (2012) is the temperature spread in the condenser which is 10 K in EN 255 (1997) and 5 K in EN 14511 (2012) which leads to approximately 7% lower CoP values for EN 14511 (2012) (WPZ, 2009).

#### Performance Factor

In normal heat pump operation the source as well as the sink temperatures constantly change and with them the operating point varies. The heat source temperature changes seasonally and diurnally. This is obvious for the outdoor air but also occurs for the ground temperature surrounding the ground source heat exchanger depending on the amount of heat extracted from it (which is usually higher in winter). The sink temperature (here the supply water temperature) usually depends on the application. Domestic hot water (DHW) demand and radiator heating systems need high supply temperatures in contrast to floor heating systems. The supply temperature often is

[1] For example A2W35 stands for a air inlet temperature of 2 °C and a water outlet temperature of 35 °C.

controlled according to the heat load. During an operating interval the supply temperature usually increases.

This shows that in standard applications of heat pumps, the efficiency at one operation point does not predict its efficiency for a longer operation. Therefore, the heat pump is evaluated by the performance factor PF. It is the quotient of the usable heating energy $Q_{\text{use}}$ and the total electric energy $W_{\text{el,tot}}$:

$$\text{PF} = \frac{\int \dot{Q}_{\text{use}} dt}{\int P_{\text{el,tot}} dt} = \frac{Q_{\text{use}}}{W_{\text{el,tot}}} \tag{2.5}$$

The calculation of the PF for one year is called SPF (seasonal performance factor). Standards and guidelines exist for the estimation of the SPF for different applications. Usually a weighting of CoP values for corresponding operating condition profiles is done and empiric correlations are applied.

The calculation procedure according to the German guideline VDI 4650-1 (2009) calculates the SPF for heating mode and for hot water production separately and the overall SPF is calculated weighting the SPF for heating and the SPF for hot water demand. Heat produced through secondary heat generators is accounted for, too. The assumptions for the calculation are an average ground temperature (ground coupled devices) and a factor taking into account the annual outdoor air temperature profile (air source heat pumps). The CoP values used within this calculation are those determined according to EN 14511 (2012).

The standard DIN EN 15316 (2008) calculates the SPF according to a sum curve of the outdoor air temperature which is divided into so called bins with a characteristic operating point of the heat pump. The control volume includes storages and loading pumps and thus offers a possibility to do a system analysis.

Choosing an adequate control volume is of great importance for the calculation of SPF. It becomes especially important if heat pumps are compared to other heat generators. The efficiency of the classical heat generator, the gas boiler, is calculated by dividing the useful heat flow in the water circuit by the fuel power. This means that heat not transferred to the water circuit is considered as heat loss, even if the boiler is placed in a heated zone. In a fair comparison, those heat losses have to be considered in heat pump systems as well. The heat losses of the heat pump device are accounted for in the control volume of EN 14511 (2012). But heat pump systems often contain storages such as buffer and DHW storages. Their heat losses also have to be taken into account but often are not, e.g. in the guideline VDI 4650-1 (2009). This is also true for the electricity used for loading pumps in the storage loading circuit.

Within this work two control volumes for SPF are used. The first one corresponds to the one used in DIN EN 15316 (2008), indicated by the index 1. The second one corresponds to VDI 4650-1 (2009), indicated by the index 2.

Control volume 1 is meant to represent the substitute system to a standard boiler system. It includes all components that are required if a boiler is replaced by a heat pump. Depending on the

given measurement positions in the field test that is analyzed within this work, the control volume cannot be exactly matched: The field test objects do not consistently contain a direct heat metering of domestic hot water (DHW). Generally, DHW is directly measured if a combined storage is used which allows to calculate a complete energy balance of the storage. In the case of separated DHW storage and buffer storage, in most cases only the heat being supplied to the DHW is metered. The control volume is indicated in figure 2.4 and the involved components are listed in table 2.1.

For the same reason, the system in control volume 1 is not always the correct substitute system for a boiler system. The boiler usually does not need a DHW storage. In spite of these constraints, control volume 1 is used as it shows the influence of storage losses and supplementary electrical energy consumption on the SPF compared to control volume 2. For all field test objects measurement data exists to calculate the $SPF_2$. It is also shown in figure 2.4 and table 2.1.

**Table 2.1:** Comparison of control volumes 1 and 2.

| | system boundary 1 | system boundary 2 |
|---|---|---|
| heat energy | - delivered to heating system<br><br><br>- for domestic hot water generation | - delivered to the buffer storage (+heating energy delivered by heating rod, if in buffer storage)<br>- for domestic hot water generation |
| electric work of | - compressor<br>- source pump or ventilator<br>- heating rod<br>- loading pumps | - compressor<br>- source pump or ventilator<br>- heating rod |

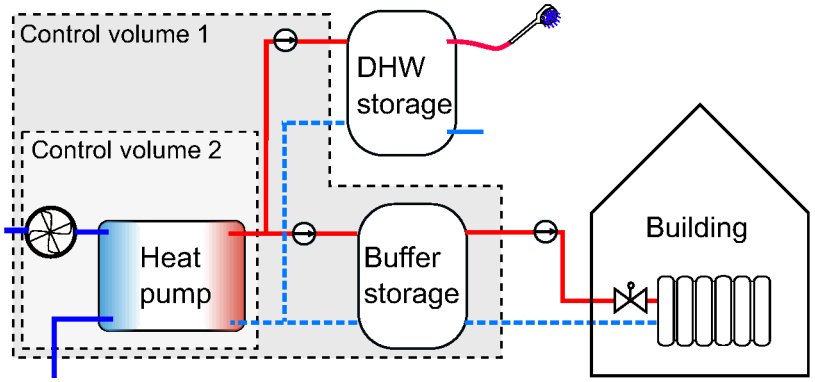


**Figure 2.4:** Scheme of the two control volumes using the example of an AWHP system.

## 2.2 Heating of buildings

### 2.2.1 Heat load

The heated building is one part of the system analyzed in this work. The heat load of the building largely depends on the outdoor air temperature.

The nominal heat load of a building is usually determined according to the standard EN 12831 (2003). This standard defines nominal outdoor air temperatures $T_{\text{out,nom}}$ and nominal indoor air temperatures $T_{\text{room,nom}}$ that are used to identify the nominal heat load of each room by summing the transmission heat load, the heat load caused by air exchange and an eventual additional heat load for the heat-up of the room in a specified time period. For the transmission heat losses each room component's heat loss is calculated by the product of heat transmission coefficient $k$ and the temperature difference between the two nominal temperatures:

$$\dot{Q}_{\text{hl,trans,nom}} = k \cdot A \cdot \left(T_{\text{room,nom}} - T_{\text{out,nom}}\right) \tag{2.6}$$

where $k$ includes the heat conduction in the building part and the convection on the inside and outside of the building. Both convection coefficients are assumed as being constant. $A$ is the component's surface area relevant for the heat flow. Additional effects (such as thermal bridges or temperature differences other than the aforementioned, e.g. towards the ground) are accounted for by factors. The sum of the heat loads of all components is the overall nominal transmission loss of the room. The nominal air exchange heat losses of a room are calculated by

$$\dot{Q}_{\text{hl,vent,nom}} = c_{p,\text{air}} \cdot n \cdot \rho_{\text{air}} \cdot V_{\text{room}} \cdot \left(T_{\text{room,nom}} - T_{\text{out,nom}}\right) \tag{2.7}$$

with the specific thermal capacity of air $c_{p,\text{air}}$, its density $\rho_{\text{air}}$, the volume of the room $V_{\text{room}}$ and the air exchange rate $n$. Overall, the standards uses thermal resistances which are multiplied by the temperature difference between the nominal temperatures.

The sum of all nominal transmission heat losses and all air exchange heat losses of a building is the nominal heat load of the building. Considering equations 2.6 and 2.7 and presuming constant convection coefficients on the inside and outside of all building parts the heat load of a building can be simplified to a linear characteristic. It is shown in figure 2.5 on page 18 and given in the equation

$$\dot{Q}_{\text{hl,tot}} = H_{\text{tot}} \cdot \left(T_{\text{room}} - T_{\text{out}}\right) \tag{2.8}$$

with $H_{\text{tot}}$ as the total heat loss coefficient. It neglects different temperatures in different rooms and inner heat gains as well as weather influences[2] other than the outdoor air temperature but is commonly used to dimension heat generation systems.

[2] For example different wind speeds that would effect the convection on the outside of the building shell are not taken into account.

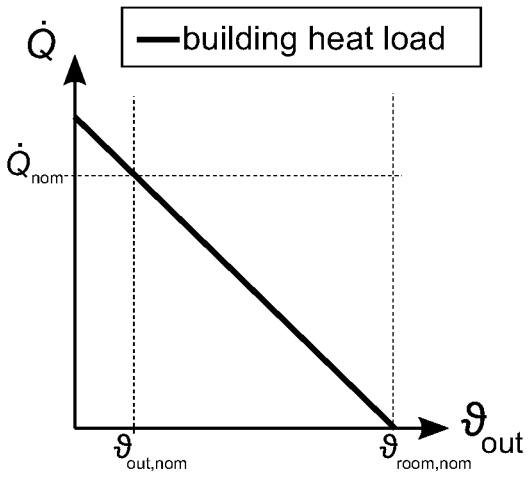


**Figure 2.5:** Simplified linear heat load characteristic of a building.

The highest amount of heat demand during a heating season usually does not occur at nominal conditions. The heat load of a building rises with decreasing outdoor air temperatures. However, very low temperatures are infrequent. In Germany, usually at temperatures between 0 and 5 °C the highest heat demand occurs during one heating period (Burger and Rogatty, 2003).

The capacity of a heat generation system often is not only fitted for handling of the nominal heat load. The capacity of the heat generator is often chosen to fit for DHW generation. Heat pumps are usually equipped with a DHW storage to avoid largely over-dimensioned devices for heating.

### 2.2.2 Evaluation of energy demand

The annual final energy demand of a building does not only depend on the outdoor air temperature. Inner and solar gains reduce the heat demand, DHW demand $Q_{\mathrm{DHW}}$ increases it. According to DIN V 4701-10 (2003) the heat demand for room heating $Q_{\mathrm{heating}}$ is calculated with the thermal resistances[3] multiplied by degree-day numbers, which are the integrated temperature differences between the nominal room temperature and the outdoor air temperature. Solar and inner gains during heating season are subtracted from this demand.

The resulting final energy demand can be multiplied by a primary energy factor $f_{\mathrm{PE}}$ to calculate the primary energy demand PE of the building.

$$\mathrm{PE} = Q_{\mathrm{final}} \cdot f_{\mathrm{PE}} \tag{2.9}$$

with

$$Q_{\mathrm{final}} = (Q_{\mathrm{heating}} + Q_{\mathrm{DHW}}) \cdot \Pi e_i \tag{2.10}$$

[3] The resistances determined in EN 12831 (2003) can be utilized, see section 2.2.1.

whereas $\Pi e_i$ is the product of expenditure factors for heat control, emission, distribution, storage, and generation. Calculation of primary energy demand is particularly interesting if heat generators that work with different types of final energy are compared to each other[4]. Primary energy factors for Germany are usually applied according to DIN SPEC 4701-10-A1:2012 (2012), whereas in this work due to the time that the field test was executed, DIN SPEC 4701-10-A1-2009 (2009) was applied. These standards offer two types of mean primary energy factors: One that considers renewable energies as primary energy and another one that only considers the non-renewable part. The latter is usually chosen for evaluation. The primary energy factor for electricity is $f_{\mathrm{PE}} = 2.6$ and for natural gas it is $f_{\mathrm{PE}} = 1.1$ for the non-renewable share (DIN SPEC 4701-10-A1-2009, 2009). In the current version DIN SPEC 4701-10-A1:2012 (2012) the primary energy factor of electricity is 2.4. This reflects the increased share of renewable energy in the electricity mix of Germany. It shows that on the level of primary energy heat pumps are becoming increasingly efficient.

A study comparing the field test evaluated in chapter 3 to gas condensing boilers was conducted in Huchtemann and Müller (2012). It showed that regarding primary energy, heat pumps in existing buildings can be advantageous when compared to gas condensing boilers. In the field test, however, a lot of them are not, as illustrated by the mean SPF of 2.3 for air-coupled devices and 2.9 for ground-coupled devices. The aforementioned trend of decreasing primary energy factors for electricity will change this situation in the future.

In this work, the evaluation of primary energy demand is not necessary as it is not the goal to compare different heat generators but different mono-energetic heat pump systems. Therefore, a comparison of the final energy and the SPF is sufficient and this is thus the main concept of energetic evaluation in this work.

### 2.2.3 Thermal comfort

Fanger (1970) defines factors that influence thermal comfort sensed by human beings. Besides the ambient and mean radiant temperature, these are humidity, air movement, metabolic rate and clothing. Whereas thermal comfort is usually assessed with PMV/PPD[5], DIN EN 15251 (2007) also defines methods to evaluate operative temperatures alone. It defines a temperature band around a reference temperature which is outdoor air temperature dependent. Discomfort is calculated either by determining the percentage of hours that the operative temperature is not within the boundaries or by integrating the differences between operative temperature and these boundaries. The latter is a commonly used approach to evaluate comfort, e.g. applied by Hoogmartens and Helsen (2011). Liao and Dexter (2004) describe a method to evaluate discomfort in multiple zones by weighting integrals of different zones according to their importance. Hube (2004) uses the quadratic sum of deviations from a comfort band which thus penalizes high deviations.

[4] The analysis of primary energy demand allows for a comparison of the heat pump to other heat generation systems. The standard heat generator and main competitor for heat pumps on the German heat generator market is the condensing gas boiler, cf. BDH (2012).

[5] PMV: predicted mean vote, PPD: predicted percentage dissatisfied, see Fanger (1970).

Freitas (1985) asserts that people prefer warm over cold thermal sensation. Mayer (2001) states that the original correlation of PMV and PPD has to be shifted towards positive PMV, which could be confirmed through experiments at EBC (Streblow, 2010).

## 2.3 Heat pump systems

Within this section, components of heat pump systems are described from the system point of view, focusing on the interaction of multiple components.

### 2.3.1 Heat pump

The heating capacity of boilers usually is chosen equal to or higher than the nominal heat load of the building which allows for a monovalent operation. According to the characteristic of a heat pump, the CoP characteristic and the frequency of outdoor air temperatures (and according supply temperatures) a monovalent operation might not be the optimal operation strategy. Figure 2.6 shows linearized characteristics of the building heat load and heat pump capacity. In a monovalent layout the heat pump is strongly over-dimensioned in the typical operation points. If the heat pump is on/off controlled, which is the capacity control commonly used[6], this leads to a strong cycling behavior. To avoid a fast wear-out of the heat pump compressor through a high number of operating intervals per heating season and to avoid a strongly fluctuating supply temperature, heat pump systems are often designed for bivalent-parallel operation (figure 2.6). This allows for lower heat pump capacities. The cycling of a heat pump is also reduced by an application of heating systems with high thermal masses. Therefore, radiator heating systems are often equipped with buffer storages, whereas floor heating systems usually can operate without an additional buffer storage. Nevertheless, there are also heat pump systems that are designed for monovalent operation.

In bivalent heat pump systems with electrically driven compression heat pumps the second heat generator often is an electrical heater[7]. The heat generation system thus is mono-energetic. The low efficiency with respect to primary energy demand of such heat generators can be justified with a small number of operating hours, its low cost and the reduced heat pump cost. In Germany, only 15% of heating energy in buildings is applied below outdoor air temperatures of -5 °C (Burger and Rogatty, 2003). Therefore, a typical bivalent temperature for heat pump systems is -5 °C (Brugmann, 2006). The additional electrical heat generators are either installed directly into the heat pump device or into a buffer storage.

The dimensioning of capacity controlled heat pumps follows the same principle. Indeed, within certain boundaries the heat pump capacity can follow the heat load characteristic. But as a lower and upper modulation boundary exists, the same considerations have to be taken into account as

[6] See Uhlmann and Bertsch (2010).
[7] Bivalent heat pump systems are studied in Huchtemann and Müller (2010); Klein et al. (2014).

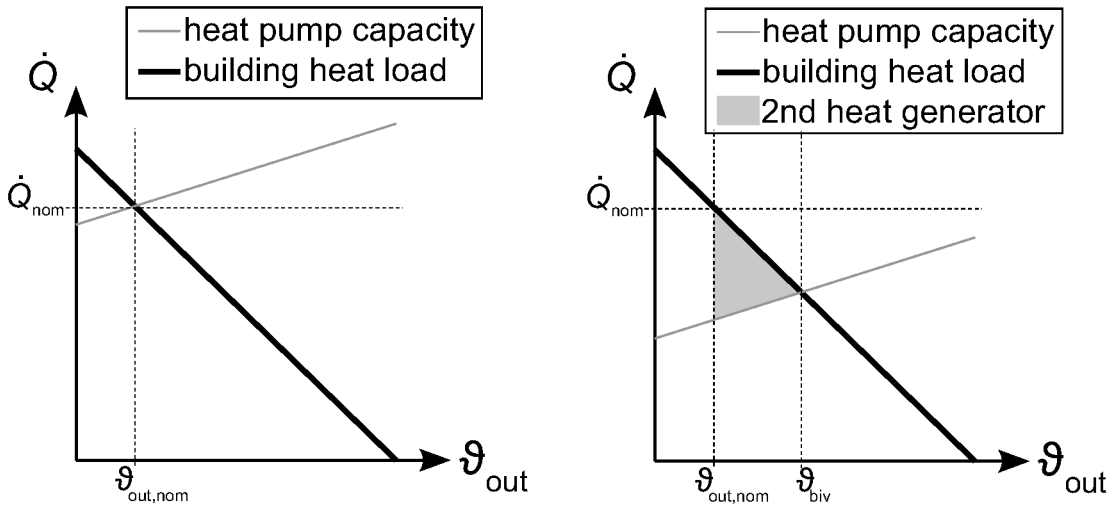


(a) Monovalent

(b) Bivalent-parallel

**Figure 2.6:** Simplified heat load characteristic of building and heat pump capacity characteristic: Monovalent and Bivalent operation strategy.

with on-off controlled heat pumps. It might be favorable to use a second heat generator to avoid an over-dimensioning of the heat pump.

### 2.3.2 Storages

As mentioned above, it might be necessary to equip heat pumps, especially on-off-controlled heat pumps, with a buffer storage that increases the inertia of the heating system in order to minimize the number of operation cycles.

Different rules can be found for the layout of the buffer storage volume. Ochsner (2008) proposes 20 to 30 l/kW of heat pump capacity at B0W35. According to Viessmann GmbH (2011) a value of 20 l/kW is recommended for run-time optimization. However, no information is given on the power value this figure refers to. In (Viessmann GmbH, 2011) a value of 60 l/kW can be found for storages that are to bridge off-periods of 2 h.

### 2.3.3 Heat sources

The most commonly used heat sources for heat pump heating systems are the outdoor air and ground. Outdoor air can be utilized with different concepts: Either the heat pump is installed indoors or outdoors. If it is installed indoors, either the air can be directed indoors, too, to pass the evaporator, or the working fluid is lead to a evaporator split unit which is installed outdoors. For heat pumps installed outdoors, higher demands are required for insulation of the unit and

the heating water pipes against the ambient. All evaporators of air source heat pumps have to be equipped with a fan forcing convection on the heat exchanger. If air has to be lead indoors, pressure losses and thus required power for the fan is higher than for outside evaporators. Depending on the conditions, icing of the humidity contained in the outdoor air can occur. This is why it has to be arranged for defrosting. Several types of defrosting are known whereas the most common is the reversal of the heat pump circuit which uses heat from the heating system (Hubacher and Ehrbar, 2000).

The most common options of using the ground as heat source are vertical (borehole) and horizontal (collector) heat exchangers. Whereas borehole heat exchangers need a restricted surface for installation, horizontal heat exchangers consume much more space during installation. Generally, with the higher depth of boreholes a more stable and higher temperature level can be achieved. Usually, plastic u-pipes or double u-pipes are used. In all ground source heat exchangers an antifreeze fluid ("brine") is used which has lower heat capacity than water. A specialized brine pump is used for circulation. Usually, a plate heat exchanger is used as evaporator.

## 2.4 Hydronic heating systems

Hydronic or water based heating systems are common in German one family homes. A standard is the two pipe system with a supply and return line. The heat delivery system in existing buildings is usually a radiator. Floor heating systems are also applied with water based distribution systems.

### 2.4.1 Distribution

Heating at nominal conditions, the two-pipe hydronic heating system has to deliver the nominal mass flow to each distribution unit (radiator or floor heating). Usually this is accomplished by executing the hydraulic balance. It means that the hydraulic section with the highest pressure drop at nominal mass flow conditions is detected. In a next step all other sections are equipped with an additional pressure drop to allow their nominal mass flows to pass at the same pressure difference. Therefore, radiator control valves are often equipped with an adjustable hydraulic resistance.

The pump of the heating system is designed according to the maximal pressure drop and the total nominal mass flow rate which is the sum of nominal mass flows of all distribution units.

### 2.4.2 Heat delivery

Radiator heating systems are generally designed to deliver a heat flow rate matching the nominal heat load [8] of the building. During the design process, the nominal heat load is determined for every room of the building and the radiator for each room is chosen accordingly. The radiator has

[8] See section 2.2.1.

a sufficient heat emitting surface to deliver the nominal heat load of the room using the nominal supply temperature $T_{\mathrm{su,nom}}$ and the nominal temperature spread $\left(T_{\mathrm{su,nom}} - T_{\mathrm{re,nom}}\right)$ (with $T_{\mathrm{re,nom}}$ as the nominal return temperature). The nominal temperature spread implies a nominal mass flow, presuming the design heat emission of the radiator is met.

The heat flow to the heated room can be expressed with the mass flow rate $\dot{m}$, the specific thermal capacity of water $c_{p,\mathrm{W}}$ and the supply and return temperature of a radiator:

$$\dot{Q} = \dot{m} \cdot c_{p,\mathrm{W}} \cdot (T_{\mathrm{su}} - T_{\mathrm{re}}) \tag{2.11}$$

The dependency of the radiator heat flow on the involved temperatures (assuming a constant mass flow rate in the radiator) can be described by the following equation (Glück, 1990):

$$\frac{\dot{Q}}{\dot{Q}_{\mathrm{nom}}} = \left(\frac{\Delta T_{\mathrm{log}}}{\Delta T_{\mathrm{log,nom}}}\right)^{n} \tag{2.12}$$

$\dot{Q}$ is the radiator heat flow rate, $n$ is the radiator index which accounts for operation outside of nominal conditions. The subscript 'nom' indicates the nominal value. The mean logarithmic temperature difference is defined by

$$\Delta T_{\mathrm{log}} = \frac{T_{\mathrm{su}} - T_{\mathrm{re}}}{ln\left(\frac{T_{\mathrm{su}} - T_{\mathrm{room}}}{T_{\mathrm{re}} - T_{\mathrm{room}}}\right)} \,. \tag{2.13}$$

Here $T_{\mathrm{su}}$ and $T_{\mathrm{re}}$ are the supply and return temperature of the heating fluid and $T_{\mathrm{room}}$ is the room air temperature.

Figure 2.7 on page 24 shows qualitative characteristics of a radiator according to equation 2.12 and the following equation:

$$\frac{\dot{Q}}{\dot{Q}_{\mathrm{nom}}} = \frac{\dot{m}}{\dot{m}_{\mathrm{nom}}} \cdot \frac{T_{\mathrm{su}} - T_{\mathrm{re}}}{T_{\mathrm{su,nom}} - T_{\mathrm{re,nom}}} \tag{2.14}$$

It shows the possibilities of influencing the heat flow rate of the radiator by adjusting the flow temperature and the mass flow rate.

### 2.4.3 Control

In two-pipe water based heating systems generally two possibilities of controlling the heat emission exist: The excess temperature can be controlled (equation 2.12) or the the mass flow can be controlled (equation 2.11). Typically both types of control are used in a typical hydronic heating system. The supply temperature is controlled centrally depending on the outdoor air temperature (heating curve). In this way, the main influence on the heat load of a building (see figure 2.5 on page 18) is considered. A decentralized control of the heat emission according to solar and inner gains of a heated zone is done with thermostatic valves.

Presuming a constant nominal room temperature and nominal mass flow, the heating curve can

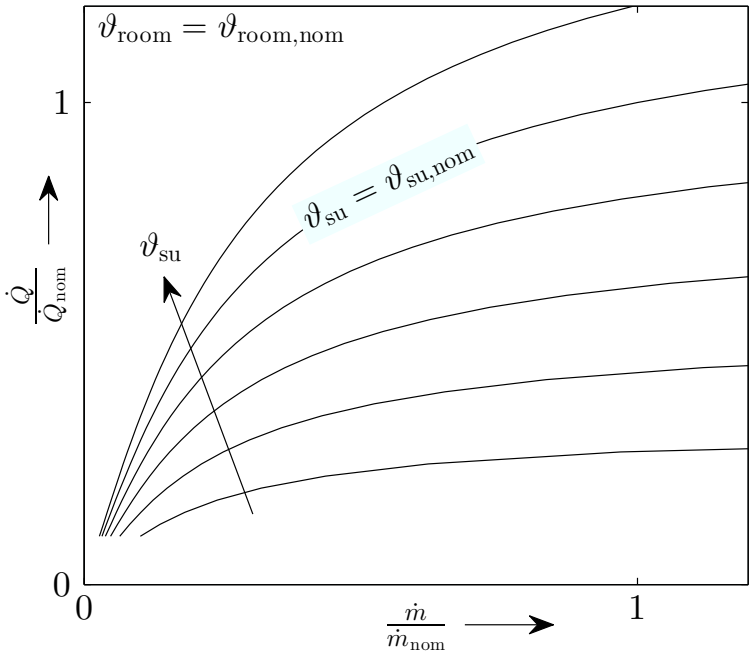


(a) Dependency of heat emission on mass flow

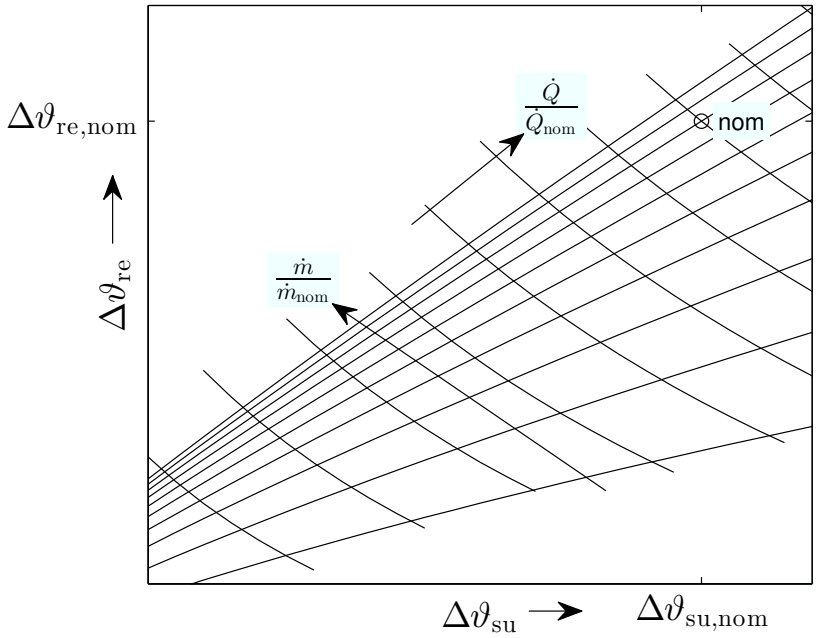


(b) Complete characteristics

**Figure 2.7:** Qualitative characteristics of a radiator. Supply temperature $\vartheta_{\mathrm{su}}$, return temperature $\vartheta_{\mathrm{re}}$, room temperature $\vartheta_{\mathrm{room}}$, radiator heat emission $\dot{Q}$, mass flow rate $\dot{m}$, $\Delta\vartheta_{\mathrm{su}} = \vartheta_{\mathrm{su}} - \vartheta_{\mathrm{room}}$, $\Delta\vartheta_{\mathrm{re}} = \vartheta_{\mathrm{re}} - \vartheta_{\mathrm{room}}$. Nominal values: 'nom'.

be calculated with equations 2.8, 2.11, 2.12 and 2.13:

$$T_{\mathrm{su,hcu}}(\Delta T_{\mathrm{out}}) = \frac{T_{\mathrm{room,nom}} - \left(T_{\mathrm{room,nom}} + c_1 \cdot \Delta T_{\mathrm{out}}\right) \cdot e^{c_2 \cdot \Delta T_{\mathrm{out}}^{1-1/n}}}{1 - e^{c_2 \cdot \Delta T_{\mathrm{out}}^{1-1/n}}} \tag{2.15}$$

with $c_1 = \frac{T_{\mathrm{su,nom}} - T_{\mathrm{re,nom}}}{T_{\mathrm{room,nom}} - T_{\mathrm{out,nom}}}$, $c_2 = \frac{c_1 \cdot \left(T_{\mathrm{room,nom}} - T_{\mathrm{out,nom}}\right)^{-1/n}}{\Delta T_{\mathrm{log,nom}}}$, $\Delta T_{\mathrm{out}} = T_{\mathrm{room,nom}} - T_{\mathrm{out}}$.

The heating curve is often calculated in a simpler way using an arithmetical instead of a logarithmic temperature difference or using substitute equations with a similar characteristic. By lowering the supply temperature, the mean logarithmic temperature difference between the heating fluid inside the radiator and the room air volume $\Delta T_{\log}$ is decreased. This implies a lower heat flow rate which is transmitted to the room (assuming a constant mass flow rate in the radiator, figure 2.8). A heating curve can also be calculated for the return temperature.

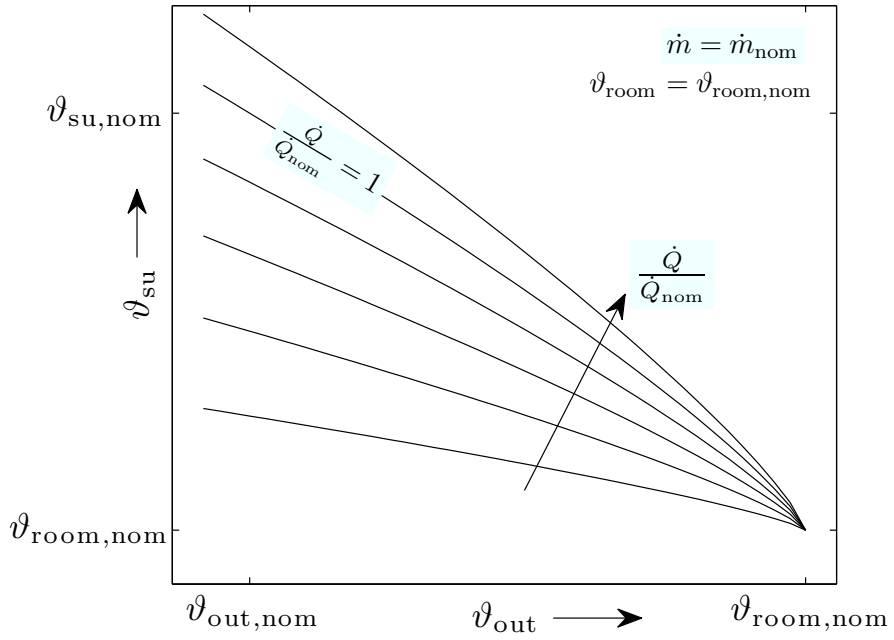


**Figure 2.8:** Qualitative heating curve and dependency of heat emission on supply temperature. Supply temperature $\vartheta_{\mathrm{su}}$, outdoor air temperature $\vartheta_{\mathrm{out}}$, room temperature $\vartheta_{\mathrm{room}}$, radiator heat emission $\dot{Q}$, mass flow rate $\dot{m}$. Nominal values: 'nom'.

Besides the outdoor air temperature, inner loads and solar gains influence the heat load of a building. Therefore, on room level, thermostatic valves are used as controllers[9]. Thermostatic valves usually adapt the mass flow rate in each section of the hydraulic network to control the heat flow rate of the radiator.

The valve position $x$ is defined as the relative valve lift. At a valve position of $x = 0$ the valve is fully closed, at the maximum valve lift $x = 1$, the valve is fully opened. Figure 2.9 shows a typical control

[9] See Recknagel et al. (2009), p. 663.

characteristic of a thermostatic valve. At the room set temperature, the valve position is $x_{\mathrm{nom}} = 0.5$ which allows the nominal mass flow rate to pass the valve. Above and near to the position 0.5 the characteristic is linear. The proportional range $\Delta T_{\mathrm{p}}$ is the difference in room temperature between the position $x = 0$, and the nominal position $x_{\mathrm{nom}} = 0.5$.

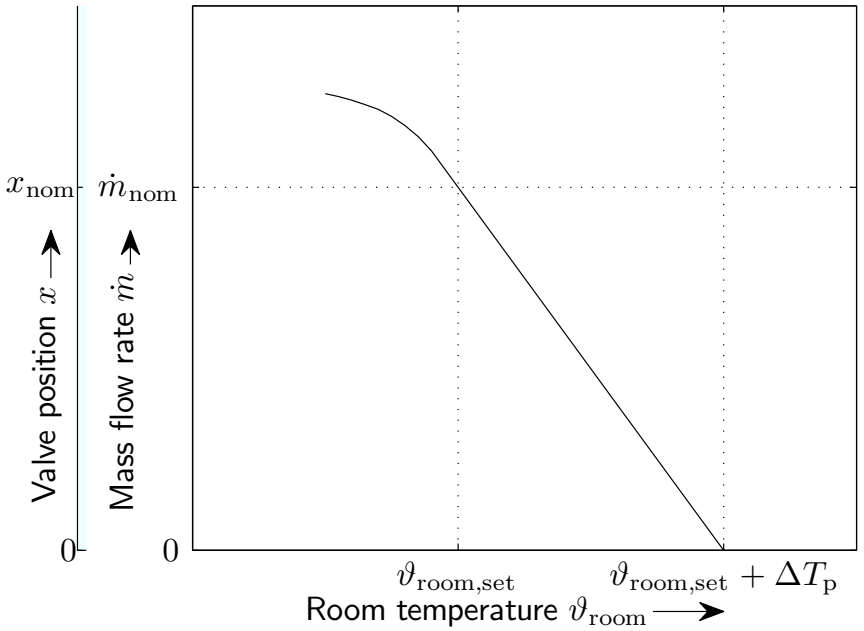


**Figure 2.9:** Characteristic of the thermostatic valve. Proportional range $\Delta T_{\mathrm{p}}$, valve position $x$, mass flow rate $\dot{m}$, room temperature $\vartheta_{\mathrm{room}}$, room set temperature $\vartheta_{\mathrm{room,set}}$.

The typical control of a heating system with radiators is shown as a functional diagram in figure 2.10. For simplification only one heated zone is shown. The two control loops are shown: The supply temperature control is controlled by the operation of the heat generator, mostly implemented with a sufficient hysteresis to avoid strong cycling behavior (in the case of an on/off controlled heat generator). The mass flow rate through the radiator is controlled by a valve which in turn is controlled by the thermostatic head .

## 2.5 Heat pump heating systems

### 2.5.1 Composition

The heat pump system and the heating system are usually hydraulically separated from each other. This can be done using a low loss header or a hydraulic switch[10], whereas often a buffer storage serves as hydraulic switch. The separation allows for different mass flow rates in the condenser

[10] See Ochsner (2008).

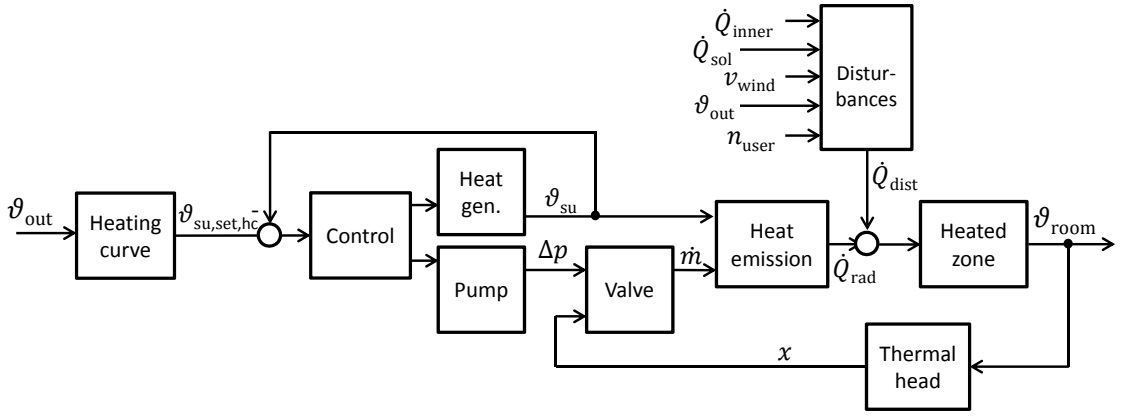


**Figure 2.10:** Functional diagram of a heating system with heating curve control and thermostatic valves (simplified with one heated zone).

circuit and the heating circuit, which is beneficial as the mass flow rate in the condenser cycle can be higher than in the heating circuit. In addition, when the heat pump is off, the heating system can still be operated.

When zones with different heat emission systems exist in one heating system, the hydraulics can be split into parts that are operated with different supply temperatures.

Domestic hot water (DHW) storages are usually integrated into heat pump heating systems by an additional loading circuit that is connected to the condenser of the heat pump by using a three way valve. Either heat is delivered to the heating circuit or to the DHW storage.

### 2.5.2 Control

This section does not cover the internal control[11] of the working fluid cycle but the upper level control of the heat pump system. Likewise, security control features are not part of this section.

Most standard concepts as well as most advanced concepts[12] separate the control of the room or heat emitting surface from the heating temperature or system control. However, a typical way of including the room temperature in the system control is to apply a reference room temperature sensor that calculates an off-set on the heating curve.

On-off controlled heat pumps are controlled using a hysteresis of the supply or return temperature. The set temperature is calculated by a heating curve. The hysteresis can either be a constant or a variable one. The return temperature control has the advantage of providing information from the heated rooms. A high return temperature means that heat cannot be transferred to the heated rooms, a low one means that heat is transferred to the heated zones. However, in this kind of

[11] A brief literature overview on this subject is given in section 1.3.
[12] See section 1.3.4.

system there is no direct control of the highest system temperature. Either it has to be assured that the system is well designed or additional sensors or controls have to be applied.

Besides the heating system inertia and the heat pump capacity, the hysteresis determines the length or number of operating cycles of an on-off controlled heat pump. Whereas a constant hysteresis leads to relatively short cycling with low heat loads (at low supply temperatures) and long operation cycles at high heat loads (at high supply temperatures), an integral hysteresis[13] evens out this mismatch. Thus high hysteresis leading to unnecessary over-heating at high supply temperatures is avoided.

For capacity controlled heat pumps a combination of a hysteresis control and continuous control (e.g. PI) is required because in a certain range the capacity can be adapted to the heat load of the building. Step-wise adjustment, however, is also common.

[13] See Madani et al. (2013).

# 3 Field test analysis

## 3.1 Description of the field test

### 3.1.1 General description

The analyzed field test, launched in 2007, was conducted by the Fraunhofer Institute for Solar Energy Systems in Freiburg (Miara et al., 2007; Russ et al., 2008). It contains 77 heat pump systems installed all over Germany. In this work, the field test was evaluated for the years 2008 and 2009 and for 42 objects based on available data records. 18 air-to-water heat pump (AWHP) systems as well as 24 brine-to-water heat pump (BWHP), i.e. ground-coupled systems, are analyzed. The heat pumps, produced by a variety of manufacturers, were installed by local companies. The institute conducting the test did not have any influence on system design or choice of components. The test does not show 'best practices' but 'as built in'-results for heat pump systems for space heating and domestic hot water generation in existing one family houses with water based heating systems.

Since the field test has been launched, several years have passed and there are new developments for the heat pump as domestic heat generator. One main development is that today, capacity controlled heat pumps are introduced to the heat generator market[1].

Other developments concern the hydraulic setup or integrated solutions (EHPA, 2012). So called reversible heat pumps are applied more often. Here the word reversible refers to the heat pump function that can be reversed, thus it can be used for cooling purposes[2]. Working with BWHP during cooling mode, mostly during summer, the heat inserted to the ground can recover the ground temperature and raise efficiency during heating mode in winter. The ground works as a seasonal storage (De Ridder et al., 2011).

Despite these developments, on/off-controlled heat pumps as used in the field test are still widely used. However, manufacturers have reacted to the growing use of heat pumps in existing buildings by introducing devices with economizers and injection working fluid cycles (Trockel, 2011).

### 3.1.2 Typology of buildings

The buildings of the field test are existing buildings that were formerly heated with oil boilers. The users are clients of different regional electricity companies associated with E.ON SE.

[1] E.g. see (Bugbee and Swift, 2013).
[2] E.g. see Self et al. (2012).

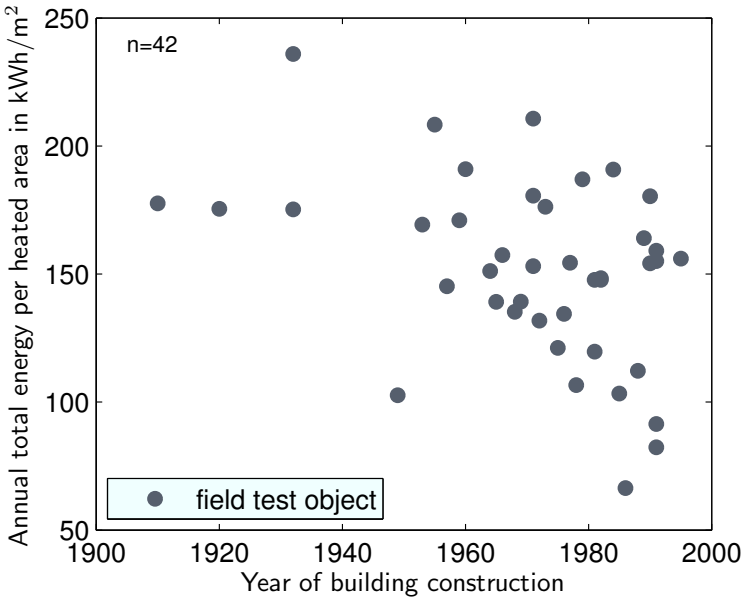


**Figure 3.1:** Annual specific heat consumption and corresponding year of construction of buildings in the field test.

Figure 3.1 shows the construction years of the buildings represented in the field test and their specific heat demands. A correlation of heat demand (or insulation standard) with the year of construction cannot be identified. In a diploma thesis dealing with this aspect no correlation of the year of construction, the respective building insulation standard and the heat consumption or heat pump efficiency could be found (Fütterer, 2010). Even some of the newest buildings achieve high heat demands, probably generated by user behavior. A comparable observation is made with respect to the design supply temperatures of heating systems: some of the newest buildings are equipped with heating systems that need relatively high supply temperatures.

### 3.1.3 Measurement and data processing

An overview on measurement equipment and data processing and transmission is given by Miara et al. (2007). For loading and heating circuits heat meters with ultra sonic sound flow meters with error margins according to EN 1434-1:2007 (2007) (grade 2) are used. For a temperature difference of 3 K and a mass flow rate of 0.1 kg/s, a relative error of ±7% is calculated according to EN 1434-1:2007 (2007). It has to be noted that measured temperature differences have the strongest influence on the error margin and temperature differences of 3 K or less are likely to occur in the condenser water circuit of a heat pump. Electric currents are measured with three phase current meters of grade 1 according to EN 62053-21 (2003) which means that error margins of ±1 % occur. For the calculation of seasonal performance factors overall relative errors of ±8% have to be ex-

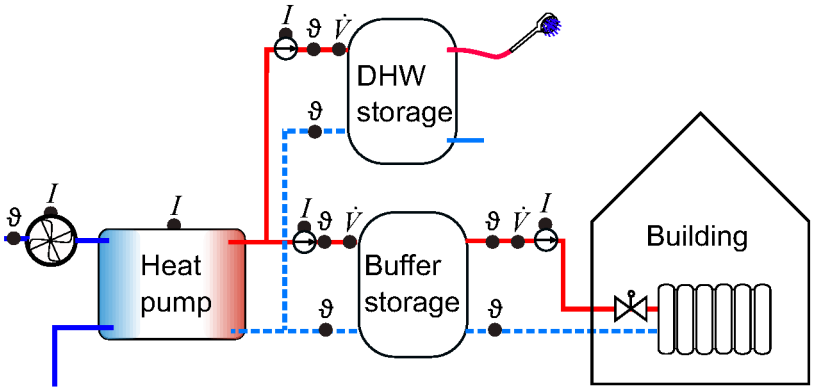


**Figure 3.2:** Scheme of an AWHP system with typical measurement points in the field test.

pected. The heat meters in brine circuits and directly measuring DHW have higher error margins because mechanical flow meters are used.

The field test data are available as time series of measurements of temperatures, volume flows, and electric currents (1 minute time steps). Not all data is available for every time step and every object due to breakdowns of measurement equipment or data transmission. In some cases, measurement points are missing to calculate values within the desired control volume. To allow for the comparability of objects, a small amount of missing data is tolerated and filled up with data calculated by outdoor air temperature-dependent regression functions. Missing data of the outdoor temperature is taken from the German Metrological Service weather station nearest to the field test object. Objects with more than 15% of the 2008 and 2009 data missing are not taken into account (Fütterer, 2010). Finally, 42 objects have a sufficient data basis, whereof 18 are AWHP, 17 are BWHP with vertical, and 7 are BWHP with horizontal ground source heat exchangers.

The typical measurement points of a heat pump system in the field test are shown in figure 3.2 for a sample AWHP system. Each system has a different configuration and partly different measurement points. In most cases, there are no measurement points closer to the distribution system than the ones shown in the figure. This means that no conclusions can be drawn about the exact heat distribution and user behavior. The exact positioning of sensors is not known.

The coverage of measurement differs between field test objects, as also system arrangements differ in the field test. Thus, not every balance or examination can be accomplished for all field test objects. For this reason, analyses in this chapter contain different numbers of objects (in figures, the number of objects is indicated by the value $n$).

Within this work the data processing was done using the software MATLAB®[3]. The basic structure of data handling was developed in a diploma thesis and is described in Fütterer (2010). Curve

[3] See MATLAB (2014)

fittings, which are mostly applied to fill up missing data are done using linear or nonlinear least squares with the trust region method.

The measurement data series of electric power and heat flow show a certain delay to each other which might be due to the sampling interval and reaction time of different measurement equipment as well as data processing. When the time series of electrical power assumes a positive value this shows a start-up of the heat pump. The same applies for the volume flow rate in the condenser circuit. In figure 3.3 these time instants are compared to each other for the time of one day. The delay is not constant over time.

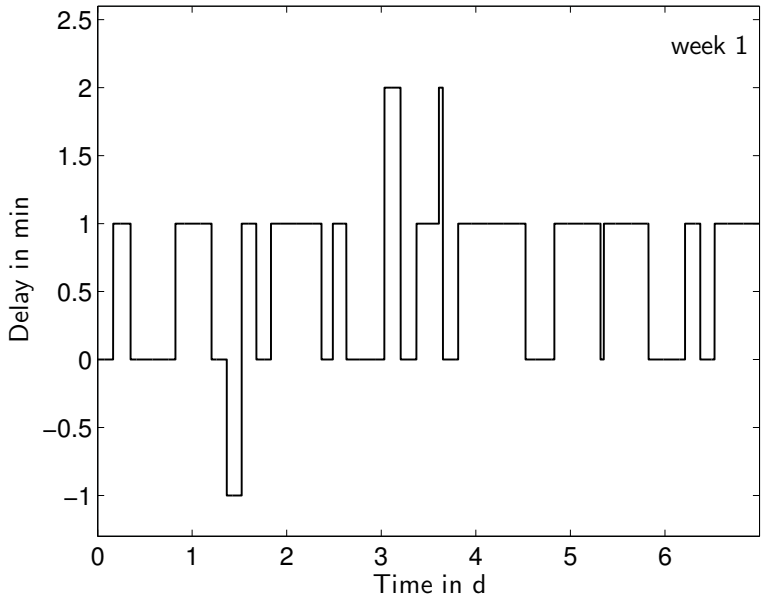


**Figure 3.3:** Measurement data, object 6: Delay of electrical power start-up and volume flow rate start-up at the beginning of an operating interval. "week 1" refers to the reference weeks (see section 4.2).

### 3.1.4 Heat pumps and heating systems

The heat pumps used in the evaluated field test objects are electrically driven compression heat pumps with standard refrigerants, such as R407C (29 objects), R404A (6 objects), R410A (4 objects) and R134A (2 objects). They are not speed controlled. The heat pumps either operate at full load or are off (on/off-controlled). This is why most of the heating systems are equipped with a buffer storage to reduce the number of operation cycles. The heating supply temperature is generally controlled depending on the outdoor air temperature.

Of the 42 analyzed objects, 26 are equipped with radiators, 6 with floor heating systems and 10 have both heating systems. In the latter case, it is not known how the two distribution systems are

connected (serially or in parallel). Usual nominal heating supply temperatures for floor heating systems are 40 °C, for radiator heating systems 55 °C[4]. DHW flow temperatures are in a range of 45 °C to 60 °C in the field test. The fraction of heat used for DHW generation related to the overall heat used is between 5 and 15% for most field test objects. Only four buildings with low specific heating demands have values between 20 and 40%. In buildings with low heating demands the percentage used for DHW generation is higher. This generally leads to a lower overall heat pump efficiency because of a higher mean temperature lift.

## 3.2 Seasonal performance factors

### 3.2.1 Determination of SPF

The determination of performance factors requires the determination of the electric and thermal energies in the respective control volumes. For each object a different amount of data at different times of the year is missing. But a comparability of the field test objects has to be ensured. Therefore, as mentioned above, the missing data is replaced by regression functions. Regressions are done for the daily values of thermal energy output of the heat pump $Q_\mathrm{d}$ and the daily values of electric energy consumption of the heat pump $W_\mathrm{el,d}$ depending on the daily mean outdoor air temperature. The daily thermal energy output consists of the thermal output for heating and for domestic hot water generation:

$$Q_\mathrm{d} = Q_\mathrm{d,H} + Q_\mathrm{d,DHW} \tag{3.1}$$

Depending on the considered control volume, the thermal energy for heating can be measured in the loading cycle (LC) or the heating cycle (HC) of the heat pump system. Usually, the LC connects the heat pump condenser and a storage, the HC connects the storage and the heating system of the building. If the system has no buffer storage, the HC is directly connected to the condenser of the heat pump.

The aforementioned quantities are fitted to a sigmoid function according to BGW (2006):

$$E_\mathrm{d} = \frac{c_1}{1 + \frac{c_2}{(\bar{\vartheta}_\mathrm{out,d} - \vartheta_0)_3^c}} + c_4 \tag{3.2}$$

Here, $E_\mathrm{d}$ stands for the daily energy which is thermal or electrical energy depending on the quantity fitted. $c_1$ to $c_4$ are fitted constants. $\vartheta_0$ is a parameter set to 40 °C (BGW, 2006).

Deviation of data occurs because of the non-outdoor air temperature dependent influences such as other weather influences (wind, solar radiation), user influences such as inner gains, ventilation or controller settings and transient effects (history of above influences).

[4] The nominal outdoor air tempreature usually is -16 °C to -12 °C in Germany.

The data of each field test object is manually revised. Non-typical data is deleted. For example, relatively low values of heating energy on days with low outdoor air temperatures is not used for regression. The data is plausible (e.g. the house is not used and the heating is therefore turned off) and used for overall evaluation. However, the regression is supposed to be calculated for a typical day of the according mean outdoor air temperature.

Figure 3.4 shows the data of thermal energy in control volume 2 for object 30. The regression fits the original data set very well. Figure 3.5 shows the same kind of data for object 33. Here, a data processing as described above is necessary (see right side of figure). This approach is also used for the electric energy.

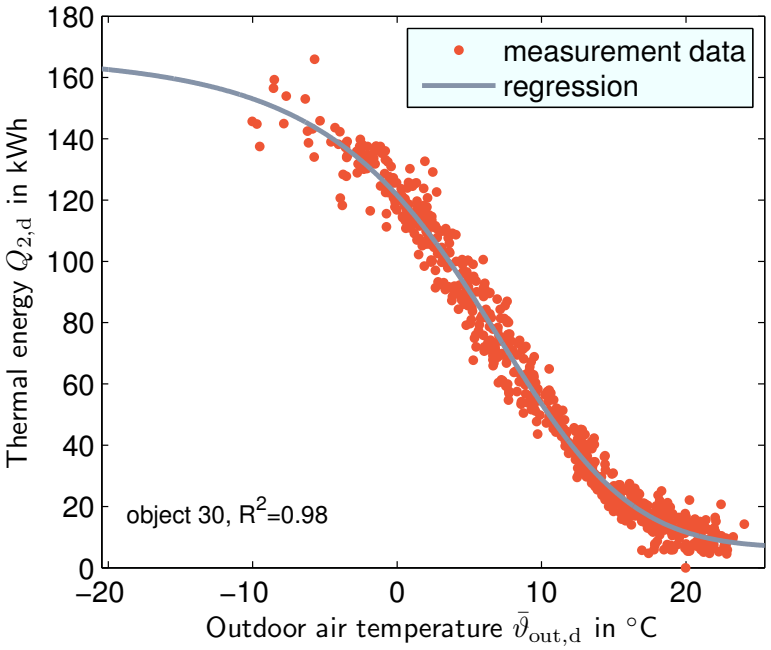


**Figure 3.4:** Daily thermal energy and daily mean outdoor air temperature dependent regression according to equation 3.2 for object 30.

The mean $SPF_1$ for all AWHP is 2.28, for all BWHP 2.90. The $SPF_2$ values are 2.51 respectively 3.19. Figure 3.6 on page 36 shows that both groups achieve a wide range of $SPF_1$ (AWHP: 1.77 to 2.87, BWHP: 1.94 to 3.95). And the same applies to the $SPF_2$ (AWHP: 1.63 to 3.45, BWHP: 2.15 to 3.95).

A comparison of the SPF according to the two control volumes in figure 3.7 on page 36 shows no constant offset between them. Whereas the difference for certain objects is up to 0.8, both SPF of object 2 are equal (value 3.95). This object does not include a storage. Four heat pump systems have solar thermal collectors (three BWHP, one AWHP). Three of them achieve SPF below the mean value. This is a common effect, as solar heat replaces thermal energy. This particularly takes place in transition seasons when boundary conditions are advantageous for heat pump operation, too.

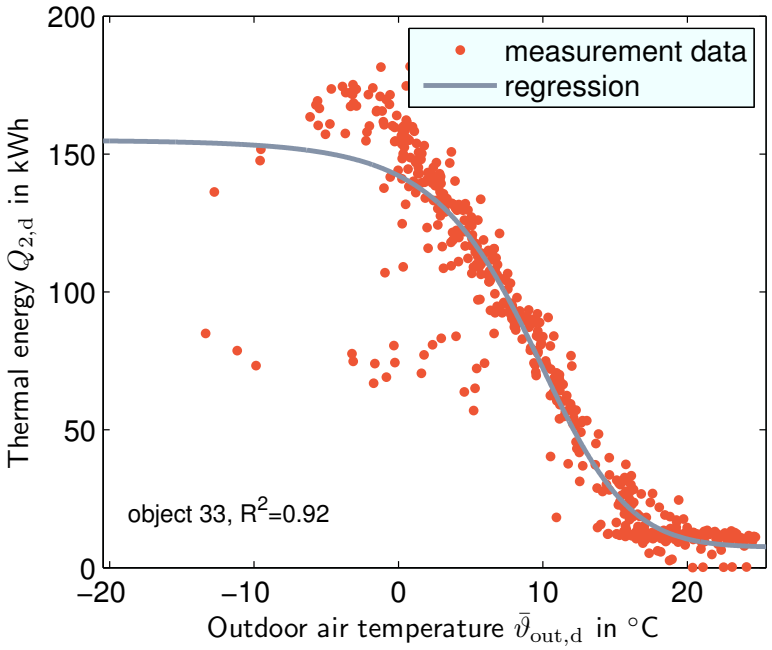


(a) Regression with all data

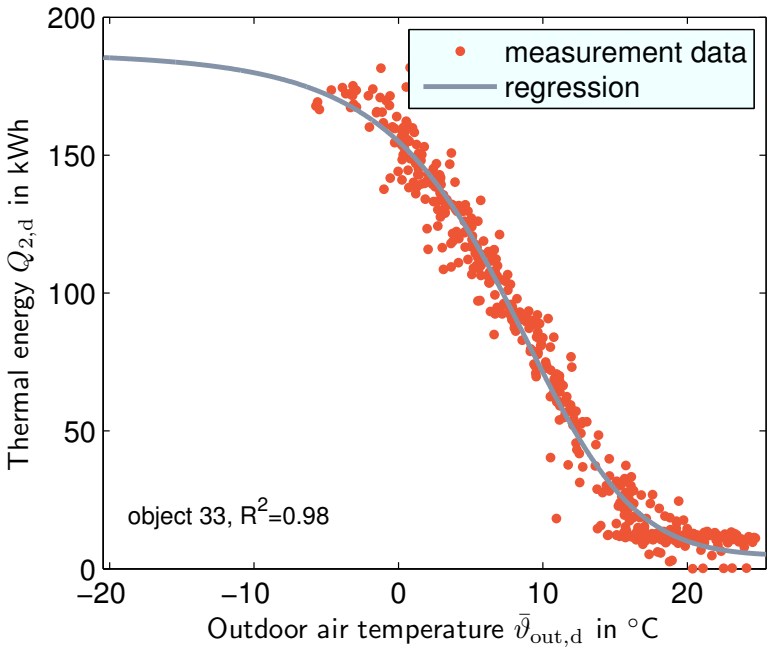


(b) Regression with revised data set

**Figure 3.5:** Daily thermal energy and daily mean outdoor air temperature dependent regression according to equation 3.2 for object 33.

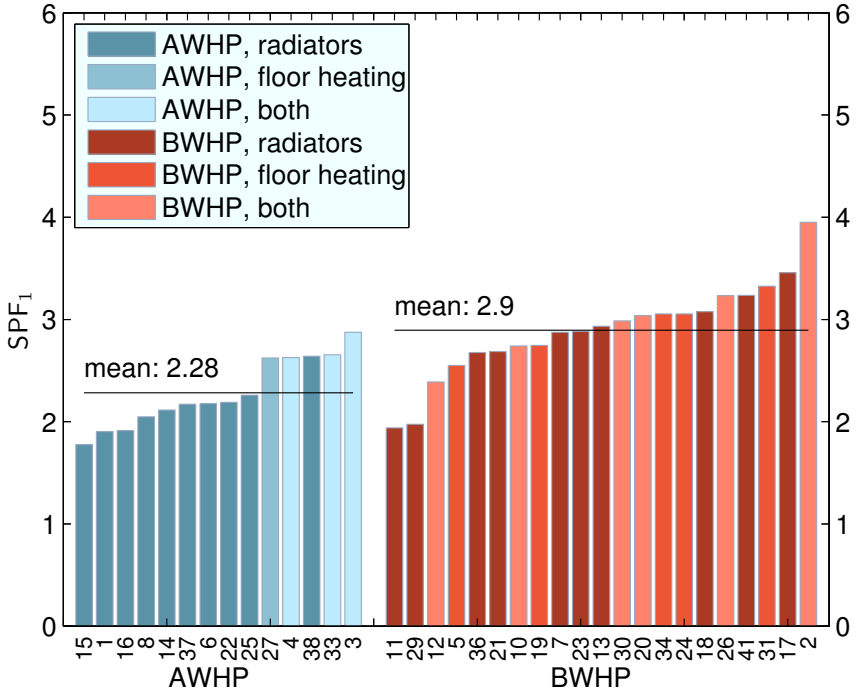


**Figure 3.6:** Seasonal performance factors in the control volume 1 of evaluated field test objects, years 2008 and 2009. AWHP (left) and BWHP (right).

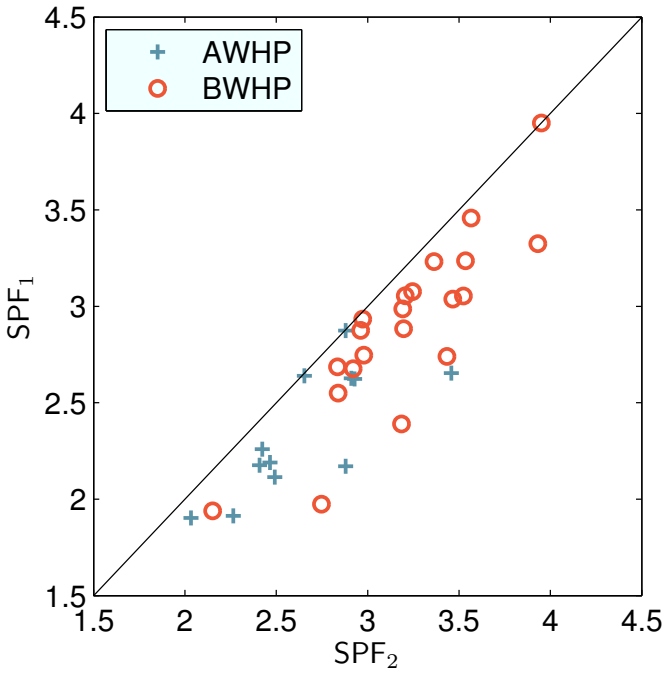


**Figure 3.7:** Comparison of SPF calculated according to control volume 1 and 2, years 2008 and 2009.

### 3.2.2 Classification of heat pump heating systems

The major parameters influencing the performance of heat pump systems are determined by classifying the objects. Conclusion have to be drawn from this carefully as cross correlations occur. For example, all systems without buffer or combined storages are BWHP systems.

Tables 3.1 and 3.2 show the mean $SPF_1$ and $SPF_2$ for groups of field test objects classified according to heat source and heat emitting type. The tables also show the number of objects and the standard deviation of the SPF in each group.

**Table 3.1:** $SPF_1$ for field test objects grouped according to heat source and heat sink type. In brackets: number of systems, standard deviation. The group "Both" contains heat emission with radiators as well as floor heating.

| $SPF_1$ | Radiators | Floor heating | Both | All systems |
|---|---|---|---|---|
| AWHP | 2.12 (10, 0.24) | 2.62 (1, 0.00) | 2.72 (3, 0.14) | 2.28 (14, 0.34) |
| BWHP | 2.77 (10, 0.49) | 2.95 (5, 0.30) | 3.06 (6, 0.53) | 2.90 (21, 0.46) |
| BWHP, hor. GSHX | 3.00 (5, 0.29) | 3.05 (1, 0.00) | 3.04 (1, 0.00) | 3.02 (7, 0.24) |
| BWHP, ver. GSHX | 2.54 (5, 0.57) | 2.92 (4, 0.34) | 3.06 (5, 0.59) | 2.84 (14, 0.54) |
| All heat sources | 2.45 (20, 0.50) | 2.89 (6, 0.30) | 2.94 (9,0.45) | 2.65 (35, 0.51) |

**Table 3.2:** $SPF_2$ for field test objects grouped according to heat source and heat sink type. In brackets: number of systems, standard deviation. The group "Both" contains heat emission with radiators as well as floor heating.

| $SPF_2$ | Radiators | Floor heating | Both | All systems |
|---|---|---|---|---|
| AWHP | 2.32 (11, 0.36) | 2.93 (1, 0.00) | 3.08 (3, 0.33) | 2.51 (15, 0.47) |
| BWHP | 3.03 (11, 0.40) | 3.30 (5, 0.44) | 3.36 (7, 0.32) | 3.19 (23, 0.40) |
| BWHP, hor. GSHX | 3.13 (5, 0.27) | 3.52 (1, 0.00) | 3.47 (1, 0.00) | 3.24 (7, 0.29) |
| BWHP, ver. GSHX | 2.95 (6, 0.49) | 3.24 (4, 0.49) | 3.34 (6, 0.34) | 3.17 (16, 0.44) |
| All heat sources | 2.68 (22, 0.52) | 3.23 (6, 0.42) | 3.28 (10, 0.33) | 2.92 (38, 0.54) |

Generally, the BWHP are more efficient which can be explained with higher source temperatures in the main heating season. Floor heating systems are generally operated with lower supply temperatures than radiator heating systems which leads to higher efficiency of the heat pump. Systems with both heat emission types reach SPF values on the same level as systems with floor heating. This allows the conclusion that low supply temperatures are used within these systems. Nevertheless, because of the number of objects in each group and the standard deviation a more detailed evaluation of the heat pump efficiency is required. An analysis of quality grades of the heat pump types is done in section 3.3.5.

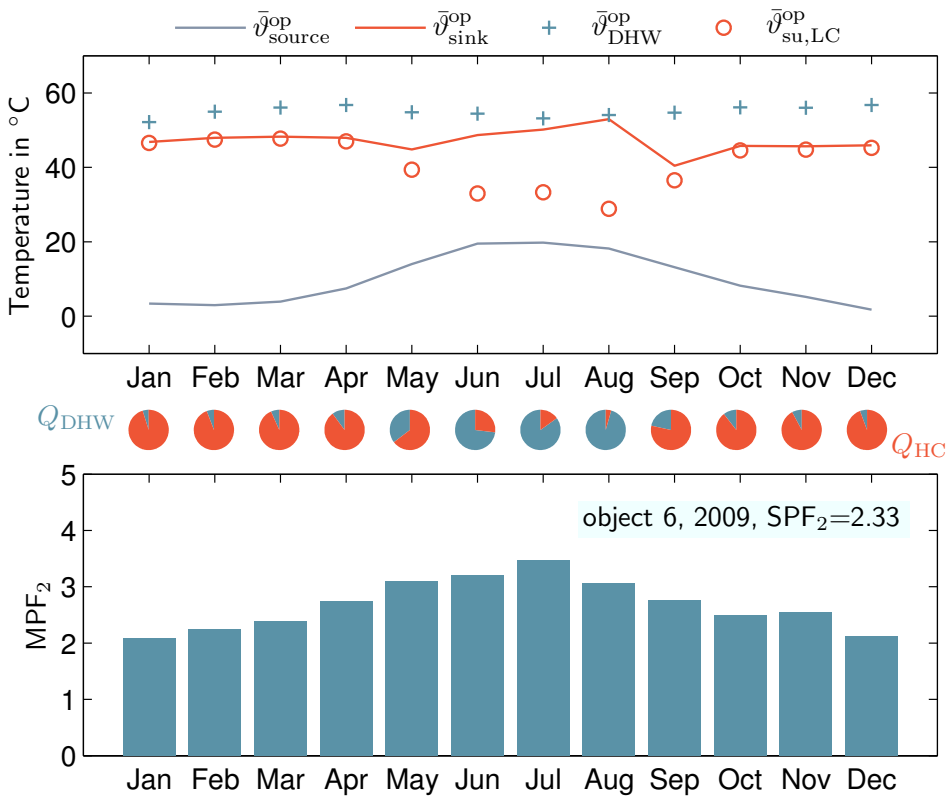


**Figure 3.8:** Monthly temperature lift and performance factor of object 6 (AWHP), field test results for 2009, control volume 2.

## 3.3 The temperature lift

Figure 3.8 shows the monthly average of the operation temperatures in the loading circuits for heating and DHW, as well as the average of these two temperatures which is weighted according to the particular heat consumption (indicated in pie charts). In this case the source temperature of the heat pump is the outdoor air temperature. Thus, the mean temperature lift for each month is shown in the upper chart. The monthly performance factors are influenced by the temperature lift. This becomes even more obvious with the characteristics of a BWHP object in figure 3.9. The strong impact of the temperature lift on the heat pump performance is shown as well as its yearly deviation and the influence of DHW generation.

### 3.3.1 Main outdoor temperature of heating

A main outdoor temperature of heating $\vartheta^{main,heating}_{out}$ is defined as the outdoor air temperature at which the highest amount of heating energy is delivered to a heated zone. For the years of 2008 to 2009 it is calculated for the field test data set as follows: A frequency distribution of $\bar{\vartheta}_{out,d}$ values is generated which can be plotted to a histogram as shown in figure 3.10.

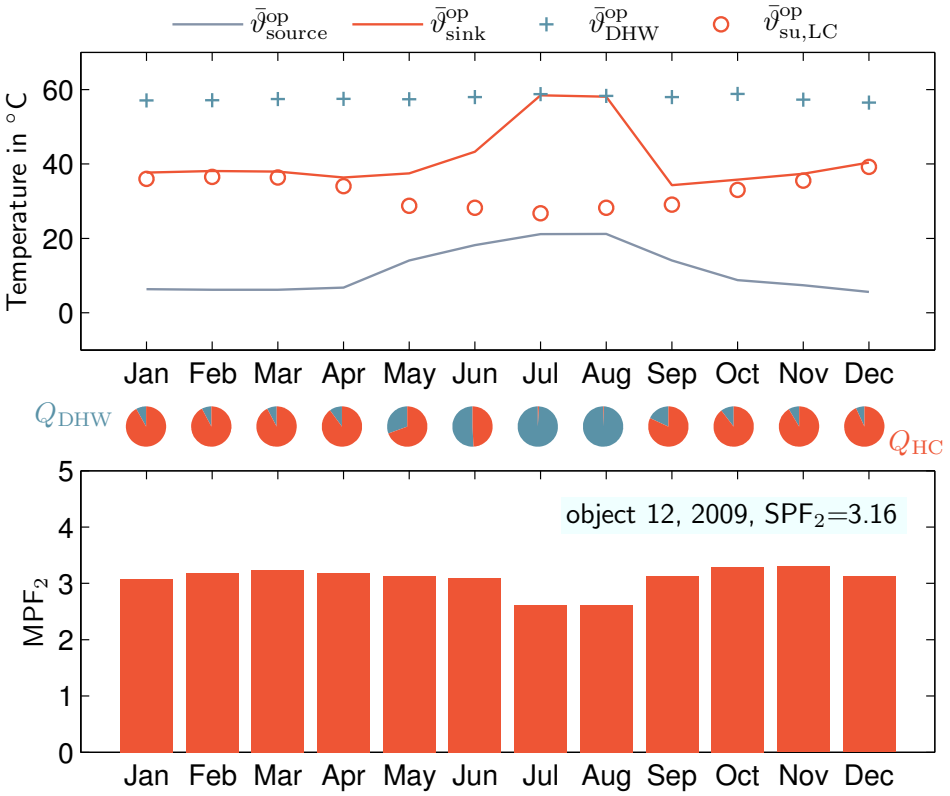


**Figure 3.9:** Monthly temperature lift and performance factor of object 12 (BWHP), field test results for 2009, control volume 2..

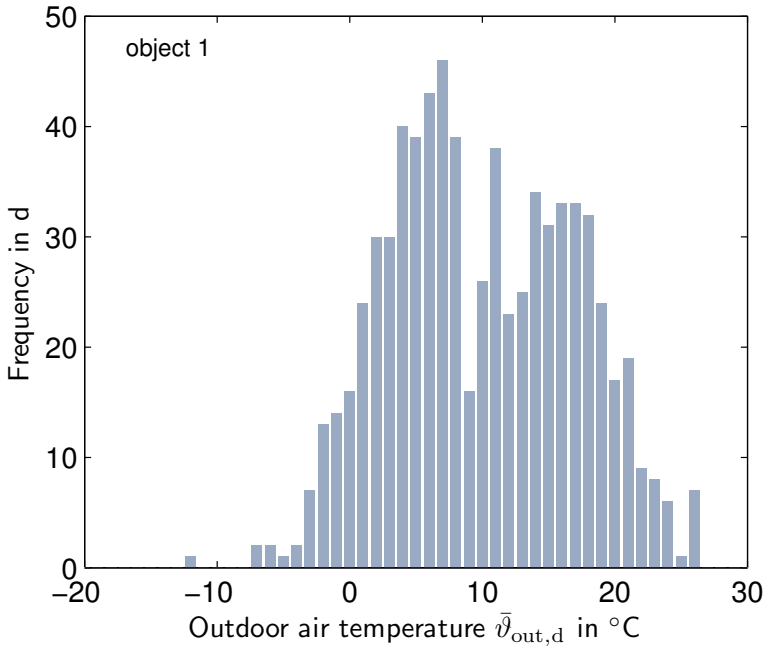


**Figure 3.10:** Histogram of mean outdoor air temperature of field test object 1 (years 2008 and 2009).

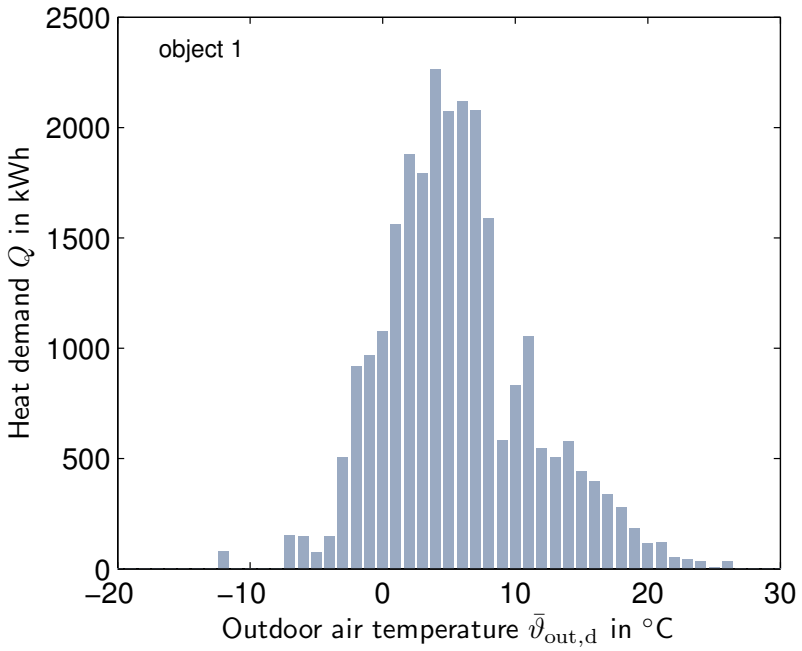


**Figure 3.11:** Histogram of the heating energy demand of field test object 1 (years 2008 and 2009).

From the correlation of daily heating energy and daily mean outdoor temperature[5] the histogram in figure 3.10 can be transformed into the one in figure 3.11. The maximum value in this example is at $\bar{\vartheta}_{\mathrm{out,d}} = 4°\mathrm{C}$, which is the main outdoor air temperature of heating for object 1. For all field test objects $\bar{\vartheta}_{\mathrm{out,d}}^{\mathrm{heating,main}}$ have values between -2 and 12 °C, whereas 2 °C is the most common, see figure 3.12. This verifies the common use of an air temperature of 2 °C as the nominal operating condition in Germany for AWHP (Burger and Rogatty, 2003).

### 3.3.2 Main source temperature, heating operation

For AWHP the source temperature is the outdoor air temperature. For heat pump heating operation, not the daily mean outdoor air temperature $\bar{\vartheta}_{\mathrm{out,d}}$, but the outdoor air temperature at heating operation determines the efficiency of the working fluid cycle. Therefore, the daily mean outdoor air temperature at heating operation $\bar{\vartheta}_{\mathrm{out,d}}^{\mathrm{heating}}$ is calculated. It is the daily mean value of measured outdoor air temperatures at times that the heat pump electric power is positive and when no DHW generation is active. Figure 3.13 shows that the two temperatures differ particularly at high outdoor air temperatures, when the operation time is short compared to the time of one day. It makes sense that heating operation occurs in colder times of the day. Hence $\bar{\vartheta}_{\mathrm{out,d}}^{\mathrm{heating}}$ tends to be lower than $\bar{\vartheta}_{\mathrm{out,d}}$. At main outdoor air temperatures of heating operation $\bar{\vartheta}_{\mathrm{out,d}}^{\mathrm{heating}}$ generally equals $\bar{\vartheta}_{\mathrm{out,d}}$.

For BWHP, the brine flow temperature is the source temperature. The brine temperature changes

[5] See section 3.2.

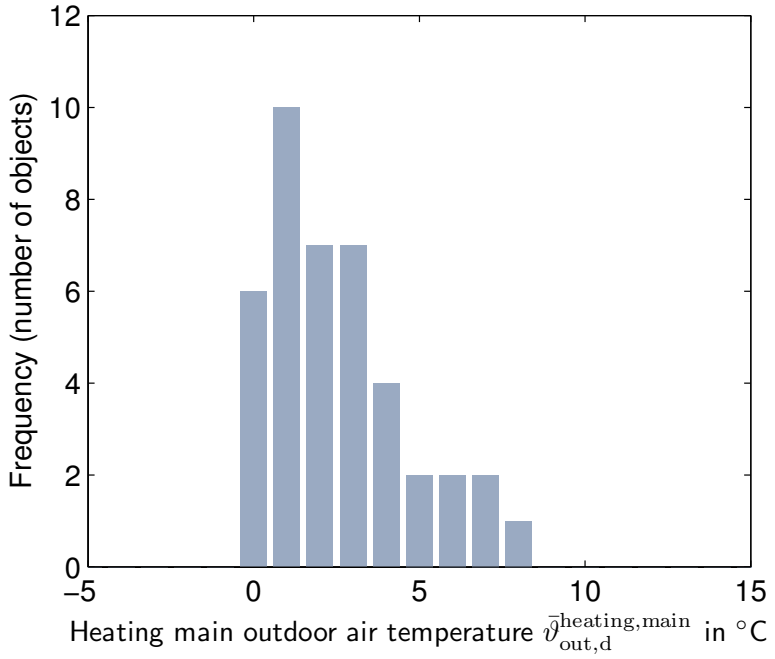


**Figure 3.12:** Frequency of the main outdoor air temperature of heating for all field test objects (years 2008 and 2009).

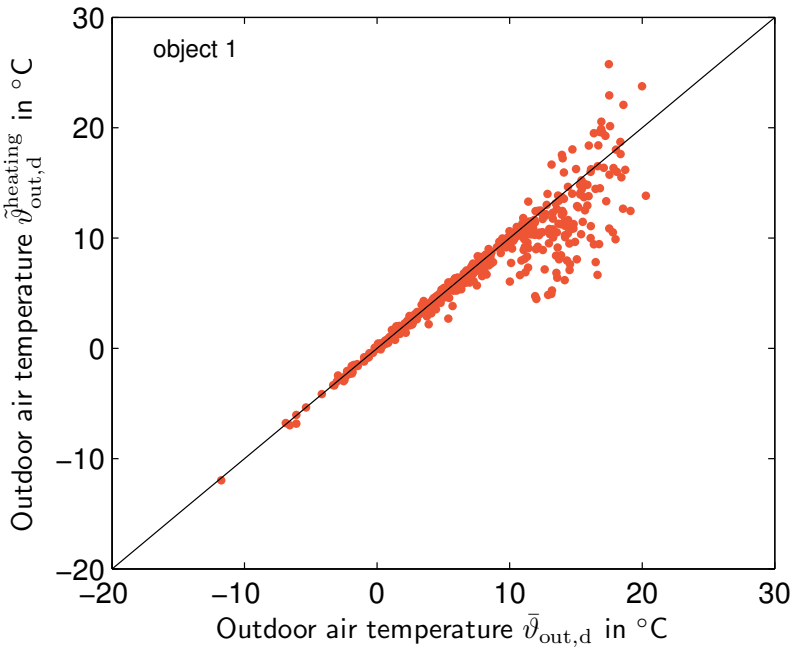


**Figure 3.13:** Comparison of main daily outdoor air temperature and main daily outdoor air temperature in heating operation for field test object 1 (years 2008 and 2009).

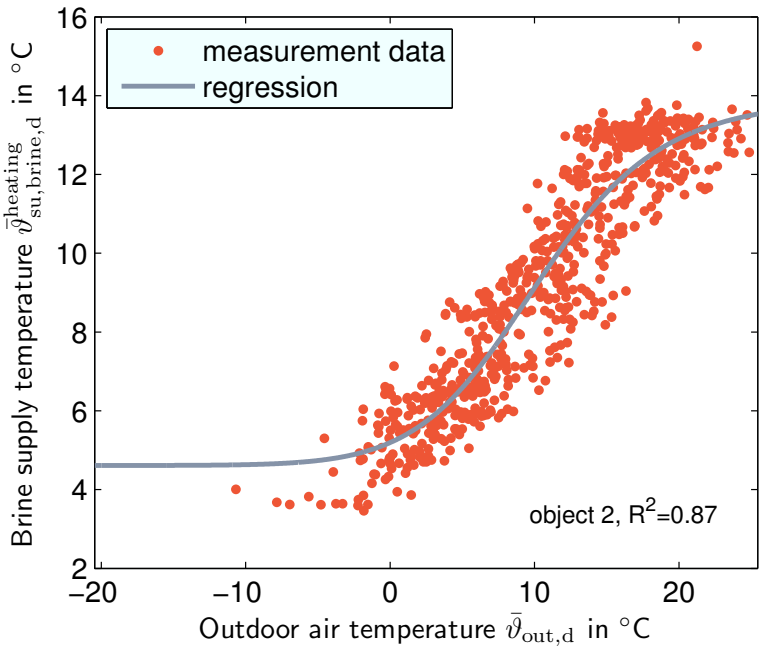


**Figure 3.14:** Daily mean of brine supply temperature in heating operation for field test object 2 (years 2008 and 2009), fit according to equation 3.3.

according to the direct outdoor air temperature influence and particularly according to the thermal heat which is extracted from the borehole. The latter again depends on the outdoor air temperature as has been stated in section 3.2. Given the inertia of the borehole, the daily mean of the brine supply temperature at heat pump operation $\bar{\vartheta}^{\text{heating}}_{\text{brine,su,d}}$ can be correlated to the daily mean of the outdoor air temperature $\bar{\vartheta}_{\text{out,d}}$. A typical correlation is shown in figure 3.14. It shows that with lower outdoor air temperatures the brine supply temperature decreases to a certain point (here it is around 0 °C) below that it stays on a constant level. An arc tangent function can describe this type of correlation and is used as regression function to fill in missing data:

$$\bar{\vartheta}^{\text{heating,main}}_{\text{brine,su,d}} = c_1 \cdot \arctan c_2 \cdot \bar{\theta}_{\text{out,d}} + c_3 + c_4 \tag{3.3}$$

With the correlations for AWHP and BWHP the main source temperatures $\bar{\vartheta}_{\text{source,main}}$ can be determined using the main outdoor air temperature of heating. For AWHP the two temperatures are the same, for BWHP the main outdoor air temperature of heating is used in equation 3.3. The main source temperatures of the field test objects are shown in figure 3.15. Its mean value is 2.1 °C respectively 4.5 °C for AWHP and BWHP.

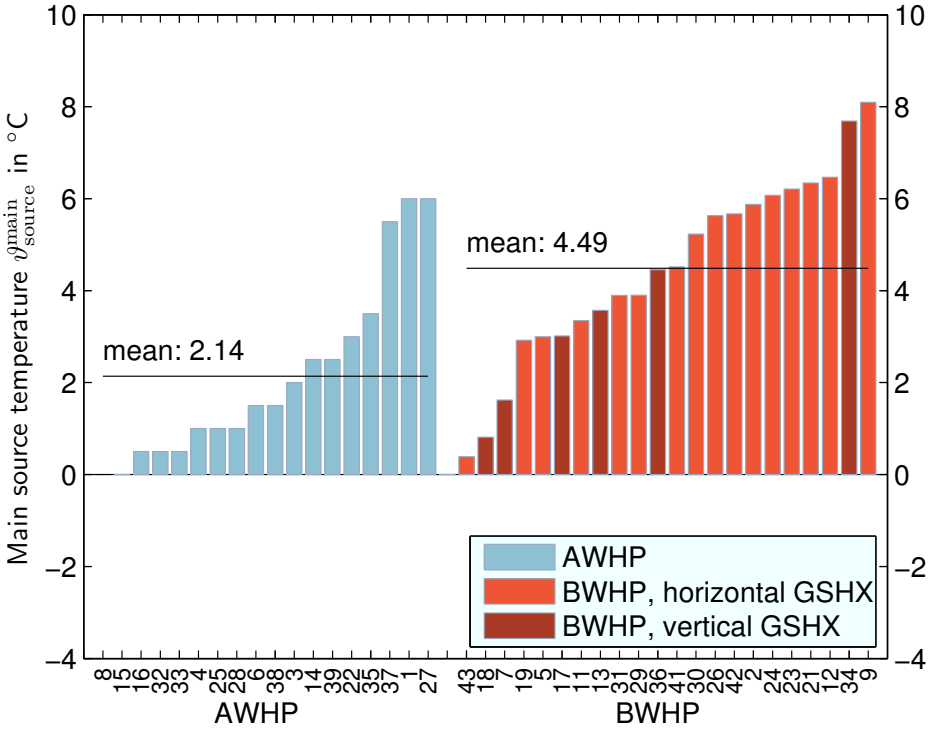


**Figure 3.15:** Main source temperatures in the field test.

### 3.3.3 Main heating supply temperature

A heating curve[6] usually describes a supply temperature control strategy that determines the supply set temperature of a heat generator according to the outdoor air temperature as a feed-forward control.

In the field test, outdoor air temperature dependent control of heating temperature can be detected. It is not known and one cannot determine from the data which kind of control is used (supply or return temperature). A linear function therefore fits the supply temperature to the outdoor air temperature. This is shown in figure 3.16 on page 44 for the example of object 12.

The main heating supply temperature $\vartheta_{su}^{heating,main}$ is determined by the linear heating curve value at the main source temperature in heating operation. Figure 3.17 on page 44 shows the respective values for the loading circuit. The mean values for the three groups "floor heating", "radiator and floor heating" and "radiator" increase in this order. However, in all groups there is a wide range of supply temperatures which makes a grouping according to the distribution questionable.

[6] See section 2.4.3.

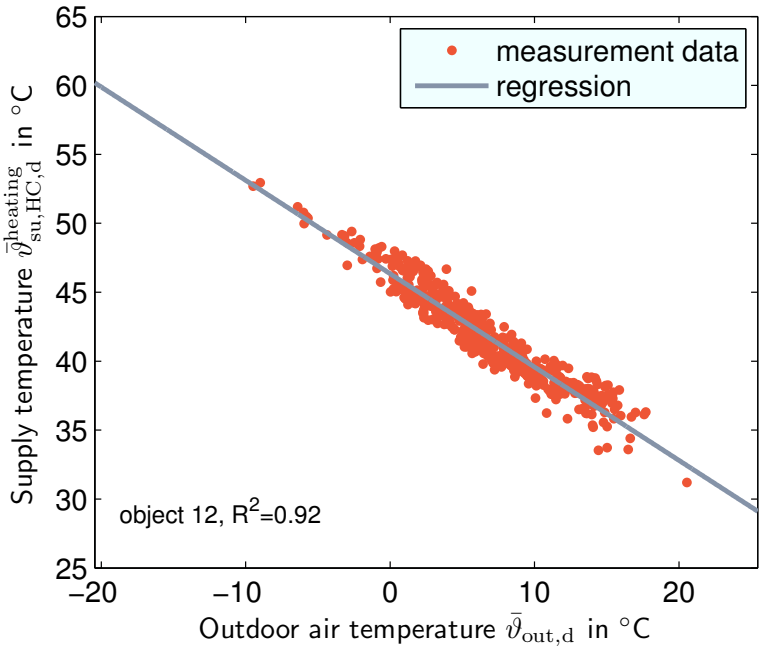


**Figure 3.16:** Daily mean supply temperatures of object 12, linearly fitted with the outdoor air temperature (linear heating curve).

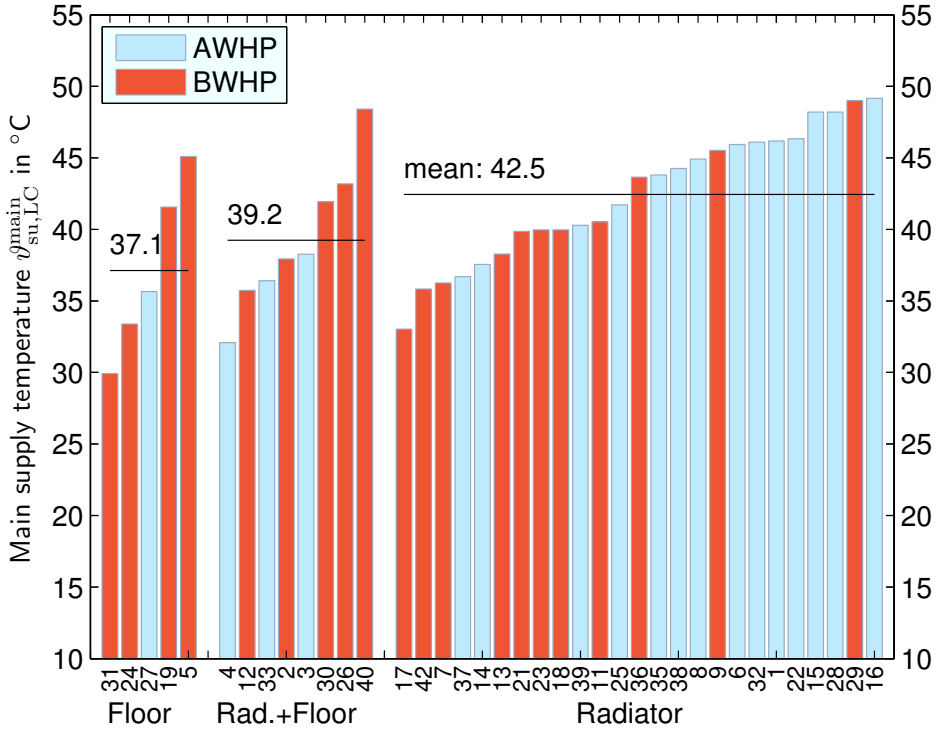


**Figure 3.17:** Main supply temperatures in the loading circuit (LC) in the field test.

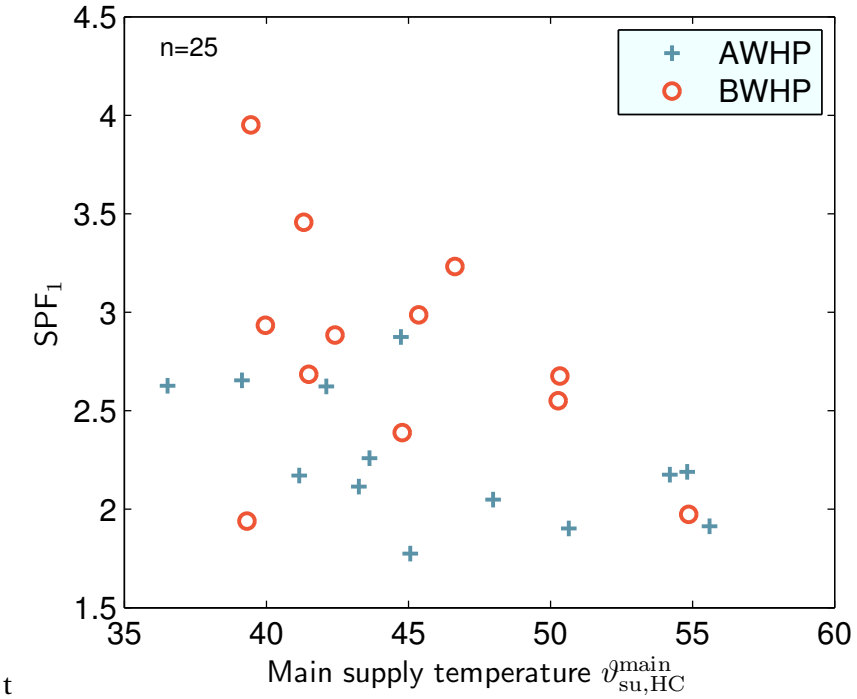


t

**Figure 3.18:** $SPF_1$ and main supply temperature in the heating circuit (HC).

### 3.3.4 Temperature lift and heat pump efficiency

Given the dependency of the COP on the temperature lift, the supply temperature is the main influence on the efficiency of heat pumps presuming a given source temperature.

A clear dependency of the SPF on the heating supply temperature cannot be detected (figure 3.18). Nevertheless, it can be seen from the figure that the supply temperature limits the efficiency. There are obviously additional influences. In this figure it has to be noted that DHW supply temperature and ratio are not taken into account.

The relevant control volume for an evaluation of the influence of the supply temperature on heat pump efficiency is control volume '2', as temperatures are measured directly in the condenser water circuit. The main correlation of the $SPF_2$ with the main supply temperature (according to section 3.3.3) can be described by equations 2.2 and 2.3. This leads to the following regression function:

$$SPF_2 = \frac{\vartheta^{main}_{su,HC} + 273.15\,K}{\vartheta^{main}_{su,HC} - \vartheta^{main}_{source}} \cdot \eta_{C,fit} \tag{3.4}$$

Figure 3.19 (page 46) shows the regression classified for AWHP and BWHP of the field test. The coefficient of determination $R^2$ is 0.47 for the data set of AWHP $\eta_{C,fit,AWHP} = 0.32$ and 0.12 for BWHP

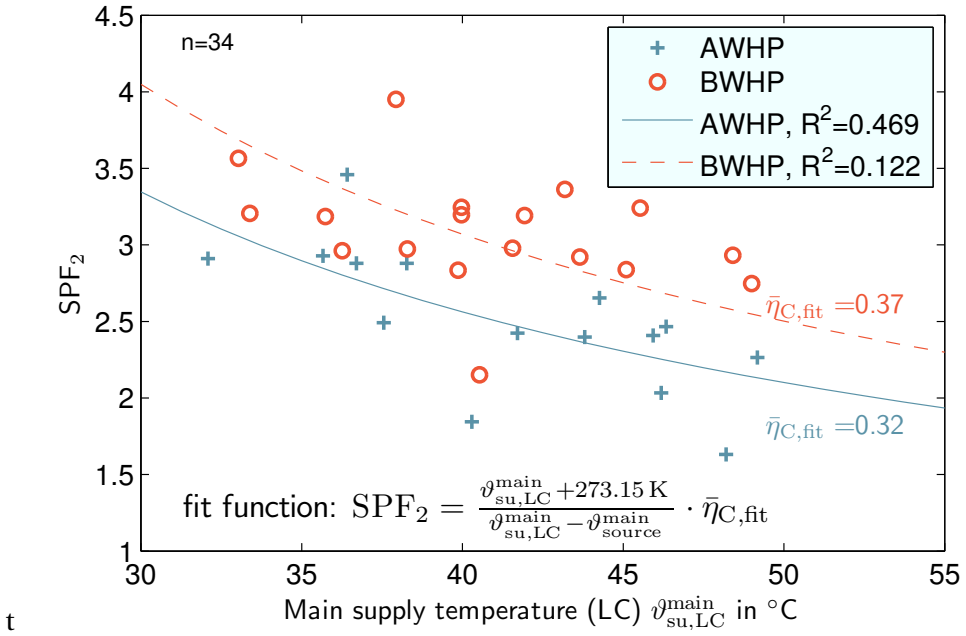


t

**Figure 3.19:** $SPF_2$ depending on main supply temperature in the loading circuit. Coefficient of determination $R^2$ for the given fitting function is given in the legend separately for AWHP and BWHP.

with $\eta_{C,fit,BWHP} = 0.37$. The quality grades achieved in the field test are at the lower boundary of the range defined by Zogg (2009)[7].

Regarding the low coefficient of determination, the evaluation method with mean temperatures described before does not seem appropriate. Instead of this, in the following paragraphs, the characteristic of the quality grade is evaluated at first and more detailed static calculation methods are then applied to the field test data.

### 3.3.5 Quality grades

The quality of a heat pump device is expressed by the quality grade[7]. To evaluate the quality grades of the devices used in the field test, the standard CoP is divided by the $CoP_C$. The latter is calculated according to equation 2.2 with the standard temperatures. The mean quality grade for AWHP is 0.36 in standard conditions and 0.51 for BWHP in standard conditions. The values range from 0.33 to 0.42 for AWHP and 0.49 to 0.57 for BWHP.

The quality grades achieved within the field test within 2008 and 2009 are calculated by :

$$\eta_C = SPF_2 \cdot \frac{\bar{T}_{su,LC} - \bar{T}_{source}}{\bar{T}_{su,LC}} \tag{3.5}$$

[7] See section 2.1.2 for more detail on quality grades.

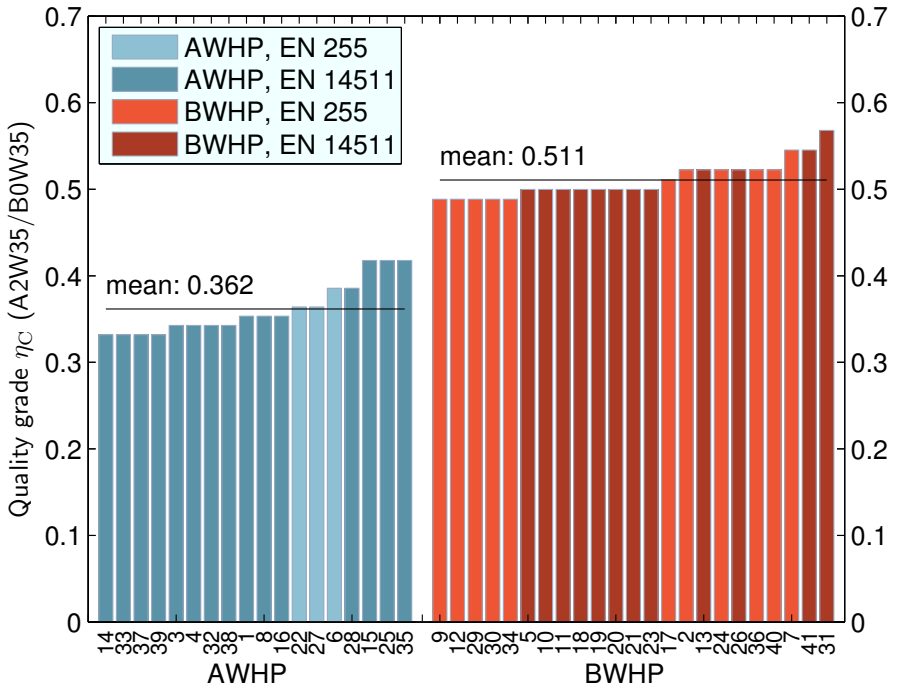


**Figure 3.20:** Quality grades of heat pumps used in the field test. Values are calculated with CoP data from heat pump tests according to EN 14511 (2012) at operating points A2W35 and B0W35 (manufacturer data).

The results show lower values than in standard conditions which are shown in figure 3.20. The quality grades calculated with equation 3.5 are 0.32 for AWHP and 0.37 for BWHP. These values equal the quality grades resulting from the fit of equation 3.4 to measurement data, in spite of the low correlation coefficients shown in figure 3.19. A correlation between the quality grades calculated from measurement data and those computed from CoP data can not be found. Especially the mean value for BWHP shows a big difference to the one in standard conditions.

For each heat pump, a typical characteristic of the quality grade depending on the temperature lift is identified from the manufacturer's data. Quality grades calculated from field test data analogously to equation 3.5 and quality grades calculated with manufacturer's data and the mean daily source and sink temperatures are compared. Qualitatively, the basic temperature dependent characteristic can be modeled this way, but generally, an offset is detected. This can be seen in figure 3.21 (page 48): Two typical characteristics are each compared to the ones calculated with table data using the daily mean temperatures as input data. Whereas for object 6 the calculated data does not fit the measurements well, for object 33 it does.

Possible reasons for the differences are

- the uncertainty of measurements,

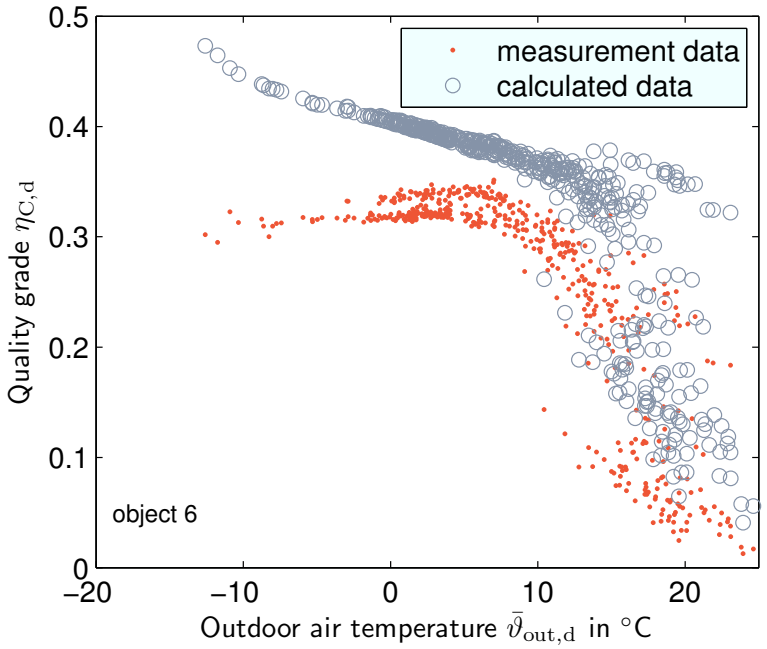


(a) Object 6

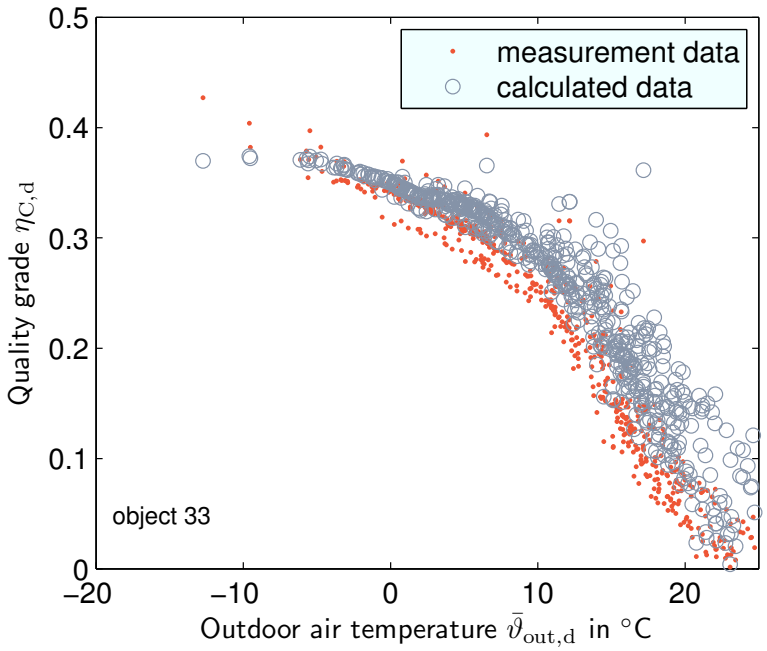


(b) Object 33

**Figure 3.21:** Daily quality grades measured during 2008 to 2009 and calculated with manufacturer's data.

- ▷ heat losses that are not accounted for in the manufacturer's data,
- ▷ auxiliary energy demands that are not accounted for in the manufacturer's data,
- ▷ mass flow rates different from nominal conditions,
- ▷ transient influences shorter than one day (such as on/off control and other control influences, DHW generation) and
- ▷ user interactions.

## 3.4 Static calculation methods

Calculation methods exist that try to include several of the aforementioned influences. As mentioned in section 1.3.3, the guideline VDI 4650-1 (2009) is commonly used in Germany for a rough prediction of a SPF, usually in the design phase. It uses CoP at one (BWHP) or three (AWHP) operating conditions. As expected, the results of this kind of calculation method correlate badly with the field test results. However, a rough ranking of heat pump heating systems is possible (see figure 3.22).

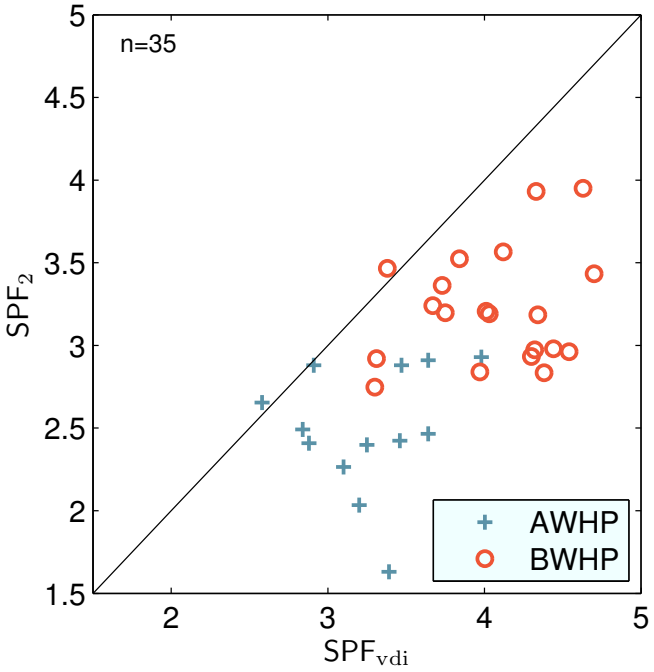


**Figure 3.22:** Comparison of SPF calculated according to control volume 2, years 2008 and 2009 and according to VDI 4650-1 (2009).

Another, more sophisticated calculation method for heat pump annual performance calculation is described in DIN EN 15316 (2008). It calculates the heat pump performance in time steps based on

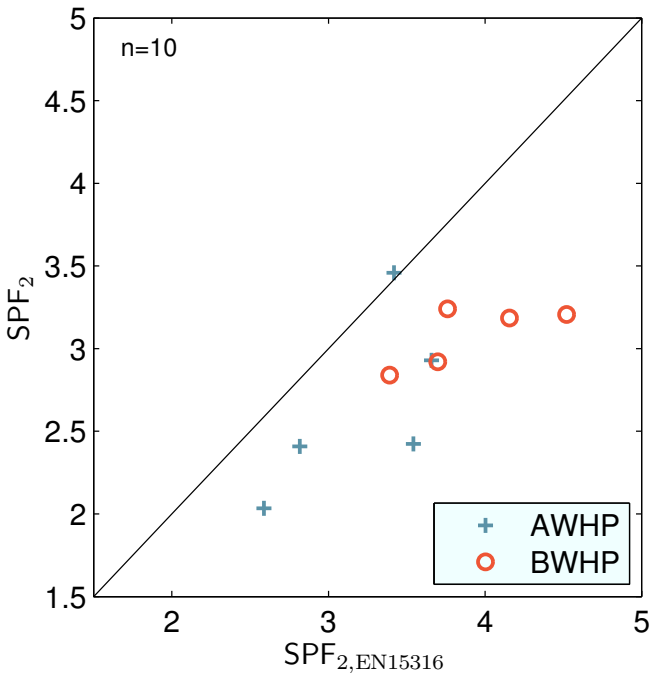


**Figure 3.23:** Comparison of SPF calculated according to control volume 2, years 2008 and 2009 and according to DIN EN 15316 (2008) with temperature input data from the field test.

the time step of the given outdoor air temperature data. CoP values are calculated for all occurring air temperatures in 1 K steps. They are then weighted according to a frequency distribution of air temperatures. For CoP calculation, performance maps of heat pumps can be used. Additionally, DIN EN 15316 (2008) considers the following influences on heat pump performance:

- Back-up heaters in a bivalent operation,
- heat losses of storages and distribution,
- DHW generation,
- auxiliary electric energy demand and
- heating curve control.

Here, the calculation method is executed with input data from the field test: The outdoor air, supply and brine temperature (the latter in the case of BWHP) and the ratio of heat demand for DHW and heating are used as input data. When a comparison to $SPF_2$ is done, heat losses of the storage are not accounted for. Ten field test objects are chosen for this evaluation - the results are displayed in figure 3.23. The according table data is shown in appendix A.

The deviations are too high to be explained by the uncertainty of measurements[8]. Here, too, a number of influences are not taken into account in the calculation. As a result of these analyses,

[8] See section 3.1.3.

the need for even more detailed calculation methods becomes evident. With the given methods, it is not possible to fully understand and evaluate the functioning of heat pump heating systems. An approach for a calculation method including additional effects is developed in chapter 4. However, the field test is further evaluated in order to additionally detect typical operating characteristics of heat pump heating systems.

## 3.5 Operational characteristics

### 3.5.1 On-off cycling

The analyzed field test objects operate with on/off controlled heat pumps. This leads to a discontinuous operating behavior where the number and length of operating cycles depend on various influences.

The main influences are the head load with its level, its dynamics and the thermal mass or inertia of the heating system. The basic characteristic of cycles can be explained by a simplified model of the heating system: In a given AWHP system the heat pump capacity and the heat load are known. A buffer storage represents the main thermal mass in the hydraulic system and is assumed being fully mixed. Furthermore it is assumed that during heat pump operation the whole thermal mass is heated up by a constant temperature difference $\Delta T_{\mathrm{ctrl}}$. One is able to calculate the time $\Delta t_{\mathrm{on}}$ during which the heat pump operates using an energy balance:

$$Q_{\mathrm{HP}} - Q_{\mathrm{BS}} - Q_{\mathrm{hl}} = 0 \tag{3.6}$$

By assuming a linear increase of temperature we can calculate $\Delta t_{\mathrm{on}}$:

$$\Delta t_{\mathrm{on}} = \frac{m_{\mathrm{BS}} \cdot c_{\mathrm{p,W}}}{\dot{Q}_{\mathrm{hp}} - \dot{Q}_{\mathrm{hl}}} \tag{3.7}$$

The same can be done for the time that the water temperature decreases $\Delta t_{\mathrm{off}}$. In this case the energy balance is

$$Q_{\mathrm{BS}} - Q_{\mathrm{hl}} = 0 \tag{3.8}$$

This leads to

$$\Delta t_{\mathrm{off}} = \frac{m_{\mathrm{BS}} \cdot c_{p,\mathrm{W}}}{\dot{Q}_{\mathrm{hl}}} \tag{3.9}$$

The time for one operating period is

$$\Delta t_{\mathrm{per}} = \Delta t_{\mathrm{on}} + \Delta t_{\mathrm{off}}. \tag{3.10}$$

Assuming the AWHP and a building with outdoor air temperature dependent characteristics as shown in figure 2.6 on page 21, it is possible to calculate the daily number of operating cycles and the length of operating cycles both as outdoor air temperature dependent characteristics. This

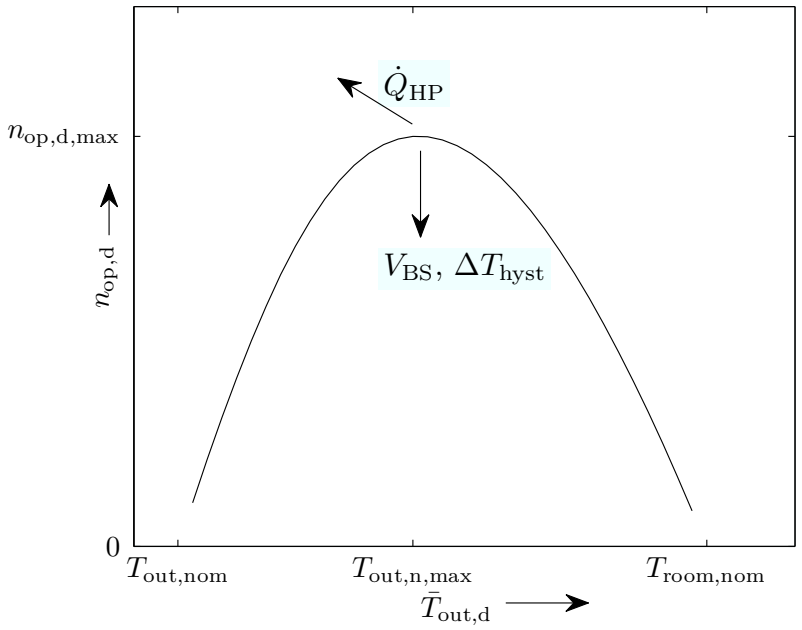


**Figure 3.24:** Qualitative characteristic of number of daily operating cycles $n_{\mathrm{op,d}}$ depending on the mean daily outdoor air temperature $\bar{T}_{\mathrm{out,d}}$. The arrows indicate the shift of the curve's maximum with increased heat pump capacity $\dot{Q}_{\mathrm{HP}}$, buffer storage volume $V_{\mathrm{BS}}$ and control hysteresis $\Delta T_{\mathrm{hyst}}$.

kind of characteristic is shown in figure 3.24. For a given building (with its given heat load characteristic) the influences of increasing heat pump capacity, buffer storage volume and on/off control hysteresis are indicated.

Figure 3.25 shows the daily number of operating cycles $n_{\mathrm{op}}$ depending on the daily mean outdoor air temperature for field test object 3. It was found that a Gaussian curve as shown in figure 3.25 describes the basic dependency of the daily operating cycles on the outdoor air temperature. The correlation used is as follows:

$$n_{\mathrm{op,d}} = c_1 \cdot e^{-((\bar{\vartheta}_{\mathrm{out,d}} - c_2)/c_3)^2} + c_4 \tag{3.11}$$

When the heat pump capacity is lower than the building heat load, theoretically, the heat pump can operate continuously. When the heat pump capacity is higher than the heat load (generally at outdoor air temperatures above the bivalent point) the heat pump operates discontinuously. At high outdoor air temperatures the heat load decreases or attains zero. A small number of operating cycles suffices to deliver the daily heating energy (or only domestic hot water energy). There are clearly other influences on the number of operating cycles than the outdoor air temperature, as there are influences on the heat load other than the outdoor air temperature, too. The dynamic during one day alone is one reason for different numbers of cycles at the same $\bar{\vartheta}_{\mathrm{out,d}}$.

The distribution of the number of daily operating cycles across the outdoor air temperature and the maximum of the curve can be identified. The according outdoor air temperature $\vartheta_{\mathrm{out,n,max}}$

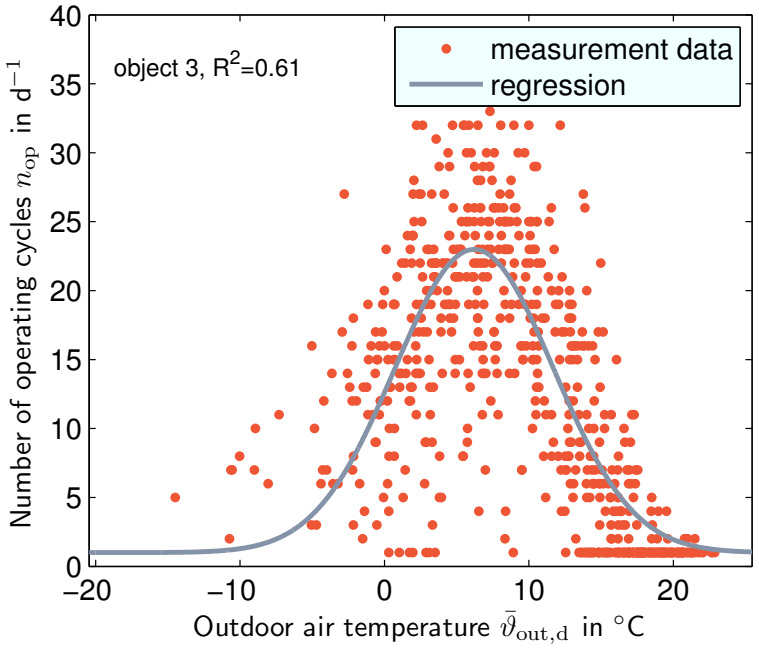


**Figure 3.25:** Daily operating cycles depending on the daily mean outdoor air temperature. Field test data of object 3, years 2008 and 2009.

(it equals $c_3$ in equation 3.11) correlates with the bivalent temperature $\vartheta_{biv}$, as can be seen in figure 3.26 (page 54). This indicates that the characteristic of operating cycles correlates with the dimensioning of the heat pump. The set-off of the curve is given by $c_4$ in equation 3.11 and is close to 1 for most of the objects which indicates that aside from heating operation most heat pumps load a DHW storage once a day.

For the calculation of annual operation cycles missing daily values are replaced by values from the correlation in equation 3.11. The mean total number of operating cycles for AWHP and BWHP are 4370 and 4930. A dependency on the heat distribution system (and its thermal inertia) cannot be observed.

The correlation of operating cycles and the buffer storage volume is studied as well as the one of operating cycles and control hysteresis temperature difference. Both do not correlate well. The two systems with the highest numbers of cycles, however, have no buffer storage.

The aforementioned correlations show high deviations which imply the existence of additional influences on the number of cycles. However, the analysis of operating cycles with respect to additional influences is limited given the available data. These influences are controller settings, layout of the hydraulic system and possible heat input from additional heat generators such as solar collectors. An impact of the number of cycles on efficiency as described in literature (Uhlmann and Bertsch, 2010) cannot be detected with the available data.

The effect of on/off control on the supply temperatures can be seen in figure 3.27, page 54. The

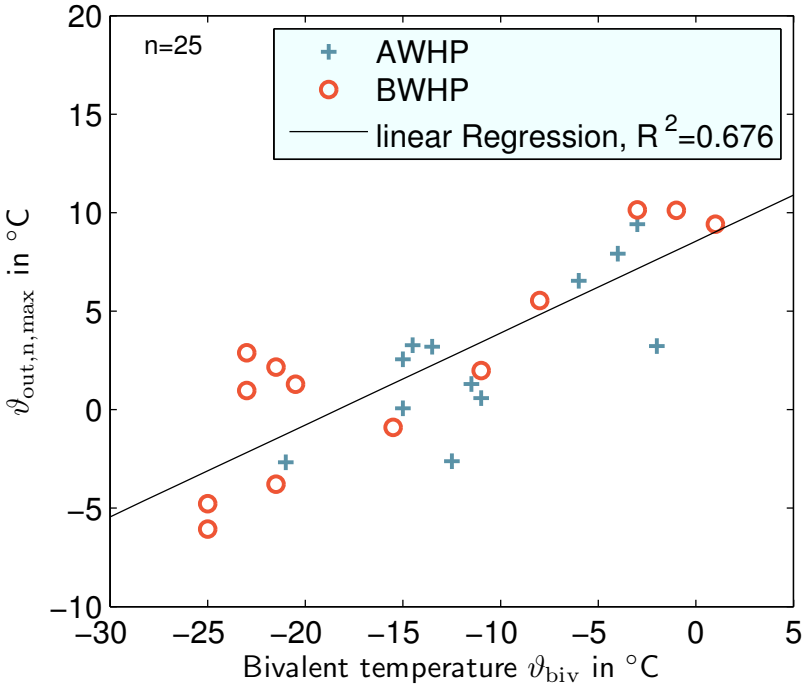


**Figure 3.26:** Bivalent temperature and daily mean outdoor air temperature at maximum number of daily operating cycles $\vartheta_{\mathrm{out,n,max}}$, field test data for 2008 and 2009.

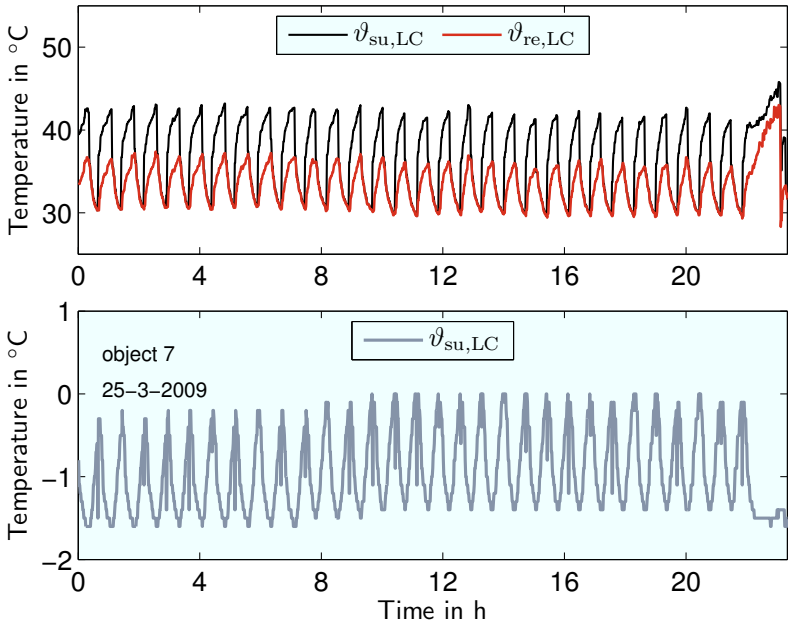


**Figure 3.27:** Supply and return temperatures in the loading cycle (LC), brine supply temperature, object 7, March 25, 2009.

supply temperature in the LC variates strongly with every cycle of the heat pump. The brine temperature variates, too.

### 3.5.2 Auxiliary electric energy

The electric energy consumption of heat pump systems consists of the energy consumed by

- ▷ the heat pump compressor and its control,
- ▷ the drives for supply of the heat source (AWHP: ventilator, BWHP: brine pump),
- ▷ the drives for supply of the heat sink and
- ▷ the electrical back-up heater.

These energies are considered in the static calculation methods described in 3.4 either by being included in the heat pump performance data or they are accounted for by approximate factors.

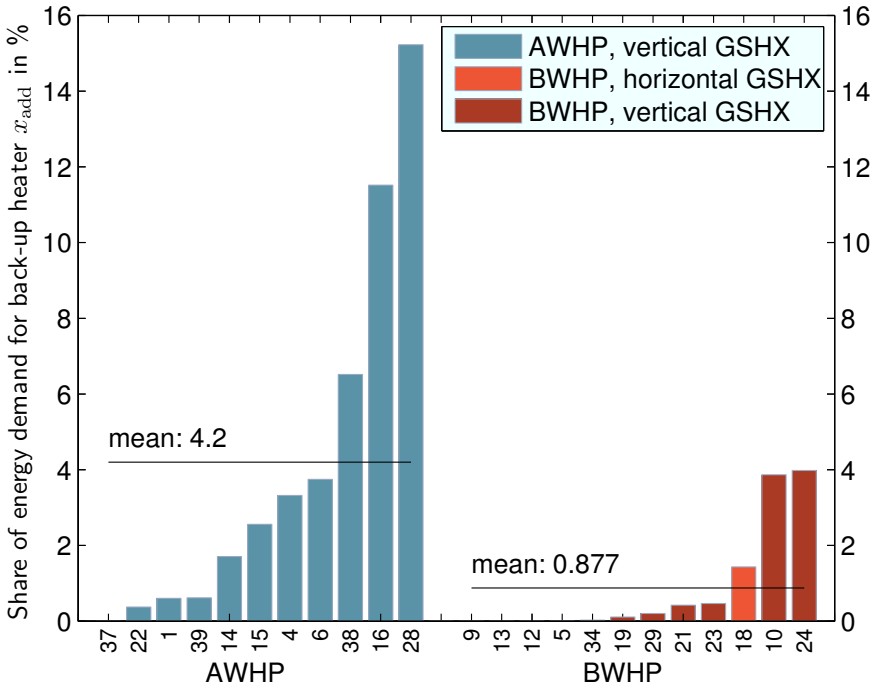


**Figure 3.28:** Field test: Ratio of electric energy demand of additional back-up heater and total electric energy demand $x_{\mathrm{add}}$.

Figures 3.28 and 3.29 show percentages of auxiliary energy (back-up heater and source drives). Both values differ strongly between field test objects. The back-up heater is extensively used in AWHP systems. Two BWHP systems have relatively high ratios which is apparently due to an error in the control as they are operating throughout the whole year. The ratios for source drives is higher

for BWHP on average, but variates strongly for AWHP as well as BWHP. These results show the importance of carefully designed heat pump systems including all components and the control.

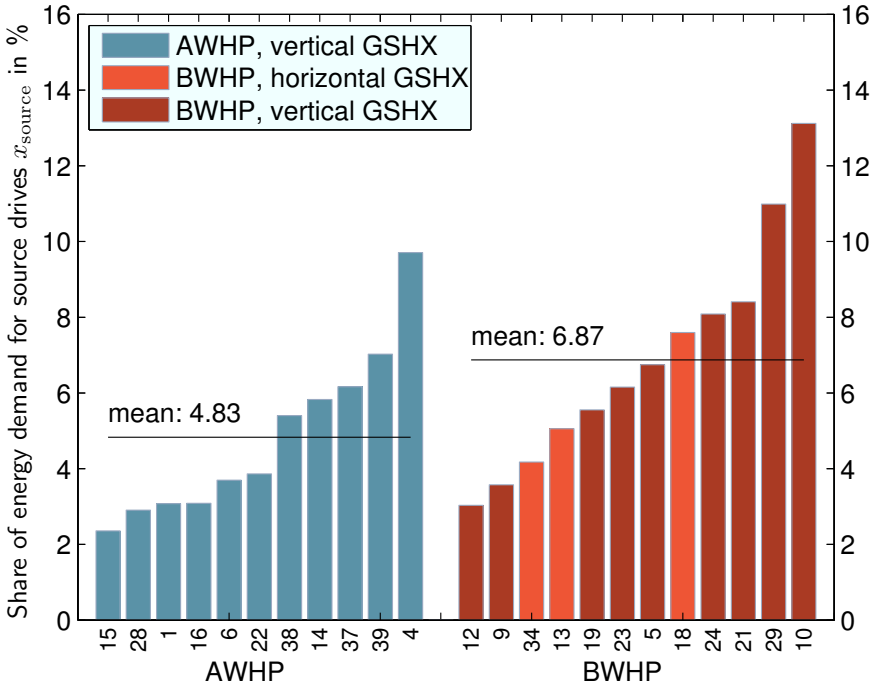


**Figure 3.29:** Field test: Ratio of electric energy demand of source drives (AWHP: ventilator, BWHP: brine pump) and total electric energy demand $x_{source}$.

However, the differences between static calculation methods and measurements cannot solely be explained by different percentages of auxiliary electricity consumption. This has been tested by correcting static calculations with the measured values (however, standard deviation decreases from 0.46 to 0.41 with this correction).

### 3.5.3 Mass flow rates

The mass flow rate of water in the condenser cycle (storage loading cycle or heating cycle directly connected to the heat pump) is important for the efficiency of the heat pump as it determines the temperature spread along the condenser. Pahud and Lachal (2004) present an approximation model for the CoP correction according to the condenser cycle mass flow rate which has been verified by Pärisch et al. (2012)[9]. Figure 3.30 shows the ratio of mean mass flow rates in the condenser cycle to the nominal value. The nominal value refers to the standard operating point of the heat pump. This operating points is chosen according to the standard which is used for heat pump testing.

[9]The model is described in section 4.2.1.

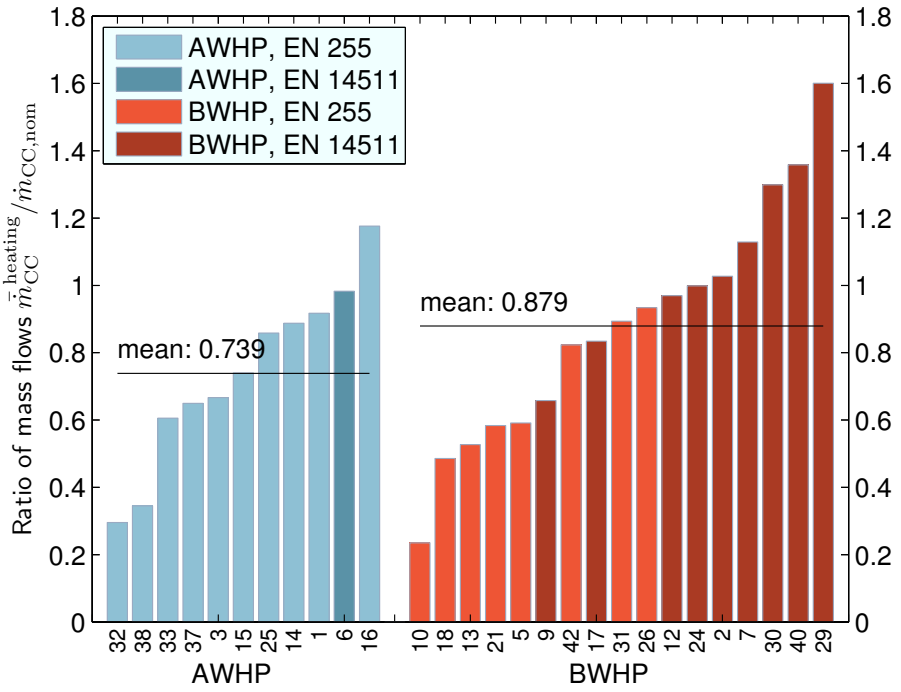


**Figure 3.30:** Field test: Ratio of mean mass flow $\bar{\dot{m}}_{CC}^{heating}$ to nominal mass flow $\dot{m}_{CC,nom}$ in condenser circuit (CC).

The performance maps of heat pumps are usually determined using this mass flow rate. In parts, the measured mass flows in the field test differ strongly from the nominal ones. This may explain differences between calculated and measured values as described in section 3.4. However, an application of the model of Pahud and Lachal (2004) in the static calculation of DIN EN 15316 (2008) does not lead to noticeably better results (the standard deviation decreases from 0.41 to 0.39). Also, a relation of mass flow rates to the residuals of the $SPF_2$ fit in figure 3.19 cannot be found (linear fits have coefficients of determination below 0.3).

Objects without buffer storage or with a serial buffer storage have only one heating circuit which means that the mass flow in the heating circuit equals the one in the condenser circuit of the heat pump. This is the case for object 38, which has a low mass flow rate. Objects 32 and 10, however, do have buffer storages that would allow to increase the condenser cycle (CC) mass flow.

### 3.5.4 System control

As mentioned before, no information is available on the system control concepts or settings. Nevertheless, certain control concepts can be deduced from the measurement data, e.g. an outdoor air temperature dependent control[10].

[10] See section 3.3.3

A night set-back can be detected in 15 of the 42 field test objects. A night set-back is either done by lowering the heating curve or by setting down the mass flow rate of the pump in the heating circuit during nighttime. Start and end times differ from object to object. It generally begins in the late evening (9 to 12 p.m.) and ends in the early morning (4 to 6 p.m.). In 5 objects, the HC pump is turned off or set back during the night while the heat pump is operating to balance the heat losses of the storage. Energy demand could be reduced by turning off the heat pump during nighttime.

## 3.6 Concluding remarks on field test analysis

The analysis of the field test only can give general information on the correlations that influence heat pump efficiency. Not enough data is available on the heating system, the building, its users and control settings.

The main influences on heat pump efficiency are understood as described by standard calculation procedures: i.e. source and sink temperatures, auxiliary energy demands and heat losses. It can be deduced from field test data that the temperatures vary not only on a seasonal level but also in shorter periods, meaning during one heat pump cycle. Auxiliary energy demand varies strongly from object to object. Heat losses cannot be correctly identified with the available data and its uncertainty.

Static calculation methods cannot correctly model the various influences in such systems. It has to be considered that the buffer storage and the building form thermal masses that are not considered in these calculations. Additionally, user influences are not taken into account. It is shown that the on/off control dominates the system behavior which leads to strongly varying temperatures in the hydraulic system.

For each analyzed object, the results are plausible regarding energy balances. As several boundary conditions are not known, it cannot be evaluated if the systems operate optimally. E.g. it cannot be definitely evaluated, whether

- ▷ supply temperatures are correctly controlled and if heat pumps operate optimally with regard to the heat emission system and the room comfort,
- ▷ each use of back-up heaters is necessary
- ▷ the dimensioning of the components is correct.

However, the large differences between systems allows the conclusion that there is room for optimization with respect to these points. Nevertheless, the main influences on heat pump efficiency could be detected and the operating behavior of on/off controlled heat pumps is analyzed. This knowledge is used in the following chapter.

# 4 Modeling and simulation

## 4.1 Requirements and method

### 4.1.1 Requirements

One objective of this work is the development of a heat pump heating system model that allows to study supply temperature and single room heating concepts. Possible characteristics of such systems are listed in table 4.1.

**Table 4.1:** Options for system components and decisions (bold font).

| Source | Heat pump control | Storage | Heat distribution | Building physics |
|---|---|---|---|---|
| **air** | **on/off controlled** | no storage | floor heating | new building |
| ground | capacity controlled | **buffer storage** | **radiator heating** | **existing building** |
| water | | DHW storage combined storage | | |

A system model that only considers the heating of a building and no DHW production is therefore developed. As heat source, outdoor air is chosen as it is the more challenging source taking into account its seasonally changing temperature level. Additionally it can be modeled more easily and thus be simulated faster. An on/off controlled heat pump is chosen over a capacity controlled one. This has to be considered for control and further system design. The field test can deliver data for model validation. A buffer storage is chosen to cope with differences of heat pump capacity and building heat load and to reduce operating cycles. An existing building with a radiator heating system is modeled.

A dynamic simulation model should consider the heat pump performance and operating behavior, the heating systems dynamics including the buffer storage and the building with multiple heated zones. The interaction of the involved components has to be implemented in a multi-directional way.

### 4.1.2 Review on heat pump models

The general literature review in section 1.3 revealed that many theoretical studies on heat pump systems exist and thus a large number of heat pump models exist. Nevertheless, it is possible to identify three categories: Static calculation methods, dynamic models and design models. This classification is also used by Afjei and Dott (2011) who, beyond that, introduce two subgroups each:

1. Calculation methods
    a) Seasonal CoP (SCoP)
    b) SPF
2. Dynamic Simulation
    a) quasi steady state
    b) dynamic effect
3. heat pump design models
    a) refrigerant cycle model
    b) heat pump component

SCoP describes a method in which a CoP characteristic is weighted according to weather data, whereas SPF calculation methods consider additional influences (cf. methods mentioned in 3.4). In dynamic simulation, performance maps represented by look-up tables or equation fits can be supplemented by dynamic effects such as the modeling of a PT1 behavior. Models generally used in dynamic simulation are black-box models. Design models are deterministic ones based on characteristics of the working fluid cycle or the detailed modeling of heat pump components. They are usually not combined with dynamic models of the source and sink but used within the design process of heat pump working fluid circuits.

The dynamic simulation of heat pumps usually is done with dynamic source and sink models. Common examples are most of the TRNSYS studies mentioned in section 1.3.3 that use heat pump models as the one presented by Wetter and Afjei (1996) which is table-based with an added PT-1 behavior. Several enhanced or slightly changed models exist, just as the one by Marx and Spindler (2011), which adds transient behavior to a heat pump model.

Jin (2002) gives a detailed review on black box and design models and presents a parameter estimation model that implements a working fluid cycle which is parametized with manufacturer's data. It is stated that accuracy of component models is higher than for equation fit models, notably when operating points are extrapolated.

Generally, black box models have a sufficient accuracy for heat pump system simulation. Carbonell et al. (2012) compare an equation fit and refrigerant cycle based model. It is stated that the equation fit model extrapolates better and has higher accuracy, provided that both models are fitted to

measurement data. Corberan et al. (2011) fit equations to the outcomes of a detailed heat pump design model. The equations are used within a system model of a ground coupled heat pump using the software EES.

Fisher and Rees (2005) present a model that implements the refrigerant properties along with the basic components of the refrigerant cycle in Energy Plus. In the same software, He et al. (2009) use an equation-fit model based on manufacturer's performance data which does not allow the modeling of on/off cycling. Salvalai (2012) creates a simple table based heat pump model in the software IDA-ICE and validates it with data from German heat pump field tests.

Uhlmann and Bertsch (2009) develop a model of the refrigerant cycle in the equation software EES, (EES, 2014), which uses working fluid medium models of Lemmon et al. (2002). It considers the thermal inertia of the refrigerant cycle components. Kinab et al. (2010) present a component heat pump model which also uses RefProp as a source for working fluid implementation. Richter (2008) presents a library for the programming language Modelica for modeling of working fluid cycles. Trockel (2011) uses the simulation environment Dymola with the programming language Modelica for component based models of heat pump cycles. Quoilin et al. (2014) present an open-source Modelica library for the implementation of thermodynamic cycles which uses the CoolProp library for medium data (Bell et al., 2014).

In this work, in order to conduct simulations of whole heating periods, a table-based black-box model has been chosen. Three different types of heat pump models were compared during the decision process: One is table-based and two two of them contain models of the refrigerant cycle with its components. One of them uses the *External Media library* (Casella and Richter, 2008) which means that external media models of Lemmon et al. (2002) are used. The other one is the commercially available library called *TIL* initially developed by Richter (2008).

Within this work, a decision on an appropriate heat pump model for simulation of heating periods was made comparing different types of heat pump models[1]. The table based model is chosen for its accuracy on the whole operating range and its computation speed. For the system analysis, a more detailed model is not required.

### 4.1.3 Review on storage models

Literature about storage tank models is often associated with studies on solar thermal heating systems. Storage tank models used within system simulation are usually multiple node models. The water volume is discretized in one dimension with finite volume or finite differences method.

[1] Twelve simulations, each simulating 3000 s with a linear change of operating conditions are carried out for each heat pump model. According to Schmidt-Holzmann (2010), the table based model takes 0.8 s on average for simulation, the *TIL* model needs 122 times as much, for the *External Media library* model the simulation time has to be multiplied by factor 1433. A high share of this time is used for initialization of the detailed models. In longer simulation runs with a lot of events through starts and stops of the heat pump this would cause very long computing.

Phillips and Dave (1982) introduce a stratification coefficient that puts into relation the energy of a stratified tank and a ideally mixed storage tank which can be used to model stratification in storage tanks. The basic storage models used in TRNSYS[2] use either an approach of multiple nodes that are connected to each other allowing flow of mass and heat, or a "plug flow" that models fluid volumes of a constant temperature which pass the storage volume without mixing. Kleinbach (1990) extends these models by implementing a calculation procedure that considers buoyancy effects. Nowadays, more complex models exist as the one by Druck (2006), which has multiple nodes, heat exchangers and auxiliary heaters.

More sophisticated models using a two- or three-dimensional discretization of the fluid volume are often not used in annual system simulations because their computing time is too high. Kenjo et al. (2003) developed a zonal, two dimensional radial fluid volume. In this way the outer zone of the volume which can be heated or cooled from the storage wall is separated from the central zone which is not directly influenced by the wall. The model has been successfully tested against measurements and is introduced into the TRNSYS environment.

Within this work, field test results are used for testing the model. The model has to assess the thermal behavior of a buffer storage and is used within simulations of heating periods. A model discretized in one dimension is chosen (see section 4.2.2).

### 4.1.4 General method

Many simulation studies on heat pump heating systems and building heating systems in general use the TRNSYS environment, whereas implementation in EnergyPlus, EES and Simulink are common, too.

Modelica[3] is a object-oriented language which allows for equation-based programming. The Modelica model libraries developed at the Institute for Energy Efficient Buildings and Indoor Climate (*EBC libraries*) allow a detailed modeling of the whole thermo-hydraulic system of a building and thus are used within this work. The libraries have constantly been developed and expanded[4]. Similar approaches of modeling buildings and HVAC systems with Modelica can be found. Merz (2002) developed a library called *ATplus* which was used as a basis for the *EBC libraries*. In recent years, Wetter (2009) developed a library which focuses on HVAC systems. Nowadays, Modelica is used increasingly in building and building system simulation (IEA EBC Annex 60, 2014).

A previous version of the models used within this work has been presented in Huchtemann and

[2] See TRNSYS (2014).

[3] See Modelica Association (2013)

[4] They are described in several publications (cf. Hoh et al. (2005, 2006); Matthes et al. (2006); Haase et al. (2007); Huchtemann and Müller (2009); Müller and Badakhshani (2010)).

Müller (2009)[5]. Within this work, as modeling environment for compiling and simulation the software Dymola[6] is used.

## 4.2 Model components

### 4.2.1 On/off controlled heat pump model

The general characteristics of on/off-controlled heat pumps can be described by two-dimensional polynomials or look-up tables. Usually the source input temperature and the sink output temperature, $T_{\text{source,in}}$ and $T_{\text{sink,out}}$, are used as inputs to these calculation procedures.

The heat pump is modeled as a black-box model which uses data from static tests of heat pumps according to standards EN 255 (1997) and EN 14511 (2012). In most cases, this is data provided by manufacturers. But also heat pump test centers as the one in Buchs, Switzerland publish this kind of data[7]. It usually contains heat pump capacities, CoP and/or electric power values at standard and additional operating points.

The electric power $P_{\text{el,HP}}$ and condenser heat flow rate $\dot{Q}_{\text{cond}}$ at different operating points is listed in look-up tables which are read out at $T_{\text{source,in}}$ and $T_{\text{sink,out}}$. The internal energy balance of the heat pump is used to calculate the evaporator heat flow:

$$\dot{Q}_{\text{evap}} = \dot{Q}_{\text{cond}} - P_{\text{hp}} \tag{4.1}$$

The look-up tables linearly interpolate and use the first or last two values of the table for extrapolation[8].

The heat pump capacity is corrected for mass flows of the source and sink medium different from those under standard conditions by a correlation according to Pahud and Lachal (2004). It presumes the arithmetic mean of inlet and outlet temperature as the relevant value for the calculation of the CoP and follows The internal energy balance of the heat pump (Pahud and Lachal, 2004):

$$\begin{aligned} \frac{\vartheta_{\text{in}} + \vartheta_{\text{out}}}{2} &= \frac{\vartheta_{\text{in,nom}} + \vartheta_{\text{out,nom}}}{2} \\ &\text{and} \\ \dot{m} \cdot c_p \left(\vartheta_{\text{out}} - \vartheta_{\text{in}}\right) &= \dot{m}_{\text{nom}} \cdot c_p \left(\vartheta_{\text{out,nom}} - \vartheta_{\text{in,nom}}\right) \end{aligned} \tag{4.2}$$

Pärisch et al. (2012) verify the use of this assumption with measurements: It is concluded that the

[5] They allow for the modeling of heat pump systems including geothermal heat exchangers and the surrounding ground. Models for geothermal sources have been described along with their validation in Rewitz (2010) and Huchtemann and Müller (2014). They allow to model BWHP systems combined with the set of models presented here. However, due to a focus on the heat sink and the use of AWHP, these models are not part of this work.

[6] See Dassault Systems (2011).

[7] See e.g. WPZ - Wärmepumpen-Testzentrum (2011), WPZ - Wärmepumpen-Testzentrum (2012).

[8] The Modelica `Modelica.Blocks.Tables.CombiTable2D` model is used therefore, see Modelica Association (2013).

deviation of the calculated CoP is notably reduced using the correlation in equation 4.2 (from 5 to 2%).

The fluid volumes of the two heat exchangers are modeled with the thermal capacity of a water volume[9]. The condenser fluid volume is connected to a heat loss element which can be parametrized by a heat loss coefficient, which models heat losses of the heat pump device[10]. Generally, this means that the thermal mass of the heat pump and its heat loss is modeled as being located in the condenser. In real heat pumps the maximum supply water temperature is limited because of a limited achievable pressure ratio of the compressor. In the model, a PI controller limits the condenser heat flow assuring a supply water temperature under a given limit, which models the maximum temperature constraints given by the working fluid.

### 4.2.2 Buffer Storage

The buffer storage model[11] consists of $n_{\text{lay}}$ fluid volumes[12] representing horizontal fluid layers that are connected to each other allowing for fluid and heat transfer. The heat flow between adjacent fluid layers $\dot{Q}_{i,i+1}$ is implemented by a constant heat conduction and an effective heat conductance, the latter representing buoyancy effects:

$$\dot{Q}_{i,i+1} = (\lambda_{\text{W}} + \lambda_{\text{eff}}) \cdot \pi \cdot \frac{d^2}{4} \cdot (T_{i+1} - T_i) \tag{4.3}$$

with heat conductivity of water $\lambda_{\text{W}}$, the inner diameter of the buffer storage $d$ and the temperature of the adjacent layers $T_i$ and $T_{i+1}$, whereas $T_{i+1}$ is the upper layer. The effective heat conductivity $\lambda_{\text{eff}}$ is modeled in three different ways. The first one, referred to as "1", implements no additional conductivity:

$$\lambda_{\text{eff},1} = 0 \tag{4.4}$$

This implies a solely conductive heat flow (see equation 4.3). The second model "2" is a turbulent heat conductance based on the work of Viskanta et al. (1977). It is a function of the layer thickness $s$, its temperature and the temperature difference to the above layer:

$$\lambda_{\text{eff},2} = 0, \; T_{i+1} > T_i \tag{4.5}$$

$$\lambda_{\text{eff},2} = \frac{2}{3} \cdot \rho \cdot c_p \cdot \kappa \cdot s^2 \cdot \sqrt{g \cdot \beta \cdot \frac{(T_{i+1} - T_i)}{s}}, \; T_{i+1} < T_i \tag{4.6}$$

$\rho$ is the density of water, $c_p$ is the specific heat capacity, $\kappa$ is the von Kármán constant, $s$ represents the turbulent mixing-length (which equals the height of the layer here), $g$ is the gravitational ac-

[9] The fluid volumes are closed fluid volumes from the *Modelica.Fluid* library: `Modelica.Fluid.Vessels.ClosedVolume` Modelica Association (2013).

[10] Measurements done by Miura and Ogino (2011) show that such modeling is appropriate.

[11] A former version of this model was implemented by Bartonicek (2007).

[12] The same as in heat pump model is used, `Modelica.Fluid.Vessels.ClosedVolume` Modelica Association (2013).

celeration, $\beta$ is the thermal coefficient of expansion. This is a common modeling which is e.g. also used by Wu and Han (1978) and Lüdemann (2001).

An additional model is implemented as a linear function of the temperature gradient as done in the *Buildings* library (Wetter, 2009; Modelica Buildings, 2014):

$$\lambda_{\text{eff},3} = 0,\ T_{i+1} > T_i \tag{4.7}$$

$$\lambda_{\text{eff},3} = s \cdot \frac{\rho \cdot c_p}{\tau} \cdot (T_{i+1} - T_i),\ T_{i+1} < T_i \tag{4.8}$$

where $\tau$ is the mixing time constant[13]. Combined with equation 4.3, the heat flow increases quadratically with the temperature gradient between two layers.

Furthermore, the cylindrical surface of each layer transmits heat to the storage wall. This heat flow is modeled with a constant heat transfer coefficient. Heat conduction and thermal capacity of the storage walls and the insulation layer are implemented and parametized with manufacturer's data and with standard material data for steel (storage wall) and polyurethane foam (insulation) which are stored in a parameter set. The fluid inlets and outlets are connected to the layers according to their height which is given in the parameter set. The convective heat transfer on the outside of the storage is implemented with a constant heat convection coefficient and a constant surrounding air temperature[14]. Pressure losses at the storage inlets and outlets as well as those on the inside are neglected. The model has one dimension with respect to fluid and heat transfer inside the fluid volume. This means that flow structures in other dimensions (e.g. convective mixing) are neglected or have to be approximated adapting the heat transfer between the fluid layers.

### 4.2.3 Validation procedure

The validation of the core components heat pump and buffer storage are done for three sample weeks with the mean outdoor air temperatures 0 °C, 7.5 °C and 15 °C. The intention is to validate the model for different operating conditions. In the first week with outdoor air temperatures of around 0 °C, heating operation dominates and AWHP defrosting occurs. In weeks with 7.5 °C mean outdoor air temperature heating operation dominates DHW operation but defrosting occurs less. With 15 °C being the general heating limit temperature for existing buildings (Recknagel et al., 2009, p. 75), in the third week DHW operation dominates over heating operation.

Aside from graphic analysis, two measures are calculated to compare measurement data and simulation results. The relative error is calculated for the heat pump electric energy and the heating energy in the loading cycle during one week:

$$f_E = \frac{E_{\text{week,sim}} - E_{\text{week,meas}}}{E_{\text{week,meas}}} \tag{4.9}$$

[13] It is set to 1 s as default in the library which leads to very high heat flows. Here, it is set to 100 s which still produces higher heat conductivity than using $\lambda_{\text{eff},2}$.

[14] set to 18 °C

$E$ stands for energy and is replaced by the heating energy measured in the condenser cycle $Q_{cc}$ or the electric work $W_{el,HP}$ in the validation process. Measured and simulated temperatures are likewise compared by the relative error, whereas their differences refer to the temperature range of the measured temperature.

$$f_\vartheta = \frac{\frac{1}{n_{data}} \cdot \sum_{i=1}^{\vartheta_i}}{max(\vartheta_i) - min(\vartheta_i)} \tag{4.10}$$

where $n_{data}$ is the number of valid data points used in the calculation. Data points are valid under the condition of volume flows different from zero. The temperature decrease of the sensors during non-operation times due to heat losses cannot be appropriately simulated as information about the installation is missing. During operation, these heat losses are assumed to be negligible.

The coefficient of determination is used to compare different parameter settings of the same simulation. It is defined by

$$R^2_X = \frac{\sum_{i=1}^{n_{data}} \left(X_{sim,i} - X_{meas,i}\right)^2}{\sum_{i=1}^{n_{data}} \left(X_{sim,i} - \bar{X}_{sim}\right)^2} \tag{4.11}$$

where $X$ represents either the electric power $P_{el}$, the heat flow rate in the condenser circuit $\dot{Q}_{cc}$ or the supply temperature in the heating circuit $\vartheta_{su,hc}$.

### 4.2.4 Heat pump model validation

Ten heat pumps have been parametrized with manufacturer's data[15] with respect to the tables for electric power and condenser heat output. As an example, the results for field test object 6 are shown in detail. At the end of this section the results for all ten objects are summarized.

The simulation set-up for the validation of the heat pump model is shown in figure 4.1. It consists of fluid sinks and sources on the condenser and evaporator side of the heat pump. These sources supply mass flow rates and inlet temperatures that were measured in the field test. An on/off signal is generated from measurement data and the heat pump model is controlled accordingly. It turns the heat pump on when the measured electric power is positive and turns it off when it is zero.

No information is available on thermal masses of the heat pump. Thus, the first step of validation involves an optimization of simulated condenser water volume. As pointed out in section 4.2.1, in the model the condenser volume represents the thermally relevant mass of the heat pump. Different water volumes are simulated for each selected week and afterwards compared on the basis of the coefficient of determination $R^2$.

Figure 4.2 (page 68) shows $R^2_{\dot{Q}_{cc}}$ and the relative error with respect to the simulated heat pump heating energy $f_{Q,cc}$ that were simulated in steps of 1 l condenser water volume. In this example for object 6 a condenser volume of 24 l is chosen as the overall coefficient of determination $R^2_{\dot{Q}_{cc}}$ is maximal. $R^2_{\dot{Q}_{cc}}$ in the validation week 1 is the lowest because of intensive use of the defrost mode

[15] This data is summarized in appendix A.

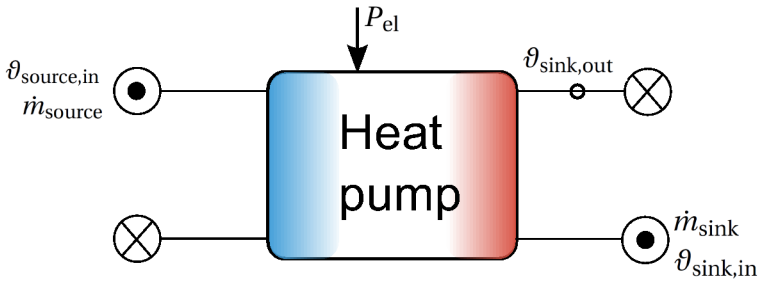


**Figure 4.1:** Simulation set-up for validation of heat pump model.

which is only quantitatively modeled. In the case shown here, also the relative error is the highest in week 1. As week 1 is the coldest of the three simulated weeks, the most operating intervals are found (cf. section 3.5.1). With each operating interval an error occurs, if the on/off signal is not exactly synchronized with the measurement data (cf. section 3.1.3).

Furthermore, the model is optimized by including the calculation of a condenser heat loss to the surrounding air. If the heat pump is located outside of the building shell, the measured outdoor air temperature is assumed to be the air surrounding the heat pump. Otherwise, a constant air temperature of 18 °C is used in the heat loss calculation. In the case of object 6, this heat loss does not lead to any improvement with respect to $R^2_{\dot{Q}_{cc}}$. Anyhow, the relative error can be reduced as figure 4.2 (page 68) shows.

Figure 4.3 (page 69) shows the electric power consumption of the heat pump for the second day of the first validation week (mean outdoor air temperature of 0 °C). The electric power is well represented by the model. During defrosting mode, measured power is positive and simulated power is zero. The model represents defrosting by higher values of electric power.

The heat flow rate in the condenser circuit shows higher deviation, see figure 4.4, page 69. The measurement data contains negative values for two reasons: At the beginning of operating intervals the return temperature might be higher than the supply temperature for short periods of time. This effect is partly reproduced by the model. The second reason is defrosting mode, when the volume flow is reversed. This means that a heat flow rate is extracted from the heating system. This is only quantitatively considered by the model by lower total heat flow rates.

The validation results for the heat pump of object 6 are summarized in table 4.2, page 70. The electric energy is very well met by the model with a relative error of up to 4%. The simulated quantity of heat has a relative error of up to 11%. This means that also the performance factor for the different weeks has an error (up to -15% and overall -11%). The error is especially high in the first week.

The results of the validation process are listed in appendix C. The best fitting condenser water volumes range from 1 to 36 l, the heat loss coefficients vary between 0 and 28 W/K (table C.1) with 28 W/K as an outlier. It has to be considered that these values do not represent real water volumes

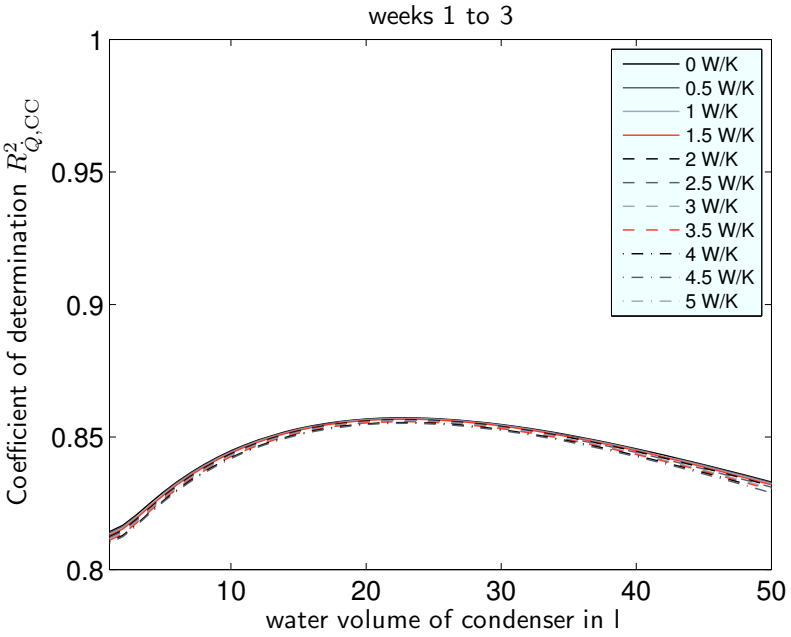


(a) coefficient of determination

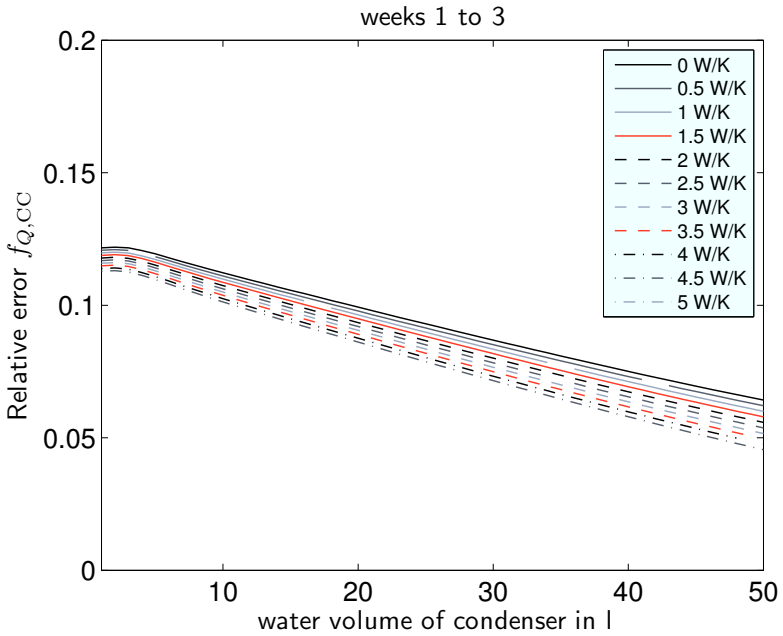


(b) relative error

**Figure 4.2:** Heat pump model validation, object 6: Comparison of coefficients of determination and relative errors for different simulated condenser volumes. Condenser volumes are changed in steps of 1 l.

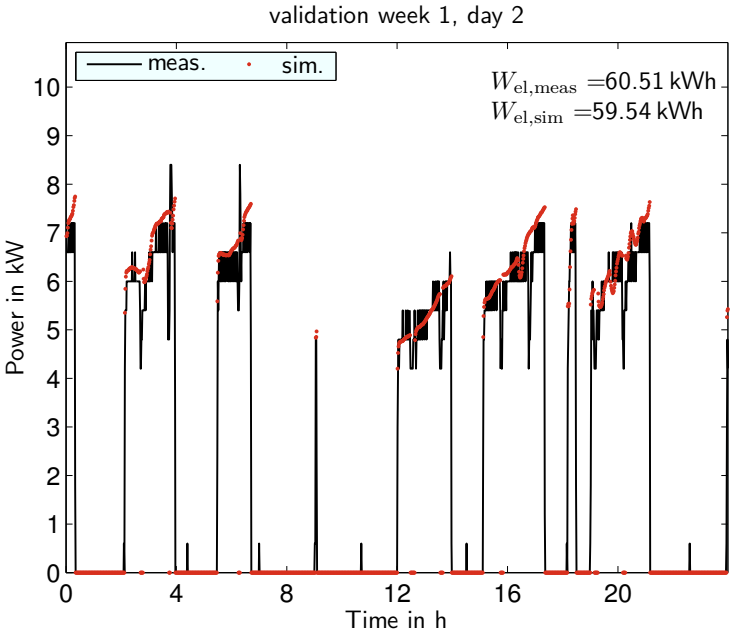


**Figure 4.3:** Heat pump model validation, object 6: Heat pump electric power without heat loss of condenser.

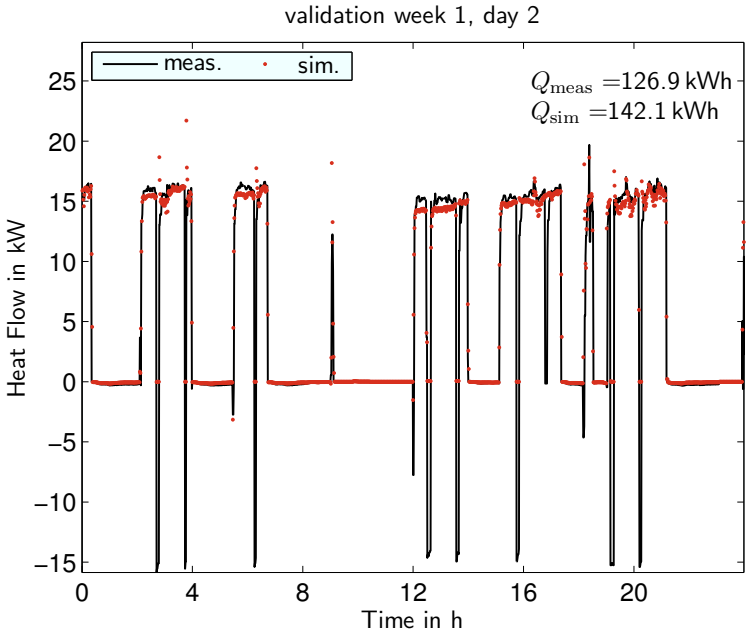


**Figure 4.4:** Heat pump model validation, object 6: Heat pump capacity without heat loss of condenser.

**Table 4.2:** Heat pump model validation, object 6: Results without heat loss of condenser.

| week | $W_{\text{el,meas}}$ in kWh | $W_{\text{el,sim}}$ in kWh | $f_{\text{W,el}}$ | $R^2_{\text{W,el}}$ | $Q_{\text{meas}}$ in kWh | $Q_{\text{sim}}$ in kWh | $f_{\text{Q}}$ | $R^2_{\text{Q}}$ |
|---|---|---|---|---|---|---|---|---|
| **1** | 482.05 | 465.19 | -0.03 | 0.87 | 985.15 | 1095.10 | 0.11 | 0.79 |
| **2** | 202.81 | 208.71 | 0.03 | 0.93 | 482.37 | 507.70 | 0.05 | 0.87 |
| **3** | 56.58 | 58.84 | 0.04 | 0.95 | 140.19 | 154.42 | 0.10 | 0.90 |
| **1 to 3** | 741.44 | 732.74 | -0.01 | 0.91 | 1607.72 | 1757.23 | 0.09 | 0.86 |

but thermally used capacities which also depend on mass flow rates and sensor positioning. However, for same heat pump types, the same values are calculated (objects 12 and 36 in table C.1).

The goodness of the model compared to the test data does not clearly depend on the outdoor air conditions[16]. With the consideration of a heat loss, $R^2_{\dot{Q}_{\text{cc}}}$ only slightly increases but the overall relative error is reduced[17]. The chosen volume of condenser has a small influence on the goodness of the model. The maximum relative error without heat loss optimization $f_Q$ is 15%, with it is 10%. For electric energy, maximum errors are 9%, for the performance factor 12%, independent from the optimization. The lowest determination is for objects 1 and 33; both use heat pumps with an insufficient number of data points in the look-up tables. Table 4.3 summarizes relative errors and coefficients of determination for all objects that were optimized with condenser volume and heat loss.

**Table 4.3:** Heat pump model optimization *with* heat loss: Relative error and coefficient of determination for week 1 to 3 of all objects.

| | $f_{\text{Q}}$ | $f_{\text{W,el}}$ | $f_{\text{PF}}$ | $R^2_{\dot{\text{Q}}}$ | $R^2_{\text{P,el}}$ |
|---|---|---|---|---|---|
| **01** | 0.07 | 0.06 | 0.02 | 0.85 | 0.57 |
| **05** | 0.07 | 0.06 | 0.06 | 0.96 | 0.93 |
| **06** | 0.10 | -0.01 | 0.11 | 0.86 | 0.91 |
| **09** | -0.09 | -0.09 | 0.03 | 0.93 | 0.91 |
| **12** | -0.02 | -0.06 | 0.04 | 0.95 | 0.98 |
| **24** | 0.08 | -0.04 | 0.12 | 0.81 | 0.96 |
| **25** | 0.01 | -0.02 | 0.06 | 0.98 | 0.96 |
| **27** | 0.02 | 0.09 | 0.00 | 0.97 | 0.95 |
| **33** | 0.06 | -0.01 | 0.07 | 0.79 | 0.88 |
| **36** | 0.04 | 0.02 | 0.02 | 0.94 | 0.99 |

Particularly the thermal energy is well modeled: The relative errors of seven objects is within the range of the uncertainty of measurements[18]. The errors in computing the electric energy are below the measurement error margins in only two out of ten objects. The relative errors range from -9%

[16] See tables C.2 and C.3.
[17] See table C.4.
[18] See section 3.1.3

to 10% for thermal energy and from -9% to 9% for electrical energy. As can be seen from the coefficients of determination, in most cases, the model fits well the behavior seen in the measurement data well.

Generally, the modeling of a heat loss at the condenser is not necessary. Five out of ten objects show better results with consideration of a heat loss, but only two at considerably high values of heat loss. These two cases could be caused by bad insulation of connection pipes. The correct parametrization of the condenser water volume however has a considerable influence on the goodness of the model.

### 4.2.5 Buffer storage model validation

Five buffer storages have been chosen for validation. Figure 4.5 shows the validation set-up. The supply temperature and mass flow of the loading circuit is given as well as the return temperature and mass flow of the heating circuit. The simulated supply temperature of the heating circuit is compared to the measured one.

Limitations to this analysis are as follows: On the one hand information on the buffer storages and their layout is limited. The measurement is limited to data of temperatures outside the storage. Thus the storage can only be investigated as a black box.

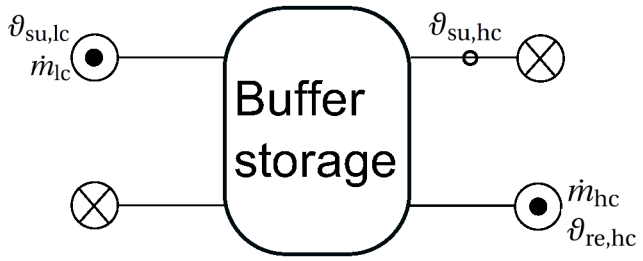


**Figure 4.5:** Simulation set-up for validation of buffer storage model.

The model does not exactly match the real storage behavior as can be seen from figure 4.6, page 73. The real temperature shows some fast changes that the model evens out. This might result from certain flow conditions which are not modeled in detail. The general curve progression is well met.

For fitting the model to the measured data $n_{lay}$ (in steps of 5) as well as the heat transfer model (model 1 to 3) are studied. The three test weeks are simulated for each parameter. The coefficient of determination as well as the relative error are calculated for each set of three week simulations. Figure 4.7 on page 73 shows the coefficient of determination and the relative error depending on $n_{lay}$ and the heat transfer model. The highest $R^2$ is yielded with 35 layers and using model 2. It has

to be noted that this is the overall result for three weeks. If only the first week is considered, model 3 has the highest $R^2$, for the other weeks it is model 2.

A different behavior can be found for object 35 (see figure 4.8, page 74). Here, a low stratification models the storage the best. It can be deduced that no stratification occurs in this storage.

Table 4.4 summarizes the results with the highest $R^2_\vartheta$ for each object and the according heat transfer models and number of layers. Of all simulations but the one for object 6, model 3 leads to the highest results with relatively low numbers of layers. The maximum relative errors are 4%. Both the type of model and the number of layers indicate that generally stratification in the buffer storage does not occur. Only the buffer storage of object 6 seems to have a certain level of stratification. Stratification is prevented when the mass flows are to high. The level of stratification can be increased by measures such as deflectors at the inlet of the storage.

**Table 4.4:** Results of buffer storage model validation

| object | heat transfer model | $n_{\mathrm{lay}}$ | $f_\vartheta$ | $R^2_\vartheta$ |
|---|---|---|---|---|
| 06 | 2 | 35 | 0.01 | 0.97 |
| 22 | 3 | 15 | 0.02 | 0.96 |
| 27 | 3 | 5 | 0.01 | 0.98 |
| 35 | 3 | 5 | 0.04 | 0.92 |
| 36 | 3 | 20 | 0.04 | 0.81 |

Model 1 is the simplest one and simulates the fastest. Models 2 and 3 take nearly the same time to simulate. The simulation time increases exponentially with an increasing number of layers (figure 4.9, page 74).

The model does not consider all physical effects that occur. Because of this, adjusting the number of fluid layers is necessary to fit the measured values. The mixing of the fluid through influences other than buoyancy are not considered in the model. In the real storages mixing probably occurs because of turbulence caused by the fluid entering the storage. Mixing in more dimensions than the modeled one also occurs because of convection on storage walls. When low numbers of fluid layers fit the best, it can be concluded that thermally the fluid volume is well mixed, or in other words, that it is not stratified.

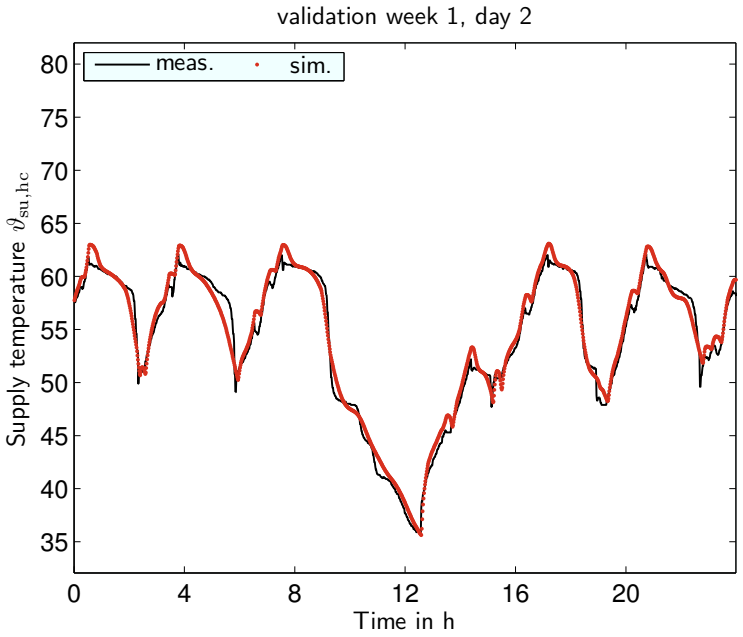


**Figure 4.6:** Buffer storage model validation, object 6: Measured and simulated supply temperature.

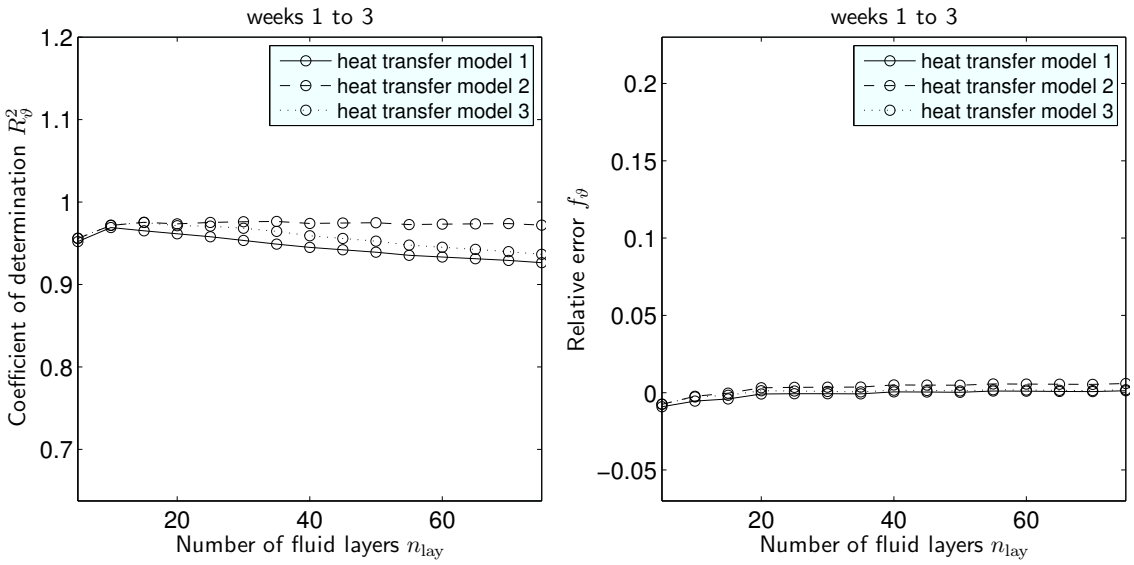


(a) coefficient of determination

(b) relative error

**Figure 4.7:** Buffer storage model validation, object 6: Comparison of coefficients of determination and relative errors for different numbers of simulated fluid layers and three heat transfer models.

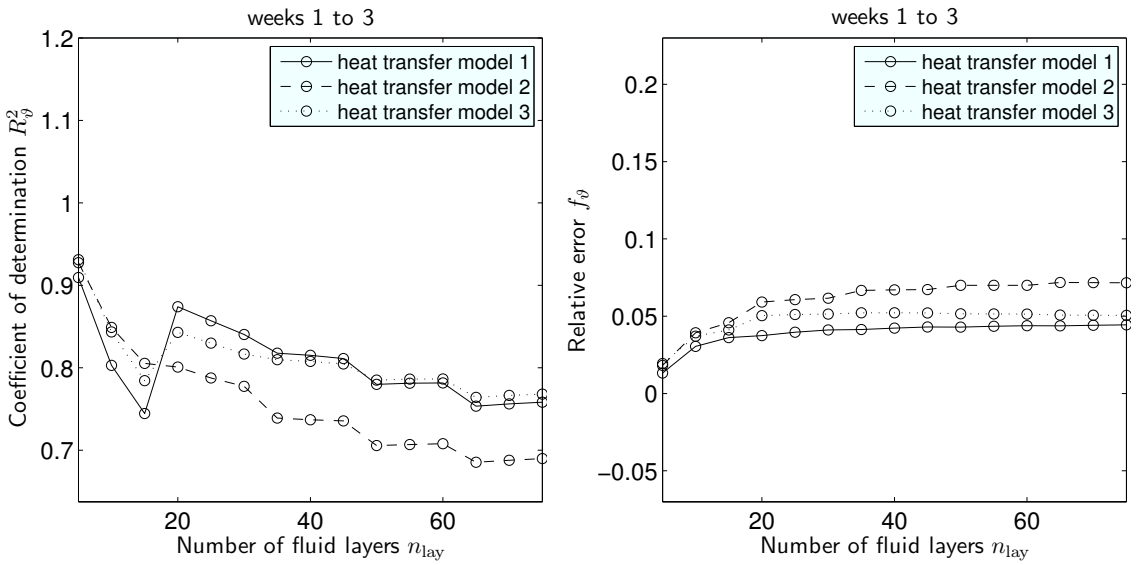


(a) coefficient of determination

(b) relative error

**Figure 4.8:** Buffer storage model validation, object 35: Comparison of coefficients of determination and relative errors for different numbers of simulated fluid layers and three heat transfer models.

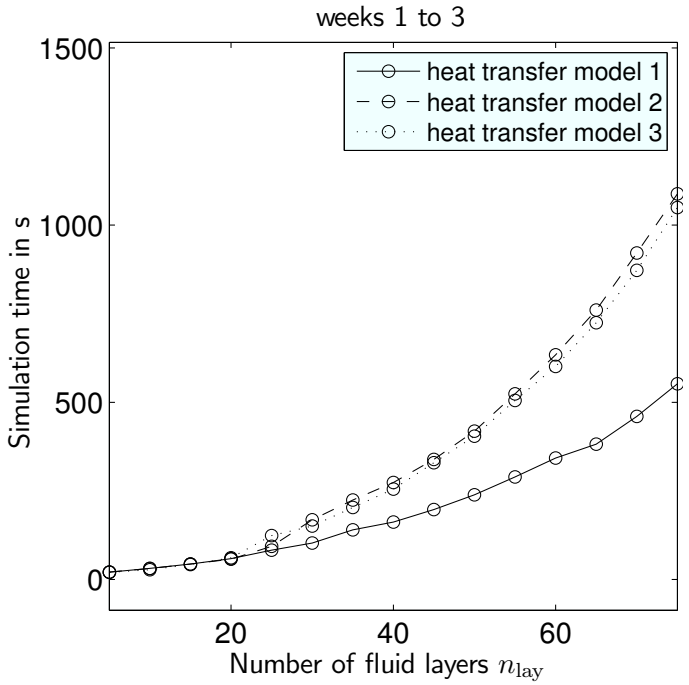


**Figure 4.9:** Duration of the validation simulation of the three sample weeks for the buffer storage of object 22 depending on the number of layers and the heat transfer model.

### 4.2.6 Additional model components

Additional model components are used for composing a model of the total system. They are part of the *EBC libraries* (see paragraph 4.1.2). The most important of these models are briefly described in the following paragraphs.

The pump model computes the pumping head according to equation 4.12, where $x$ is a value between 0.3 and 1 which represents the modulation rate:

$$H = x^2 \cdot c_0 + x \cdot c_1 \cdot \dot{V} + c_2 \cdot \dot{V}^2 \tag{4.12}$$

The radiator model is part of the EBC libraries (see section 4.1.2) and is based on the works of Glück (1990), Nadler (1991) and Tritschler (1999).

The water volume of the radiator is lumped into several water volumes (here, five volumes are modeled for each radiator) which allows for an estimation of the temperature gradient along the length of the radiator. The thermal mass of the radiator wall and conduction is equally lumped. Radiative heat flow from the radiator surface to the room is modeled according to the Stefan-Boltzmann law. The convective heat flow is calculated considering the logarithmic excess temperature [19]. The ratio of convetive to radiative heat flow is a constant parameter. The pressure drop inside the radiator is computed using a quadratic coefficient which is given in the manufacturer's data[20].

The model of the thermostatic valve consists of the valve model and the model of the thermal head and is also part of the *EBC libraries* whereas the valve model extends a model of the *Modelica.Fluid* library[21]. The valve uses a linear characteristic of opening position to flow coefficient. The thermal head implements the characteristic shown in figure 2.9 and adds the influence of the heating fluid temperature on the temperature of the sensor, the influence of the pressure drop inside the valve, the influence of the static pressure and a PT1 behavior.

A building model developed at the Institute for Energy Efficient Buildings and Indoor Climate is used (Constantin et al., 2014). The one-family dwelling consists of nine heated rooms on two floors of which one is the corridor containing the staircase and thus extending over the two floors. It also contains an attic. A radiator heating system with the nominal supply temperature of 55 °C and a return temperature of 45 °C is chosen. The layout of the hydraulic system is shown in figure 4.10, page 76. A detailed plan of the building are shown in appendix F.

## 4.3 Development of a reference model

The following sections describe the parameters chosen for the different model components and boundary conditions in order to complete the reference system model.

[19] See equation 2.13
[20] See Kermi (2010).
[21] See Modelica Association (2013).

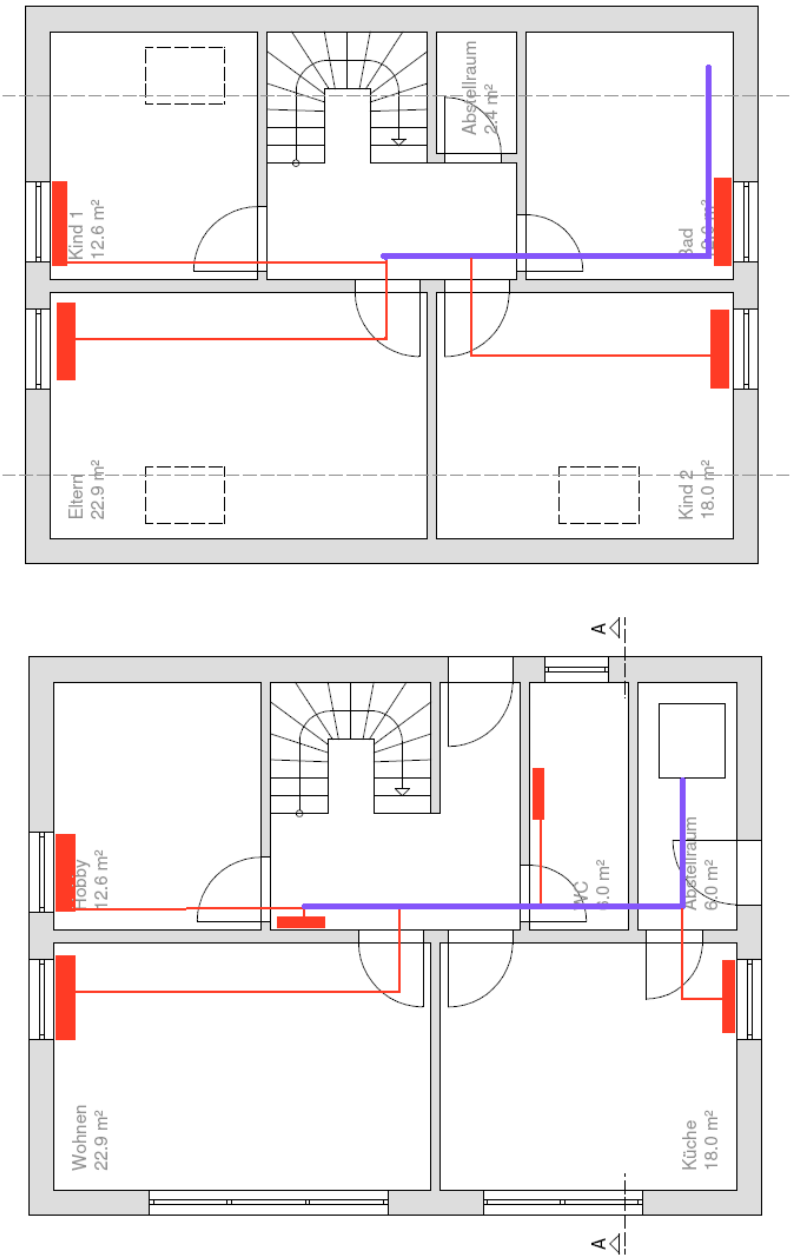


**Figure 4.10:** Layout of the hydraulics of the modeled building (Constantin et al., 2014).

**Table 4.5:** Description of the heated rooms of the reference building.

| Heated room | | $\vartheta_{i,nom}$ °C | $\dot{Q}_{hl,nom,WSchV84}$ $m^2$ | $\dot{Q}_{hl,nom,EnEV09}$ W | W |
|---|---|---|---|---|---|
| 1 | Livingroom | 20 | 23.8 | 2298 | 1222 |
| 2 | Hobby | 20 | 13.3 | 1229 | 654 |
| 3 | Corridor | 18 | 31.1 | 1169 | 396 |
| 4 | WC | 18 | 13.3 | 1132 | 559 |
| 5 | Kitchen | 20 | 18.9 | 1753 | 939 |
| 6 | Sleeping | 20 | 23.8 | 1803 | 910 |
| 7 | Children 1 | 20 | 13.3 | 1238 | 629 |
| 8 | Bath | 24 | 13.3 | 1494 | 870 |
| 9 | Children 2 | 20 | 18.9 | 1442 | 700 |

### 4.3.1 Building

The building model provides parameter sets for different insulation standards that apply for the building physics as well as for the dimensioning of the hydraulic system. Within this work two insulation standards are used: "WSchV84" (W) and "EnEV 2009" (E)[22]. The nominal heat load is calculated for a nominal outdoor air temperature of -12 °C. For each room adequate radiators are chosen fitting the heat load at nominal supply, return and room temperatures (55, 45, 20 °C). Table 4.5 gives an overview of heated rooms with their areas, nominal air temperatures and nominal heat loads according to the two insulation standards.

### 4.3.2 Dimensioning of components

For the layout of the heating circuit pump, the coefficients $c_1$ to $c_3$ (see equation 4.12) are extracted from a pump maximum characteristic[23]. The characteristic is scaled to match the nominal mass flow of the two building in both insulation standards.

The heat pump is dimensioned as described in section 2.3.1. For each insulation standard a monovalent layout ('M') is chosen as well as a bivalent one ('B') with a bivalent temperature of -5°C. The data of the heat pump *Viessmann Vitocal 350 AWI 114* (cf. appendix A, table A.4) is scaled accordingly. This means, each configuration has the same CoP characteristic. The bivalent configurations are completed by an electrical heater.

As stated in section 2.3, no consistent rules exist for the dimensioning of the buffer storage in heat pump systems. It should be mentioned that in the field test in AWHP systems an average volume of 50 l/kW can be found, referring to the nominal heat load. Here, the buffer storage model is

[22] "WSchV84" stands for the "Wärmeschutzverordnung 1984", the German Heat Insulation Ordinance of the year 1984, and "EnEV 2009" denotes "Energieeinsparverordnung 2009", the German Energy Saving Ordinance of 2009.
[23] Wilo Stratos Eco 25-1-5 BMS($x = 1$), see appendix E.

parametrized according to data of the *Viessmann Vitocell 750* storage. For the different insulation standards, the diameter of the storage is scaled ensuring a value of 50 l/kW.

In order to conduct the hydraulic balance of the hydronic heating system, valves with different flow coefficients were chosen. The hydraulic balance is executed ensuring that each radiator is supplied with the correct mass flow in the nominal point (see section 2.4.1). In reality, this is accomplished by a pre-adjustment of the valves. The flow coefficients with the according nominal mass flow of each radiator is listed in table E.2, appendix E. Each radiator valve is equipped with a thermostatic head with a proportional range of 1 K.

### 4.3.3 Inner loads and natural ventilation

Standardized profiles of inner loads for one family homes are hard to find. However, the Swiss standard SIA 2024 (2006) gives hourly values of occupancy and utilization of machines and lights for different types of rooms. Heimrath and Haller (2007) have developed an occupancy profile with the hourly presence of inhabitants in the whole building for a day. It is a mean value for occupancy profiles derived from surveys in Austrian low energy houses that were documented in Streicher (2004).

For the heat gained from humans, an occupancy schedule is developed on an hourly basis for each room. It differentiates between weekdays and weekends. On average it matches the occupancy profile given in Heimrath and Haller (2007) scaled to a presence of 4 persons during night time. This profile specifies the occupancy in the whole building. In order to determine profiles for different rooms, indications of SIA 2024 (2006) can be used. This is done for the living room, the sleeping rooms and the kitchen. Whereas the occupancy profile for the kitchen matches the overall building's profile well, the peak at noon in living rooms given by SIA 2024 (2006) could not be implemented as it would have interfered with matching the overall occupancy profile. The profile is shown in appendix D along with a reduced profile with a maximum occupancy of three persons and less occupancy at daytime during weekdays. The heat emission from people is calculated depending on the convective room temperature for low activity according to the guideline VDI 2078 (1996).

The inner loads through appliances are applied within the living room, sleeping room, children's rooms and the kitchen according to the profiles of SIA 2024 (2006). The profile is shown in appendix D along with a reduced profile.

In addition to a lighting schedule, a hysteresis controls the lighting in each room of the building. The schedule is shown for two scenarios in appendix D. Lighting is activated when the solar radiation on horizontal surface falls below 150 W/m$^2$; it is turned off when it rises above 180 W/m$^2$.

Referring to the two schedules of internal gains (3/4 persons), two ventilation profiles have been developed that can be found in appendix D, too.

### 4.3.4 Boundary conditions

The weather data used for the simulation of the system is the test reference year data of the German meteorological service for the city of Essen[24].

The outdoor air temperature serves as input to the AWHP model and the building model. It is also used for the system control. The wind speed is used for the calculation of convection on outside walls of the building model. The weather data also gives horizontal values of the solar radiation which are processed to radiation on vertical and differently orientated tilted surfaces of the building (Hoh et al., 2005).

### 4.3.5 Basic system control

The reference control of the system is described in the following paragraph. The supply set temperature which is generated by a heating curve. The heating curve is calculated according to the radiator equations[25] with a nominal room temperature of 20 °C. The supply temperature is measured in the upper part of the buffer storage. The on/off control of the heat pump is implemented with a hysteresis of ±3 K, the control hysteresis temperature difference thus is $\Delta T_{\mathrm{ctrl}} = 6\,\mathrm{K}$. Additionally, a heating threshold of 15 °C is implemented. At outdoor air temperatures higher than this, the heat pump is off. The heating system operates from September 15 to April 15 (heating season). An additional control is implemented for the electrical auxiliary heater. Its operation is restricted to outdoor air temperatures below the statically calculated bivalent point[26]. Its operation starts one minute after heat pump operation has started. The electrical power is controlled by a PI controller with the water temperature as measured value and the supply set temperature as target.

Changes to this control set-up are analyzed in chapter 5.

## 4.4 Evaluation of system configurations

The two main goals of the heating control in this work are

1. thermal comfort in all controlled zones and
2. energy efficiency of the heat pump system.

Energy efficiency is evaluated by comparing the electric energy demand of the systems studied[27]. The evaluation of thermal comfort needs a more sophisticated evaluation, which is described in the following.

[24] Referring to region 5, see Christoffer et al. (2004).
[25] See section 2.4.2.
[26] See section 2.3.
[27] See section 2.2.2.

The system analyzed within this work controls the room temperature. In addition, it is assumed that the room set temperature is the operative temperature desired by the user. Assuming the other influences on thermal comfort[28] as being the same in the systems compared, it is adequate to focus on the analysis of operative room temperature.

The comfort band is set from -0.5 K to +0.5 K. Excess of the comfort band not only happens due to bad control but also because of inner and solar gains. Overall, violation of the temperature band is defined as discomfort and calculated as follows:

- ▷ Only rooms 1, 2, 5, 6, 7, 8 and 9 are considered. In other words, the corridor and the WC/storage room are not included in the evaluation.
- ▷ Temperatures not meeting the comfort band are squared and integrated, positive (too warm) and negative (too cold) violations are treated separately (called cool/warm discomfort in the following).
- ▷ Discomfort is summed up for all considered rooms during the analyzed period. This can be either be done
  - for the whole heating period (which is done in this chapter) or
  - only during occupied periods on day time[29] (which is done in chapter 5).

As mentioned above, within this chapter discomfort is defined as the violations of the comfort band during the whole heating period. This is a theoretical approach which allows to compare different user schedules on the same reference time period. Positive violations (too warm) are analyzed when needed for a detailed comprehension of the system behavior. However, analyzing configurations with changing room set temperature, in chapter 5 only discomfort in times of user presence are compared. Then, comparison of the systems is done only with negative (too cold) comfort violations (DIN EN ISO 7730, 2006).

Following DIN EN 15251 (2007), reference systems are also evaluated with PPD-weighted hours in which a PMV comfort band is violated during occupation. This comfort band is defined ranging from PMV of -0.5 to 0.5 (category II, DIN EN 15251 (2007)).

## 4.5 System model verification

The reference system is simulated for the whole heating period. Its characteristics are presented in this section along with parameter studies on the buffer storage size, the control hysteresis and the mass flow rate in the condenser cycle. Table 4.6 shows the different variations of the basic system that are described in the previous chapters with the according abbreviations. The reference system contains a building with the insulation standard according to WSchV84, a bivalent set-up and high

[28] See section 2.2.3.
[29] These periods are between 6 am and 11 pm when users are in the room and windows are not opened.

occupancy (W-B-H). This system is analyzed in the following sections along with studies of basic parameters, a basic scheme of the system is shown in figure 4.11.

**Table 4.6:** Options for system layout.

| | | | |
|---|---|---|---|
| insulation standard | **W - WSchV84** | E - EnEV09 | see section 4.3.1 |
| Bivalent set-up | **B - bivalent** | M - monovalent | see section 4.3.2 |
| occupancy/inner gains and ventilation | **H - high** | L - low | see section 4.3.3 |

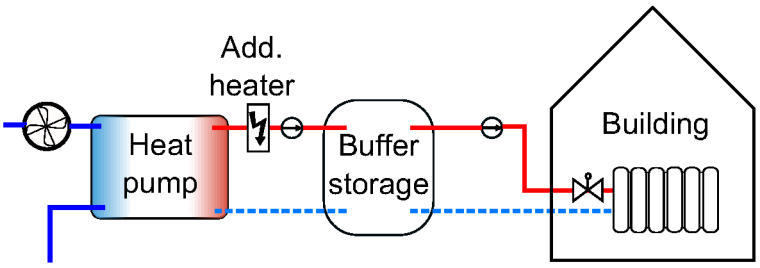


**Figure 4.11:** Scheme with the main components of the reference model.

### 4.5.1 Basic characteristics

The overall simulation results of the reference system are listed in table 4.7. An $SPF_1$ of 3.12 is achieved with a heating demand of 13570 kWh and a simulated electrical energy of 4319 kWh in one heating season. The additional electrical heater is rarely used. The heat pump works 25% of the total heating hours (4849 h). The characteristic of the supply temperature is studied in section 4.5.5.

**Table 4.7:** Simulation results of the reference system WBH for one heating season.

| $SPF_1$ | $W_{el,HP}$ kWh | $W_{el,add}$ kWh | $Q_{LC}$ kWh | $Q_{HC}$ kWh | $t_{on}$ h | $n_{op}$ |
|---|---|---|---|---|---|---|
| 3.12 | 4319.2 | 32.8 | 13552.5 | 13570.3 | 1224.1 | 4217 |

The monthly values of energies and performance factors are shown in figure 4.12. The highest ratios for heating are in December and January, when PF are lowest.

The distribution of operative room temperature differs depending on the room. The two rooms that are analyzed are room 1, the living room and room 8, the bath. Room 1 has a set temperature of 20 °C and has lots of inner gains that change throughout the day. Room 8 has a set temperature of 24 °C, which is the highest in the building, but comparatively low inner or solar gains. Figure 4.13 shows the cumulative temperature deviation of these two rooms. The mean room temperature of room 1 is 2.1 K too high with a standard deviation of 1.8, whereas in room 8, the mean temperature

**Table 4.8:** Discomfort of reference system WBH, calculated according to section 4.4.

| Type of discomfort | too cold | too warm |
|---|---|---|
| Squared Kelvin-hours | 5022 $K^2h$ | 95562 $K^2h$ |
| Squared Kelvin-hours, occupied periods | 1325 $K^2h$ | 37049 $K^2h$ |
| PPD weighted PMV, occupied periods | 198.5 h | 5002 h |
| Percentage of hours out of PMV comfort band, occupied periods | 2.2% | 22% |

is -0.17 K too low and there is a standard deviation of 1 K. The latter can be explained through the heating curve which is theoretically too low for the high nominal room temperature of 24 °C. This, however, is partially compensated by the over-dimensioning of the radiator and inner gains. In all rooms, the opening of windows is the main reason for temperature falling below the set point.

The total calculated discomfort is shown in table 4.8. The warm discomfort is much higher than cool values, mainly resulting from inner gains.

The reference system is analyzed in an annual simulation considering DHW generation (see appendix G). The $SPF_1$ for this configuration is 2.59 and successfully reproduces a typical profile of monthly performance factors as identified in the field test.

### 4.5.2 Insulation standard and bivalent set-up

The insulation standard has a strong effect on the efficiency of the heat pump system. Whereas the building with the lower standard (W) has a heating demand during the whole heating season, the building with high insulation standard (E) has a smaller number of operating hours. It is heated throughout the times of lowest outdoor air temperatures when the inner and solar gains do not suffice to heat the rooms. In times of low outdoor air temperatures the heat pump efficiency is the lowest. Analogously, systems with the high level insulation yield smaller numbers of operating cycles: Figure 4.14 on page 84 shows that operating time and number of cycles is lower for the insulation standard E. The operating time is lower for high inner gains (H) than for low inner gains (L) because inner gains partly substitute heating. The monovalent (M) systems have less operating hours than the bivalent (B) ones because the heat pump capacity is higher. With high insulation standard (E) high inner gains (H) lead to a lower number of operating intervals, for low insulation standard (W) it is the opposite: whereas in buildings of standard E the inner gains can fully substitute heating during longer periods, in the buildings of standard W the heating demand is only partly substituted. This means that the heating demand is decreased and leads to a stronger cycling of the heat pump.

The aforementioned effects result in lower SPF of the high insulation standard building. Electric energy demand of bivalent systems is a little higher than that of the monovalent system; the comfort of the systems is not affected. The high insulation level results in strongly over-heated rooms

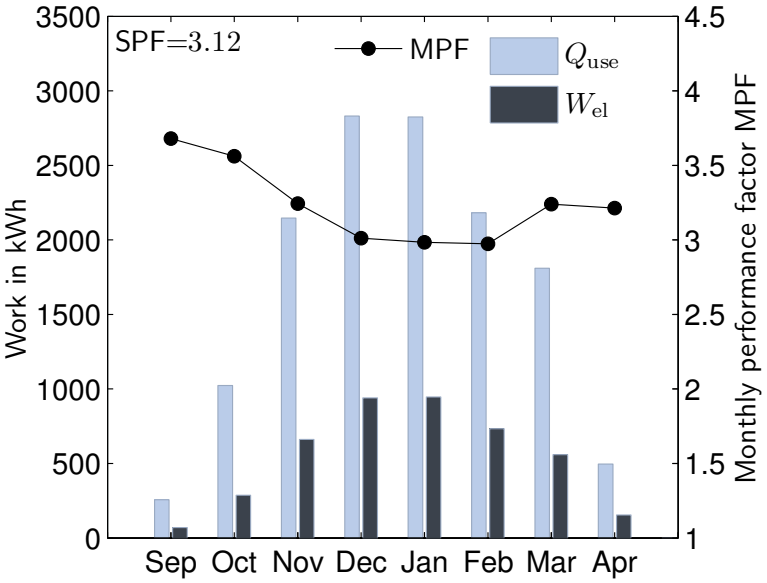


**Figure 4.12:** Monthly performance factors, heat demand and energy of the reference system WBH.

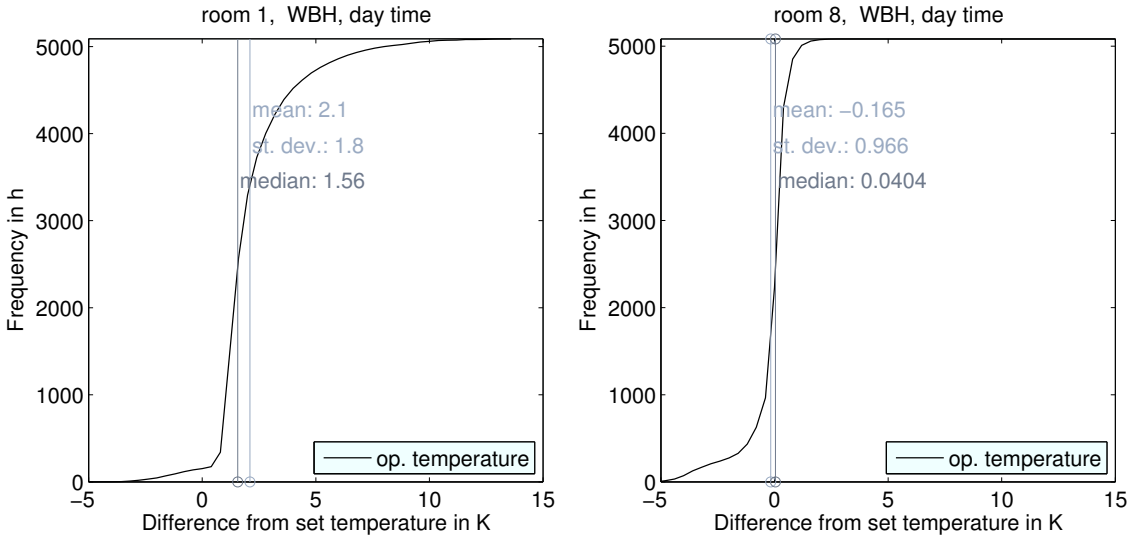


(a) Room 1

(b) Room 8

**Figure 4.13:** Operative room temperatures of rooms 1 and 8. Simulation results of the reference system WBH.

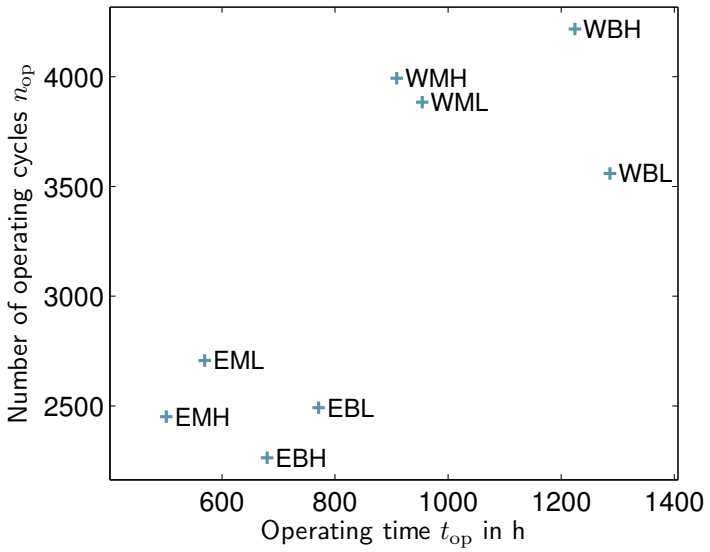


**Figure 4.14:** Simulation results for different insulation standards and bivalent set-ups: Number of operating cycles and time. W/E: Low/high insulation standard. M/B: Monovalent/bivalent system. H/L: High/low occupation profile.

which leads to much higher warm discomfort. Taking into account only negative violation (too cold) of the comfort criteria, the buildings perform roughly the same for same system design. Figure 4.15 summarizes the relative differences of positive (too warm) and negative (too cold) comfort violation as well as electrical energy demand compared to the reference system WBH.

There is no strong difference with respect to efficiency between monovalent and bivalent systems. The monovalent system performs slightly better, the number of operating cycles is not dramatically higher. However, the investment in a high capacity heat pump seems unreasonable, given the small differences; a bivalent system design is adequate.

It becomes clear from the analysis in this section that user influences play an important role in system behavior which is why they will be analyzed in depth.

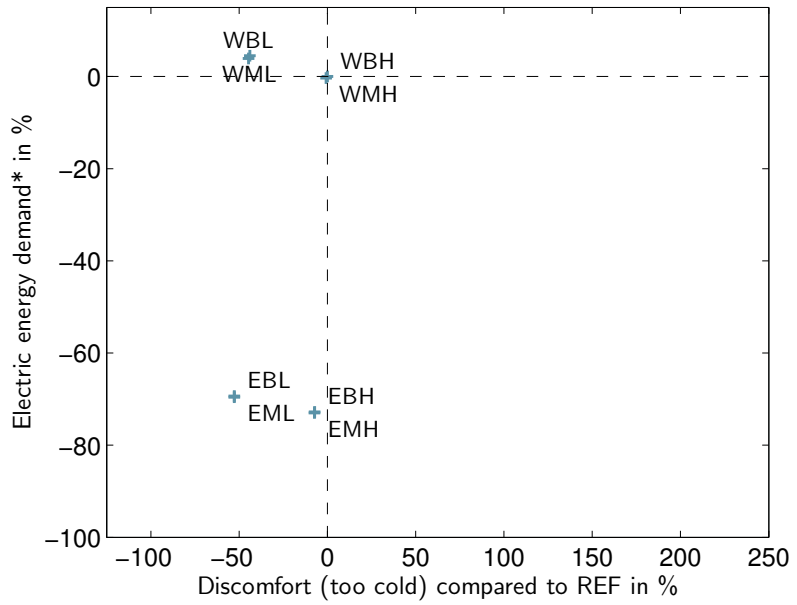


(a) Cool discomfort

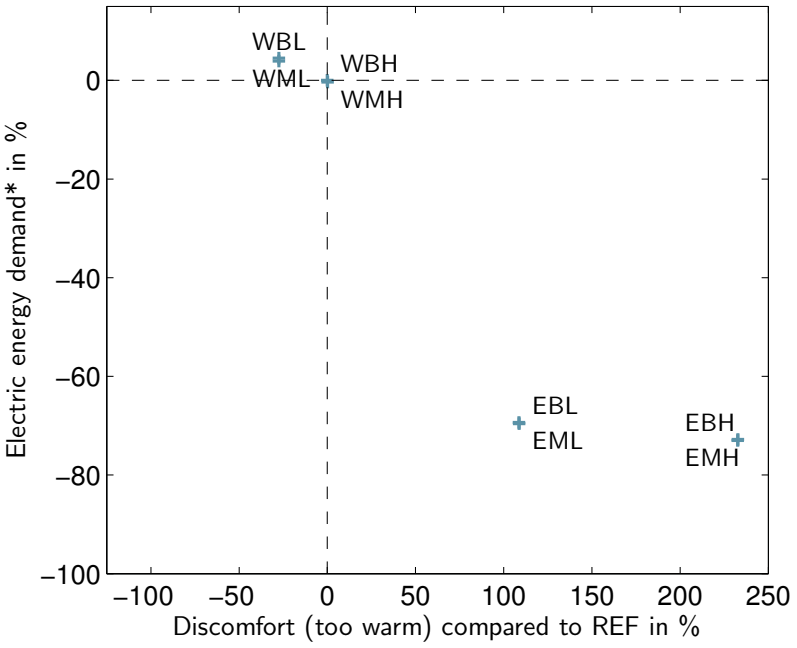


(b) Warm discomfort

**Figure 4.15:** Relative differences in electricity demand and discomfort, simulation results for different insulation standard and bivalent set-ups. W/E: Low/high insulation standard. M/B: Monovalent/bivalent system. H/L: High/low occupation profile.

### 4.5.3 Inner gains and user influences

Beside the two user profiles already presented (H and L), a theoretical one with no inner gains, no user presence and no ventilation schedule is introduced (N). The occupancy can thus be studied on the basis of three profiles.

As mentioned above, the SPF increases with lower inner gains because the heating period is extended (see figure 4.16). Accordingly, figure 4.17 (page 88) shows that the total electricity demand is increased, too. An interesting effect is observed for operating cycles: With a decreasing level of occupancy (H to N) the number of cycles increases in the low insulation standard building. For insulation standard E it is the opposite. In the first case lower internal gains lead to longer and through this fewer operating intervals, in the latter a longer heating season allows for an extended operating time with more cycles.

Furthermore, figure 4.17 (page 88) shows that with respect to cold discomfort there is no difference between the insulation standards: With a decreasing level of occupancy it is reduced by 50% (L) or even 100% (N). The warm discomfort is not reduced in the same way. For insulation standard W smaller reduction is yielded lowering the occupancy (up to 50%). This shows that too high room temperatures are not only due to occupancy but also due to solar gains and the control: The thermostatic radiator valves are proportional controllers that fully shut when the room set temperature is exceeded by 1 K[30]. In the configurations with high insulation standard (E) much stronger overheating is detected.

### 4.5.4 Building mass

The building inertia is studied by varying the wall construction from lime sand brick masonry (heavy) over porous concrete (middle) to a wood beam construction[31] (light) within the reference system WBH.

The capacity of the building construction has a negligible influence on the heat pump performance and the number of operating cycles which can be explained by the buffer storage water volume having the much stronger effect on the heating system inertia. However, positive comfort violations (too warm) can be reduced by the higher thermal building mass, cool discomfort is not affected.

[30] See section 2.4.3.

[31] The wall parameters for different building constructions are part of the building model described in section 4.3.1. They are in accordance with DIN 4108-2-2011 (2011), table 9, where heavy, middle and light wall constructions are defined.

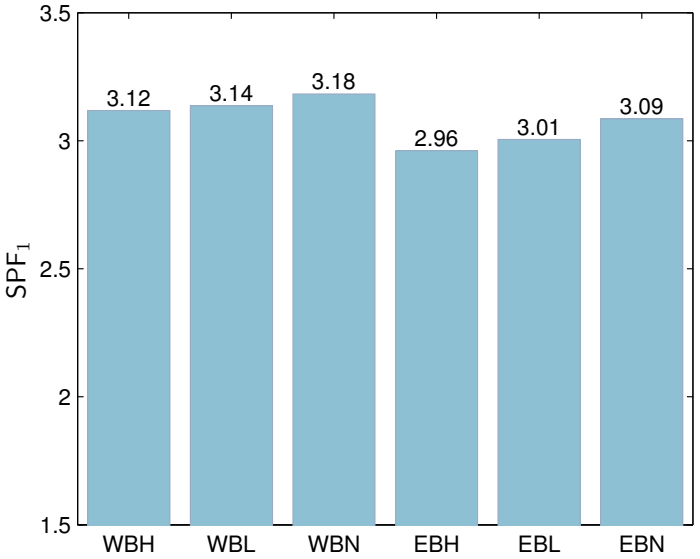


(a) SPF

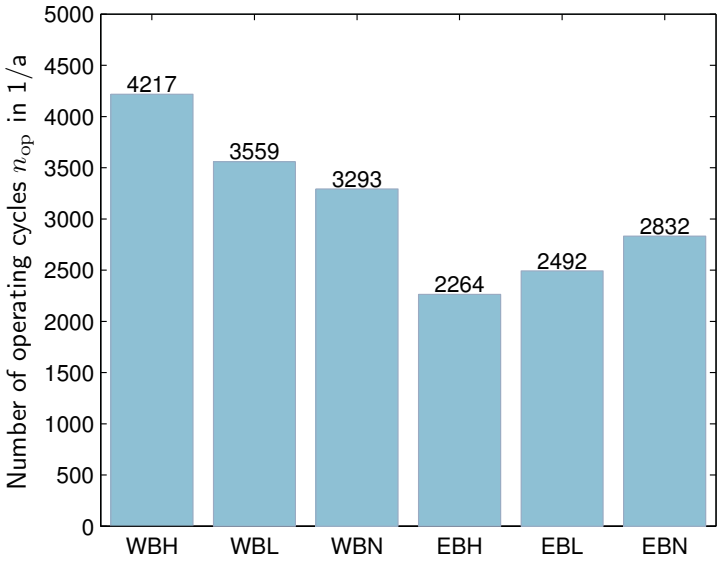


(b) Operating cylces

**Figure 4.16:** Simulation results: $SPF_1$ and operating cycles for different user schedules. W/E: Low/high insulation standard. B: Bivalent system. H/L: High/low occupation profile.

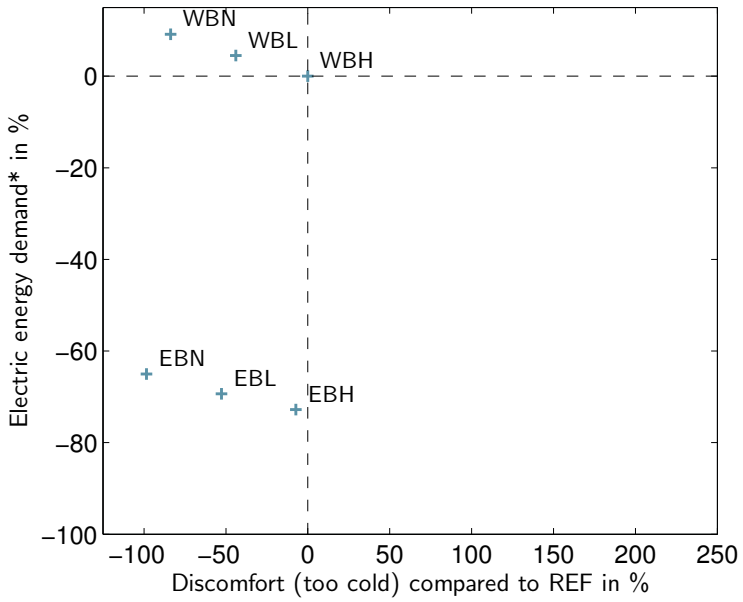


(a) Cool discomfort

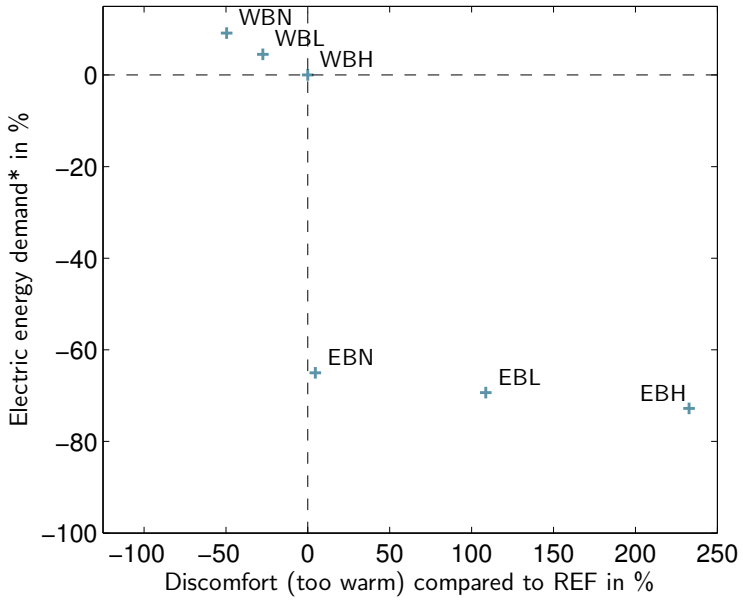


(b) Warm discomfort

**Figure 4.17:** Relative differences in electricity demand and discomfort, simulation results for different user schedules and bivalent set-ups. W/E: Low/high insulation standard. B: Bivalent system. H/L: High/low occupation profile.

### 4.5.5 Measurement of supply temperature

Several system layouts exist for heat pump heating systems. Likewise, different control concepts exist including different supply temperature controls. Generally, an on/off controlled heat pump is controlled with a hysteresis controller. The input of this controller is the supply temperature in the heating circuit, one buffer storage temperature or two temperatures measured in the buffer storage. Four implementations of the supply temperature control hysteresis are analyzed:

(a) The supply temperature is measured in the upper part of the buffer storage.

(b) The supply temperature is measured in the heating circuit. The measurement is only valid if the water is circulating in the heating circuit.

(c) The water temperature in the upper and lower part of the storage are measured. The heat pump turns on when the upper temperature falls below the lower hysteresis set point (supply temperature heating curve value minus 3 K), the heat pump turns off when the lower storage temperature reaches the upper hysteresis set point (return temperature heating curve plus 3 K).

(d) The water temperature in the upper and lower part of the storage are measured. The heat pump turns on when the upper temperature falls below the lower hysteresis set point (target temperature minus 3 K), the heat pump turns off when the lower storage temperature reaches the upper hysteresis set point (target temperature minus 3 K).

Depending on the place of measurement, different reaction times and time constants are reached, which is the main difference between configuration (a) and (b). Configuration (c) is designed to fully load the buffer storage. Configuration (d) attempts to minimize excess of supply temperature compared to (c).

Figure 4.18 on page 90 shows the heating curve and the daily mean values of supply temperature related to the daily mean outdoor air temperature. Both configurations (a) and (b) match the heating curve well. On average, (c) and (d) lead to excess of supply set temperatures.

There are only small differences between the SPF in these configurations (see figure 4.19, page 91): Whereas (a) has the lowest mean supply temperatures resulting in to the highest efficiency. The number of operating cycles, however, differs strongly with configuration (a) having the highest number. Configuration (c) operating with two heating curves yields only 31% of cycles of configuration A. It optimally uses the buffer storage regarding the temperature spread required by the heating system.

The differences in supply temperatures between the four configurations are too small to noticeably affect the comfort.

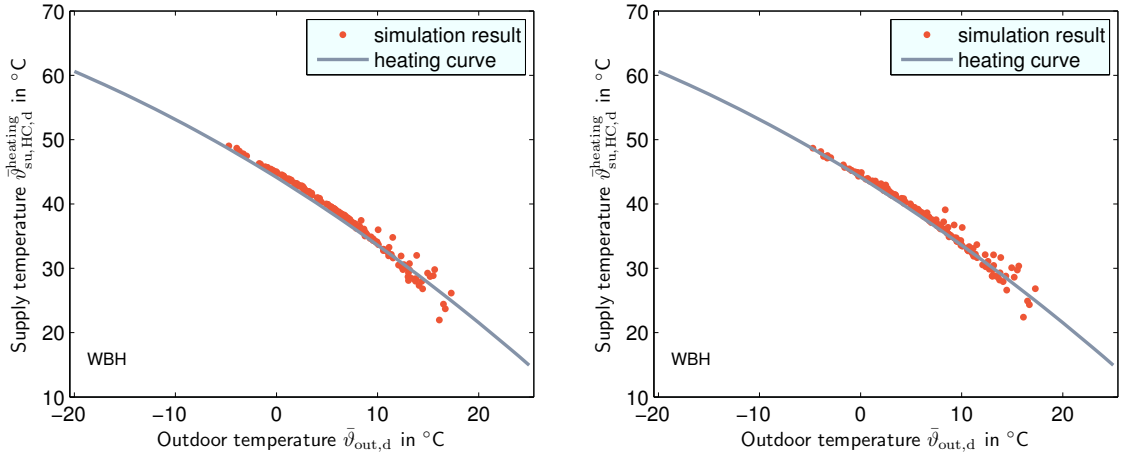


(a) Supply temperature measured in upper buffer storage.

(b) Supply temperature measured in heating circuit.

(c) Supply temperature measured in upper and lower part of buffer storage.

(d) Supply temperature measured in upper and lower part of buffer storage, adapted hysteresis.

**Figure 4.18:** Daily mean supply temperatures depending on daily mean outdoor air temperatures for different types of hysteresis control.

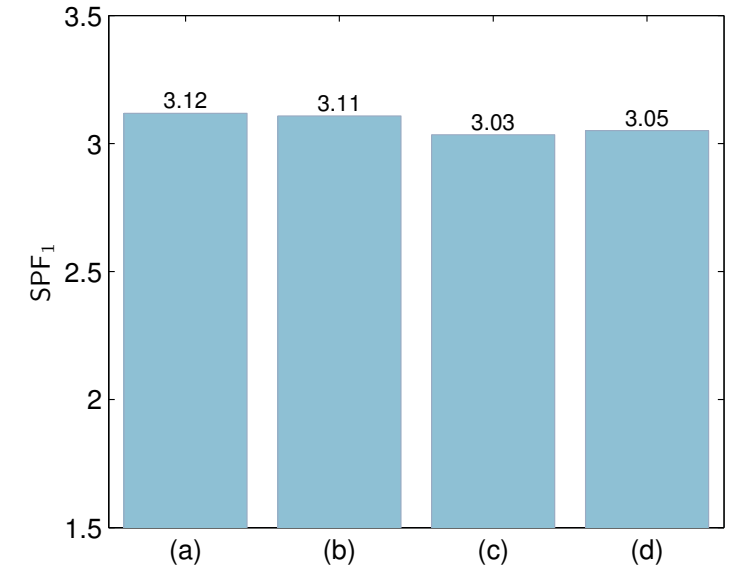


(a) SPF

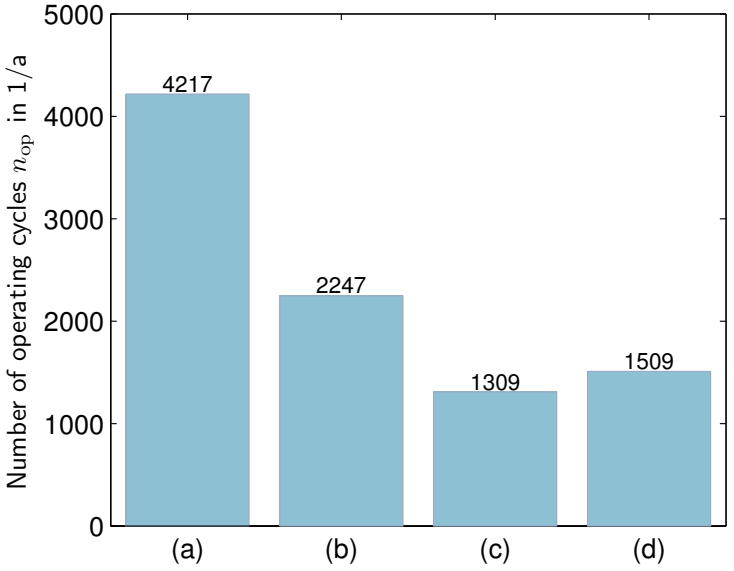


(b) Operating cylces

**Figure 4.19:** Simulation results: $SPF_1$ and operating intervals for different types of hysteresis control; reference system WBH. (a): Supply temperature measured in upper buffer storage. (b): Supply temperature measured in heating circuit. (c): Supply temperature measured in upper and lower part of buffer storage. (d): Supply temperature measured in upper and lower part of buffer storage, adapted hysteresis.

### 4.5.6 Buffer storage size and control hysteresis

Both the buffer storage volume, i.e. the inertia of the heating system and the control hysteresis influence the number of operating intervals and the variation of the supply temperature. The volume of the buffer storage is varied by changing the inner diameter, all other parameters are unchanged. Figure 4.20 shows the number of operating cycles during the heating period which is distinctly influenced by the storage volume as well as the control hysteresis.

Figure 4.20 on page 93 also shows that the main influence on SPF with different storage volumes can be explained by storage heat losses that lead to decreasing PF with increasing volumes.

The effect of the hysteresis on the supply temperature can be seen in figure 4.20, too. The characteristic of the Carnot CoP (see equation 2.2) leads to the effect that, even with the same mean supply temperature a higher hysteresis band leads to lower heat pump efficiency. The efficiency strongly decreases with higher supply temperatures which frequently occur with higher hysteresis bandwidths.

### 4.5.7 Discussion of reference system simulation results

It has to be noted that results in energy efficiency and comfort differ strongly for a variation of single influences that are not directly associated with the heat generation system and cannot be modeled with static calculation methods. Figure 4.21 on page 95 shows the relative differences in electrical energy demand and discomfort compared to the reference system WBH.

The configurations with less occupancy, L and N have the strongest impacts on the violation of the temperature band. Especially the negative violations (too cold) can be reduced with less occupancy, as also less window opening events occur.

The results of the monovalent system (M) virtually show no difference to those of the bivalent system. The mass flow rate and with it the temperature spread in the condenser cycle has an impact on the efficiency of the heat pump as has been pointed out in section 3.5.3. Simulations of the reference system with three different mass flow rates are therefore executed. The reference system with the nominal mass flow rate achieves an $SPF_1$ of 3.12. With half the mass flow rate the $SPF_1$ is 2.87, with the double of the nominal value it reaches 3.21. This means a 9% higher or 3% lower electric energy demand. The adaption of the mass flow rate ($\dot{m}\uparrow/\dot{m}\downarrow$) in the CC offers the highest influence on energy demand without noticeably influencing the thermal comfort.

Whereas a higher building mass ($C\uparrow$) can smooth out overshoot of temperature and analogously a lower mass ($C\downarrow$) yields more warm discomfort, the effect on cool discomfort is negligible. The adjustment of the control hysteresis ($\Delta T_{\mathrm{ctrl}}\uparrow$, $\Delta T_{\mathrm{ctrl}}\downarrow$) in the given range (2 K to 14 K) has a strong effect on comfort; 18% more negative violations of comfort (too cold) are calculated for a hysteresis with 14 K instead of 6 K. The volume of the buffer storage is varied from 0.083 $m^3$ to 0.83 $m^3$. Lower heat losses of a small buffer storage are gained by higher discomfort.

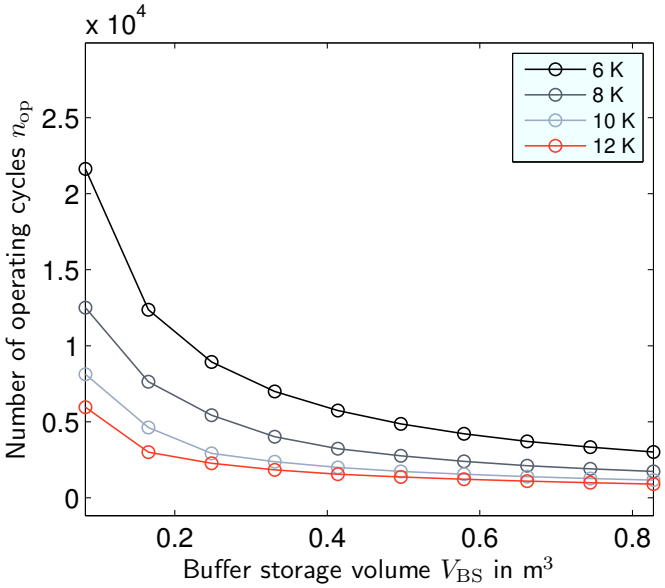


(a) Operating cycles

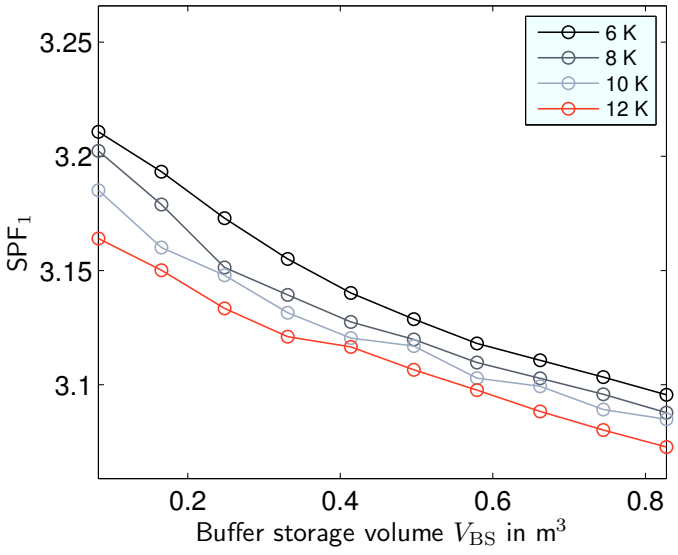


(b) SPF

**Figure 4.20:** Number of operating cycles and SPF depending on the buffer storage volume and the control hysteresis.

The heating curve is calculated for a room temperature of 20 °C in the reference case. The highest room set temperature in the building is 24 °C which should be used for heating curve calculation. Nevertheless, usually 20 °C is sufficient, as heating surfaces are over-dimensioned through the standard layout procedure[32].

The heating curve is calculated presuming a nominal room temperature of 20 °C in the reference system. A heating curve calculated for a nominal room temperature of 24 °C is also shown in figure 4.21 (hcu↑). With the higher heating curve, the energy demand is 6% higher. The $SPF_1$ is 2.98 instead of 3.12. The comfort is improved especially in the bath which is the only room with a 24 °C set temperature. But the higher heating curve also leads to higher warm discomfort in other rooms.

[32] See section 2.2.1

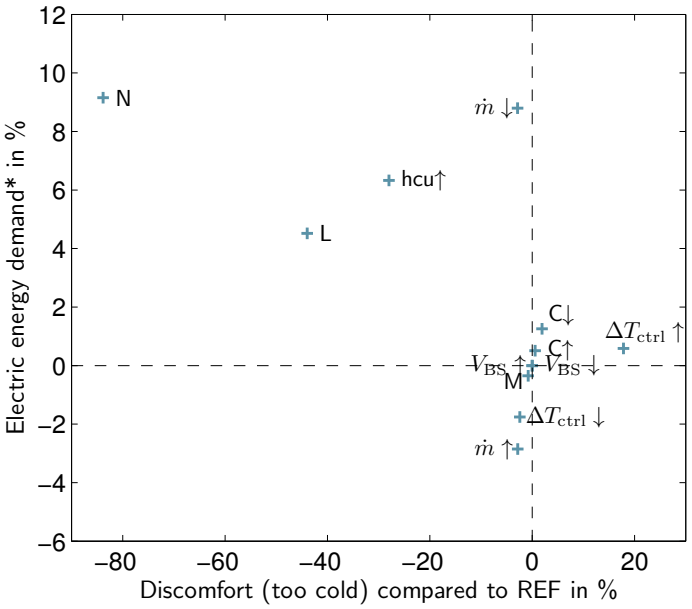


(a) Cool discomfort

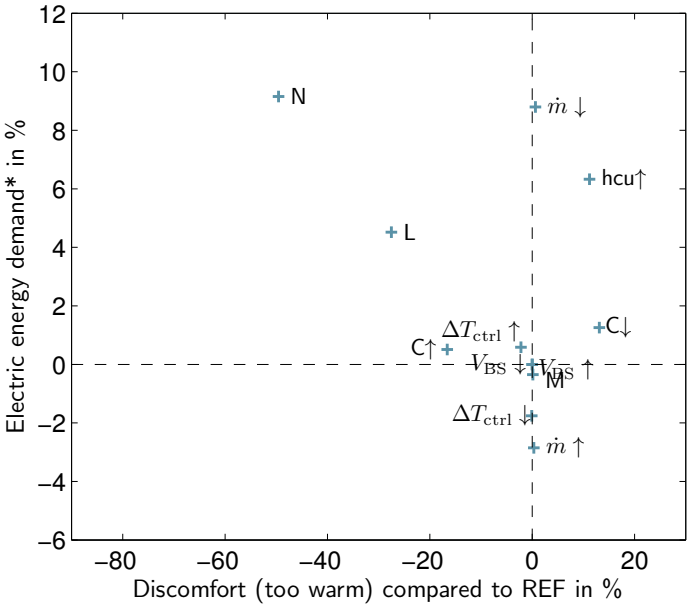


(b) Warm discomfort

**Figure 4.21:** Relative differences in electrical energy and discomfort of single measures compared to the reference system WBH. $\dot{m}\uparrow/\dot{m}\downarrow$: Higher/lower mass flow rate in the condenser cycle. $C\uparrow/C\downarrow$: Higher/lower building mass. $\Delta T_{\mathrm{ctrl}}\uparrow/\Delta T_{\mathrm{ctrl}}\downarrow$: Larger/smaller control hysteresis. hcu↑: Heating curve set higher. N/L: No/lower occupation profile.

# 5 Application of model

In chapter 4 a comprehensive tool for evaluating heat pump systems was described. A reference system was demonstrated in the last sections. On the one hand it showed that the mean supply temperature considerably influences heat pump efficiency. On the other hand, user interactions are detected to have a strong impact on seasonal performance.

In this chapter, using the reference system model of chapter 4, different control schemes are evaluated which take into account information from the heated zones.

## 5.1 Additional reference systems

Electrical actuators functioning as radiator valve controls allow the programming of the room set temperature. This can either be done manually or automatically with an intelligent adaptive algorithm as described by Adolph et al. (2013). In the latter case, the set temperature is lowered in non-occupied rooms. The algorithm learns user profiles and raises the set room temperature before periods of occupancy, providing comfort when the user enters the room.

In this control concept, the standard thermostatic valve heads in each room are exchanged by electric actuators which are PI controlled. The actuators are modeled as ideal which means they can perfectly access every position within the range of valve positions. In reality, actuators usually move in steps[1]. One important difference of PI controlled actuators compared to thermostatic heads (P controllers) is the lag of a permanent control offset. This can be seen in figure 5.1 (a) and (b) on page 98: The air temperature in the room is kept at a value approximately 1 K higher than the set value in the reference system REF[2]; in the system with electric valve actuator and PI control (EA), the air temperature is controlled to the set value. However, in this case it means that the operative temperature is evaluated as too low for system EA because the mean radiant temperature is lower in room 8.

Based on the user presence profiles (see section 4.3.3 and appendix D) room set temperature profiles are generated. The set value is lowered by 2 K in times of no user presence and during nighttime (11 pm to 6 am). One hour before user presence or daytime starts, it is set to the nominal value.

[1] Challenges occurring with real electric actuators are addressed by Reulen (2014).

[2] The bivalent reference system has the insulation standard of "WSchV84" and the "high" occupancy profile WBH, see section 4.3.

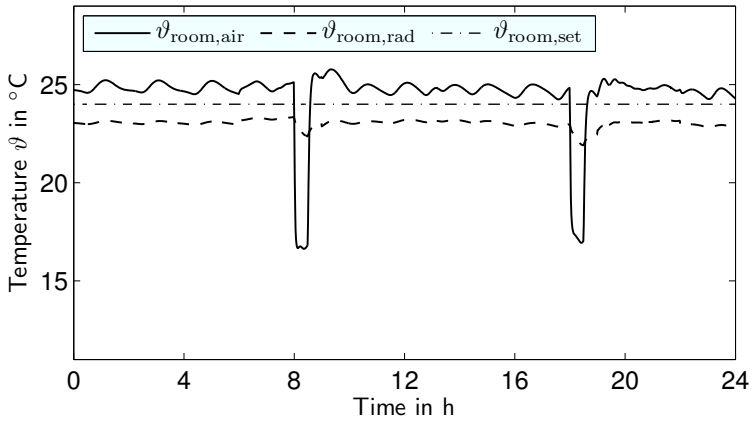


(a) Reference system (REF)

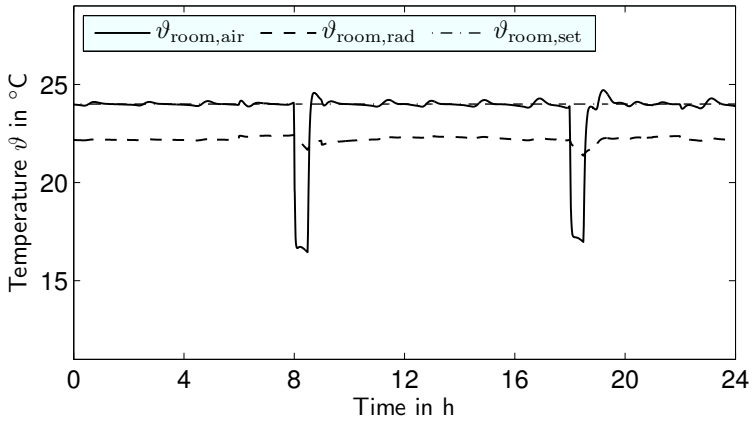


(b) Electrical valve actuators with PI control (EA)

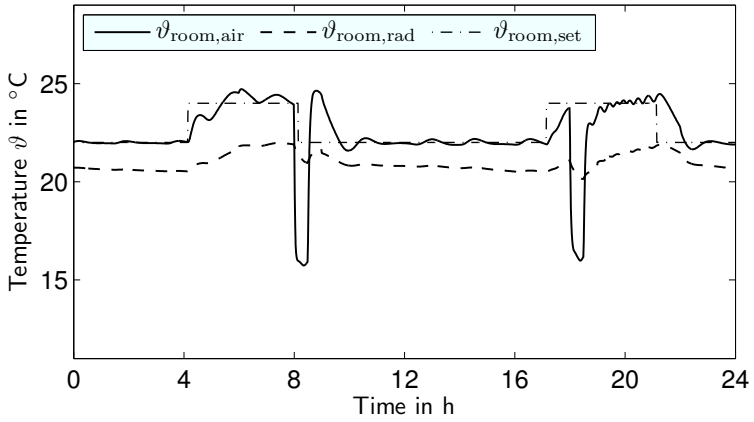


(c) Electrical valve actuators with PI control, variable set temperature profile (EAvar)

**Figure 5.1:** Daily variation of air, radiative and set temperature of room 8 for reference system (REF) and systems with electrical valve actuators (EA) and variable set temperature profile (var) (December 24).

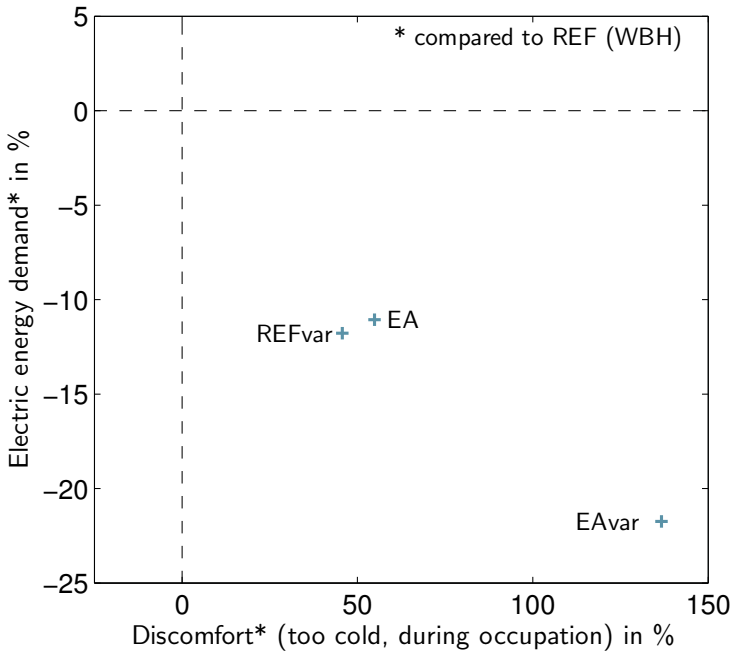


**Figure 5.2:** Relative differences in electrical energy and cool discomfort during occupation of systems with electrical valve actuators (EA) and variable room set-points (var) compared to the reference system (REF).

Figure 5.2 shows a comparison of a system with the variable set temperature profile (REFvar) to the reference system (REF). Discomfort is only compared during times of user presence in the heated zones. In addition, electrical valve actuators with PI controls (EA) are simulated instead of thermostatic valve heads which use P controls. The results of this system using a variable set temperature profile are also shown (EAvar). The total values for the calculation of discomfort are listed in tables 5.1 and 5.2 on page 100.

By lowering the room set temperature in times of no user presence, 12% of electrical energy demand can be saved. This is because of a lower heat demand. Another reduction of heat demand is achieved by using PI controls instead of P controllers. Whereas a P control always has a offset, the PI controller yields an exact match of room temperature to set temperature. This means that with thermostatic heads the mean room temperature generally is too high. However, in both cases deviations occur due to heat gains (positive deviations) and window opening (negative deviations).

In the case of variable room set temperatures, discomfort is considerably higher than for the configurations with constant set temperature. Generally, the air temperature rises quickly after a period of lower set temperature and as mentioned before, time for heating-up is part of the schedule. Nevertheless, the mean radiant temperature needs much longer to increase. Especially in the bath, which is only occupied during short periods, this is a problem. In addition, with adjacent rooms being on a lower temperature level, heat loads of heated rooms are higher and walls need even

**Table 5.1:** Discomfort of the reference system with variable set temperature profile (REFvar), calculated according to section 4.4.

| Type of discomfort | too cold, occupied periods | too warm, occupied periods |
|---|---|---|
| Squared Kelvin-hours | 1931 $K^2h$ | 4381 $K^2h$ |
| PPD weighted PMV | 636.2 h | 3006 h |
| Percentage of hours out of PMV comfort band | 3.9% | 17% |

**Table 5.2:** Discomfort of the system with electrical valve actuators and variable set temperature profile (EAvar), calculated according to section 4.4.

| Type of discomfort | too cold, occupied periods | too warm, occupied periods |
|---|---|---|
| Squared Kelvin-hours | 3137 $K^2h$ | 3221 $K^2h$ |
| PPD weighted PMV | 2521 h | 2532 h |
| Percentage of hours out of PMV comfort band | 15% | 14% |

longer to be heated up. This aspect has to be carefully addressed by the potential algorithm that calculates the room set temperatures.

Figure 5.1 on page 98 shows the daily variation of the room air, radiation and set temperature of room 8 for the reference system WBH with P controlled thermostatic valves (REF) and the system with PI controlled electrical valve actuators (EA) for a constant and variable set temperature profile. Room 8 is the bath which has higher room set temperatures than the other rooms of the building. In all three figures the periods of window opening can be seen when the air temperature abruptly declines and rises half an hour later. The P control in part (a) of the figure shows a deviation of the air temperature: The deviation of supply temperature due to on/off control of the heat pump is transferred to the room temperature. With the PI control in part (b) these deviations are smoothed out by the control. Indirectly, this comparison shows the high amount of work of the PI controller for adjusting the radiator valve position. With the variable profile the mean radiant temperature is considerably lower because the room is only heated to the target temperature of 24 °C two times a day. The air temperature attains the set value during periods of user presence. The second window opening strongly interferes with a period of heating up. The development of the air temperature after the first window opening shows that no precaution in the valve controller is implemented; when the air temperature falls it fully opens the valve. When the window is closed the valve is still open and the air temperature strongly overshoots the set value.

The main reason for thermal discomfort in the heated rooms is the pulse ventilation. In room 5 which uses constant ventilation during daytime, no discomfort occurs (see figure 5.3). The highest values for discomfort occur in room 8 which has been discussed above. The reasons for additional discomfort with PI control and variable set temperatures have also been discussed before; figure 5.3

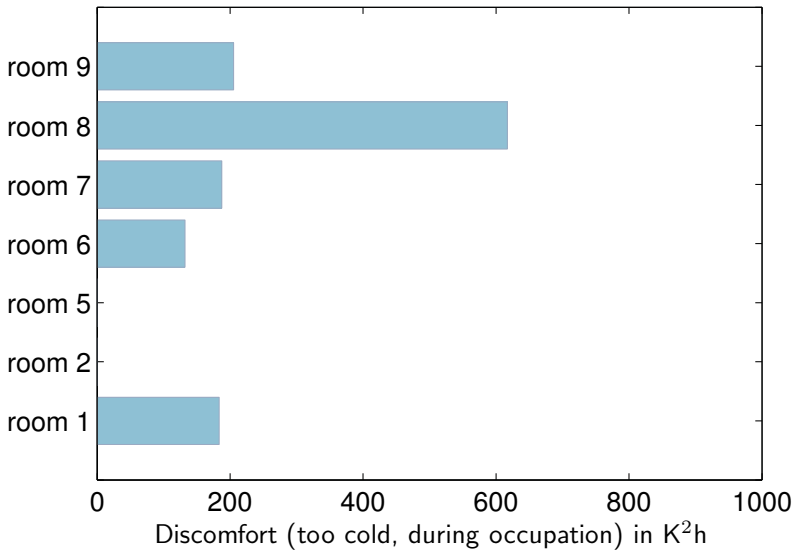


(a) absolute values of discomfort of reference system (REF).

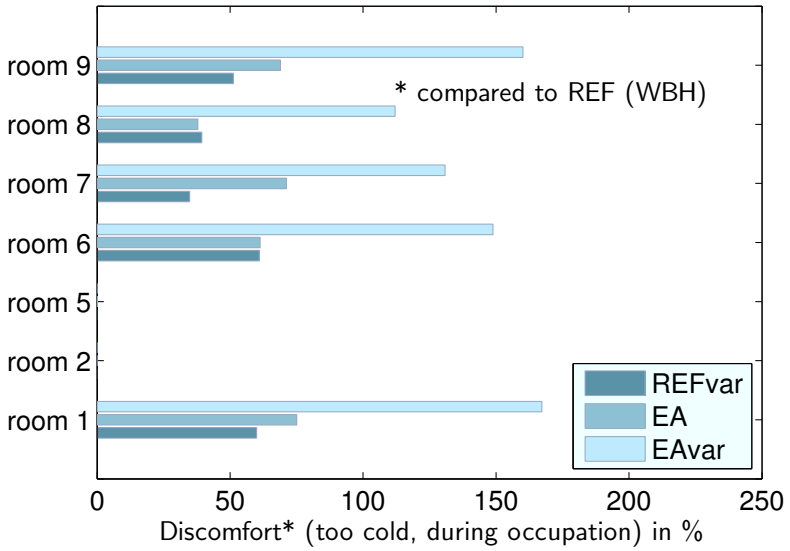


(b) Relative differences of systems with variable set temperature (var) and electrical valve actuators (EA) compared to reference system (REF).

**Figure 5.3:** Discomfort of reference systems without and with variable room set temperature profile and without and with electrical valve actuators with PI control.

shows that all rooms but room 5 are affected by this discomfort. Differences between the rooms are due to various reasons, mainly the schedules of occupation, inner gains and ventilation.

In the following paragraphs, certain model configurations are calculated with a variable set temperature profile or PI valve controls. They are then compared to the reference configurations described above and are marked accordingly.

## 5.2 Standard supply temperature adaption concept

The standard concept for implementing an influence of the room temperature on the supply temperature is the *reference room* (RR) concept. Usually, one room temperature of a reference room is measured. According to this temperature, an offset is subtracted from the supply set temperature.

The functional diagram in figure 5.4 shows this type of control. Basically, the diagram shown in figure 2.10 is extended by a connection of the measured room temperature to the block calculating the offset on supply set temperature. This offset can also take positive values when the room temperature is too low which can lead to a lower efficiency.

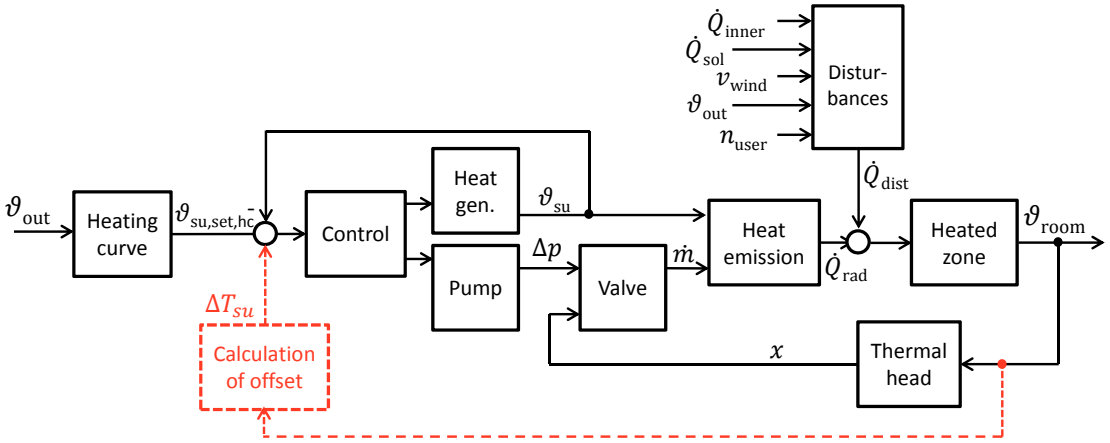


**Figure 5.4:** Functional diagram of a heating system with heating curve control, room temperature offset calculation and thermostatic valves (simplified with one heated zone).

Here, the living room (room 1 of the building model) is chosen as reference room. This concept is based on the idea that the reference room is representative for the whole building. This leads to discomfort in the other rooms if they do not behave like the reference one, e.g. if inner gains do not occur at the same time. In existing buildings in Germany this poses a problem in reality because it is unlikely that all zones behave similarly.

This concept is also tested with multiple reference rooms. In all rooms but rooms 3 and 4 (the corridor and WC/storage) the air temperature is measured. For the calculation of the offset, the minimum error signal of all rooms is used. Both concepts can save energy compared to the reference system (see figure 5.5). Yet, when controlling multiple rooms energy savings of the concept

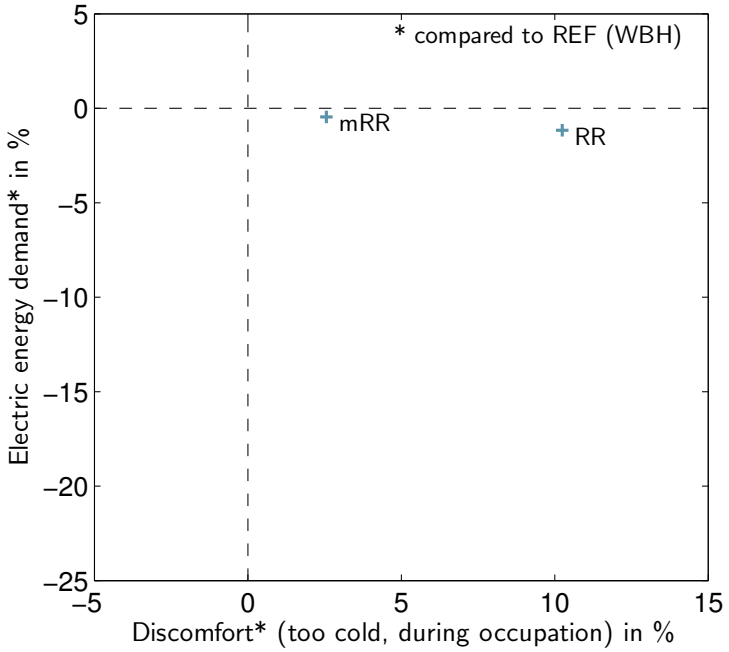


(a) Constant room set temperature

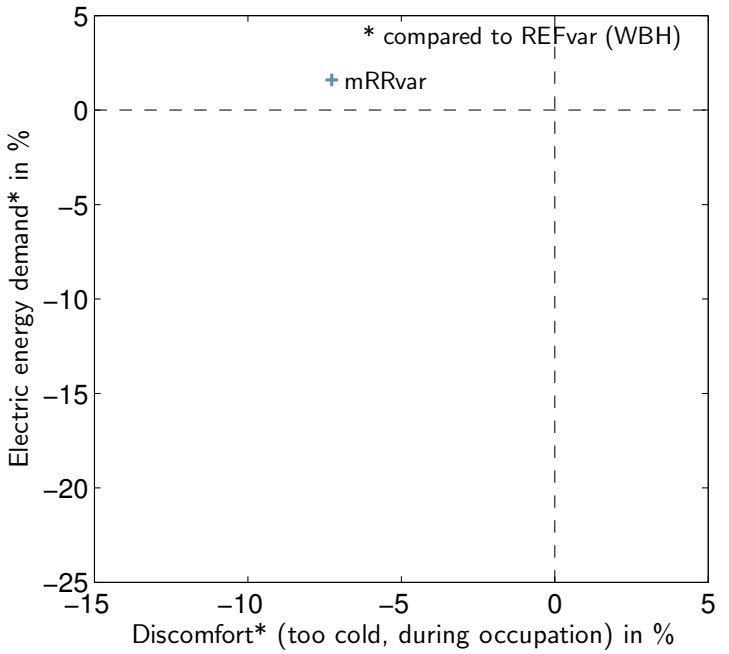


(b) Variable room set temperature

**Figure 5.5:** Relative differences in electrical energy and cool discomfort during occupation of systems reference room offset (RR), multiple reference rooms (mRR), without and with variable room set-points (var) compared to the reference system (REF).

(mRR) are negligible. The savings for the single reference room configuration are 1.2%. In the case of a variable room set temperature, the concept yields a higher comfort than the reference system. However, it has a higher energy demand (1.6% compared to REFvar).

## 5.3 Advanced supply temperature control concepts

When all thermostatic valves in a heating system are in a position[3] below the nominal value $x_{\mathrm{nom}}$, the supply temperature can be lowered to a value at which one valve position reaches $x_{\mathrm{nom}}$. This kind of control requires a communication interface with the (electronic) thermostatic valves (Rietschel, 2005). To ensure that all rooms of the building are heated properly, only the maximum valve position is taken into account for the supply temperature adaption. The adaption process has to be designed carefully to prevent instabilities (Kähler and Ohl, 2008). This is achieved through a delayed adaption process (Rietschel, 2005) implemented either through a filter element or through a discrete algorithm (Kraft, 2002). The first two of three control concepts which are proposed in the following sections operate similarly to this supply temperature adaption concept.

### 5.3.1 Rule-based supply temperature adaption concept (RB)

#### Description of RB controller

A rule-based controller is presented in Huchtemann and Müller (2013). It uses the position of the radiator valve as control variable. It is proportional to the difference of the room set temperature and the room temperature, the latter being the control variable. If it is measured directly, the room temperature also can be taken as control variable, which is done here. The heating curve calculates the basic supply set temperature. The functional diagram shown in figure 5.4 also applies for this concept. It calculates an offset $\Delta T_{\mathrm{su,set}}$ which is added to the supply set temperature:

$$T_{\mathrm{su,set}} = T_{\mathrm{su,set,hcu}} + \Delta T_{\mathrm{su,set}} \tag{5.1}$$

Yet, the offset is calculated differently. The controller changes $\Delta T_{\mathrm{su,set}}$ step-wise. If the difference between room temperature and room set temperature $\Delta T_{\mathrm{room}}$ is within a given range, $\Delta T_{\mathrm{su,set}}$ is not changed.

$$\Delta T_{\mathrm{room,min}} < \Delta T_{\mathrm{room}} < \Delta T_{\mathrm{room,max}} \Rightarrow \Delta T_{\mathrm{su,set}}(k) = \Delta T_{\mathrm{su,set}}(k-1) \tag{5.2}$$

[3] See section 2.4.3 for the characteristic of thermostatic valve heads.

$k$ denotes the current time step of the controller. When $\Delta T_{\text{room}}$ falls below or exceeds this range, the offset is increased respectively decreased.

$$\Delta T_{\text{room}} < \Delta T_{\text{room,min}} \Rightarrow \Delta T_{\text{su,set}}(k) = \Delta T_{\text{su,set}}(k-1) + \Delta T_{\text{rise}} \tag{5.3}$$

$$\Delta T_{\text{room}} > \Delta T_{\text{room,max}} \Rightarrow \Delta T_{\text{su,set}}(k) = \Delta T_{\text{su,set}}(k-1) - \Delta T_{\text{drop}} \tag{5.4}$$

$\Delta T_{\text{room}}$ is limited to negative values which means that the supply set temperature is not increased above the heating curve value. In addition, a lower boundary $\Delta T_{\text{su,set,min}}$ is defined:

$$\Delta T_{\text{su,set}} > \Delta T_{\text{su,set,min}} \tag{5.5}$$

At set temperature changes the required supply temperature may abruptly increase. Therefore, in one simulated configuration, $\Delta T_{\text{su,set}}$ is always set to zero when the room set temperature in any room is increased. Research of Huchtemann and Müller (2013) was used to find the parameters which are listed in table 5.3.

**Table 5.3:** Parameters of the rule-based controller.

| $\Delta T_{\text{room,min}}$ K | $\Delta T_{\text{room,max}}$ K | $\Delta T_{\text{rise}}$ K | $\Delta T_{\text{drop}}$ K | $\Delta T_{\text{su,set,min}}$ K |
|---|---|---|---|---|
| -0.5 | 0.5 | 1 | 1 | 10 |

In the system simulations, the minimum $\Delta T_{\text{room}}$ of all rooms is taken as input to the controller. The controller only takes into account rooms with closed windows to prevent a rising supply temperature during times of window ventilation.

### Simulation results of RB controller

The rule-based control concept uses standard thermostatic valve heads and therefore is compared to the reference system REF. Figure 5.6 on page 106 shows discomfort and electric energy savings. With constant room set temperature the concept yields 7.4% energy savings and has a discomfort 60% higher than the reference system. When using a variable room temperature profile, only 1.9% energy is saved and the discomfort is 5% higher (RBvar(a)). The reason for this is that with every room set temperature raise the supply set temperature returns to the heating curve value. As described above, this is done as a measure to ensure a sufficient heat flow for heating up the room. The system without this feature RBvar(b) yields higher energy savings (11%) but also higher discomfort (90%).

Figure 5.7 on page 107 shows the simulation results of the supply temperature for both configurations. Diagram (a) shows that supply temperatures are particularly lowered at colder outdoor air temperatures when longer periods of heating occur. This is due to the functionality of the control

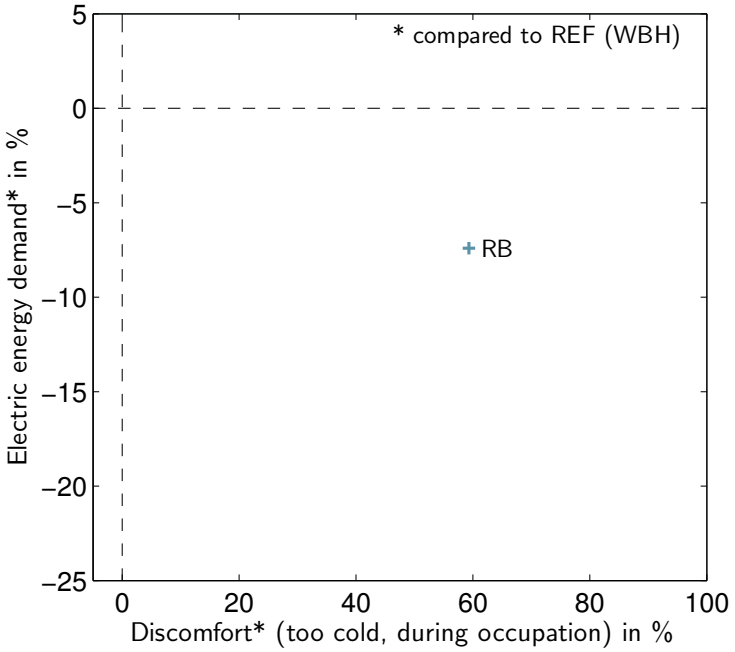


(a) Constant room set temperature

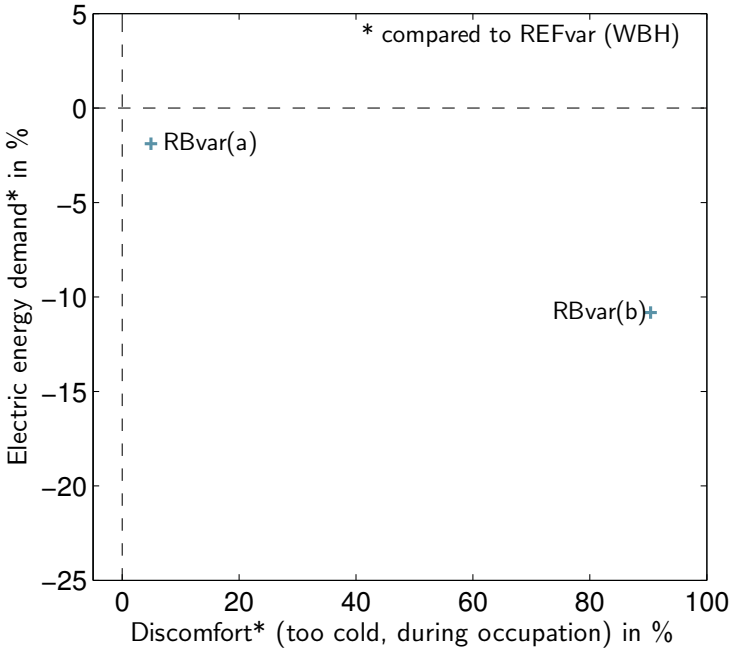


(b) Variable room set temperature

**Figure 5.6:** Relative differences in electrical energy and cool discomfort during occupation of systems with rule-based supply temperature control (RB) and variable room set-points (var) compared to the reference system (REF).

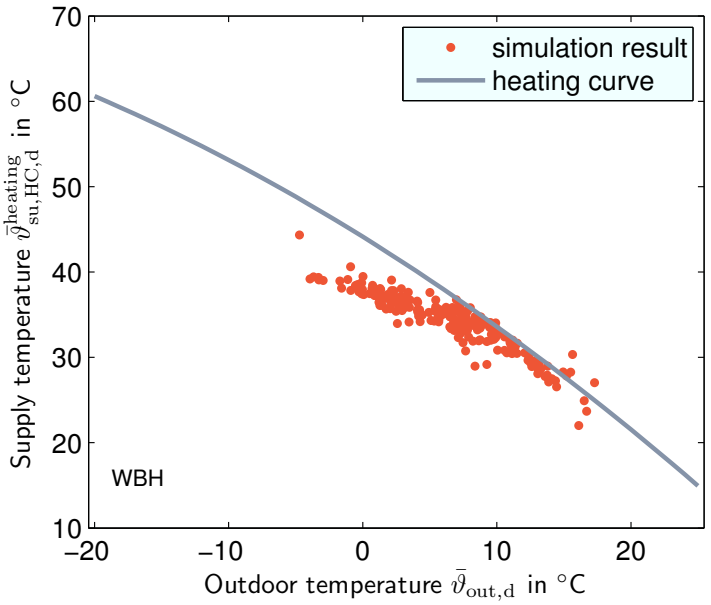


(a) Rule-based control (RB)

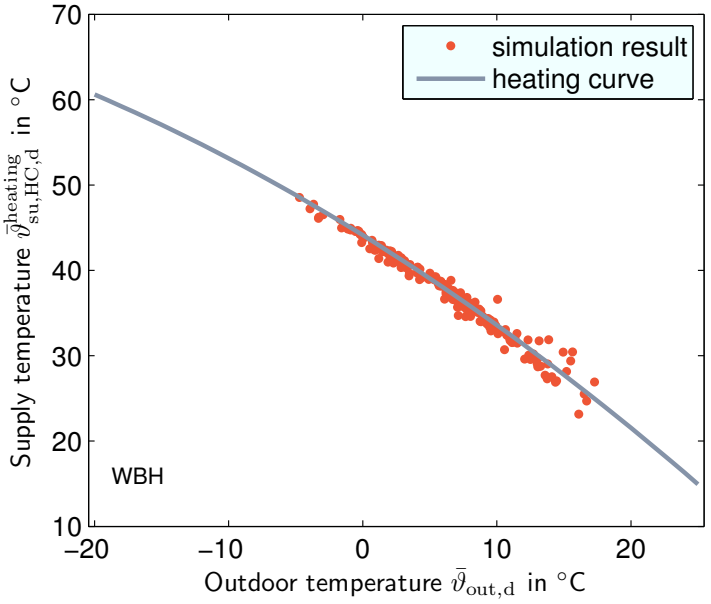


(b) Rule-based control, variable set temperature profile (RBvar)

**Figure 5.7:** Daily mean supply temperatures depending on daily mean outdoor air temperatures of systems with rule-based supply temperature control.

concept which successively lowers the supply temperature. Part (b) of the figure shows that with variable room set temperature supply temperature is not substantially lowered compared to the heating curve value.

### 5.3.2 PI supply temperature controller concept (PI)

#### Description of PI controller

The second control analyzed uses a PI controller. The input is the maximum of all valve positions that are measured in the heating system. The target value for valve opening is 1 (fully open). A PI valve control in each room controls the valve position between a value of 0 and a theoretical value of 1.2. The range for the actuating variable submitted to the valve is limited between 0 and 1. The range submitted to the PI supply temperature control is limited between 0.8 and 1.2. This approach allows for a sufficient actuating range of the PI supply temperature control. It is depicted in figure 5.8. The most obvious difference to the rule based control is that no heating curve is required in this control concept. The controller does not take into account valve positions of rooms with open windows.

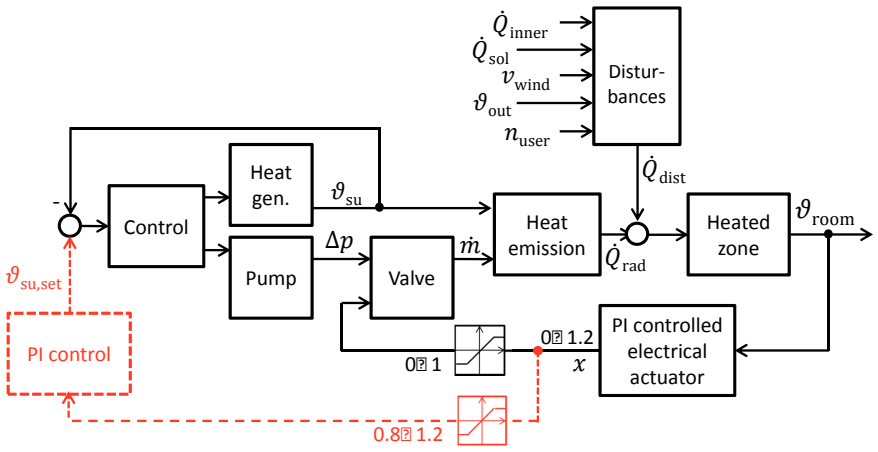


**Figure 5.8:** Functional diagram of the heating system with the PI controller.

#### Simulation results of PI controller

The system with PI controlled supply temperature mPI(a) saves 6.1% energy and has higher discomfort (39%) than configuration EA (see figure 5.9 (a)).

PI control can be optimized with respect to valve travel which is crucial for the energy demand of electric valve actuators. Here, two parameter settings with a integrator time constant of 600 s (a) and 300 s (b) are evaluated. As mentioned before, the highest discomfort occurs in room 8.

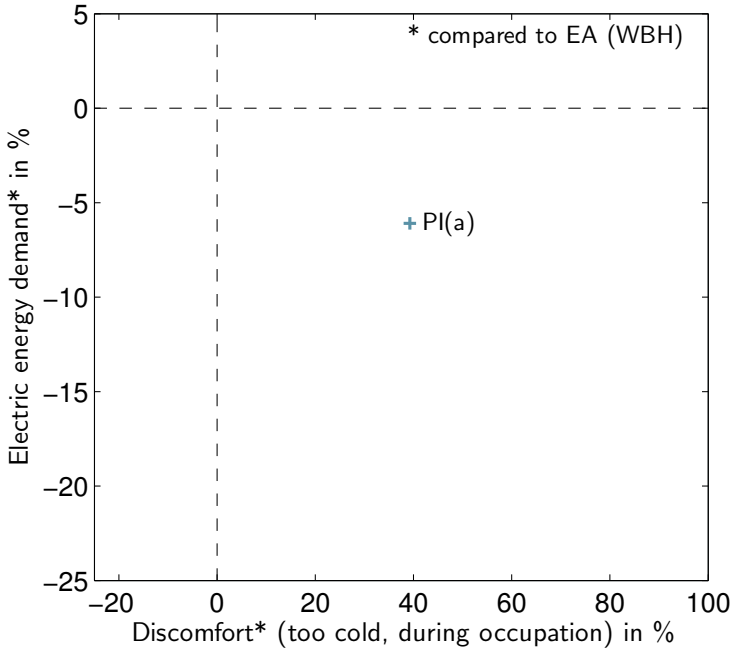


(a) Constant room set temperature

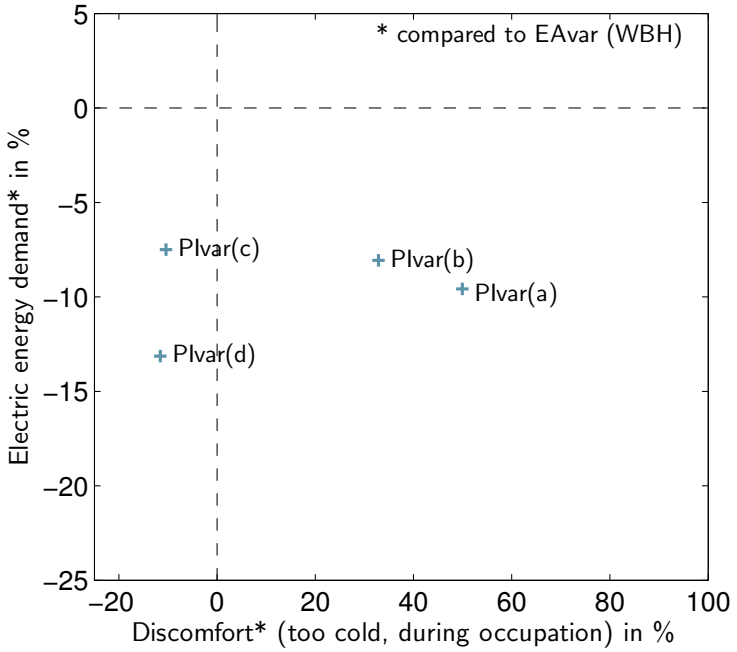


(b) Variable room set temperature

**Figure 5.9:** Relative differences in electrical energy and cool discomfort during occupation of systems with PI supply temperature control (PI) compared to the reference system with electrical valve actuators (EA) and variable room set-points (var). (a) to (d) refer to configurations described on page 108.]

Beside the standard configurations (a) and (b), two different measures are presented to prevent low operative temperature in this room:

c In the first one, during user presence, the radiator valve is fully opened and the radiator supplies a base heat load. An electric wall heating supplies the remaining power to heat the room to the comfort temperature. The electric wall heating has a surface of 2 $m^2$ and a high ratio of radiation to convection heat emission (90%). It is activated one hour before user presence.

d The second measure employs a heating panel instead of the standard radiator in the bath. A high share of the total heat is emitted as radiation and it is operated with low supply temperatures. It is parametrized with a ratio of radiation to convection heat emission of 75% and a surface area of 4 $m^2$.

With variable room set temperature 9.6% energy savings are yielded and discomfort is 50% higher (PIvar(a), see figure 5.9, page 109). Savings and comfort can be considerably influenced by the parametrization of the PI controller: With the faster controller of PIvar(b), discomfort can be lowered compared to PIvar(a), but energy savings are lower, too.

Summing up the values of all rooms, configurations PIvar(c) and PIvar(d) both can reduce discomfort compared to the reference system and nevertheless yield substantial savings in electrical energy (7.5% and 13% respectively). However, as can be learned from figure 5.10 discomfort is only reduced in room 8 at the expense of higher discomfort in the other rooms. This allows the conclusion that the thermal comfort of all rooms benefits from higher supply temperatures.

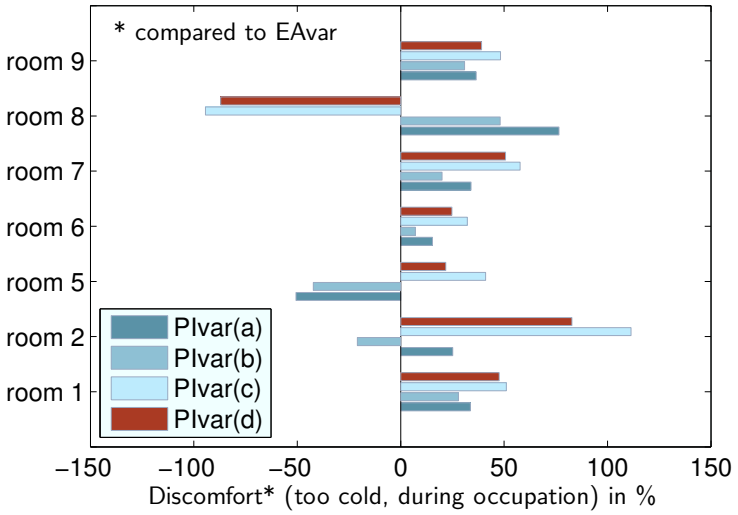


**Figure 5.10:** Discomfort in single rooms of reference systems with PI supply temperature control (PI) and variable room set temperature profile (var), relative values compared to the system with electrical valve actuators and variable room set temperature profile (EAvar).

Figure 5.11 compares the supply temperatures of configurations PIvar(a) and PIvar(c). The char-

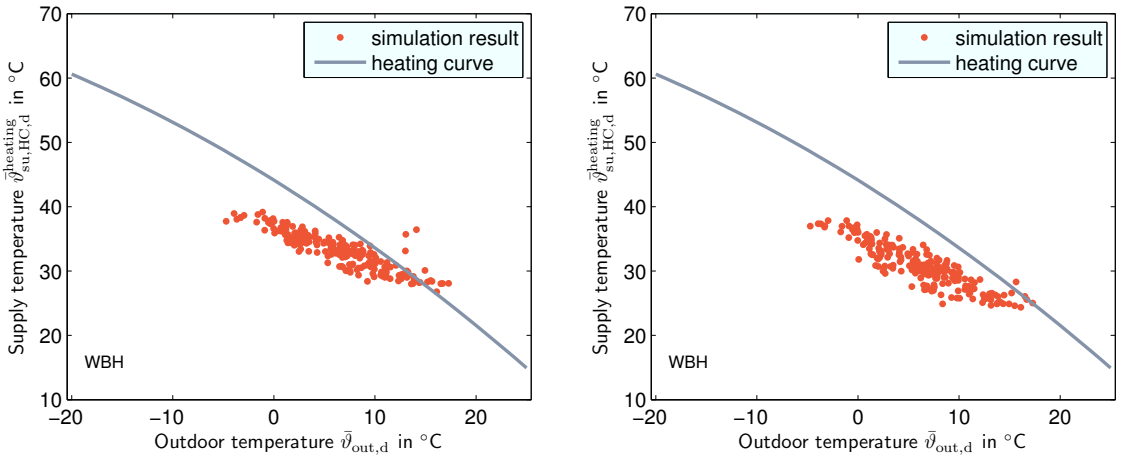


(a) PI supply temperature control, PIvar(a)

(b) PI supply temperature control, PIvar(c)

**Figure 5.11:** Daily mean supply temperatures depending on daily mean outdoor air temperatures of systems with PI supply temperature control (PI) and variable room set temperature profile (var). (a) and (c) refer to configurations described on page 108.

acteristic of supply temperature to outdoor air temperature is less steep than the original heating curve. For configuration PIvar(c) it can be seen that the limitation of the set temperature in room 8 results in lower supply temperatures. However, as an electrical heating is operated as an additional heat source in this room, overall energy demand is higher than in configuration PIvar(a).

### 5.3.3 Supply temperature prognosis control (MPC)

As the heat pump operates periodically due to the on-off control, the supply temperature cannot be controlled continuously but only during operation of the heat pump. The previous control concept for the optimization of the supply temperature does not require information about the room, the user behavior, weather influences other than the outdoor air temperature and the layout of the heating system. However, in modern houses and with new concepts of room control equipment (e.g. electronic valve actuators and control concepts as described by Adolph et al. (2013)), a lot of this information is available.

With this information and a prediction of the according data, it is possible to calculate a heat load estimation for each room. It allows to estimate the needed supply temperature for each room during the next operating cycle of the heat pump. Such predictions can be done using the concept of model predictive control.

### Description of MPC controller

Model predictive control (MPC) uses a simplified model of the controlled process to calculate the optimal control sequence at each time step $k$ for the next $N_1$ time steps, i.e. the prediction horizon. Usually, the first value of this control sequence is used as manipulated variable whereas the rest of the sequence is omitted. At the next time step the next sequence is calculated, this time from time step $k+1$, and again only the first value is used. This is also called *rolling horizon* concept.

In the controller presented here, the required supply temperature is calculated from a predicted heat load sequence for each heated zone. Instead of using only the first value, the maximum of the next $N_{\mathrm{op}}$ predicted values is used as actuating variable. $N_{\mathrm{op}}$ times the length of a time step is the estimated time that the heat pump is off between two operating cycles. In this way it is assured that the supply temperature is sufficient during the off-periods.

The concept of the controller is illustrated in figure 5.12, its integration to the heating system is shown in figure 5.13. The MPC receives the actual measured room temperature, the outdoor air temperature and their future set-points respectively predictions. It also has an input for the prediction of the inner and solar gains of the room. The output is the sequence of predicted values of heat load which are used to calculate the future supply temperatures (using the radiator equations in section 2.4.2) as well as $N_{\mathrm{op}}$ (using equation 3.9). The maximum supply temperature within the horizon of $N_{\mathrm{op}}$ is chosen as output. Like with the rule-based controller, only rooms with closed windows are taken into account. Using this control scheme for multiple rooms, one MPC controller is used for each room, the calculation of $N_{\mathrm{op}}$ is executed for the sum of heat load vectors and the maximum of all calculated supply temperatures is chosen as controller output (see figure 5.12).

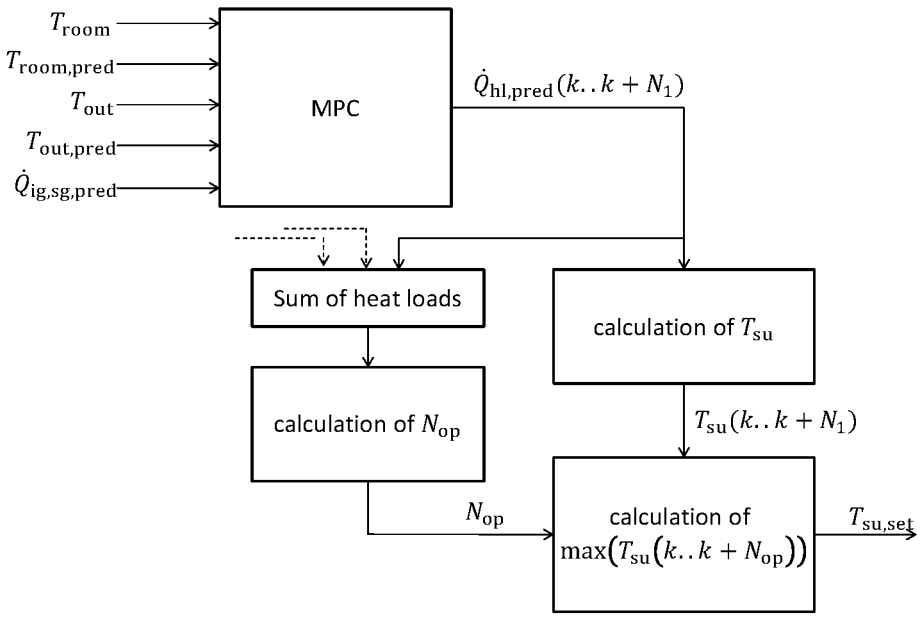


**Figure 5.12:** Concept of the MPC controller.

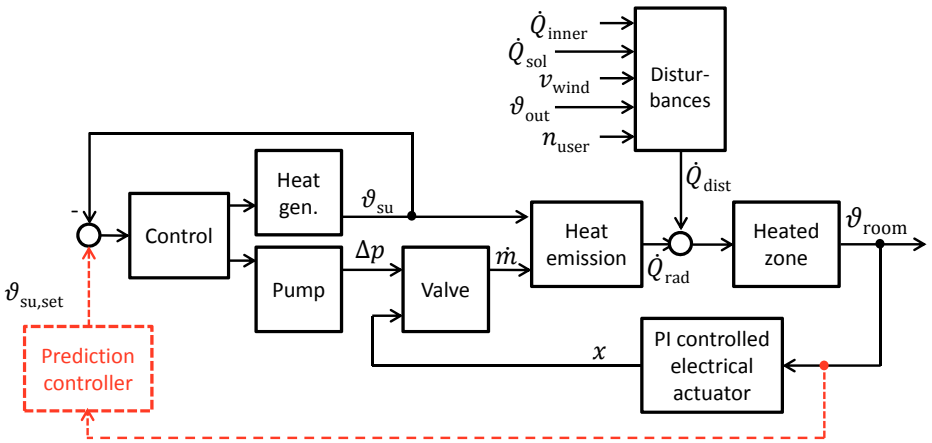


**Figure 5.13:** Functional diagram of the heating system with the MPC controller.

The MPC uses a room model with three capacities: the air volume, the outer wall and a capacity representing inner walls, floors and ceiling. Half of the heat gains through inner and solar gains are transferred to the room air node, the other half to the capacity of inner walls. Heat emitted by the radiator is split into 80% that are transferred to the air node and 20% that are transmitted to the inner wall capacity, corresponding to the characteristics of the radiator with respect to radiation and convection. The outer wall is modeled with two thermal resistances, one between the air volume of the room and the capacity of the wall and one between the capacity and the exterior. Heat transfer to adjacent rooms is not accounted for. The model does not distinguish between radiation and convection. The model is described in detail in appendix H and has been tested against the Modelica room model to assure a realistic response of the room temperature.

The optimization within a MPC is done according to a cost function which here is chosen as:

$$J = \sum_{j=N_1}^{N_2} \left(w_T \cdot \left(T_{\mathrm{room},k} - T_{\mathrm{room,set},k}\right)\right)^2 + \sum_{j=N_1}^{N_2} \left(w_{\dot{Q}} \cdot \left(\dot{Q}_{\mathrm{H},k} - \dot{Q}_{\mathrm{H},k-1}\right)\right)^2 \tag{5.6}$$

Within the control horizon, this function is minimized by taking into account the constraints, which are the boundaries of the heat emission of each radiator:

$$0 < \dot{Q}_{\mathrm{H}} < \dot{Q}_{\mathrm{hl,nom}} \tag{5.7}$$

According to the weights $w_T$ and $w_{\dot{Q}}$ of the cost function, the optimization is done for compliance of room temperature $T_{\mathrm{room}}$ ($w_T > 0$) or for a smaller variation of the actuating variable $\dot{Q}_{\mathrm{H}}$ ($w_{\dot{Q}} > 0$). Here, this means that for each room the controller can be tuned for higher comfort or higher energy efficiency.

The controller is implemented in the MATLAB®-Simulink[4] software which contains a MPC tool-

[4] See SIMULINK (2014).

box that allows direct implementation of the model in state space representation. For simulations Simulink and Dymola (which runs the heat pump heating system and building model) are coupled using the software TISC[5].

This control concept requires very detailed knowledge on the controlled building. Therefore, especially when being implemented in existing buildings, the controller models should be equipped with a model identification process which makes manual parametrization unnecessary (e.g. as described in Bianchi (2006)).

### Simulation results of MPC controller

Three different strategies are simulated for the MPC controller.

(a) In the first one, only the compliance of the room temperature is part of the cost function which means that for all rooms, $w_{\dot{Q}} = 0$ and $w_T = 1$.

(b) The second strategy includes the weighting of the actuating variable in all rooms ($w_{\dot{Q}} = 0.005$ and $w_T = 1$).

(c) In the last configuration $w_{\dot{Q}}$ is twice as high as in (b) in room 8. This is a scenario in which the user decides to accept discomfort in the bath in return for energy efficiency of the heat pump.

With constant room set temperature, the control optimized for the compliance of room set temperature MPC(a) yields higher comfort than the reference configuration EA (see figure 5.14). This is at the expense of energy savings; the electric energy demand is 24% higher. The configuration tuned for room temperature compliance and smaller variation of heat emission attains 6.9% energy savings and a 76% higher discomfort.

Being tuned for higher energy savings in room 8 (MPC(c)) the control yields higher energy savings (13%) and higher overall discomfort (263%). And in figure 5.15 on page 116 it is shown that this is mainly due to a considerably higher discomfort in room 8. However, the operative temperatures of the other rooms are also affected. In reverse, this shows that supply temperatures increased because of a demand in room 8 are advantageous for the thermal comfort of other rooms. This has been detected for the PI control already (see section 5.3.2).

With variable set temperature profile all configurations of the MPC control have higher discomfort than the reference EAvar. With the configuration tuned for room temperature compliance MPCvar(a) the discomfort is 39% higher but energy savings only sum up to 2.9%. The other two configurations yield higher savings and higher discomfort (MPCvar(b): 13% savings, 140% higher discomfort; MPCvar(c): 19% savings, 251% higher discomfort, both compared to EAvar). Figure 5.16 on page 116 shows that discomfort is not as clearly concentrated in room 8 as in the systems with

[5] See TISC (2014).

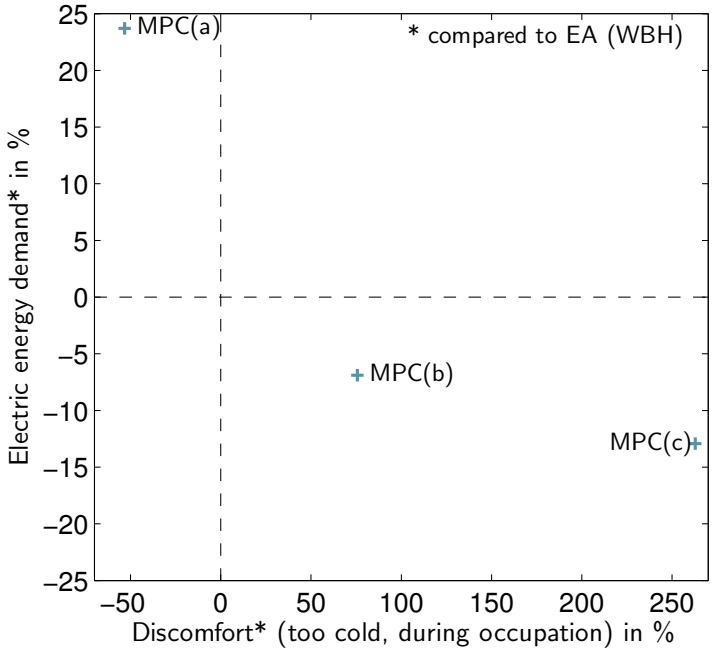


(a) Constant room set temperature

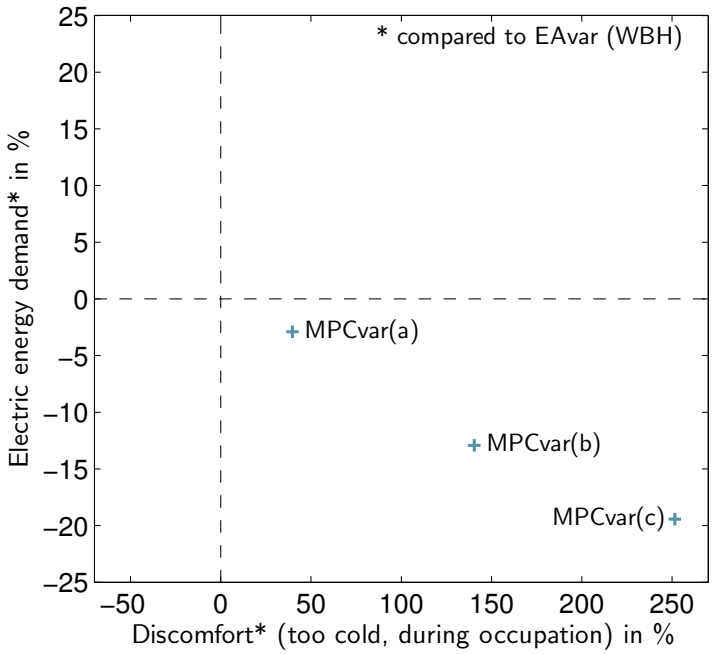


(b) Variable room set temperature

**Figure 5.14:** Relative differences in electrical energy and cool discomfort during occupation of systems with MPC supply temperature control (MPC) compared to the reference system with electrical valve actuators (EA) and variable room set temperature profile (var). (a) to (c) refers to configurations described on page 114.

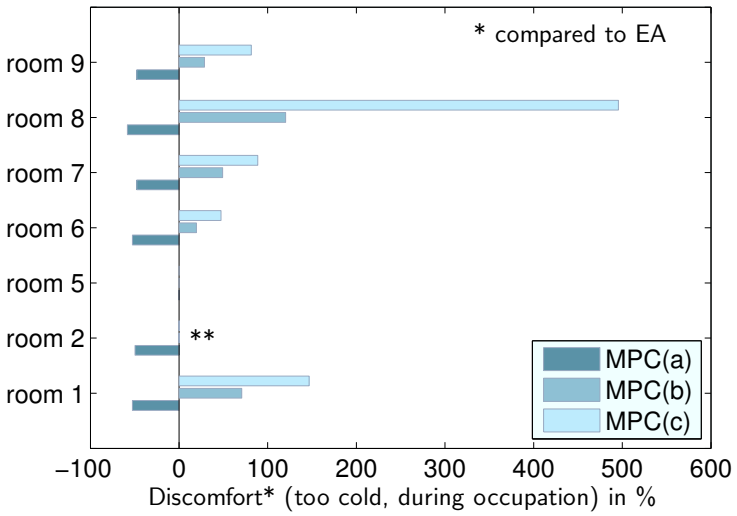


**Figure 5.15:** Relative differences of discomfort in single rooms during occupation of systems with MPC supply temperature control (MPC) compared to the reference system with electrical valve actuators (EA). (a) to (c) refers to configurations described on page 114. **: Values for room 2, configurations MPC (b) and (c) are very high (up to 10 times the reference value) and therefore not shown in this diagram; however, reference values for this room are near zero.

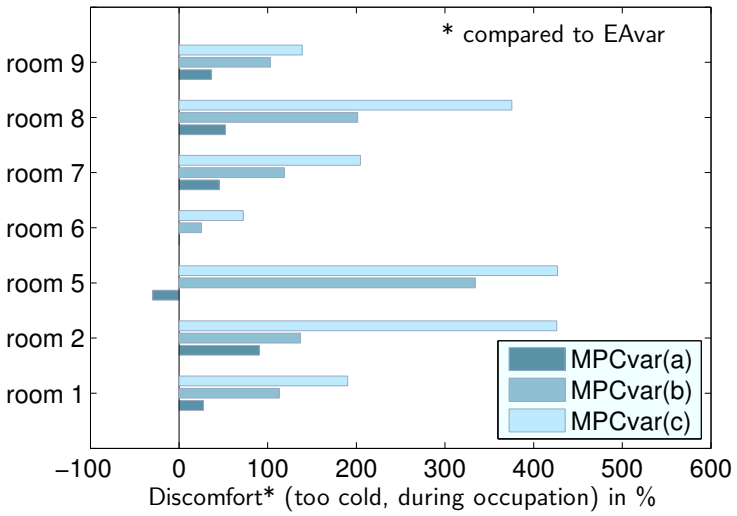


**Figure 5.16:** Relative differences of discomfort in single rooms during occupation of systems with MPC supply temperature control (MPCvar) compared to the reference system with electrical valve actuators and variable room set temperature profile (EAvar). (a) to (c) refers to configurations described on page 114.

constant set temperature profile. However, when looking at this figure, it has to be considered that the absolute values of discomfort in room 5 are very low.

Figure 5.17 on page 118 shows the daily variation of the air, radiation and set temperature of room 8 for the three differently weighted cost functions in MPC controlled systems with variable room set temperature. In all diagrams the mean radiant temperature is too low with values around 20 or 21 °C which is a general problem of this room, especially when setting back the set temperature when the room is not used[6]. With the optimization for room temperature compliance, the air temperature is well controlled to the target value for most of the day.

With increased weighting of the cost function for slower adaption of heat flow, the room set temperature is less frequently kept. Especially in case of MPCvar(c) the valve in room 8 is opened throughout most of the day and the room air temperature is influenced mainly by the supply temperature which fluctuates due to on/off control of the heat pump and due to demand of the remaining rooms.

## 5.4 Discussion of control concepts

Generally, every reduction of supply temperature results in a higher discomfort than a reference systems without such reduction. This is because at periods that the room is heated up, without supply temperature reduction a higher heat flow rate is available. These periods occur after times of no user presence, at set temperature changes or window openings. These effects are considered in the simulations. Another reason is that positive discomfort is not accounted for in the evaluation. By overheating heated zones, a safety buffer for the prevention of cool discomfort is build up. With an intelligent supply temperature control, overheating is decreased. The model used in this work does not consider the user intentionally using this overheating.

However, in real systems the user interacts with the control system, which is not considered in the simulated model. If the user feels thermal discomfort he is likely to change the set temperature. In this context systems that allow a fast reaction to these changes are favorable.

Additionally, it has to be answered if the lower energy demands of supply temperature controlled configurations are due to higher efficiency or due to lower heat demand. Figure 5.18 on page 119 offers an answer to that question. In diagram (a) of this figure the heat demand and the energy demand of different configurations are compared to the reference system EAvar. On the right side of the dashed line savings in heat demand are smaller than the savings in energy demand. The efficiency of the system (the SPF) is thus higher in this zone than the efficiency of the reference system. The opposite applies for the zone left of the dashed line. On the dashed line the same efficiency as in the reference system is yielded.

[6] This has also been detected for the reference systems in section 5.1

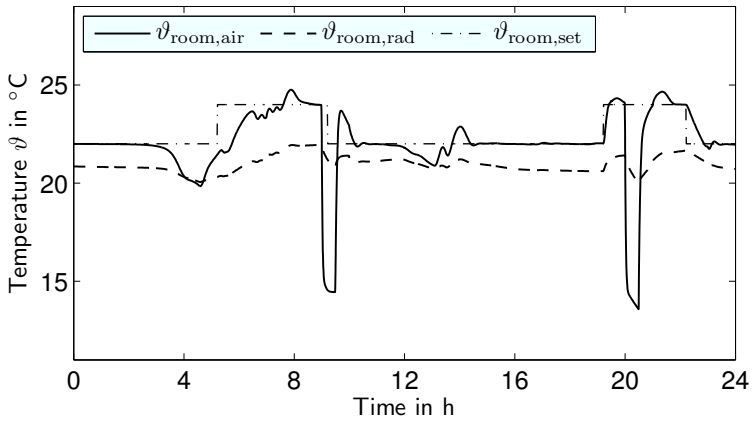


(a) MPCvar(a)

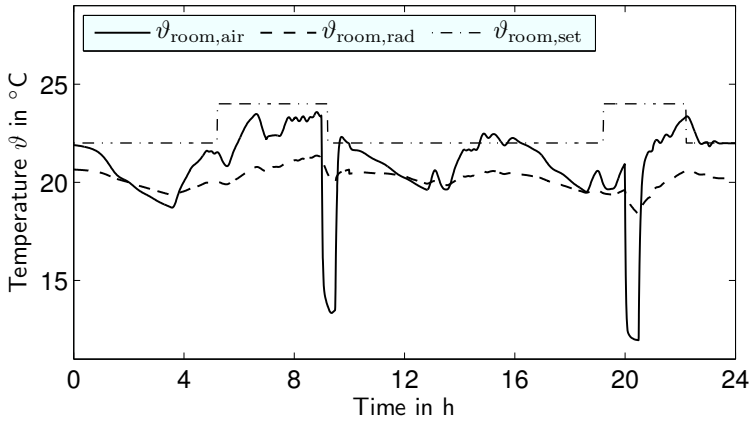


(b) MPCvar(b)

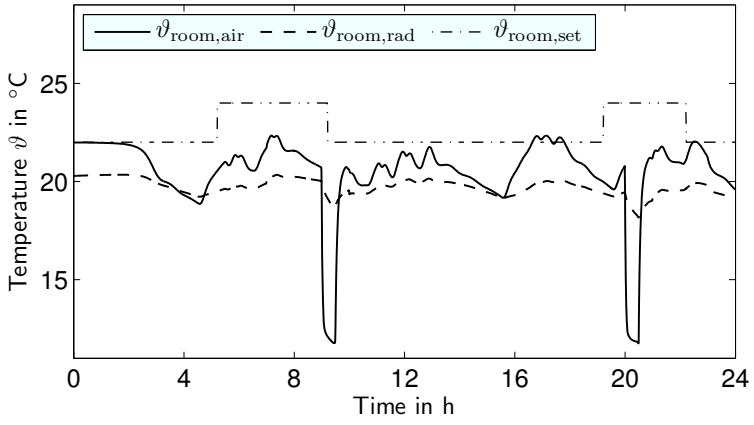


(c) MPCvar(c)

**Figure 5.17:** Daily variation of air, radiative and set temperature of room 8 for systems with MPC supply temperature control and variable room set temperature profile (MPCvar) (December 1). (a) to (c) refers to configurations described on page 114.

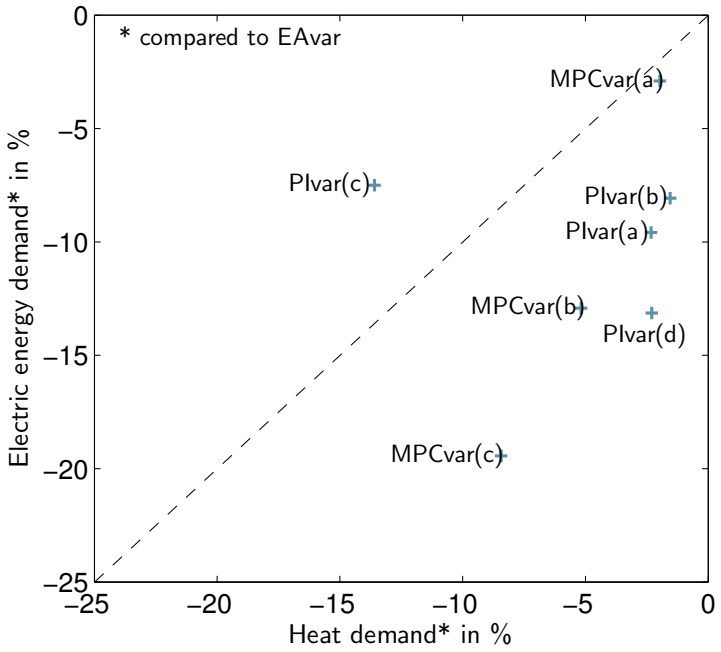


(a) Electrical energy and heating demand

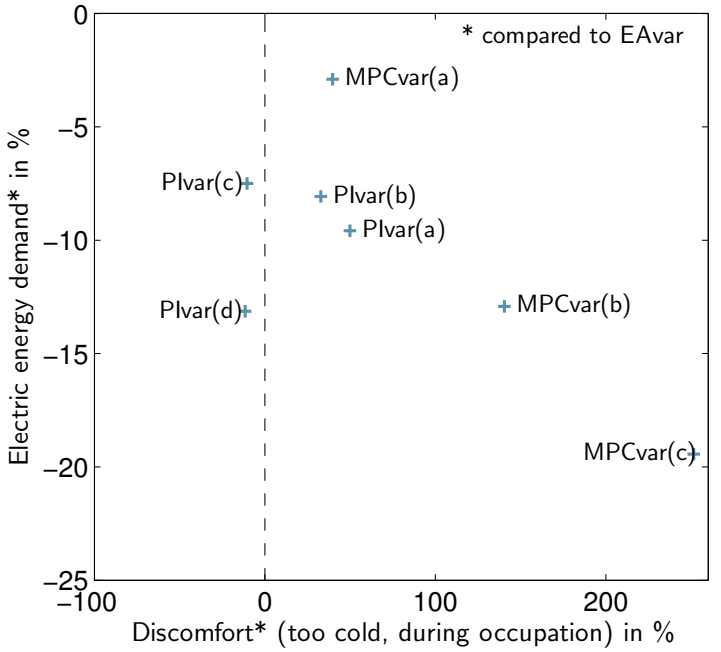


(b) Electrical energy and discomfort

**Figure 5.18:** Comparison of different supply temperature control concepts in systems with variable room set temperature (var) with respect to electrical energy, heating demand and discomfort. The systems are compared to the reference system with electrical valve actuators (EA).

Most of the systems with PI or MPC supply temperature control have a heating demand lowered by less than 5%. Only one system has a lower efficiency than the reference system. It is system PIvar(c) which features a direct electrical heating in room 8. The systems performing most efficiently and with the lowest constraints regarding comfort (see diagram (b) of figure 5.18, page 119) are PIvar(a), PIvar(b) and PIvar(d). They yield seasonal performance factors of 3.3 (PIvar(a) and PIvar(b)) and 3.5 (PIvar(d), compared to 3.1 of configuration EAvar). Apart from system PIvar(c), the SPF clearly depends on the mean supply temperature of the heating season, see figure 5.19.

In order to qualitatively compare the simulated control concepts with respect to applicability, performance and comfort, an overview of system characteristics is given in table 5.4.

**Table 5.4:** Selected characteristics of systems with different supply temperature control concepts: Rule-based (RB), PI and MPC.

| | **RB** | **PI** | **MPC** |
|---|---|---|---|
| Required knowledge about the system | normal | low | very high |
| Effort for parametrizing the controller | normal | normal | very high |
| Computational effort | low | high | very high |
| Comfort | good | fair | tunable |
| Energy savings | low | high | tunable |
| Required information transmitted from room to controller | difference from set temperature | valve position | room temperature |

The RB control does not require special knowledge of the controlled system. However, the hydraulic system has to be well designed. Errors in the determination of the heating curve can be partly corrected by this controller. The heating curve is still required and with it an outdoor air temperature sensor has to be installed which is, however, a standard component of heating system controls. The computational effort of the RB supply temperature control is low. This means that today's controller hardware suffices for an implementation.

In a system with constant room set temperature, the RB concept works fine. This controller is well suited to work in existing buildings without changing the radiator valve control. Theoretically, it functions with standard P-controlled valve heads as long as the room temperature and the set temperature is known. The easiest way for implementation is by transmitting the actual valve position to the supply temperature controller. Energy savings are low, especially when many set temperature changes occur. Yet, comfort is assured as the set temperature can always be set back to the heating curve value when rooms need to be heated up.

The PI control concept has the lowest requirements for knowledge about the controlled system when parametrizing it. Though, besides the simple functioning of such a control it can be opti-

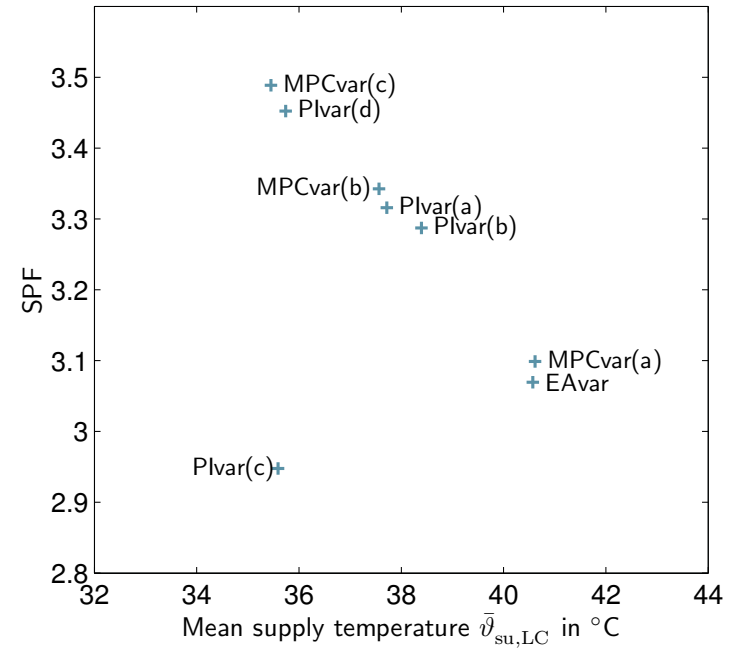


(a) SPF and mean supply temperature

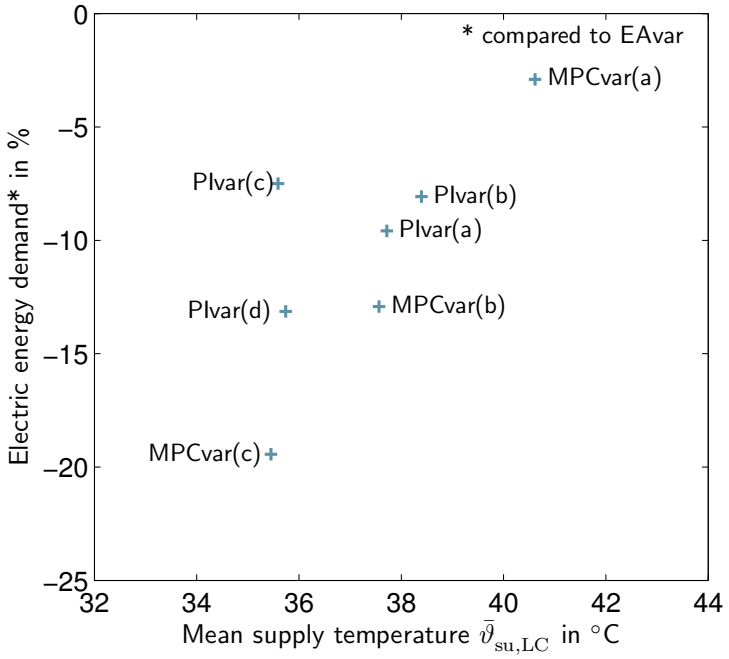


(b) Electrical energy and mean supply temperature

**Figure 5.19:** Influence of mean supply temperature in the loading circuit on SPF and electrical energy demand.

mized for different purposes such as comfort, energy efficiency or minimized valve travel. This requires more knowledge of the system or an automatized system identification process. In any case it requires more computing capacity than the RB controller. A heating curve and a sensor measuring the outdoor air temperature are not needed.

The PI supply temperature control needs electrical valve actuators on room level that transmit their actual valve position to the central supply temperature control. Yielded comfort is generally lower than with the RB control. It has been shown that measures such as the implementation of additional heaters can be applied to assure comfort in special cases and still energy savings are achieved (here: bathroom with substantially higher room temperature than the rest of the rooms).

The MPC control has the highest demands with respect to system knowledge, effort for parametrizing the controller and computational requirements. It needs to be combined with a system identification method (e.g. as described in Bianchi (2006)). However, this additionally increases computational effort. As a result, this kind of control is hardly applicable with today's controller hardware in one-family houses or standard heat pump heating system controller hardware. However, the MPC control uses data which is available when using modern room temperature control systems.

The proposed control concept can be tuned either for the purpose of increased comfort or increased energy efficiency. The control provides data to give the user information about the consequences of control settings. The models implemented in the controller are not detailed enough to fully consider the consequences of reduced comfort in single rooms.

Figure 5.20 shows how systems with different building insulation standards[7] and occupancy profiles[8] perform with the PI supply temperature control. Each system is compared to a reference system with the same insulation standard and occupancy profile but without advanced supply temperature control. Energy savings of systems with a high insulation standard E are considerably higher than with the lower level of insulation W. Increased occupation also leads to higher savings when applying the advanced supply temperature control. Generally, inner gains are more efficiently utilized for the purpose of heating the room to the set temperature; they do not lead to the same amount of overheating as in the reference systems[9]. But also energy efficiency of the heat pump is considerably increased ($SPF_1$ of 3.3 compared to 2.9 for configuration EBH).

The reference systems within this work are ideally dimensioned systems. In real buildings, notably in existing buildings, this is not typical. Often supply temperatures are set too high or radiators are over-dimensioned. The latter often is the case in existing buildings where insulation measures have been implemented. In order to illustrate the effect of different reference systems on the results, the PI supply temperature control PIvar(a) is compared to three additional systems. Compared to the initial reference system savings in electrical energy of 9.6% are yielded (comparison to a system with electrical valve actuators and variable set temperature profile EAvar).

[7] The insulation standards are presented in section 4.3.1.
[8] These profiles are presented in section 4.3.3.
[9] See section 4.5.1.

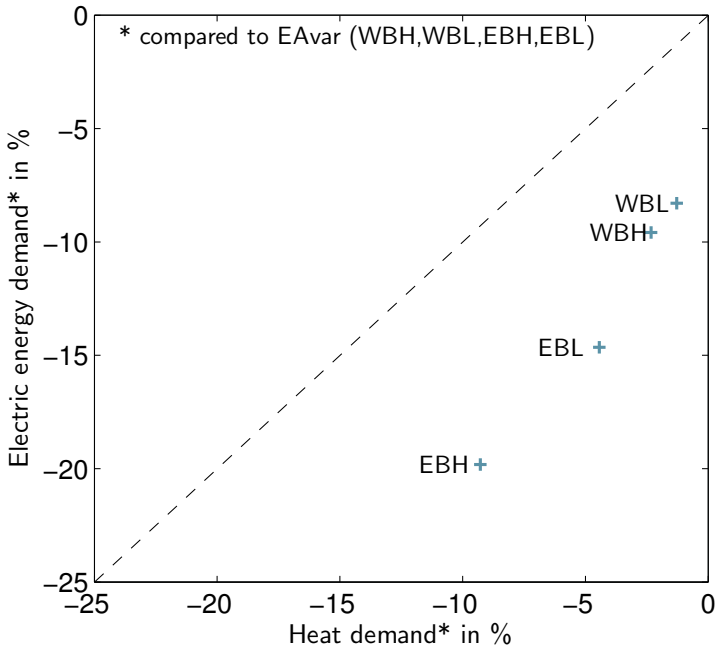


(a) Electrical energy and heating demand

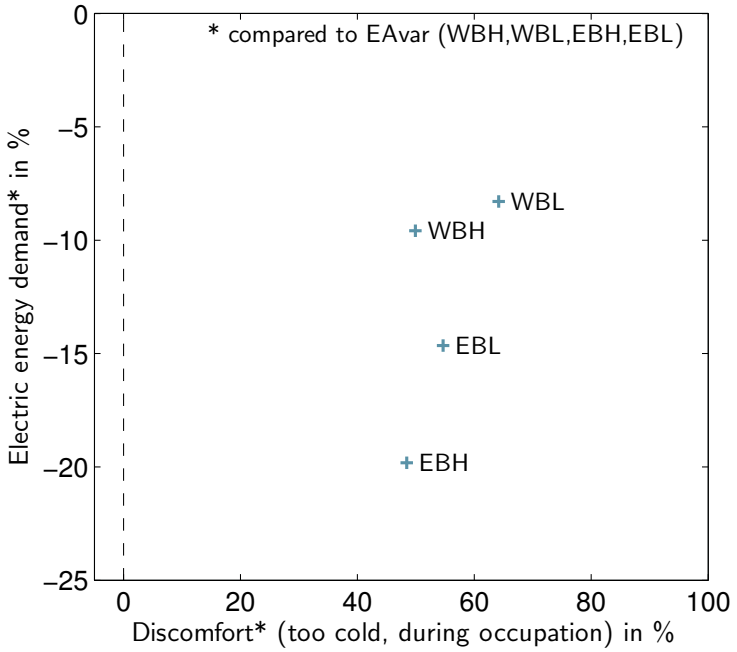


(b) Electrical energy and discomfort

**Figure 5.20:** Comparison of PI supply temperature control concept PIvar(a) for different insulation standards and user schedules with respect to electrical energy, heating demand and discomfort. W/E: Low/high insulation standard. B: Bivalent system. H/L: High/low occupation profile

If PIvar(a) is applied to a building with a strongly over-dimensioned heating system[10] the savings are 12%. Presuming reference system EAvar with a heating curve calculated for a too high room temperature[11], PIvar(a) yields savings in electrical energy of 15%. Savings of 29% are calculated if the system with supply temperature control is compared to a reference system with standard thermostatic radiator valves and no user-dependent room set temperature profile. In conclusion, savings in real buildings are likely higher than when comparing ideal systems in simulation.

The simulation results show large relative differences of discomfort between systems with supply temperature control and reference systems. They mainly result from discomfort directly after times of strong natural ventilation. It is disputable if a real user would judge thermal comfort during those periods in the same way he would in other periods. Nevertheless, in this work, this difference in perception is not taken into account.

[10] Therefore, the building shell is insulated according to "WSchV 1995" (German Heat Insulation Ordinance of the year 1995) and the heating system is dimensioned for "WSchV 1984". The heating system is over-dimensioned by 46%. For simulation results of the additional reference systems see appendix I.

[11] The same heating curve as has been applied in section 4.5.7. For simulation results of the additional reference systems see appendix I.

# 6 Conclusion and outlook

## 6.1 Conclusion

Within this work heat pump heating systems were analyzed. The focus was on the interaction of the heat pump with the heat sink. A field test was evaluated and a system model was developed. This model was tested and applied to study advanced supply temperature control concepts.

The field test offers the opportunity to analyze heat pumps of different manufacturers operating in existing buildings in Germany. A classification of field test objects according to type of heat sink and heat emission system reveals the main influences on the system efficiency which were found to be the source and sink temperature. Both directly influence the temperature lift that the heat pump has to provide. However, the performance of heat pump systems depends on many more system parameters and operating conditions. These were studied and documented comprehensively but in many cases a definite correlation was not found or data was not sufficient for a detailed study. Without data on usage, room temperature and control settings, the potential of the field test cannot be fully realized.

The mean seasonal performance factors in the system control volume are 2.3 for air-coupled devices and 2.9 for ground-coupled devices. The best systems in the field test achieved seasonal performance factors of 3.0 (air-source) and 4.0 (ground-coupled). The large difference to the mean values indicates both the high potential of this technology and the necessity to optimize the total heating system, including its control and heat emission system.

Static calculation methods were tested with field test data. They are able to give a rough ranking of the efficiency of field test objects. However, even detailed procedures do not allow a sufficient prediction of seasonal performance factors of heat pump heating systems.

Models of heat pump and buffer storage were developed and they were tested with field test data. Considering the uncertainty of measurements the heat pump and the buffer storage are well modeled. Based on an existing Modelica model library an overall heat pump heating system model was developed. The used building model was implemented with nine heated zones. The influence of the insulation standard of the heated building, user presence and ventilation profiles were studied with this model and parameters such as the buffer storage volume and the control hysteresis temperature difference for on/off control. Building insulation standard and user influences were detected to have a profound effect on system efficiency and compliance with a band of operative temperature in the heated zone.

The model allows to comprehensively study control concepts in heat pump heating systems. The type of room temperature control and the variation of room set temperature were analyzed as well as one standard and three advanced supply temperature control concepts. These concepts were compared with respect to energy demand, thermal comfort and energy efficiency. Generally, energy efficiency of heat pump heating systems can be increased and savings in electrical energy are yielded with these control concepts. However, an increased thermal discomfort cannot be fully avoided. Single rooms with higher set temperature can limit overall savings.

An MPC controller can be tuned for increased energy savings or increased comfort but requires a very detailed programming and high computational effort. A simple rule-based control successively adapting the supply set temperature given by the heating curve yields low savings in electrical energy when room set temperature changes occur. A PI supply temperature control using the information of electrical actuators for radiator valves is the best compromise in terms of energy efficiency, discomfort and feasibility (regarding computational and parametrization effort).

It is possible to yield higher energy efficiency through an intelligent supply temperature control. Attained energy savings crucially depend on the type of building physics and the user influences.

## 6.2 Outlook

Future field tests with heat pump systems require a comprehensive scheduling of user occupancy, control decisions and room temperature. The documentation has to contain detailed information on the type of heating system and building physics. A detailed documentation of sensor placement allows for an accurate modeling; additional temperature sensors, for example in the buffer storage and on working fluid cycle level, can enable a sound understanding of model components.

However, the gap between a field test with as many objects as the one analyzed within this work and the level of detail achieved with the system model can be filled by *hardware in the loop* (HiL) testing which combines real components and simulation. Single components and controller implementations can be tested interacting with each other and interacting with a simulation environment by using a test bench which emulates the behavior of a building or a heat source. The proposed control concepts have to be tested in a HiL environment to assure a sound functioning with real components.

Parts of the proposed system model can be used for an application in HiL test benches. Through its object oriented type of modeling the system model enables a user-friendly extension or exchange of model parts. The library including the proposed heat pump heating system model already contains models for ground source heat exchangers, DHW storages, capacity controlled heat pumps and a floor heating system. These models allow for a broader research of different types of heat pump heating systems.

Weather is expected to have an important influence on system efficiency as well as the control's or user's reaction to it. Within this context and the context of the proposed control algorithms, the

most obvious influence is solar radiation which accounts for solar gains depending on the possible usage of shading appliances. Different weather scenarios are to be studied in future work.

Interactions of the main system components were implemented in the heat pump heating system model. User influences are considered by internal gains, ventilation and room set temperature schedules which have an impact on the control and system behavior. The scheme in figure 6.1 shows the interactions of a heat pump heating system, the user and control. The particular interactions of the control with the heat pump heating system and the user with the heat pump heating system are implemented in the model. A question which has not been addressed is how the user would react to different levels of comfort. Instead of schedule-based implementation a dynamic user model that makes control decisions could be implemented.

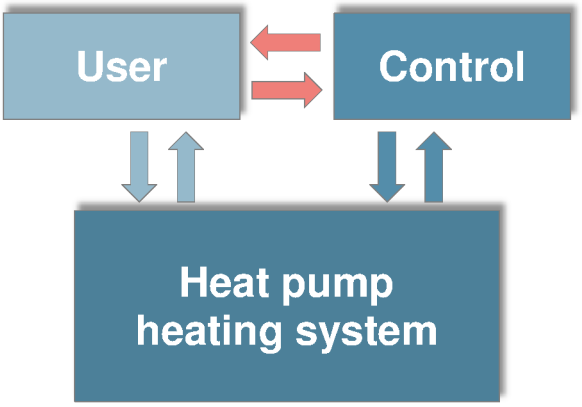


**Figure 6.1:** Interaction of heat pump heating systems, user and control.

The main field of future development of the supply temperature control concepts should include their combination with an adaptive room set temperature algorithm. The objective should be the development of a controller that automatically finds the optimal room temperature and uses it to calculate the optimal supply temperature. The MPC control concept has to be extended. By taking into account the dynamics of the heat generation system the concept allows for an optimal use of electricity tariffs. Literature provides different approaches for this kind of control.

Generally, another field of study with respect to heat pump heating systems is their interaction with the environment (see figure 6.2). This does not only include the environmental impact of the usage of energy but also the interaction with energy grids and the surrounding buildings. The control of heat pumps cannot only be optimized for energy efficiency or comfort but also for the best usage of renewable energies or their storage as heat in the buffer storage, the ambient ground or by intentionally overheating the building structure.

Key components of the heat pump heating system offering research possibilities regarding system control are the working fluid cycle with the compressor as the main controllable component and the radiator valve. In this work, radiator valves and their actuators are implemented with ideal

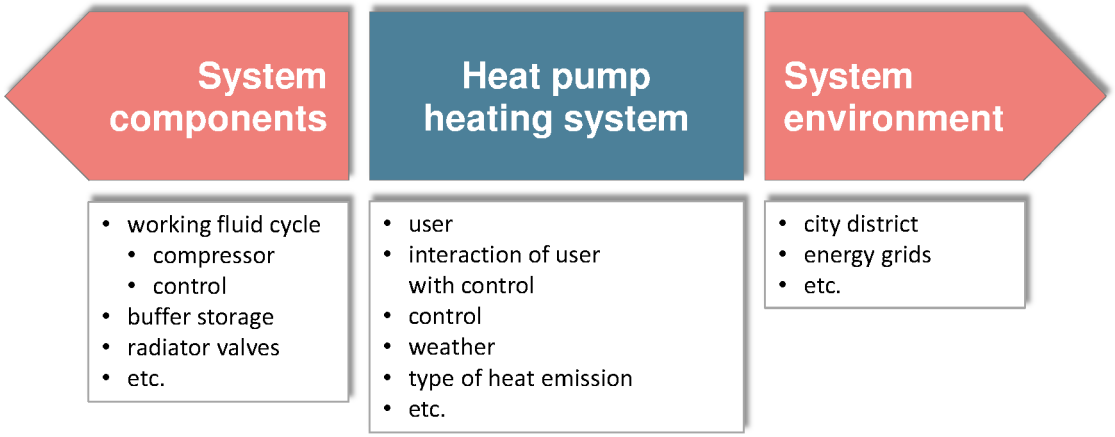


**Figure 6.2:** Fields of further research in context of this work.

characteristics. They are a key component for the implementation of supply temperature control concepts and should thus be studied in detail.

The model developed in this work represents a basic tool for these studies. The findings on supply temperature control strategies will be helpful for the practical implementation of advanced heat pump heating system controllers with single room temperature control.

# Appendix

# A Heat pump table data

**Table A.1:** List of heat pumps used for model validation

| object number | manufacturer | type | reference to table | source type |
|---|---|---|---|---|
| 1 | Alpha Innotec | LW 80 M-A | A.2 | AWHP |
| 5 | Ochsner | GMSW 15 plus | A.3 | BWHP |
| 6 | Viessmann | Vitocal AWI 114 | A.4 | AWHP |
| 9 | Viessmann | Vitocal BWH 110 | A.5 | BWHP |
| 12 | Viessmann | Vitocal BWH 113 | A.6 | BWHP |
| 24 | Nibe | Fighter 1140-15 | A.8 | BWHP |
| 25 | Ochsner | GMLW 19 plus | A.9 | AWHP |
| 27 | Stiebel Eltron | WPL 18 | A.7 | AWHP |
| 33 | Dimplex | LA 11 AS | A.10 | AWHP |
| 36 | Viessmann | Vitocal BWH 113 | A.6 | BWHP |

**Table A.2:** Data of "Alpha Innotec LW 80 MA" according to manufacturer's data ("Alpha Innotec Wärmepumpen-Guide 2007/08"). Data according to EN 14511 (2012).

| operating condition | $\dot{Q}_{cc}$ | $P_{el}$ |
|---|---|---|
| | in W | in W |
| A-7W35 | 6,300 | 2,625 |
| A2W35 | 8,000 | 2,424 |
| A7W35 | 9,400 | 2,410 |
| A10W35 | 10,300 | 2,395 |
| A7W45 | 9,000 | 3,000 |

**Table A.3:** Data of "Ochsner GMSW 15 plus", according to data from heat pump test center "WPZ Buchs", Swiss and EN 14511 (2012).

| operating condition | $\dot{Q}_{cc}$ | $P_{el}$ |
|---|---|---|
| | in W | in W |
| B-5W35 | 12,762 | 3,225 |
| B0W35 | 14,500 | 3,300 |
| B5W35 | 16,100 | 3,300 |
| B-5W45 | 12,100 | 4,000 |
| B0W45 | 13,900 | 4,000 |
| B5W45 | 15,600 | 4,000 |
| B0W55 | 13,200 | 4,900 |
| B5W55 | 14,900 | 4,900 |

**Table A.4:** Data of "Viessmann Vitocal 350 AWI 114". Extracted from diagram given in manufacturer's data sheet, according to EN 255 (1997).

| operating condition | $\dot{Q}_{cc}$ | $P_{el}$ |
|---|---|---|
| | in W | in W |
| A-20W35 | 9204.5 | 3295.5 |
| A-15W35 | 11136.4 | 3522.7 |
| A-10W35 | 11477.3 | 3750 |
| A-5W35 | 12215.9 | 3977.3 |
| A0W35 | 13863.6 | 4034.1 |
| A5W35 | 15056.8 | 4090.9 |
| A10W35 | 16931.8 | 4204.5 |
| A15W35 | 19090.9 | 4375 |
| A20W35 | 21250 | 4488.6 |
| A25W35 | 21477.3 | 4488.6 |
| A30W35 | 21761.4 | 4545 |
| A-20W50 | 10795.5 | 4659.1 |
| A-15W50 | 11988.6 | 4886.4 |
| A-10W50 | 12215.9 | 5113.6 |
| A-5W50 | 13068.2 | 5227.3 |
| A0W50 | 14545.5 | 5511.4 |
| A5W50 | 15681.8 | 5568.2 |
| A10W50 | 17613.6 | 5738.6 |
| A15W50 | 20284.1 | 5909.1 |
| A20W50 | 22500 | 6022.7 |
| A25W50 | 23181.8 | 6250 |
| A30W50 | 23863.6 | 6477.3 |
| A-15W65 | 12954.5 | 6875 |
| A-10W65 | 13465.9 | 7159.1 |
| A-5W65 | 14431.8 | 7500 |
| A0W65 | 15965.9 | 7727.3 |
| A5W65 | 17386.4 | 7897.7 |
| A10W65 | 19204.5 | 7954.5 |
| A15W65 | 21250 | 7954.5 |
| A20W65 | 22897.7 | 8181.8 |
| A25W65 | 23863.6 | 8409.1 |
| A30W65 | 24886.4 | 8579.5 |

**Table A.5:** Data of "Viessmann Vitocal 350 BWH 110". Extracted from diagram given in manufacturer's data sheet, according to EN 255 (1997).

| operating condition | $\dot{Q}_{cc}$ | $P_{el}$ |
|---|---|---|
| | in W | in W |
| B-5W35 | 9522 | 2478 |
| B0W35 | 11000 | 2522 |
| B5W35 | 12520 | 2609 |
| B10W35 | 14000 | 2696 |
| B15W35 | 15520 | 2783 |
| B-5W45 | 11610 | 3608 |
| B0W45 | 12740 | 3652 |
| B5W45 | 13910 | 3696 |
| B10W45 | 15090 | 3739 |
| B15W45 | 16220 | 3783 |
| B-5W55 | 11610 | 4217 |
| B0W55 | 12740 | 4261 |
| B5W55 | 13910 | 4304 |
| B10W55 | 15090 | 4348 |
| B15W55 | 16220 | 4391 |
| B-5W65 | 11610 | 5087 |
| B0W65 | 12740 | 5130 |
| B5W65 | 13910 | 5174 |
| B10W65 | 15090 | 5217 |
| B15W65 | 16220 | 5261 |

**Table A.6:** Data of "Viessmann Vitocal 350 BWH 113". Extracted from diagram given in manufacturer's data sheet, according to EN 255 (1997).

| operating condition | $\dot{Q}_{cc}$ | $P_{el}$ |
|---|---|---|
| | in W | in W |
| B-5W35 | 14500 | 3750 |
| B0W35 | 16292 | 3750 |
| B5W35 | 18042 | 3750 |
| B10W35 | 19750 | 3750 |
| B15W35 | 21583 | 3833 |
| B-5W45 | 14708 | 4833 |
| B0W45 | 17167 | 4917 |
| B5W45 | 18583 | 4958 |
| B10W45 | 20083 | 5042 |
| B15W45 | 21583 | 5125 |
| B-5W55 | 15708 | 5583 |
| B0W55 | 17167 | 5667 |
| B5W55 | 18583 | 5750 |
| B10W55 | 20083 | 5833 |
| B15W55 | 21583 | 5958 |
| B-5W65 | 15708 | 7000 |
| B0W65 | 17167 | 7125 |
| B5W65 | 18583 | 7250 |
| B10W65 | 20083 | 7417 |
| B15W65 | 21583 | 7583 |

**Table A.7:** Data of "Stiebel Eltron WPL 18", according to data from heat pump test center "WPZ Buchs", Swiss and EN 14511 (2012).

| operating condition | $\dot{Q}_{cc}$ | $P_{el}$ |
|---|---|---|
| | in W | in W |
| A-7W35 | 9700 | 3300 |
| A2W35 | 11600 | 3400 |
| A7W35 | 13000 | 3500 |
| A10W35 | 14800 | 3700 |
| A20W35 | 16300 | 3800 |
| A-7W50 | 10000 | 4500 |
| A2W50 | 11200 | 4400 |
| A7W50 | 12900 | 4600 |
| A10W50 | 16700 | 5000 |
| A20W50 | 17500 | 5100 |

**Table A.8:** Data of "Nibe Fighter 1140-15", according to manufacturer's data. Data according to EN 255 (1997).

| operating condition | $\dot{Q}_{cc}$ | $P_{el}$ |
|---|---|---|
| | in W | in W |
| B-5W35 | 13260 | 3360 |
| B0W35 | 15420 | 3380 |
| B2W35 | 16350 | 3380 |
| B5W35 | 17730 | 3390 |
| B10W35 | 19930 | 3400 |
| B-5W55 | 12560 | 4830 |
| B0W55 | 14490 | 4910 |
| B2W55 | 15330 | 4940 |
| B5W55 | 16590 | 4990 |
| B10W55 | 18900 | 5050 |

**Table A.9:** Data of "Ochsner GMLW 19 plus", according to manufacturer's data. Data according to EN 14511 (2012).

| operating condition | $\dot{Q}_{cc}$ | $P_{el}$ |
|---|---|---|
| | in W | in W |
| A-10W35 | 12600 | 4100 |
| A2W35 | 16800 | 4300 |
| A7W35 | 19800 | 4400 |
| A-10W50 | 11700 | 5500 |
| A2W50 | 15900 | 5700 |
| A7W50 | 18900 | 5800 |
| A-10W60 | 11400 | 6300 |
| A2W60 | 15600 | 6500 |
| A7W60 | 18600 | 6600 |

**Table A.10:** Data of "Dimplex LA 11 AS", according to data from heat pump test center "WPZ Buchs", Swiss and EN 255 (1997).

| operating condition | $\dot{Q}_{cc}$ | $P_{el}$ |
|---|---|---|
| | in W | in W |
| A-7W35 | 6600 | 2444 |
| A2W35 | 8800 | 2839 |
| A7W35 | 11300 | 3139 |
| A10W35 | 12100 | 3103 |
| A-7W45 | 6400 | 2783 |
| A2W45 | 7898 | 2974 |
| A7W45 | 9600 | 3097 |
| A10W45 | 10145 | 3013 |

# B Buffer Storage data

**Table B.1:** List of buffer storages used for model validation

| object number | manufacturer | type | reference to table |
|---|---|---|---|
| 6 | Viessmann | Vitocell 100E SVP 750 | B.2 |
| 22 | Stiebel Eltron | SBP 700E | B.3 |
| 27 | Stiebel Eltron | SBP 700E | B.3 |
| 35 | Ochsner | PU 500 | B.4 |
| 36 | Viessmann | Vitocell 050 600 | B.5 |

**Table B.2:** Data of "Viessmann Vitocell 100 E SVP, 750 l" according to manufacturer's data sheet, 4/2007.

| | | |
|---|---|---|
| inner height | m | 1.873 |
| height of lower port, LC | m | 0.272 |
| height of upper port, LC | m | 1.605 |
| height of lower port, HC | m | 0 |
| height of upper port, HC | m | 1.873 |
| diameter | m | 0.750 |
| thickness of insulation | m | 0.105 |

**Table B.3:** Data of "Stiebel Eltron SBP 700 E SOL", according to manufacturer's data sheet, values partly extracted from drawing.

| | | |
|---|---|---|
| inner height | m | 1.66 |
| height of lower port, LC | m | 0.205 |
| height of upper port, LC | m | 1.315 |
| height of lower port, HC | m | 0.345 |
| height of upper port, HC | m | 1.455 |
| diameter | m | 0.75 |
| thickness of insulation | m | 0.080 |

**Table B.4:** Data of "Ochsner PU 500" storage, according to manufacturer's data sheet

| | | |
|---|---|---|
| inner height | m | 1.51 |
| height of lower port, LC | m | 0.1 |
| height of upper port, LC | m | 1.41 |
| height of lower port, HC | m | 0.1 |
| height of upper port, HC | m | 1.51 |
| diameter | m | 0.65 |
| thickness of insulation | m | 0.085 |

**Table B.5:** Data of "Viessmann Vitocell 050, 750 l" according to manufacturer's data sheet.

| | | |
|---|---|---|
| inner height | m | 1.873 |
| height of lower port, LC | m | 0.269 |
| height of upper port, LC | m | 1.604 |
| height of lower port, HC | m | 0 |
| height of upper port, HC | m | 1.873 |
| diameter | m | 0.750 |
| thickness of insulation | m | 0.105 |

# C Model optimization and validation results

**Table C.1:** Heat pump model optimization: Best fits for condenser volumes and heat loss coefficients.

| | optimization *without* heat loss | optimization *with* heat loss | |
|---|---|---|---|
| | condenser volume in l | condenser volume in l | heat loss coefficient in W/K |
| **01** | 6.00 | 6.00 | 1.00 |
| **05** | 8.00 | 10.00 | 28.00 |
| **06** | 23.00 | 23.00 | 0.00 |
| **09** | 17.00 | 19.00 | 9.00 |
| **12** | 19.00 | 19.00 | 0.00 |
| **24** | 25.00 | 25.00 | 0.00 |
| **25** | 36.00 | 34.00 | 0.50 |
| **27** | 13.00 | 9.00 | 3.50 |
| **33** | 1.00 | 1.00 | 0.00 |
| **36** | 19.00 | 19.00 | 0.00 |

**Table C.2:** Heat pump model optimization *without* heat loss: $R^2$ for best fits (see table C.1).

| | $R^2_{\dot{Q}}$ | $R^2_{\dot{Q}}$ | $R^2_{\dot{Q}}$ | $R^2_{\dot{Q}}$ | $R^2_{P,\mathrm{el}}$ | $R^2_{P,\mathrm{el}}$ | $R^2_{P,\mathrm{el}}$ | $R^2_{P,\mathrm{el}}$ |
|---|---|---|---|---|---|---|---|---|
| **week→** | **1** | **2** | **3** | **1 to 3** | **1** | **2** | **3** | **1 to 3** |
| **01** | 0.84 | 0.84 | 0.80 | 0.85 | 0.49 | 0.48 | 0.65 | 0.57 |
| **05** | 0.95 | 0.95 | 0.94 | 0.95 | 0.91 | 0.94 | 0.92 | 0.93 |
| **06** | 0.79 | 0.87 | 0.90 | 0.86 | 0.87 | 0.93 | 0.95 | 0.91 |
| **09** | 0.91 | 0.93 | 0.91 | 0.92 | 0.89 | 0.93 | 0.91 | 0.91 |
| **12** | 0.95 | 0.95 | 0.94 | 0.95 | 0.98 | 0.98 | 0.97 | 0.98 |
| **24** | 0.80 | 0.82 | 0.62 | 0.81 | 0.95 | 0.96 | 0.93 | 0.96 |
| **25** | 0.98 | 0.98 | 0.97 | 0.98 | 0.94 | 0.95 | 0.98 | 0.96 |
| **27** | 0.95 | 0.94 | 0.97 | 0.95 | 0.92 | 0.95 | 0.94 | 0.95 |
| **33** | 0.55 | 0.80 | 0.82 | 0.79 | 0.77 | 0.87 | 0.91 | 0.88 |
| **36** | 0.94 | 0.94 | 0.89 | 0.94 | 0.99 | 0.99 | 0.98 | 0.99 |

**Table C.3:** Heat pump model optimization *with* heat loss: $R^2$ for best fits (see table C.1).

| | $R^2_{\dot{Q}}$ | $R^2_{\dot{Q}}$ | $R^2_{\dot{Q}}$ | $R^2_{\dot{Q}}$ | $R^2_{P,\mathrm{el}}$ | $R^2_{P,\mathrm{el}}$ | $R^2_{P,\mathrm{el}}$ | $R^2_{P,\mathrm{el}}$ |
|---|---|---|---|---|---|---|---|---|
| **week→** | **1** | **2** | **3** | **1 to 3** | **1** | **2** | **3** | **1 to 3** |
| **01** | 0.84 | 0.84 | 0.80 | 0.85 | 0.49 | 0.48 | 0.65 | 0.57 |
| **05** | 0.96 | 0.96 | 0.94 | 0.96 | 0.91 | 0.94 | 0.92 | 0.93 |
| **06** | 0.79 | 0.87 | 0.90 | 0.86 | 0.87 | 0.93 | 0.95 | 0.91 |
| **09** | 0.92 | 0.94 | 0.92 | 0.93 | 0.89 | 0.92 | 0.91 | 0.91 |
| **12** | 0.95 | 0.95 | 0.94 | 0.95 | 0.98 | 0.98 | 0.97 | 0.98 |
| **24** | 0.80 | 0.82 | 0.62 | 0.81 | 0.95 | 0.96 | 0.93 | 0.96 |
| **25** | 0.98 | 0.98 | 0.97 | 0.98 | 0.94 | 0.95 | 0.98 | 0.96 |
| **27** | 0.95 | 0.96 | 0.98 | 0.97 | 0.93 | 0.95 | 0.94 | 0.95 |
| **33** | 0.55 | 0.80 | 0.82 | 0.79 | 0.77 | 0.87 | 0.91 | 0.88 |
| **36** | 0.94 | 0.94 | 0.89 | 0.94 | 0.99 | 0.99 | 0.98 | 0.99 |

**Table C.4:** Heat pump model optimization, relative errors for week 1 to 3 with and without modeling of heat loss.

| | optimization *without* heat loss | | | optimization *with* heat loss | | |
|---|---|---|---|---|---|---|
| | $f_Q$ | $f_{W,\mathrm{el}}$ | $f_{\mathrm{PF}}$ | $f_Q$ | $f_{W,\mathrm{el}}$ | $f_{\mathrm{PF}}$ |
| **01** | 0.09 | 0.06 | 0.02 | 0.07 | 0.06 | 0.01 |
| **05** | 0.15 | 0.07 | 0.07 | 0.07 | 0.06 | 0.00 |
| **06** | 0.10 | -0.01 | 0.11 | 0.10 | -0.01 | 0.11 |
| **09** | -0.05 | -0.08 | 0.03 | -0.09 | -0.09 | 0.00 |
| **12** | -0.02 | -0.06 | 0.04 | -0.02 | -0.06 | 0.04 |
| **24** | 0.08 | -0.04 | 0.12 | 0.08 | -0.04 | 0.12 |
| **25** | 0.02 | -0.02 | 0.04 | 0.01 | -0.02 | 0.03 |
| **27** | 0.12 | 0.09 | 0.02 | 0.02 | 0.09 | -0.06 |
| **33** | 0.06 | -0.01 | 0.07 | 0.06 | -0.01 | 0.07 |
| **36** | 0.04 | 0.02 | 0.02 | 0.04 | 0.02 | 0.02 |

# D Inner load and ventilation schedules

**Table D.1:** List of tables in this chapter. More information on inner gains are given in chapter 4, section 4.3.3.

**Table D.2:** Occupancy in number of people per hour.

| Schedule for four inhabitants (high profile) | | | | | | | | | | | | | | | | | | | | | | | | |
|---|---|---|---|---|---|---|---|---|---|---|---|---|---|---|---|---|---|---|---|---|---|---|---|---|
| | Livingroom | | Hobby | | Corridor | | WC | | Kitchen | | Sleeping | | Children 1 | | Bath | | Children 2 | | | | | | | |
| **Hour** | **mo-fr** | **sa-su** | **mo-fr** | **sa-su** | **mo-fr** | **sa-su** | **mo-fr** | **sa-su** | **mo-fr** | **sa-su** | **mo-fr** | **sa-su** | **mo-fr** | **sa-su** | **mo-fr** | **sa-su** | **mo-fr** | **sa-su** | | | | | | |
| 0 | 0.00 | 0.00 | 0.00 | 0.00 | 0.00 | 0.00 | 0.00 | 0.00 | 0.00 | 0.00 | 2.00 | 2.00 | 1.00 | 1.00 | 0.00 | 0.00 | 1.00 | 1.00 | | | | | | |
| 1 | 0.00 | 0.00 | 0.00 | 0.00 | 0.00 | 0.00 | 0.00 | 0.00 | 0.00 | 0.00 | 2.00 | 2.00 | 1.00 | 1.00 | 0.00 | 0.00 | 1.00 | 1.00 | | | | | | |
| 2 | 0.00 | 0.00 | 0.00 | 0.00 | 0.00 | 0.00 | 0.00 | 0.00 | 0.00 | 0.00 | 2.00 | 2.00 | 1.00 | 1.00 | 0.00 | 0.00 | 1.00 | 1.00 | | | | | | |
| 3 | 0.00 | 0.00 | 0.00 | 0.00 | 0.00 | 0.00 | 0.00 | 0.00 | 0.00 | 0.00 | 2.00 | 2.00 | 1.00 | 1.00 | 0.00 | 0.00 | 1.00 | 1.00 | | | | | | |
| 4 | 0.00 | 0.00 | 0.00 | 0.00 | 0.00 | 0.00 | 0.00 | 0.00 | 0.00 | 0.00 | 2.00 | 2.00 | 1.00 | 1.00 | 0.00 | 0.00 | 1.00 | 1.00 | | | | | | |
| 5 | 0.00 | 0.00 | 0.00 | 0.00 | 0.00 | 0.00 | 0.00 | 0.00 | 0.00 | 0.00 | 2.00 | 2.00 | 1.00 | 1.00 | 0.00 | 0.00 | 1.00 | 1.00 | | | | | | |
| 6 | 0.00 | 0.00 | 0.00 | 0.00 | 0.00 | 0.00 | 0.00 | 0.00 | 1.10 | 0.00 | 1.00 | 2.00 | 0.50 | 1.00 | 0.25 | 0.00 | 0.50 | 1.00 | | | | | | |
| 7 | 0.00 | 0.00 | 0.00 | 0.00 | 0.00 | 0.00 | 0.00 | 0.00 | 2.00 | 0.00 | 0.00 | 1.25 | 0.00 | 1.00 | 0.25 | 0.25 | 0.00 | 1.00 | | | | | | |
| 8 | 0.00 | 0.75 | 0.00 | 0.00 | 0.00 | 0.00 | 0.00 | 0.00 | 0.50 | 1.00 | 0.00 | 0.00 | 0.00 | 1.00 | 0.25 | 0.25 | 0.00 | 1.00 | | | | | | |
| 9 | 0.00 | 1.00 | 0.00 | 0.75 | 0.00 | 0.00 | 0.00 | 0.00 | 0.00 | 0.00 | 0.00 | 0.00 | 0.00 | 1.00 | 0.00 | 0.25 | 0.00 | 1.00 | | | | | | |
| 10 | 0.00 | 1.75 | 0.00 | 1.00 | 0.00 | 0.00 | 0.00 | 0.00 | 0.00 | 0.00 | 0.00 | 0.00 | 0.00 | 0.00 | 0.00 | 0.00 | 0.00 | 1.25 | | | | | | |
| 11 | 0.00 | 0.00 | 0.00 | 1.00 | 0.00 | 0.00 | 0.00 | 0.00 | 0.70 | 0.80 | 0.00 | 0.00 | 0.00 | 0.00 | 0.00 | 0.00 | 0.00 | 1.80 | | | | | | |
| 12 | 0.30 | 0.00 | 0.00 | 0.00 | 0.00 | 0.00 | 0.00 | 0.00 | 1.20 | 2.00 | 0.00 | 0.00 | 0.00 | 0.00 | 0.00 | 0.00 | 0.00 | 0.00 | | | | | | |
| 13 | 0.00 | 3.00 | 0.00 | 0.00 | 0.00 | 0.00 | 0.00 | 0.00 | 1.00 | 0.00 | 0.00 | 0.00 | 0.00 | 0.00 | 0.00 | 0.00 | 0.00 | 0.00 | | | | | | |
| 14 | 1.00 | 0.50 | 0.00 | 2.50 | 0.00 | 0.00 | 0.00 | 0.00 | 0.00 | 0.00 | 0.00 | 0.00 | 0.00 | 0.50 | 0.00 | 0.00 | 0.00 | 0.50 | | | | | | |
| 15 | 1.00 | 0.50 | 0.00 | 2.50 | 0.00 | 0.00 | 0.00 | 0.00 | 0.00 | 0.00 | 0.00 | 0.00 | 0.00 | 0.50 | 0.00 | 0.00 | 0.00 | 0.50 | | | | | | |
| 16 | 1.00 | 1.00 | 0.00 | 1.00 | 0.00 | 0.00 | 0.00 | 0.00 | 1.00 | 0.00 | 0.00 | 0.00 | 0.00 | 0.50 | 0.00 | 0.00 | 0.00 | 0.50 | | | | | | |
| 17 | 1.00 | 3.00 | 0.00 | 0.00 | 0.00 | 0.00 | 0.00 | 0.00 | 2.00 | 0.00 | 0.00 | 0.00 | 0.00 | 0.00 | 0.00 | 0.00 | 0.00 | 0.00 | | | | | | |
| 18 | 1.00 | 1.00 | 0.00 | 0.00 | 0.00 | 0.00 | 0.00 | 0.00 | 1.00 | 1.00 | 0.00 | 0.00 | 0.50 | 1.00 | 0.00 | 0.00 | 0.50 | 1.00 | | | | | | |
| 19 | 2.00 | 2.00 | 0.00 | 0.00 | 0.00 | 0.00 | 0.00 | 0.60 | 1.00 | 0.00 | 0.00 | 0.00 | 0.20 | 0.50 | 0.25 | 0.00 | 0.20 | 0.50 | | | | | | |
| 20 | 2.00 | 3.00 | 0.50 | 0.00 | 0.00 | 0.00 | 0.00 | 0.00 | 0.00 | 0.00 | 0.00 | 0.00 | 0.50 | 0.50 | 0.00 | 0.00 | 0.75 | 0.50 | | | | | | |
| 21 | 2.00 | 2.00 | 0.00 | 0.00 | 0.00 | 0.00 | 0.00 | 0.00 | 0.00 | 0.00 | 0.00 | 0.00 | 0.75 | 0.75 | 0.25 | 0.25 | 0.75 | 0.75 | | | | | | |
| 22 | 0.00 | 1.80 | 0.00 | 0.00 | 0.00 | 0.00 | 0.00 | 0.00 | 0.00 | 0.00 | 2.00 | 0.00 | 1.00 | 1.00 | 0.00 | 0.20 | 1.00 | 1.00 | | | | | | |
| 23 | 0.00 | 0.00 | 0.00 | 0.00 | 0.00 | 0.00 | 0.00 | 0.00 | 0.00 | 0.00 | 2.00 | 2.00 | 1.00 | 1.00 | 0.00 | 0.00 | 1.00 | 1.00 | | | | | | |

| Schedule for three inhabitants (low profile) | | | | | | | | | | | | | | | | | | | | | | | | |
|---|---|---|---|---|---|---|---|---|---|---|---|---|---|---|---|---|---|---|---|---|---|---|---|---|
| | Livingroom | | Hobby | | Corridor | | WC | | Kitchen | | Sleeping | | Children 1 | | Bath | | Children 2 | | | | | | | |
| **Hour** | **mo-fr** | **sa-su** | **mo-fr** | **sa-su** | **mo-fr** | **sa-su** | **mo-fr** | **sa-su** | **mo-fr** | **sa-su** | **mo-fr** | **sa-su** | **mo-fr** | **sa-su** | **mo-fr** | **sa-su** | **mo-fr** | **sa-su** | | | | | | |
| 0 | 0.00 | 0.00 | 0.00 | 0.00 | 0.00 | 0.00 | 0.00 | 0.00 | 0.00 | 0.00 | 2.00 | 2.00 | 1.00 | 1.00 | 0.00 | 0.00 | 0.00 | 0.00 | | | | | | |
| 1 | 0.00 | 0.00 | 0.00 | 0.00 | 0.00 | 0.00 | 0.00 | 0.00 | 0.00 | 0.00 | 2.00 | 2.00 | 1.00 | 1.00 | 0.00 | 0.00 | 0.00 | 0.00 | | | | | | |
| 2 | 0.00 | 0.00 | 0.00 | 0.00 | 0.00 | 0.00 | 0.00 | 0.00 | 0.00 | 0.00 | 2.00 | 2.00 | 1.00 | 1.00 | 0.00 | 0.00 | 0.00 | 0.00 | | | | | | |
| 3 | 0.00 | 0.00 | 0.00 | 0.00 | 0.00 | 0.00 | 0.00 | 0.00 | 0.00 | 0.00 | 2.00 | 2.00 | 1.00 | 1.00 | 0.00 | 0.00 | 0.00 | 0.00 | | | | | | |
| 4 | 0.00 | 0.00 | 0.00 | 0.00 | 0.00 | 0.00 | 0.00 | 0.00 | 0.00 | 0.00 | 2.00 | 2.00 | 1.00 | 1.00 | 0.00 | 0.00 | 0.00 | 0.00 | | | | | | |
| 5 | 0.00 | 0.00 | 0.00 | 0.00 | 0.00 | 0.00 | 0.00 | 0.00 | 0.00 | 0.00 | 2.00 | 2.00 | 1.00 | 1.00 | 0.00 | 0.00 | 0.00 | 0.00 | | | | | | |
| 6 | 0.00 | 0.00 | 0.00 | 0.00 | 0.00 | 0.00 | 0.00 | 0.00 | 1.10 | 0.00 | 1.00 | 2.00 | 0.50 | 1.00 | 0.25 | 0.00 | 0.00 | 0.00 | | | | | | |
| 7 | 0.00 | 0.00 | 0.00 | 0.00 | 0.00 | 0.00 | 0.00 | 0.00 | 2.00 | 0.00 | 0.00 | 1.25 | 0.00 | 1.00 | 0.25 | 0.25 | 0.00 | 0.00 | | | | | | |
| 8 | 0.00 | 0.00 | 0.00 | 0.00 | 0.00 | 0.00 | 0.00 | 0.00 | 0.50 | 1.00 | 0.00 | 0.00 | 0.00 | 1.00 | 0.25 | 0.25 | 0.00 | 0.00 | | | | | | |
| 9 | 0.00 | 2.00 | 0.00 | 0.00 | 0.00 | 0.00 | 0.00 | 0.00 | 0.00 | 0.00 | 0.00 | 0.00 | 0.00 | 0.75 | 0.00 | 0.25 | 0.00 | 0.00 | | | | | | |
| 10 | 0.00 | 2.00 | 0.00 | 0.00 | 0.00 | 0.00 | 0.00 | 0.00 | 0.00 | 0.00 | 0.00 | 0.00 | 0.00 | 0.00 | 0.00 | 0.00 | 0.00 | 0.00 | | | | | | |
| 11 | 0.00 | 0.00 | 0.00 | 0.00 | 0.00 | 0.00 | 0.00 | 0.00 | 0.00 | 0.00 | 0.00 | 0.00 | 0.00 | 0.00 | 0.00 | 0.00 | 0.00 | 0.00 | | | | | | |
| 12 | 0.00 | 0.00 | 0.00 | 0.00 | 0.00 | 0.00 | 0.00 | 0.00 | 0.00 | 0.00 | 0.00 | 0.00 | 0.00 | 0.00 | 0.00 | 0.00 | 0.00 | 0.00 | | | | | | |
| 13 | 0.00 | 2.00 | 0.00 | 0.00 | 0.00 | 0.00 | 0.00 | 0.00 | 0.00 | 0.00 | 0.00 | 0.00 | 0.00 | 0.00 | 0.00 | 0.00 | 0.00 | 0.00 | | | | | | |
| 14 | 0.50 | 0.50 | 0.00 | 1.00 | 0.00 | 0.00 | 0.00 | 0.00 | 0.00 | 0.00 | 0.00 | 0.00 | 0.00 | 0.00 | 0.00 | 0.00 | 0.00 | 0.00 | | | | | | |
| 15 | 1.00 | 0.50 | 0.00 | 1.00 | 0.00 | 0.00 | 0.00 | 0.00 | 0.00 | 0.00 | 0.00 | 0.00 | 0.00 | 0.00 | 0.00 | 0.00 | 0.00 | 0.00 | | | | | | |
| 16 | 1.00 | 1.00 | 0.00 | 1.00 | 0.00 | 0.00 | 0.00 | 0.00 | 1.00 | 0.00 | 0.00 | 0.00 | 0.00 | 0.00 | 0.00 | 0.00 | 0.00 | 0.00 | | | | | | |
| 17 | 1.00 | 1.00 | 0.00 | 0.00 | 0.00 | 0.00 | 0.00 | 0.00 | 1.00 | 0.00 | 0.00 | 0.00 | 0.00 | 0.00 | 0.00 | 0.00 | 0.00 | 0.00 | | | | | | |
| 18 | 1.00 | 1.00 | 0.00 | 0.00 | 0.00 | 0.00 | 0.00 | 0.00 | 0.00 | 0.00 | 0.00 | 0.00 | 0.00 | 0.00 | 0.00 | 0.00 | 0.00 | 0.00 | | | | | | |
| 19 | 2.00 | 2.00 | 0.00 | 0.00 | 0.00 | 0.00 | 0.00 | 0.60 | 0.00 | 0.00 | 0.00 | 0.00 | 0.20 | 0.50 | 0.00 | 0.00 | 0.00 | 0.00 | | | | | | |
| 20 | 2.00 | 2.00 | 0.50 | 0.00 | 0.00 | 0.00 | 0.00 | 0.00 | 0.00 | 0.00 | 0.00 | 0.00 | 0.50 | 0.50 | 0.00 | 0.00 | 0.00 | 0.00 | | | | | | |
| 21 | 2.00 | 2.00 | 0.00 | 0.00 | 0.00 | 0.00 | 0.00 | 0.00 | 0.00 | 0.00 | 0.00 | 0.00 | 0.75 | 0.75 | 0.25 | 0.25 | 0.00 | 0.00 | | | | | | |
| 22 | 0.00 | 1.80 | 0.00 | 0.00 | 0.00 | 0.00 | 0.00 | 0.00 | 0.00 | 0.00 | 2.00 | 0.00 | 1.00 | 1.00 | 0.00 | 0.20 | 0.00 | 0.00 | | | | | | |
| 23 | 0.00 | 0.00 | 0.00 | 0.00 | 0.00 | 0.00 | 0.00 | 0.00 | 0.00 | 0.00 | 2.00 | 2.00 | 1.00 | 1.00 | 0.00 | 0.00 | 0.00 | 0.00 | | | | | | |

**Table D.3:** Inner gains through machines. Values from 0 to 1 that are multiplied by specific heat flows and room area. Specific heat flows are 40 W/m$^2$ for the kitchen, 1.5 W/m$^2$ for the other rooms.

High profile

| | Livingroom | | Hobby | | Corridor | | WC | | Kitchen | | Sleeping | | Children 1 | | Bath | | Children 2 | |
|---|---|---|---|---|---|---|---|---|---|---|---|---|---|---|---|---|---|---|
| **Hour** | **mo-fr** | **sa-su** | **mo-fr** | **sa-su** | **mo-fr** | **sa-su** | **mo-fr** | **sa-su** | **mo-fr** | **sa-su** | **mo-fr** | **sa-su** | **mo-fr** | **sa-su** | **mo-fr** | **sa-su** | **mo-fr** | **sa-su** |
| 0 | 0.10 | 0.10 | 0.00 | 0.00 | 0.00 | 0.00 | 0.00 | 0.00 | 0.20 | 0.20 | 0.10 | 0.10 | 0.10 | 0.10 | 0.00 | 0.00 | 0.10 | 0.10 |
| 1 | 0.10 | 0.10 | 0.00 | 0.00 | 0.00 | 0.00 | 0.00 | 0.00 | 0.20 | 0.20 | 0.10 | 0.10 | 0.10 | 0.10 | 0.00 | 0.00 | 0.10 | 0.10 |
| 2 | 0.10 | 0.10 | 0.00 | 0.00 | 0.00 | 0.00 | 0.00 | 0.00 | 0.20 | 0.20 | 0.10 | 0.10 | 0.10 | 0.10 | 0.00 | 0.00 | 0.10 | 0.10 |
| 3 | 0.10 | 0.10 | 0.00 | 0.00 | 0.00 | 0.00 | 0.00 | 0.00 | 0.20 | 0.20 | 0.10 | 0.10 | 0.10 | 0.10 | 0.00 | 0.00 | 0.10 | 0.10 |
| 4 | 0.10 | 0.10 | 0.00 | 0.00 | 0.00 | 0.00 | 0.00 | 0.00 | 0.20 | 0.20 | 0.10 | 0.10 | 0.10 | 0.10 | 0.00 | 0.00 | 0.10 | 0.10 |
| 5 | 0.10 | 0.10 | 0.00 | 0.00 | 0.00 | 0.00 | 0.00 | 0.00 | 0.20 | 0.20 | 0.10 | 0.10 | 0.10 | 0.10 | 0.00 | 0.00 | 0.10 | 0.10 |
| 6 | 0.50 | 0.50 | 0.00 | 0.00 | 0.00 | 0.00 | 0.00 | 0.00 | 0.40 | 0.40 | 0.50 | 0.50 | 0.50 | 0.50 | 0.00 | 0.00 | 0.50 | 0.50 |
| 7 | 1.00 | 1.00 | 0.00 | 0.00 | 0.00 | 0.00 | 0.00 | 0.00 | 0.80 | 0.80 | 1.00 | 1.00 | 1.00 | 1.00 | 0.00 | 0.00 | 1.00 | 1.00 |
| 8 | 0.50 | 0.50 | 0.00 | 0.00 | 0.00 | 0.00 | 0.00 | 0.00 | 0.40 | 0.40 | 0.50 | 0.50 | 0.50 | 0.50 | 0.00 | 0.00 | 0.50 | 0.50 |
| 9 | 0.50 | 0.50 | 0.00 | 0.00 | 0.00 | 0.00 | 0.00 | 0.00 | 0.20 | 0.20 | 0.50 | 0.50 | 0.50 | 0.50 | 0.00 | 0.00 | 0.50 | 0.50 |
| 10 | 0.50 | 0.50 | 0.00 | 0.00 | 0.00 | 0.00 | 0.00 | 0.00 | 0.20 | 0.20 | 0.50 | 0.50 | 0.50 | 0.50 | 0.00 | 0.00 | 0.50 | 0.50 |
| 11 | 1.00 | 1.00 | 0.00 | 0.00 | 0.00 | 0.00 | 0.00 | 0.00 | 0.40 | 0.40 | 1.00 | 1.00 | 1.00 | 1.00 | 0.00 | 0.00 | 1.00 | 1.00 |
| 12 | 1.00 | 1.00 | 0.00 | 0.00 | 0.00 | 0.00 | 0.00 | 0.00 | 1.00 | 1.00 | 1.00 | 1.00 | 1.00 | 1.00 | 0.00 | 0.00 | 1.00 | 1.00 |
| 13 | 0.50 | 0.50 | 0.00 | 0.00 | 0.00 | 0.00 | 0.00 | 0.00 | 0.40 | 0.40 | 0.50 | 0.50 | 0.50 | 0.50 | 0.00 | 0.00 | 0.50 | 0.50 |
| 14 | 0.50 | 0.50 | 0.00 | 0.00 | 0.00 | 0.00 | 0.00 | 0.00 | 0.20 | 0.20 | 0.50 | 0.50 | 0.50 | 0.50 | 0.00 | 0.00 | 0.50 | 0.50 |
| 15 | 0.50 | 0.50 | 0.00 | 0.00 | 0.00 | 0.00 | 0.00 | 0.00 | 0.20 | 0.20 | 0.50 | 0.50 | 0.50 | 0.50 | 0.00 | 0.00 | 0.50 | 0.50 |
| 16 | 1.00 | 1.00 | 0.00 | 0.00 | 0.00 | 0.00 | 0.00 | 0.00 | 0.40 | 0.40 | 1.00 | 1.00 | 1.00 | 1.00 | 0.00 | 0.00 | 1.00 | 1.00 |
| 17 | 1.00 | 1.00 | 0.00 | 0.00 | 0.00 | 0.00 | 0.00 | 0.00 | 1.00 | 1.00 | 1.00 | 1.00 | 1.00 | 1.00 | 0.00 | 0.00 | 1.00 | 1.00 |
| 18 | 1.00 | 1.00 | 0.00 | 0.00 | 0.00 | 0.00 | 0.00 | 0.00 | 0.40 | 0.40 | 1.00 | 1.00 | 1.00 | 1.00 | 0.00 | 0.00 | 1.00 | 1.00 |
| 19 | 1.00 | 1.00 | 0.00 | 0.00 | 0.00 | 0.00 | 0.00 | 0.00 | 0.20 | 0.20 | 1.00 | 1.00 | 1.00 | 1.00 | 0.00 | 0.00 | 1.00 | 1.00 |
| 20 | 0.50 | 0.50 | 0.00 | 0.00 | 0.00 | 0.00 | 0.00 | 0.00 | 0.20 | 0.20 | 0.50 | 0.50 | 0.50 | 0.50 | 0.00 | 0.00 | 0.50 | 0.50 |
| 21 | 0.50 | 0.50 | 0.00 | 0.00 | 0.00 | 0.00 | 0.00 | 0.00 | 0.20 | 0.20 | 0.50 | 0.50 | 0.50 | 0.50 | 0.00 | 0.00 | 0.50 | 0.50 |
| 22 | 0.50 | 0.50 | 0.00 | 0.00 | 0.00 | 0.00 | 0.00 | 0.00 | 0.20 | 0.20 | 0.50 | 0.50 | 0.50 | 0.50 | 0.00 | 0.00 | 0.50 | 0.50 |
| 23 | 0.10 | 0.10 | 0.00 | 0.00 | 0.00 | 0.00 | 0.00 | 0.00 | 0.20 | 0.20 | 0.10 | 0.10 | 0.10 | 0.10 | 0.00 | 0.00 | 0.10 | 0.10 |

Low profile

| | Livingroom | | Hobby | | Corridor | | WC | | Kitchen | | Sleeping | | Children 1 | | Bath | | Children 2 | |
|---|---|---|---|---|---|---|---|---|---|---|---|---|---|---|---|---|---|---|
| **Hour** | **mo-fr** | **sa-su** | **mo-fr** | **sa-su** | **mo-fr** | **sa-su** | **mo-fr** | **sa-su** | **mo-fr** | **sa-su** | **mo-fr** | **sa-su** | **mo-fr** | **sa-su** | **mo-fr** | **sa-su** | **mo-fr** | **sa-su** |
| 0 | 0.10 | 0.10 | 0.00 | 0.00 | 0.00 | 0.00 | 0.00 | 0.00 | 0.20 | 0.20 | 0.10 | 0.10 | 0.10 | 0.10 | 0.00 | 0.00 | 0.10 | 0.10 |
| 1 | 0.10 | 0.10 | 0.00 | 0.00 | 0.00 | 0.00 | 0.00 | 0.00 | 0.20 | 0.20 | 0.10 | 0.10 | 0.10 | 0.10 | 0.00 | 0.00 | 0.10 | 0.10 |
| 2 | 0.10 | 0.10 | 0.00 | 0.00 | 0.00 | 0.00 | 0.00 | 0.00 | 0.20 | 0.20 | 0.10 | 0.10 | 0.10 | 0.10 | 0.00 | 0.00 | 0.10 | 0.10 |
| 3 | 0.10 | 0.10 | 0.00 | 0.00 | 0.00 | 0.00 | 0.00 | 0.00 | 0.20 | 0.20 | 0.10 | 0.10 | 0.10 | 0.10 | 0.00 | 0.00 | 0.10 | 0.10 |
| 4 | 0.10 | 0.10 | 0.00 | 0.00 | 0.00 | 0.00 | 0.00 | 0.00 | 0.20 | 0.20 | 0.10 | 0.10 | 0.10 | 0.10 | 0.00 | 0.00 | 0.10 | 0.10 |
| 5 | 0.10 | 0.10 | 0.00 | 0.00 | 0.00 | 0.00 | 0.00 | 0.00 | 0.40 | 0.40 | 0.50 | 0.50 | 0.50 | 0.50 | 0.00 | 0.00 | 0.10 | 0.10 |
| 6 | 0.50 | 0.50 | 0.00 | 0.00 | 0.00 | 0.00 | 0.00 | 0.00 | 0.80 | 0.80 | 1.00 | 1.00 | 1.00 | 1.00 | 0.00 | 0.00 | 0.10 | 0.10 |
| 7 | 1.00 | 1.00 | 0.00 | 0.00 | 0.00 | 0.00 | 0.00 | 0.00 | 0.80 | 0.80 | 1.00 | 1.00 | 1.00 | 1.00 | 0.00 | 0.00 | 0.10 | 0.10 |
| 8 | 0.50 | 0.50 | 0.00 | 0.00 | 0.00 | 0.00 | 0.00 | 0.00 | 0.40 | 0.40 | 0.50 | 0.50 | 0.50 | 0.50 | 0.00 | 0.00 | 0.10 | 0.10 |
| 9 | 0.50 | 0.50 | 0.00 | 0.00 | 0.00 | 0.00 | 0.00 | 0.00 | 0.20 | 0.20 | 0.10 | 0.10 | 0.10 | 0.50 | 0.00 | 0.00 | 0.10 | 0.10 |
| 10 | 0.50 | 0.50 | 0.00 | 0.00 | 0.00 | 0.00 | 0.00 | 0.00 | 0.20 | 0.20 | 0.10 | 0.10 | 0.10 | 0.50 | 0.00 | 0.00 | 0.10 | 0.10 |
| 11 | 0.50 | 0.50 | 0.00 | 0.00 | 0.00 | 0.00 | 0.00 | 0.00 | 0.20 | 0.20 | 0.10 | 0.10 | 0.10 | 0.50 | 0.00 | 0.00 | 0.10 | 0.10 |
| 12 | 0.50 | 0.50 | 0.00 | 0.00 | 0.00 | 0.00 | 0.00 | 0.00 | 0.20 | 0.20 | 0.10 | 0.10 | 0.10 | 0.50 | 0.00 | 0.00 | 0.10 | 0.10 |
| 13 | 0.50 | 0.50 | 0.00 | 0.00 | 0.00 | 0.00 | 0.00 | 0.00 | 0.20 | 0.20 | 0.10 | 0.10 | 0.10 | 0.50 | 0.00 | 0.00 | 0.10 | 0.10 |
| 14 | 0.50 | 0.50 | 0.00 | 0.00 | 0.00 | 0.00 | 0.00 | 0.00 | 0.20 | 0.20 | 0.10 | 0.10 | 0.10 | 0.50 | 0.00 | 0.00 | 0.10 | 0.10 |
| 15 | 0.50 | 0.50 | 0.00 | 0.00 | 0.00 | 0.00 | 0.00 | 0.00 | 0.20 | 0.20 | 0.50 | 0.50 | 0.50 | 0.50 | 0.00 | 0.00 | 0.10 | 0.10 |
| 16 | 1.00 | 1.00 | 0.00 | 0.00 | 0.00 | 0.00 | 0.00 | 0.00 | 0.40 | 0.40 | 1.00 | 1.00 | 1.00 | 1.00 | 0.00 | 0.00 | 0.10 | 0.10 |
| 17 | 1.00 | 1.00 | 0.00 | 0.00 | 0.00 | 0.00 | 0.00 | 0.00 | 1.00 | 1.00 | 1.00 | 1.00 | 1.00 | 1.00 | 0.00 | 0.00 | 0.10 | 0.10 |
| 18 | 1.00 | 1.00 | 0.00 | 0.00 | 0.00 | 0.00 | 0.00 | 0.00 | 0.40 | 0.40 | 1.00 | 1.00 | 1.00 | 1.00 | 0.00 | 0.00 | 0.10 | 0.10 |
| 19 | 1.00 | 1.00 | 0.00 | 0.00 | 0.00 | 0.00 | 0.00 | 0.00 | 0.20 | 0.20 | 1.00 | 1.00 | 1.00 | 1.00 | 0.00 | 0.00 | 0.10 | 0.10 |
| 20 | 0.50 | 0.50 | 0.00 | 0.00 | 0.00 | 0.00 | 0.00 | 0.00 | 0.20 | 0.20 | 0.50 | 0.50 | 0.50 | 0.50 | 0.00 | 0.00 | 0.10 | 0.10 |
| 21 | 0.50 | 0.50 | 0.00 | 0.00 | 0.00 | 0.00 | 0.00 | 0.00 | 0.20 | 0.20 | 0.50 | 0.50 | 0.50 | 0.50 | 0.00 | 0.00 | 0.10 | 0.10 |
| 22 | 0.50 | 0.50 | 0.00 | 0.00 | 0.00 | 0.00 | 0.00 | 0.00 | 0.20 | 0.20 | 0.50 | 0.50 | 0.50 | 0.50 | 0.00 | 0.00 | 0.10 | 0.10 |
| 23 | 0.10 | 0.10 | 0.00 | 0.00 | 0.00 | 0.00 | 0.00 | 0.00 | 0.20 | 0.20 | 0.10 | 0.10 | 0.10 | 0.10 | 0.00 | 0.00 | 0.10 | 0.10 |

**Table D.4:** Lighting schedule. Values from 0 to 1 that are multiplied by specific heat flows and room area. Specific heat flows are 12.4 W/m$^2$ for the kitchen, 7.85 W/m$^2$ for living and sleeping rooms, 7.5 W/m$^2$ for bath rooms.

High profile

| | Livingroom | | Hobby | | Corridor | | WC | | Kitchen | | Sleeping | | Children 1 | | Bath | | Children 2 | |
|---|---|---|---|---|---|---|---|---|---|---|---|---|---|---|---|---|---|---|
| **Hour** | **mo-fr** | **sa-su** | **mo-fr** | **sa-su** | **mo-fr** | **sa-su** | **mo-fr** | **sa-su** | **mo-fr** | **sa-su** | **mo-fr** | **sa-su** | **mo-fr** | **sa-su** | **mo-fr** | **sa-su** | **mo-fr** | **sa-su** |
| 0 | 0.00 | 0.00 | 0.00 | 0.00 | 0.00 | 0.00 | 0.00 | 0.00 | 0.00 | 0.00 | 0.00 | 0.00 | 0.00 | 0.00 | 0.00 | 0.00 | 0.00 | 0.00 |
| 1 | 0.00 | 0.00 | 0.00 | 0.00 | 0.00 | 0.00 | 0.00 | 0.00 | 0.00 | 0.00 | 0.00 | 0.00 | 0.00 | 0.00 | 0.00 | 0.00 | 0.00 | 0.00 |
| 2 | 0.00 | 0.00 | 0.00 | 0.00 | 0.00 | 0.00 | 0.00 | 0.00 | 0.00 | 0.00 | 0.00 | 0.00 | 0.00 | 0.00 | 0.00 | 0.00 | 0.00 | 0.00 |
| 3 | 0.00 | 0.00 | 0.00 | 0.00 | 0.00 | 0.00 | 0.00 | 0.00 | 0.00 | 0.00 | 0.00 | 0.00 | 0.00 | 0.00 | 0.00 | 0.00 | 0.00 | 0.00 |
| 4 | 0.00 | 0.00 | 0.00 | 0.00 | 0.00 | 0.00 | 0.00 | 0.00 | 0.00 | 0.00 | 0.00 | 0.00 | 0.00 | 0.00 | 0.00 | 0.00 | 0.00 | 0.00 |
| 5 | 0.00 | 0.00 | 0.00 | 0.00 | 0.00 | 0.00 | 0.00 | 0.00 | 0.00 | 0.00 | 0.00 | 0.00 | 0.00 | 0.00 | 0.00 | 0.00 | 0.00 | 0.00 |
| 6 | 0.00 | 0.00 | 0.00 | 0.00 | 0.00 | 0.00 | 0.00 | 0.00 | 1.00 | 0.00 | 1.00 | 0.00 | 1.00 | 0.00 | 1.00 | 0.00 | 1.00 | 1.00 |
| 7 | 0.00 | 0.00 | 0.00 | 0.00 | 0.00 | 0.00 | 0.00 | 0.00 | 1.00 | 1.00 | 0.00 | 1.00 | 1.00 | 1.00 | 1.00 | 1.00 | 1.00 | 1.00 |
| 8 | 0.00 | 1.00 | 0.00 | 0.00 | 0.00 | 0.00 | 0.00 | 0.00 | 1.00 | 1.00 | 0.00 | 1.00 | 0.00 | 1.00 | 1.00 | 1.00 | 0.00 | 1.00 |
| 9 | 0.00 | 1.00 | 0.00 | 1.00 | 0.00 | 0.00 | 0.00 | 0.00 | 0.00 | 0.00 | 0.00 | 0.00 | 0.00 | 1.00 | 0.00 | 1.00 | 0.00 | 1.00 |
| 10 | 0.00 | 1.00 | 0.00 | 1.00 | 0.00 | 0.00 | 0.00 | 0.00 | 0.00 | 0.00 | 0.00 | 0.00 | 0.00 | 0.00 | 0.00 | 0.00 | 0.00 | 1.00 |
| 11 | 0.00 | 1.00 | 0.00 | 1.00 | 0.00 | 0.00 | 0.00 | 0.00 | 1.00 | 1.00 | 0.00 | 0.00 | 0.00 | 0.00 | 0.00 | 0.00 | 0.00 | 1.00 |
| 12 | 1.00 | 1.00 | 0.00 | 0.00 | 0.00 | 0.00 | 0.00 | 0.00 | 1.00 | 1.00 | 0.00 | 0.00 | 0.00 | 0.00 | 0.00 | 0.00 | 0.00 | 0.00 |
| 13 | 0.00 | 1.00 | 0.00 | 0.00 | 0.00 | 0.00 | 0.00 | 0.00 | 1.00 | 1.00 | 0.00 | 0.00 | 0.00 | 1.00 | 0.00 | 0.00 | 0.00 | 1.00 |
| 14 | 1.00 | 1.00 | 0.00 | 1.00 | 0.00 | 0.00 | 0.00 | 0.00 | 0.00 | 0.00 | 0.00 | 0.00 | 0.00 | 1.00 | 0.00 | 0.00 | 0.00 | 1.00 |
| 15 | 1.00 | 1.00 | 0.00 | 1.00 | 0.00 | 0.00 | 0.00 | 0.00 | 0.00 | 0.00 | 0.00 | 0.00 | 0.00 | 1.00 | 0.00 | 0.00 | 0.00 | 1.00 |
| 16 | 1.00 | 1.00 | 0.00 | 1.00 | 0.00 | 0.00 | 0.00 | 0.00 | 1.00 | 1.00 | 0.00 | 0.00 | 0.00 | 1.00 | 0.00 | 0.00 | 0.00 | 1.00 |
| 17 | 1.00 | 1.00 | 0.00 | 0.00 | 0.00 | 0.00 | 0.00 | 0.00 | 1.00 | 1.00 | 0.00 | 0.00 | 0.00 | 1.00 | 0.00 | 0.00 | 0.00 | 0.00 |
| 18 | 1.00 | 1.00 | 0.00 | 0.00 | 0.00 | 0.00 | 0.00 | 0.00 | 1.00 | 1.00 | 0.00 | 0.00 | 1.00 | 1.00 | 0.00 | 0.00 | 1.00 | 1.00 |
| 19 | 1.00 | 1.00 | 0.00 | 0.00 | 0.00 | 0.00 | 0.00 | 0.00 | 1.00 | 1.00 | 0.00 | 0.00 | 1.00 | 1.00 | 0.00 | 0.00 | 1.00 | 1.00 |
| 20 | 1.00 | 1.00 | 1.00 | 0.00 | 0.00 | 0.00 | 0.00 | 0.00 | 0.00 | 0.00 | 0.00 | 0.00 | 1.00 | 1.00 | 0.00 | 0.00 | 1.00 | 1.00 |
| 21 | 1.00 | 1.00 | 0.00 | 0.00 | 0.00 | 0.00 | 0.00 | 0.00 | 0.00 | 0.00 | 0.00 | 0.00 | 1.00 | 1.00 | 1.00 | 1.00 | 1.00 | 1.00 |
| 22 | 0.00 | 1.00 | 0.00 | 0.00 | 0.00 | 0.00 | 0.00 | 0.00 | 0.00 | 0.00 | 1.00 | 1.00 | 1.00 | 1.00 | 0.00 | 1.00 | 1.00 | 1.00 |
| 23 | 0.00 | 0.00 | 0.00 | 0.00 | 0.00 | 0.00 | 0.00 | 0.00 | 0.00 | 0.00 | 1.00 | 1.00 | 0.00 | 0.00 | 0.00 | 0.00 | 0.00 | 0.00 |

Low profile

| | Livingroom | | Hobby | | Corridor | | WC | | Kitchen | | Sleeping | | Children 1 | | Bath | | Children 2 | |
|---|---|---|---|---|---|---|---|---|---|---|---|---|---|---|---|---|---|---|
| **Hour** | **mo-fr** | **sa-su** | **mo-fr** | **sa-su** | **mo-fr** | **sa-su** | **mo-fr** | **sa-su** | **mo-fr** | **sa-su** | **mo-fr** | **sa-su** | **mo-fr** | **sa-su** | **mo-fr** | **sa-su** | **mo-fr** | **sa-su** |
| 0 | 0.00 | 0.00 | 0.00 | 0.00 | 0.00 | 0.00 | 0.00 | 0.00 | 0.00 | 0.00 | 0.00 | 0.00 | 0.00 | 0.00 | 0.00 | 0.00 | 0.00 | 0.00 |
| 1 | 0.00 | 0.00 | 0.00 | 0.00 | 0.00 | 0.00 | 0.00 | 0.00 | 0.00 | 0.00 | 0.00 | 0.00 | 0.00 | 0.00 | 0.00 | 0.00 | 0.00 | 0.00 |
| 2 | 0.00 | 0.00 | 0.00 | 0.00 | 0.00 | 0.00 | 0.00 | 0.00 | 0.00 | 0.00 | 0.00 | 0.00 | 0.00 | 0.00 | 0.00 | 0.00 | 0.00 | 0.00 |
| 3 | 0.00 | 0.00 | 0.00 | 0.00 | 0.00 | 0.00 | 0.00 | 0.00 | 0.00 | 0.00 | 0.00 | 0.00 | 0.00 | 0.00 | 0.00 | 0.00 | 0.00 | 0.00 |
| 4 | 0.00 | 0.00 | 0.00 | 0.00 | 0.00 | 0.00 | 0.00 | 0.00 | 0.00 | 0.00 | 0.00 | 0.00 | 0.00 | 0.00 | 0.00 | 0.00 | 0.00 | 0.00 |
| 5 | 0.00 | 0.00 | 0.00 | 0.00 | 0.00 | 0.00 | 0.00 | 0.00 | 0.00 | 0.00 | 0.00 | 0.00 | 0.00 | 0.00 | 0.00 | 0.00 | 0.00 | 0.00 |
| 6 | 0.00 | 0.00 | 0.00 | 0.00 | 0.00 | 0.00 | 0.00 | 0.00 | 1.00 | 0.00 | 1.00 | 0.00 | 1.00 | 0.00 | 1.00 | 0.00 | 0.00 | 0.00 |
| 7 | 0.00 | 0.00 | 0.00 | 0.00 | 0.00 | 0.00 | 0.00 | 0.00 | 1.00 | 1.00 | 0.00 | 1.00 | 1.00 | 1.00 | 1.00 | 1.00 | 0.00 | 0.00 |
| 8 | 0.00 | 0.00 | 0.00 | 0.00 | 0.00 | 0.00 | 0.00 | 0.00 | 1.00 | 1.00 | 0.00 | 0.00 | 0.00 | 1.00 | 1.00 | 1.00 | 0.00 | 0.00 |
| 9 | 0.00 | 1.00 | 0.00 | 0.00 | 0.00 | 0.00 | 0.00 | 0.00 | 0.00 | 0.00 | 0.00 | 0.00 | 0.00 | 1.00 | 0.00 | 1.00 | 0.00 | 0.00 |
| 10 | 0.00 | 1.00 | 0.00 | 0.00 | 0.00 | 0.00 | 0.00 | 0.00 | 0.00 | 0.00 | 0.00 | 0.00 | 0.00 | 0.00 | 0.00 | 0.00 | 0.00 | 0.00 |
| 11 | 0.00 | 0.00 | 0.00 | 0.00 | 0.00 | 0.00 | 0.00 | 0.00 | 0.00 | 0.00 | 0.00 | 0.00 | 0.00 | 0.00 | 0.00 | 0.00 | 0.00 | 0.00 |
| 12 | 0.00 | 0.00 | 0.00 | 0.00 | 0.00 | 0.00 | 0.00 | 0.00 | 0.00 | 0.00 | 0.00 | 0.00 | 0.00 | 0.00 | 0.00 | 0.00 | 0.00 | 0.00 |
| 13 | 0.00 | 1.00 | 0.00 | 0.00 | 0.00 | 0.00 | 0.00 | 0.00 | 0.00 | 0.00 | 0.00 | 0.00 | 0.00 | 0.00 | 0.00 | 0.00 | 0.00 | 0.00 |
| 14 | 1.00 | 1.00 | 0.00 | 1.00 | 0.00 | 0.00 | 0.00 | 0.00 | 0.00 | 0.00 | 0.00 | 0.00 | 0.00 | 0.00 | 0.00 | 0.00 | 0.00 | 0.00 |
| 15 | 1.00 | 1.00 | 0.00 | 1.00 | 0.00 | 0.00 | 0.00 | 0.00 | 0.00 | 0.00 | 0.00 | 0.00 | 0.00 | 0.00 | 0.00 | 0.00 | 0.00 | 0.00 |
| 16 | 1.00 | 1.00 | 0.00 | 1.00 | 0.00 | 0.00 | 0.00 | 0.00 | 1.00 | 0.00 | 0.00 | 0.00 | 0.00 | 0.00 | 0.00 | 0.00 | 0.00 | 0.00 |
| 17 | 1.00 | 1.00 | 0.00 | 1.00 | 0.00 | 0.00 | 0.00 | 0.00 | 1.00 | 0.00 | 0.00 | 0.00 | 0.00 | 0.00 | 0.00 | 0.00 | 0.00 | 0.00 |
| 18 | 1.00 | 1.00 | 0.00 | 0.00 | 0.00 | 0.00 | 0.00 | 0.00 | 1.00 | 1.00 | 0.00 | 0.00 | 1.00 | 1.00 | 0.00 | 0.00 | 0.00 | 0.00 |
| 19 | 1.00 | 1.00 | 0.00 | 0.00 | 0.00 | 0.00 | 0.00 | 0.00 | 1.00 | 1.00 | 0.00 | 0.00 | 1.00 | 1.00 | 0.00 | 0.00 | 0.00 | 0.00 |
| 20 | 1.00 | 1.00 | 1.00 | 0.00 | 0.00 | 0.00 | 0.00 | 0.00 | 0.00 | 0.00 | 0.00 | 0.00 | 1.00 | 1.00 | 0.00 | 0.00 | 0.00 | 0.00 |
| 21 | 1.00 | 1.00 | 0.00 | 0.00 | 0.00 | 0.00 | 0.00 | 0.00 | 0.00 | 0.00 | 0.00 | 0.00 | 1.00 | 1.00 | 1.00 | 1.00 | 0.00 | 0.00 |
| 22 | 0.00 | 1.00 | 0.00 | 0.00 | 0.00 | 0.00 | 0.00 | 0.00 | 0.00 | 0.00 | 1.00 | 1.00 | 1.00 | 1.00 | 0.00 | 1.00 | 0.00 | 0.00 |
| 23 | 0.00 | 0.00 | 0.00 | 0.00 | 0.00 | 0.00 | 0.00 | 0.00 | 0.00 | 0.00 | 1.00 | 1.00 | 0.00 | 0.00 | 0.00 | 0.00 | 0.00 | 0.00 |

**Table D.5:** Ventilation schedule, high profile in 1/h.

| | Livingroom | | Hobby | | WC | | Kitchen | | Sleeping | | Children 1 | | Bath | | Children 2 | |
|---|---|---|---|---|---|---|---|---|---|---|---|---|---|---|---|---|
| **Hour** | **mo-fr** | **sa-su** | **mo-fr** | **sa-su** | **mo-fr** | **sa-su** | **mo-fr** | **sa-su** | **mo-fr** | **sa-su** | **mo-fr** | **sa-su** | **mo-fr** | **sa-su** | **mo-fr** | **sa-su** |
| 0:00 | 0.00 | 0.00 | 0.00 | 0.00 | 0.00 | 0.00 | 0.50 | 0.50 | 0.00 | 0.00 | 0.00 | 0.00 | 0.00 | 0.00 | 0.00 | 0.00 |
| 0:30 | 0.00 | 0.00 | 0.00 | 0.00 | 0.00 | 0.00 | 0.50 | 0.50 | 0.00 | 0.00 | 0.00 | 0.00 | 0.00 | 0.00 | 0.00 | 0.00 |
| 1:00 | 0.00 | 0.00 | 0.00 | 0.00 | 0.00 | 0.00 | 0.50 | 0.50 | 0.00 | 0.00 | 0.00 | 0.00 | 0.00 | 0.00 | 0.00 | 0.00 |
| 1:30 | 0.00 | 0.00 | 0.00 | 0.00 | 0.00 | 0.00 | 0.50 | 0.50 | 0.00 | 0.00 | 0.00 | 0.00 | 0.00 | 0.00 | 0.00 | 0.00 |
| 2:00 | 0.00 | 0.00 | 0.00 | 0.00 | 0.00 | 0.00 | 0.50 | 0.50 | 0.00 | 0.00 | 0.00 | 0.00 | 0.00 | 0.00 | 0.00 | 0.00 |
| 2:30 | 0.00 | 0.00 | 0.00 | 0.00 | 0.00 | 0.00 | 0.50 | 0.50 | 0.00 | 0.00 | 0.00 | 0.00 | 0.00 | 0.00 | 0.00 | 0.00 |
| 3:00 | 0.00 | 0.00 | 0.00 | 0.00 | 0.00 | 0.00 | 0.50 | 0.50 | 0.00 | 0.00 | 0.00 | 0.00 | 0.00 | 0.00 | 0.00 | 0.00 |
| 3:30 | 0.00 | 0.00 | 0.00 | 0.00 | 0.00 | 0.00 | 0.50 | 0.50 | 0.00 | 0.00 | 0.00 | 0.00 | 0.00 | 0.00 | 0.00 | 0.00 |
| 4:00 | 0.00 | 0.00 | 0.00 | 0.00 | 0.00 | 0.00 | 0.50 | 0.50 | 0.00 | 0.00 | 0.00 | 0.00 | 0.00 | 0.00 | 0.00 | 0.00 |
| 4:30 | 0.00 | 0.00 | 0.00 | 0.00 | 0.00 | 0.00 | 0.50 | 0.50 | 0.00 | 0.00 | 0.00 | 0.00 | 0.00 | 0.00 | 0.00 | 0.00 |
| 5:00 | 0.00 | 0.00 | 0.00 | 0.00 | 0.00 | 0.00 | 0.50 | 0.50 | 0.00 | 0.00 | 0.00 | 0.00 | 0.00 | 0.00 | 0.00 | 0.00 |
| 5:30 | 0.00 | 0.00 | 0.00 | 0.00 | 0.00 | 0.00 | 0.50 | 0.50 | 0.00 | 0.00 | 0.00 | 0.00 | 0.00 | 0.00 | 0.00 | 0.00 |
| 6:00 | 0.00 | 0.00 | 0.00 | 0.00 | 0.00 | 0.00 | 0.50 | 0.50 | 0.00 | 0.00 | 0.00 | 0.00 | 0.00 | 0.00 | 12.00 | 0.00 |
| 6:30 | 0.00 | 0.00 | 0.00 | 0.00 | 0.00 | 0.00 | 0.50 | 0.50 | 12.00 | 0.00 | 12.00 | 0.00 | 0.00 | 0.00 | 0.00 | 0.00 |
| 7:00 | 0.00 | 0.00 | 0.00 | 0.00 | 12.00 | 0.00 | 0.50 | 0.50 | 0.00 | 12.00 | 0.00 | 0.00 | 0.00 | 0.00 | 0.00 | 0.00 |
| 7:30 | 0.00 | 0.00 | 0.00 | 0.00 | 0.00 | 0.00 | 0.50 | 0.50 | 0.00 | 0.00 | 0.00 | 0.00 | 0.00 | 0.00 | 0.00 | 0.00 |
| 8:00 | 0.00 | 0.00 | 0.00 | 0.00 | 0.00 | 12.00 | 0.50 | 0.50 | 0.00 | 0.00 | 0.00 | 0.00 | 12.00 | 0.00 | 0.00 | 0.00 |
| 8:30 | 0.00 | 0.00 | 0.00 | 0.00 | 0.00 | 0.00 | 0.50 | 0.50 | 0.00 | 0.00 | 0.00 | 0.00 | 0.00 | 0.00 | 0.00 | 0.00 |
| 9:00 | 0.00 | 12.00 | 0.00 | 0.50 | 0.00 | 0.00 | 0.50 | 0.50 | 0.00 | 0.00 | 0.00 | 12.00 | 0.00 | 12.00 | 0.00 | 0.00 |
| 9:30 | 0.00 | 0.00 | 0.00 | 0.50 | 0.00 | 0.00 | 0.50 | 0.50 | 0.00 | 0.00 | 0.00 | 0.00 | 0.00 | 0.00 | 0.00 | 0.00 |
| 10:00 | 0.00 | 0.00 | 0.00 | 0.50 | 0.00 | 0.00 | 0.50 | 0.50 | 0.00 | 0.00 | 0.00 | 0.00 | 0.00 | 0.00 | 0.00 | 0.00 |
| 10:30 | 0.00 | 0.00 | 0.00 | 0.50 | 0.00 | 0.00 | 0.50 | 0.50 | 0.00 | 0.00 | 0.00 | 0.00 | 0.00 | 0.00 | 0.00 | 0.00 |
| 11:00 | 0.00 | 0.00 | 0.00 | 0.50 | 0.00 | 0.00 | 0.50 | 0.50 | 0.00 | 0.00 | 0.00 | 0.00 | 0.00 | 0.00 | 0.00 | 0.00 |
| 11:30 | 0.00 | 0.00 | 0.00 | 0.50 | 0.00 | 0.00 | 0.50 | 0.50 | 0.00 | 0.00 | 0.00 | 0.00 | 0.00 | 0.00 | 0.00 | 0.00 |
| 12:00 | 12.00 | 0.00 | 0.00 | 0.50 | 0.00 | 0.00 | 0.50 | 0.50 | 0.00 | 0.00 | 0.00 | 0.00 | 0.00 | 0.00 | 0.00 | 12.00 |
| 12:30 | 0.00 | 0.00 | 0.00 | 0.50 | 0.00 | 0.00 | 0.50 | 0.50 | 0.00 | 0.00 | 0.00 | 0.00 | 0.00 | 0.00 | 0.00 | 0.00 |
| 13:00 | 0.00 | 0.00 | 0.00 | 0.50 | 0.00 | 0.00 | 0.50 | 0.50 | 0.00 | 0.00 | 0.00 | 0.00 | 0.00 | 0.00 | 0.00 | 0.00 |
| 13:30 | 0.00 | 0.00 | 0.00 | 0.50 | 0.00 | 0.00 | 0.50 | 0.50 | 0.00 | 0.00 | 0.00 | 0.00 | 0.00 | 0.00 | 0.00 | 0.00 |
| 14:00 | 0.00 | 0.00 | 0.00 | 0.50 | 0.00 | 0.00 | 0.50 | 0.50 | 0.00 | 0.00 | 0.00 | 0.00 | 0.00 | 0.00 | 0.00 | 0.00 |
| 14:30 | 0.00 | 0.00 | 0.00 | 0.50 | 0.00 | 0.00 | 0.50 | 0.50 | 0.00 | 0.00 | 0.00 | 0.00 | 0.00 | 0.00 | 0.00 | 0.00 |
| 15:00 | 0.00 | 0.00 | 0.00 | 0.50 | 0.00 | 0.00 | 0.50 | 0.50 | 0.00 | 0.00 | 0.00 | 0.00 | 0.00 | 0.00 | 0.00 | 0.00 |
| 15:30 | 0.00 | 0.00 | 0.00 | 0.50 | 0.00 | 0.00 | 0.50 | 0.50 | 0.00 | 0.00 | 0.00 | 0.00 | 0.00 | 0.00 | 0.00 | 0.00 |
| 16:00 | 0.00 | 0.00 | 0.00 | 0.50 | 0.00 | 0.00 | 0.50 | 0.50 | 0.00 | 0.00 | 0.00 | 0.00 | 0.00 | 0.00 | 0.00 | 0.00 |
| 16:30 | 0.00 | 0.00 | 0.00 | 0.50 | 0.00 | 0.00 | 0.50 | 0.50 | 0.00 | 0.00 | 0.00 | 0.00 | 0.00 | 0.00 | 0.00 | 0.00 |
| 17:00 | 0.00 | 0.00 | 0.00 | 0.00 | 0.00 | 0.00 | 0.50 | 0.50 | 0.00 | 0.00 | 0.00 | 0.00 | 0.00 | 0.00 | 12.00 | 12.00 |
| 17:30 | 0.00 | 0.00 | 0.00 | 0.00 | 0.00 | 0.00 | 0.50 | 0.50 | 0.00 | 0.00 | 0.00 | 0.00 | 0.00 | 0.00 | 0.00 | 0.00 |
| 18:00 | 0.00 | 0.00 | 0.00 | 0.00 | 0.00 | 0.00 | 0.50 | 0.50 | 0.00 | 0.00 | 0.00 | 12.00 | 12.00 | 0.00 | 0.00 | 0.00 |
| 18:30 | 0.00 | 0.00 | 0.00 | 0.00 | 0.00 | 0.00 | 0.50 | 0.50 | 0.00 | 0.00 | 0.00 | 0.00 | 0.00 | 0.00 | 0.00 | 0.00 |
| 19:00 | 12.00 | 12.00 | 0.00 | 0.00 | 0.00 | 0.00 | 0.50 | 0.50 | 0.00 | 0.00 | 0.00 | 0.00 | 0.00 | 0.00 | 0.00 | 0.00 |
| 19:30 | 0.00 | 0.00 | 0.00 | 0.00 | 0.00 | 0.00 | 0.50 | 0.50 | 0.00 | 0.00 | 12.00 | 0.00 | 0.00 | 0.00 | 0.00 | 0.00 |
| 20:00 | 0.00 | 0.00 | 0.50 | 0.00 | 0.00 | 0.00 | 0.50 | 0.50 | 12.00 | 12.00 | 0.00 | 0.00 | 0.00 | 12.00 | 0.00 | 0.00 |
| 20:30 | 0.00 | 0.00 | 0.50 | 0.00 | 0.00 | 0.00 | 0.50 | 0.50 | 0.00 | 0.00 | 0.00 | 0.00 | 0.00 | 0.00 | 0.00 | 0.00 |
| 21:00 | 0.00 | 0.00 | 0.00 | 0.00 | 0.00 | 0.00 | 0.50 | 0.50 | 0.00 | 0.00 | 0.00 | 0.00 | 0.00 | 0.00 | 0.00 | 0.00 |
| 21:30 | 0.00 | 0.00 | 0.00 | 0.00 | 0.00 | 0.00 | 0.50 | 0.50 | 0.00 | 0.00 | 0.00 | 0.00 | 0.00 | 0.00 | 0.00 | 0.00 |
| 22:00 | 0.00 | 0.00 | 0.00 | 0.00 | 0.00 | 0.00 | 0.50 | 0.50 | 0.00 | 0.00 | 0.00 | 0.00 | 0.00 | 0.00 | 0.00 | 0.00 |
| 22:30 | 0.00 | 0.00 | 0.00 | 0.00 | 0.00 | 0.00 | 0.50 | 0.50 | 0.00 | 0.00 | 0.00 | 0.00 | 0.00 | 0.00 | 0.00 | 0.00 |
| 23:00 | 0.00 | 0.00 | 0.00 | 0.00 | 0.00 | 0.00 | 0.50 | 0.50 | 0.00 | 0.00 | 0.00 | 0.00 | 0.00 | 0.00 | 0.00 | 0.00 |
| 23:30 | 0.00 | 0.00 | 0.00 | 0.00 | 0.00 | 0.00 | 0.50 | 0.50 | 0.00 | 0.00 | 0.00 | 0.00 | 0.00 | 0.00 | 0.00 | 0.00 |

**Table D.6:** Ventilation schedule, low profile in 1/h.

| | Livingroom | | Hobby | | WC | | Kitchen | | Sleeping | | Children 1 | | Bath | | Children 2 | |
|---|---|---|---|---|---|---|---|---|---|---|---|---|---|---|---|---|
| **Hour** | **mo-fr** | **sa-su** | **mo-fr** | **sa-su** | **mo-fr** | **sa-su** | **mo-fr** | **sa-su** | **mo-fr** | **sa-su** | **mo-fr** | **sa-su** | **mo-fr** | **sa-su** | **mo-fr** | **sa-su** |
| 0:00 | 0.00 | 0.00 | 0.00 | 0.00 | 0.00 | 0.00 | 0.40 | 0.40 | 0.00 | 0.00 | 0.00 | 0.00 | 0.00 | 0.00 | 0.00 | 0.00 |
| 0:30 | 0.00 | 0.00 | 0.00 | 0.00 | 0.00 | 0.00 | 0.40 | 0.40 | 0.00 | 0.00 | 0.00 | 0.00 | 0.00 | 0.00 | 0.00 | 0.00 |
| 1:00 | 0.00 | 0.00 | 0.00 | 0.00 | 0.00 | 0.00 | 0.40 | 0.40 | 0.00 | 0.00 | 0.00 | 0.00 | 0.00 | 0.00 | 0.00 | 0.00 |
| 1:30 | 0.00 | 0.00 | 0.00 | 0.00 | 0.00 | 0.00 | 0.40 | 0.40 | 0.00 | 0.00 | 0.00 | 0.00 | 0.00 | 0.00 | 0.00 | 0.00 |
| 2:00 | 0.00 | 0.00 | 0.00 | 0.00 | 0.00 | 0.00 | 0.40 | 0.40 | 0.00 | 0.00 | 0.00 | 0.00 | 0.00 | 0.00 | 0.00 | 0.00 |
| 2:30 | 0.00 | 0.00 | 0.00 | 0.00 | 0.00 | 0.00 | 0.40 | 0.40 | 0.00 | 0.00 | 0.00 | 0.00 | 0.00 | 0.00 | 0.00 | 0.00 |
| 3:00 | 0.00 | 0.00 | 0.00 | 0.00 | 0.00 | 0.00 | 0.40 | 0.40 | 0.00 | 0.00 | 0.00 | 0.00 | 0.00 | 0.00 | 0.00 | 0.00 |
| 3:30 | 0.00 | 0.00 | 0.00 | 0.00 | 0.00 | 0.00 | 0.40 | 0.40 | 0.00 | 0.00 | 0.00 | 0.00 | 0.00 | 0.00 | 0.00 | 0.00 |
| 4:00 | 0.00 | 0.00 | 0.00 | 0.00 | 0.00 | 0.00 | 0.40 | 0.40 | 0.00 | 0.00 | 0.00 | 0.00 | 0.00 | 0.00 | 0.00 | 0.00 |
| 4:30 | 0.00 | 0.00 | 0.00 | 0.00 | 0.00 | 0.00 | 0.40 | 0.40 | 0.00 | 0.00 | 0.00 | 0.00 | 0.00 | 0.00 | 0.00 | 0.00 |
| 5:00 | 0.00 | 0.00 | 0.00 | 0.00 | 0.00 | 0.00 | 0.40 | 0.40 | 0.00 | 0.00 | 0.00 | 0.00 | 0.00 | 0.00 | 0.00 | 0.00 |
| 5:30 | 0.00 | 0.00 | 0.00 | 0.00 | 0.00 | 0.00 | 0.40 | 0.40 | 0.00 | 0.00 | 0.00 | 0.00 | 0.00 | 0.00 | 0.00 | 0.00 |
| 6:00 | 0.00 | 0.00 | 0.00 | 0.00 | 0.00 | 0.00 | 0.40 | 0.40 | 0.00 | 0.00 | 0.00 | 0.00 | 0.00 | 0.00 | 0.00 | 0.00 |
| 6:30 | 0.00 | 0.00 | 0.00 | 0.00 | 0.00 | 0.00 | 0.40 | 0.40 | 12.00 | 0.00 | 12.00 | 0.00 | 0.00 | 0.00 | 0.00 | 0.00 |
| 7:00 | 0.00 | 0.00 | 0.00 | 0.00 | 6.00 | 0.00 | 0.40 | 0.40 | 0.00 | 12.00 | 0.00 | 0.00 | 0.00 | 0.00 | 0.00 | 0.00 |
| 7:30 | 0.00 | 0.00 | 0.00 | 0.00 | 0.00 | 0.00 | 0.40 | 0.40 | 0.00 | 0.00 | 0.00 | 0.00 | 0.00 | 0.00 | 0.00 | 0.00 |
| 8:00 | 0.00 | 0.00 | 0.00 | 0.00 | 0.00 | 6.00 | 0.40 | 0.40 | 0.00 | 0.00 | 0.00 | 0.00 | 8.00 | 0.00 | 0.00 | 0.00 |
| 8:30 | 0.00 | 0.00 | 0.00 | 0.00 | 0.00 | 0.00 | 0.40 | 0.40 | 0.00 | 0.00 | 0.00 | 0.00 | 0.00 | 0.00 | 0.00 | 0.00 |
| 9:00 | 0.00 | 12.00 | 0.00 | 0.50 | 0.00 | 0.00 | 0.40 | 0.40 | 0.00 | 0.00 | 0.00 | 6.00 | 0.00 | 8.00 | 0.00 | 6.00 |
| 9:30 | 0.00 | 0.00 | 0.00 | 0.50 | 0.00 | 0.00 | 0.40 | 0.40 | 0.00 | 0.00 | 0.00 | 0.00 | 0.00 | 0.00 | 0.00 | 0.00 |
| 10:00 | 0.00 | 0.00 | 0.00 | 0.50 | 0.00 | 0.00 | 0.40 | 0.40 | 0.00 | 0.00 | 0.00 | 0.00 | 0.00 | 0.00 | 0.00 | 0.00 |
| 10:30 | 0.00 | 0.00 | 0.00 | 0.50 | 0.00 | 0.00 | 0.40 | 0.40 | 0.00 | 0.00 | 0.00 | 0.00 | 0.00 | 0.00 | 0.00 | 0.00 |
| 11:00 | 0.00 | 0.00 | 0.00 | 0.50 | 0.00 | 0.00 | 0.40 | 0.40 | 0.00 | 0.00 | 0.00 | 0.00 | 0.00 | 0.00 | 0.00 | 0.00 |
| 11:30 | 0.00 | 0.00 | 0.00 | 0.50 | 0.00 | 0.00 | 0.40 | 0.40 | 0.00 | 0.00 | 0.00 | 0.00 | 0.00 | 0.00 | 0.00 | 0.00 |
| 12:00 | 12.00 | 0.00 | 0.00 | 0.00 | 0.00 | 0.00 | 0.40 | 0.40 | 0.00 | 0.00 | 0.00 | 0.00 | 0.00 | 0.00 | 0.00 | 0.00 |
| 12:30 | 0.00 | 0.00 | 0.00 | 0.00 | 0.00 | 0.00 | 0.40 | 0.40 | 0.00 | 0.00 | 0.00 | 0.00 | 0.00 | 0.00 | 0.00 | 0.00 |
| 13:00 | 0.00 | 0.00 | 0.00 | 0.50 | 0.00 | 0.00 | 0.40 | 0.40 | 0.00 | 0.00 | 0.00 | 0.00 | 0.00 | 0.00 | 0.00 | 0.00 |
| 13:30 | 0.00 | 0.00 | 0.00 | 0.50 | 0.00 | 0.00 | 0.40 | 0.40 | 0.00 | 0.00 | 0.00 | 0.00 | 0.00 | 0.00 | 0.00 | 0.00 |
| 14:00 | 0.00 | 0.00 | 0.00 | 0.50 | 0.00 | 0.00 | 0.40 | 0.40 | 0.00 | 0.00 | 0.00 | 0.00 | 0.00 | 0.00 | 0.00 | 0.00 |
| 14:30 | 0.00 | 0.00 | 0.00 | 0.50 | 0.00 | 0.00 | 0.40 | 0.40 | 0.00 | 0.00 | 0.00 | 0.00 | 0.00 | 0.00 | 0.00 | 0.00 |
| 15:00 | 0.00 | 0.00 | 0.00 | 0.50 | 0.00 | 0.00 | 0.40 | 0.40 | 0.00 | 0.00 | 0.00 | 0.00 | 0.00 | 0.00 | 0.00 | 0.00 |
| 15:30 | 0.00 | 0.00 | 0.00 | 0.50 | 0.00 | 0.00 | 0.40 | 0.40 | 0.00 | 0.00 | 0.00 | 0.00 | 0.00 | 0.00 | 0.00 | 0.00 |
| 16:00 | 0.00 | 0.00 | 0.00 | 0.50 | 0.00 | 0.00 | 0.40 | 0.40 | 0.00 | 0.00 | 0.00 | 0.00 | 0.00 | 0.00 | 0.00 | 0.00 |
| 16:30 | 0.00 | 0.00 | 0.00 | 0.50 | 0.00 | 0.00 | 0.40 | 0.40 | 0.00 | 0.00 | 0.00 | 0.00 | 0.00 | 0.00 | 0.00 | 0.00 |
| 17:00 | 0.00 | 0.00 | 0.00 | 0.00 | 0.00 | 0.00 | 0.40 | 0.40 | 0.00 | 0.00 | 0.00 | 0.00 | 0.00 | 0.00 | 0.00 | 0.00 |
| 17:30 | 0.00 | 0.00 | 0.00 | 0.00 | 0.00 | 0.00 | 0.40 | 0.40 | 0.00 | 0.00 | 0.00 | 0.00 | 0.00 | 0.00 | 0.00 | 0.00 |
| 18:00 | 0.00 | 0.00 | 0.00 | 0.00 | 0.00 | 0.00 | 0.40 | 0.40 | 0.00 | 0.00 | 0.00 | 0.00 | 8.00 | 0.00 | 0.00 | 0.00 |
| 18:30 | 0.00 | 0.00 | 0.00 | 0.00 | 0.00 | 0.00 | 0.40 | 0.40 | 0.00 | 0.00 | 0.00 | 0.00 | 0.00 | 0.00 | 0.00 | 0.00 |
| 19:00 | 6.00 | 6.00 | 0.00 | 0.00 | 0.00 | 0.00 | 0.40 | 0.40 | 0.00 | 0.00 | 0.00 | 0.00 | 0.00 | 0.00 | 0.00 | 0.00 |
| 19:30 | 0.00 | 0.00 | 0.00 | 0.00 | 0.00 | 0.00 | 0.40 | 0.40 | 0.00 | 0.00 | 6.00 | 0.00 | 0.00 | 0.00 | 0.00 | 0.00 |
| 20:00 | 0.00 | 0.00 | 0.50 | 0.00 | 0.00 | 0.00 | 0.40 | 0.40 | 0.00 | 0.00 | 0.00 | 0.00 | 0.00 | 8.00 | 0.00 | 0.00 |
| 20:30 | 0.00 | 0.00 | 0.50 | 0.00 | 0.00 | 0.00 | 0.40 | 0.40 | 0.00 | 0.00 | 0.00 | 0.00 | 0.00 | 0.00 | 0.00 | 0.00 |
| 21:00 | 0.00 | 0.00 | 0.00 | 0.00 | 0.00 | 0.00 | 0.40 | 0.40 | 0.00 | 0.00 | 0.00 | 0.00 | 0.00 | 0.00 | 0.00 | 0.00 |
| 21:30 | 0.00 | 0.00 | 0.00 | 0.00 | 0.00 | 0.00 | 0.40 | 0.40 | 0.00 | 0.00 | 0.00 | 0.00 | 0.00 | 0.00 | 0.00 | 0.00 |
| 22:00 | 0.00 | 0.00 | 0.00 | 0.00 | 0.00 | 0.00 | 0.40 | 0.40 | 0.00 | 0.00 | 0.00 | 0.00 | 0.00 | 0.00 | 0.00 | 0.00 |
| 22:30 | 0.00 | 0.00 | 0.00 | 0.00 | 0.00 | 0.00 | 0.40 | 0.40 | 0.00 | 0.00 | 0.00 | 0.00 | 0.00 | 0.00 | 0.00 | 0.00 |
| 23:00 | 0.00 | 0.00 | 0.00 | 0.00 | 0.00 | 0.00 | 0.40 | 0.40 | 0.00 | 0.00 | 0.00 | 0.00 | 0.00 | 0.00 | 0.00 | 0.00 |
| 23:30 | 0.00 | 0.00 | 0.00 | 0.00 | 0.00 | 0.00 | 0.40 | 0.40 | 0.00 | 0.00 | 0.00 | 0.00 | 0.00 | 0.00 | 0.00 | 0.00 |

# E Additional model parametrization data

**Table E.1:** Coefficients for the pump model, see equation 4.12

| symbol | value for WSchV84 | value for EnEV2009 | unit |
|---|---|---|---|
| $c_0$ | 4.7277 | 0.4602 | m |
| $c_1$ | 0.8982 | 0.06338 | $h/m^2$ |
| $c_2$ | -0.8831 | -0.06323 | $h^2/m^5$ |

**Table E.2:** Nominal mass flows and flow coefficients of the radiator valves. The valve data is chosen according to *Danfoss RA N 15* valve characteristic for a proportional range of 1 K.

| room nb. | $\dot{m}_{nom}$ in kg/s | $k_{vs}$ in $m^3/h$ |
|---|---|---|
| 1 | 0.055 | 0.4300 |
| 2 | 0.029 | 0.1902 |
| 3 | 0.042 | 0.2835 |
| 4 | 0.027 | 0.1727 |
| 5 | 0.028 | 0.1787 |
| 6 | 0.042 | 0.3044 |
| 7 | 0.030 | 0.1928 |
| 8 | 0.034 | 0.2250 |
| 9 | 0.036 | 0.2394 |

# F Building model

| | WSchV84 - W | EnEV09 - E |
|---|---|---|
| Outer wall | 0.6 W/(m$^2$K) | 0.28 W/(m$^2$K) |
| Ground floor | 0.7 W/(m$^2$K) | 0.35 W/(m$^2$K) |
| Floor slap | 0.45 W/(m$^2$K) | 0.2 W/(m$^2$K) |
| Saddle roof | 0.45 W/(m$^2$K) | 0.2 W/(m$^2$K) |
| Window | 2.5 W/(m$^2$K) | 1.3 W/(m$^2$K) |
| Outer door | 3.1 W/(m$^2$K) | 1.8 W/(m$^2$K) |

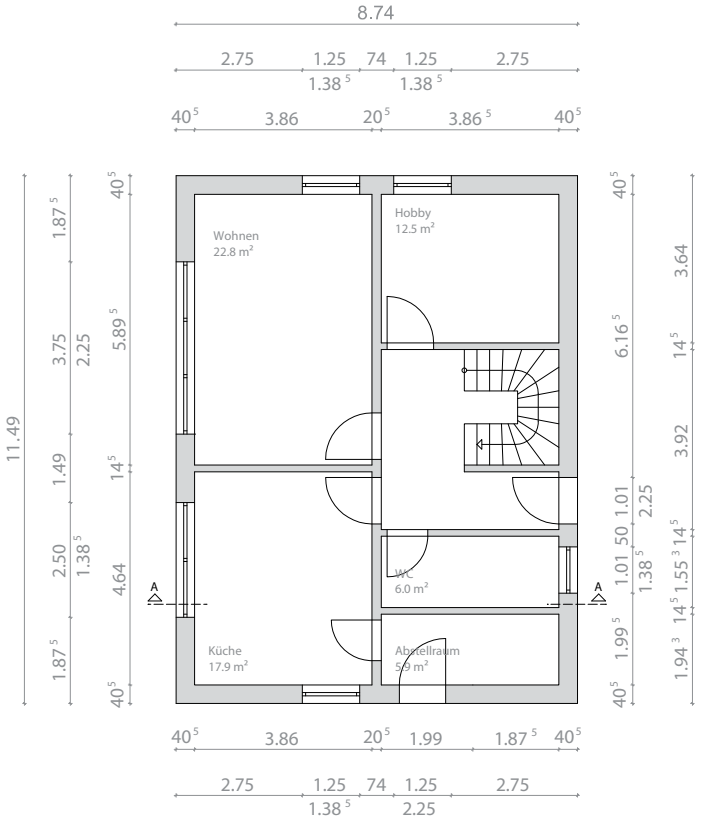


**Figure F.1:** Plan of the ground floor of the modeled building (Constantin et al., 2014).

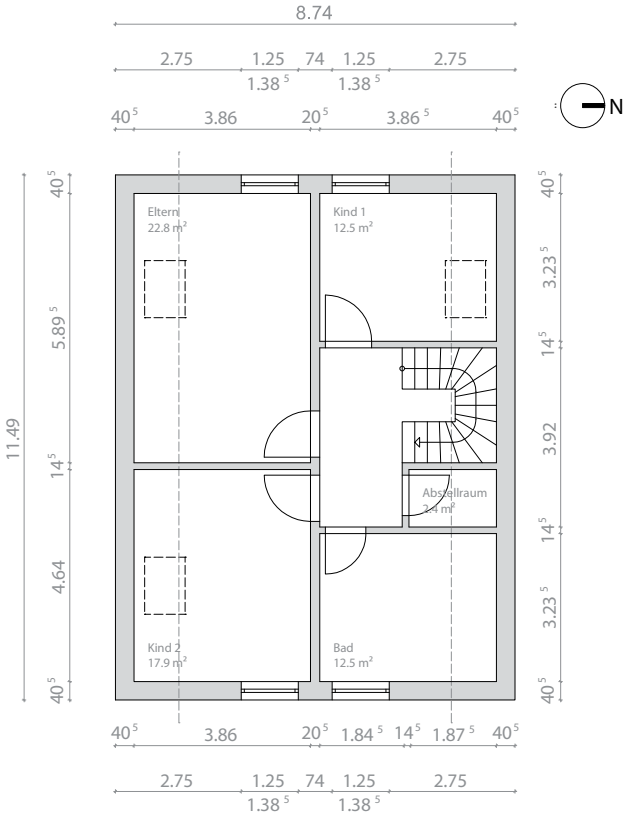


**Figure F.2:** Plan of the upper floor of the modeled building (Constantin et al., 2014).

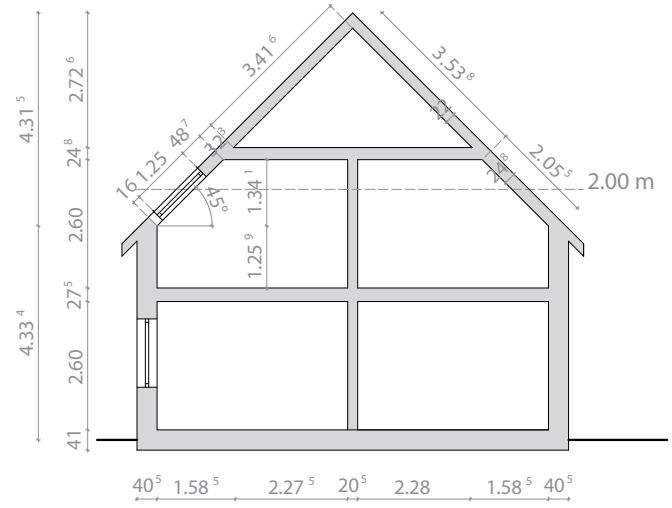


**Figure F.3:** Section view of the modeled building (see A-A in figure F.1) (Constantin et al., 2014).

# G Reference system with DHW generation

DHW demand is not part of the studies in this work. Nevertheless, the possible influence on heat pump efficiency is analyzed for one system which allows for better comparison to the field test results where many heat pump systems also generate DHW. The reference system is therefore extended by a DHW storage that can be loaded by a coiled tube heat exchanger[1]. A three way valve in the condenser circuit controls whether the buffer storage or DHW storage is charged. Loading of DHW storage has priority over loading of buffer storage and is activated if the upper DHW storage temperature falls below 45 °C and is turned of when reaching 50 °C. The cold water temperature is 10 °C during the whole year. The DHW tap profile is taken from DIN EN 16147-2011 (2011), profile M; slight adjustments to this profile are adopted according to Haller et al. (2013).

The $SPF_1$ of the reference system WBH for a year long simulation is 2.59, the $SPF_2$ is 2.89. Figure G.1, using the same representation as for field test objects in figure 3.8, shows the monthly performance factors and monthly mean temperatures. The characteristic of the system with DHW generation is in line with the field test results. This shows that the system characteristics are well modeled.

[1] Storage data from Buderus Logalux SF 300 is used.

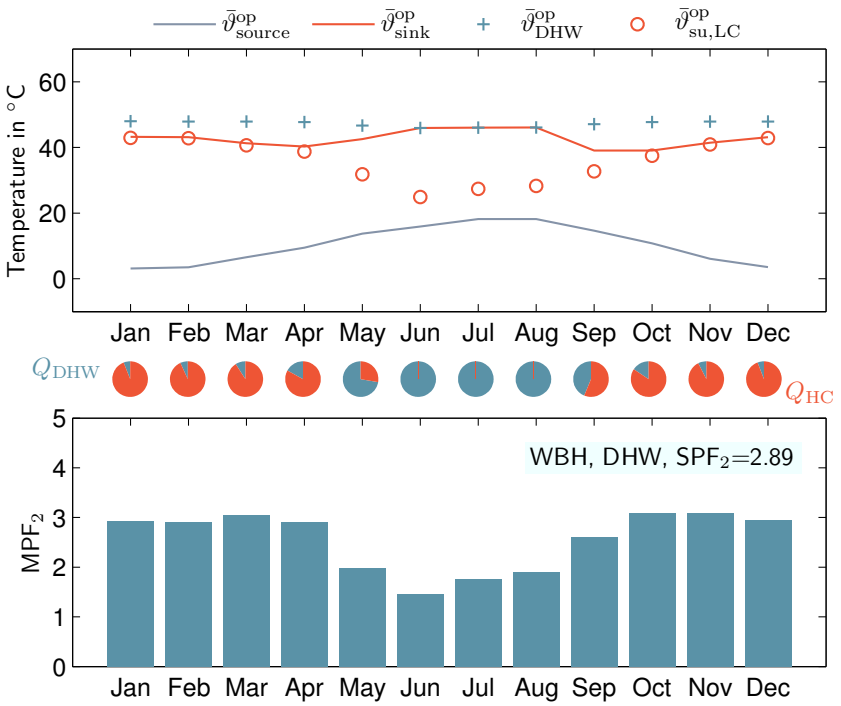


**Figure G.1:** Monthly temperature lift and performance factor of reference system WBH with DHW generation, control volume 2.

# H Room model for MPC

For the room volume the energy balance leads to:

$$\dot{T}_\mathrm{R} = \frac{-H_\mathrm{RW} - H_\mathrm{V} - H_\mathrm{RC}}{C_\mathrm{R}} \cdot T_\mathrm{R} + \frac{H_\mathrm{RW}}{C_\mathrm{R}} \cdot T_\mathrm{W} + \frac{H_\mathrm{RC}}{C_\mathrm{R}} \cdot T_\mathrm{C} - \frac{H_\mathrm{V}}{C_\mathrm{R}} \cdot T_\mathrm{O} + \frac{1}{2C_\mathrm{R}} \cdot \dot{Q}_\mathrm{H} + \frac{1}{2C_\mathrm{R}} \cdot \dot{Q}_\mathrm{G} \tag{H.1}$$

Thereby, index R is for the room air node, W for the wall, index C for the capacity of inner walls, O for outdoor. $H$ is the heat loss coefficient representing heat conductance between different nodes whereas $H_\mathrm{V}$ represents the heat loss coefficient for ventilation, i.e. between the room air node and the outdoors. $\dot{Q}_\mathrm{G}$ represents inner and solar gains, $\dot{Q}_\mathrm{H}$ represents the heat gain through the heater, i.e. the radiator.

The wall is represented as follows:

$$\dot{T}_\mathrm{W} = \frac{-H_\mathrm{RW} - H_\mathrm{WO}}{C_\mathrm{W}} \cdot T_\mathrm{W} + \frac{H_\mathrm{RW}}{C_\mathrm{W}} \cdot T_\mathrm{R} + \frac{H_\mathrm{WO}}{C_\mathrm{W}} \cdot T_\mathrm{O} \tag{H.2}$$

$H_\mathrm{WO}$ is the heat loss coefficient for heat transfer from the wall node to the outdoor air. The capacity is connected to the air node:

$$\dot{T}_\mathrm{C} = \frac{H_\mathrm{RC}}{C_\mathrm{C}} \dot{T}_\mathrm{R} - \frac{H_\mathrm{RC}}{C_\mathrm{C}} \dot{T}_\mathrm{C} + \frac{1}{2C_\mathrm{C}} \cdot \dot{Q}_\mathrm{H} + \frac{1}{2C_\mathrm{C}} \cdot \dot{Q}_\mathrm{G} \tag{H.3}$$

These three equations can be used as linear, time-invariant model for MPC in the form of

$$\dot{x} = A \cdot x + B \cdot u \tag{H.4}$$

with

$$A = \begin{bmatrix} \frac{-H_\mathrm{RW}-H_\mathrm{V}-H_\mathrm{RC}}{C_\mathrm{R}} & \frac{H_\mathrm{RW}}{C_\mathrm{R}} & \frac{H_\mathrm{RC}}{C_\mathrm{R}} \\ \frac{H_\mathrm{RW}}{C_\mathrm{W}} & \frac{-H_\mathrm{RW}-H_\mathrm{WA}}{C_\mathrm{W}} & 0 \\ \frac{H_\mathrm{RC}}{C_\mathrm{C}} & 0 & -\frac{H_\mathrm{RC}}{C_\mathrm{C}} \end{bmatrix}, B = \begin{bmatrix} -\frac{H_\mathrm{V}}{C_\mathrm{R}} & \frac{1}{2C_\mathrm{R}} & \frac{1}{2C_\mathrm{R}} \\ \frac{H_\mathrm{WA}}{C_\mathrm{W}} & 0 & 0 \\ 0 & \frac{1}{2C_\mathrm{C}} & \frac{1}{2C_\mathrm{C}} \end{bmatrix},$$

$$x = \begin{bmatrix} T_\mathrm{R} \\ T_\mathrm{W} \\ T_\mathrm{C} \end{bmatrix}, u = \begin{bmatrix} T_\mathrm{A} \\ \dot{Q}_\mathrm{H} \\ \dot{Q}_\mathrm{G} \end{bmatrix}.$$

The model is compared to the room model implemented in Modelica, which implements radiation, convection, multiple layer walls with respect to capacities and heat conductance. Figure H.1 shows a comparison of both models during two days. Short-time response of the simplified model

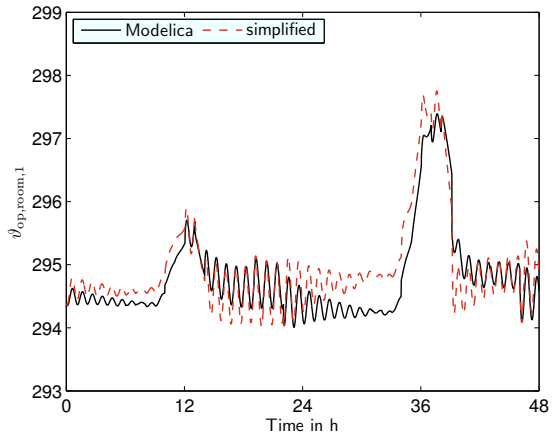


**Figure H.1:** Comparison of Modelica model and simplified room model for MPC control.

matches well the detailed model ones whereas certain behavior is not well modeled according to different shares of convective and radiative heat gains than assumed.

# I Detailed results of simulation studies

**Table I.1:** Results of system simulations: Different insulation standards and User schedules.

| | $SPF_1$ | $W_{el,HP}$ in kWh | $W_{el,HR}$ in kWh | $Q_{LC}$ in kWh | $Q_{HC}$ in kWh | $t_{on}$ in h | $n_{op}$ |
|---|---|---|---|---|---|---|---|
| WBH | 3.12 | 4319 | 32.84 | 13553 | 13570 | 1224 | 4217 |
| WBL | 3.14 | 4518 | 31.11 | 14294 | 14267 | 1286 | 3559 |
| WBN | 3.18 | 4718 | 32.65 | 15148 | 15119 | 1358 | 3293 |
| EBH | 2.96 | 1178 | 6.19 | 3622 | 3508 | 680 | 2264 |
| EBL | 3.01 | 1327 | 7.23 | 4116 | 4009 | 771 | 2492 |
| EBN | 3.09 | 1518 | 4.18 | 4793 | 4698 | 893 | 2832 |

**Table I.2:** Results of system simulations: Monovalent systems.

| | $SPF_1$ | $W_{el,HP}$ in kWh | $W_{el,HR}$ in kWh | $Q_{LC}$ in kWh | $Q_{HC}$ in kWh | $t_{on}$ in h | $n_{op}$ |
|---|---|---|---|---|---|---|---|
| WML | 3.15 | 4523 | 0.00 | 14141 | 14268 | 954 | 3884 |
| WMH | 3.13 | 4337 | 0.00 | 13437 | 13574 | 909 | 3993 |
| EML | 3.03 | 1323 | 0.00 | 4072 | 4010 | 569 | 2707 |
| EMH | 2.98 | 1175 | 0.00 | 3581 | 3507 | 502 | 2451 |

**Table I.3:** Results of system simulation: Supply temperature control.

| | $SPF_1$ | $W_{el,HP}$ in kWh | $W_{el,add}$ in kWh | $Q_{LC}$ in kWh | $Q_{HC}$ in kWh | $t_{on}$ in h | $n_{op}$ |
|---|---|---|---|---|---|---|---|
| REF (WBH) | 3.12 | 4319 | 32.84 | 13553 | 13570 | 1224 | 4217 |
| REFvar (WBH) | 3.08 | 3808 | 30.98 | 11857 | 11813 | 1073 | 3536 |
| RR (WBH) | 3.14 | 4271 | 29.96 | 13505 | 13504 | 1221 | 3840 |
| mRR (WBH) | 3.13 | 4303 | 29.18 | 13551 | 13550 | 1225 | 3905 |
| mRRvar (WBH) | 3.04 | 3870 | 30.66 | 11927 | 11873 | 1076 | 3444 |
| RB (WBH) | 3.28 | 4024 | 6.15 | 13091 | 13210 | 1199 | 6604 |
| RBvar(a) (WBH) | 3.12 | 3736 | 31.47 | 11789 | 11756 | 1069 | 3532 |
| RBvar(b) (WBH) | 3.31 | 3413 | 11.07 | 11259 | 11327 | 1037 | 5562 |
| PI(a) (WBH) | 3.29 | 3635 | 0.01 | 11803 | 11950 | 1090 | 6136 |
| PIvar(a) (WBH) | 3.32 | 3079 | 1.17 | 10130 | 10212 | 939 | 5476 |
| PIvar(a) (EBH) | 3.28 | 754 | 1.83 | 2552 | 2477 | 489 | 1648 |
| PIvar(a) (EBL) | 3.27 | 878 | 1.93 | 2954 | 2878 | 564 | 1799 |
| PIvar(a) (WBL) | 3.33 | 3212 | 0.99 | 10610 | 10700 | 982 | 5634 |
| PIvar(b) (WBH) | 3.29 | 3131 | 0.11 | 10240 | 10293 | 944 | 5253 |
| PIvar(c) (WBH) | 2.95 | 2896 | 254.2 | 8946 | 9034 | 838 | 4932 |
| PIvar(d) (WBH) | 3.45 | 2958 | 0.93 | 10110 | 10214 | 941 | 5348 |
| MPC(a) (WBH) | 2.63 | 4762 | 26.61 | 12800 | 12602 | 1106 | 2517 |
| MPC(b) (WBH) | 3.29 | 3603 | 0.48 | 11870 | 11867 | 1083 | 4049 |
| MPC(c) (WBH) | 3.41 | 3368 | 2.32 | 11428 | 11483 | 1051 | 4683 |
| MPCvar(a) (WBH) | 3.10 | 3275 | 32.02 | 10366 | 10249 | 933 | 2275 |
| MPCvar(b) (WBH) | 3.34 | 2960 | 6.37 | 9961 | 9914 | 911 | 2763 |
| MPCvar(c) (WBH) | 3.49 | 2741 | 2.54 | 9553 | 9573 | 883 | 3716 |

**Table I.4:** Results of system simulation: Study of additional reference systems. "Renovated" indicates building physics according to "WSchV 1995" (German Heat Insulation Ordinance of the year 1995). The "higher heating curve" is calculated as indicated in section 4.5.7.

| | $SPF_1$ | $W_{el,HP}$ in kWh | $W_{el,add}$ in kWh | $Q_{LC}$ in kWh | $Q_{HC}$ in kWh | $t_{on}$ in h | $n_{op}$ |
|---|---|---|---|---|---|---|---|
| REFvar, renovated | 3.11 | 2157 | 18 | 6880 | 6776 | 1279 | 2566 |
| PIvar(a), renovated | 3.44 | 1893 | 15 | 6616 | 6560 | 1250 | 2259 |
| EAvar, higher heating curve | 2.94 | 3587 | 31 | 10778 | 10630 | 966 | 2584 |

# Bibliography


Adhikari, R. S., Aste, N., Manfren, M., and Marini, D. (2011). Energy savings through variables speed compressor heat pump systems. *2nd International Conference on Advances in Energy Engineering 2011*, 6:1337–1342.

Adolph, M., Kopmann, N., Lupulescu, B., and Müller, D. (2013). Adaptive control strategies for single room heating. *Energy and Buildings*.

Afjei, T. and Dott, R. (2011). Heat pump modelling for annual performance, design and new technologies. In *Proceedings of Building Simulation 2011: 12th Conference of International Building Performance Simulation Association, Sydney, 14-16 November.*, pages 2431–2438.

BAFA (2011). Erläuterungen zur Fachunternehmererklärung für Wärmepumpenanlagen, German Federal Office of Economics and Export Control (BAFA). Online. `http://www.bafa.de/bafa/de/energie/erneuerbare_energien/publikationen/energie_ee_erlaeuterungen_fue_wp.pdf` [accessed May 7, 2013].

BAFA (2012). Wärmepumpe - Basis- und Bonusförderung, Stand: ab dem 15.08.2012, German Federal Office of Economics and Export Control (BAFA). Online. `http://www.bafa.de/bafa/de/energie/erneuerbare_energien/publikationen/energie_ee_wp_uebersicht.pdf` [accessed May 7, 2013].

Bartonicek, P. (2007). Simulation eines Schichtenspeichers in Dymola/Modelica. Master's thesis, Technische Universität Berlin. (non-published student thesis, supervised by P. Matthes).

BDH (2012). Marktentwicklung Wärmeerzeuger 2002-2012, Bundesindustrieverband Deutschland Haus-, Energie- und Umwelttechnik e.V. (BDH). Online. `http://bdh-koeln.de/uploads/media/Pressegrafik_Marktentwicklung_2002-2012.pdf` [accessed May 7, 2013].

Beghi, A. and Cecchinato, L. (2011). Modelling and adaptive control of small capacity chillers for HVAC applications. *Applied Thermal Engineering*, 31:1125–1134.

Bell, I., Wronski, J., Quoilin, S., and Lemort, V. (2014). Pure- and pseudo-pure fluid thermophysical property evaluation and the open-source thermophysical property library coolprop. *Industrial & Engineering Chemistry Research*, 53:2498–2508.

BGW (2006). Praxisinformation P 2006 / 8 Gastransport / Betriebswirtschaft - Anwendung von Standardlastprofilen zur Belieferung nichtleistungsgemessener Kunden, Bundesverband der deutschen Gas- und Wasserwirtschaft (BGW), Berlin und Brüssel. Online. `http://www.eko-netz.de/download_fcms/3.5_standardlastprofile_bgw_information_lastprofile.pdf` [accessed May 9, 2013].

Bianchi, M. (2006). *Adaptive modellbasierte prädiktive Regelung einer Kleinwärmepumpenanlage*. PhD thesis, Eidgenössische technische Hochschule Zürich.

Boait, P. J., Fan, D., and Stafford, A. (2011). Performance and control of domestic ground-source heat pumps in retrofit installations. *Energy and Buildings*, 43:1968 – 1976.

Bollin, E. (2009). *Automation regenerativer Wärme- und Kälteversorgung von Gebäuden: Komponenten, Systeme, Anlagenbeispiele*. Vieweg+Teubner Verlag.

BPIE (2014). Building Performance Institute Europe - data hub. Online. `http://www.buildingsdata.eu` [accessed March 10, 2014].

Brugmann, J. (2006). Planung von Luft/Wasser-Wärmepumpen für Altbauten. *KI Klima - Kälte - Heizung*, 05:192–197.

Bugbee, J. E. and Swift, J. R. (2013). Cold climate ductless heat pump performance. *Energy Engineering*, 110:2:47–57.

Burger, H. and Rogatty, W. (2003). *BHKS Almanach 2003*, chapter Anpassung der Kesselleistung an die Heizlast, pages 41–47. BHKS - Bundesindustrieverband Heizungs-, Klima-, Sanitärtechnik/Technische Gebäudesysteme e.V.

BWP (2011). BWP-Branchenstudie 2011, Bundesverband Wärmepumpe (BWP) e.V., Berlin, Germany. Online. `http://www.waermepumpe.de/uploads/tx_bwppublication/2012-08-23_MK_Branchenprognose2011.pdf` [accessed May 7,2013].

BWP (2013). Absatzzahlen 2012: 70.000 neue Wärmepumpen in Deutschland installiert, Bundesverband Wärmepumpe (BWP) e.V., Berlin, Germany. Online. `http://www.waermepumpe.de/uploads/tx_bwppublication/2013-01-17_BWP-PI_Absatzzahlen_2012_BDH.pdf` [accessed May 7,2013].

Carbonell, D., Cadafalch, J., Pärisch, P., and Consul, R. (2012). Numerical analysis of heat pump models. comparative study between equation-fit and refrigerant cycle based models. In *Proc. of Eurosun 2012 (ISES Europe Solar Conference, Croatian Solar Energy Association Rijeka and International Solar Energy Society Europe, Rijeka, Kroatia, September, 2012)*.

Casella, F. and Richter, C. (2008). ExternalMedia: A library for easy re-use of external fluid property code in Modelica. In *Modelica 2008*. The Modelica Association.

Chen, K., Streblow, R., Müller, D.and Molitor, C., Benigni, A., Monti, A., Stieneker, M., and de Doncker, R. W. (2012). *Hardware-in-the-Loop Test Bed for Home Energy Systems*. E.ON Energy Research Center, RWTH Aachen University.

Choi, J., Lee, G., and Kim, M. S. (2011). Capacity control of a heat pump system applying a fuzzy control method. *Applied Thermal Engineering*, 31:2332–2339.

Christoffer, J., Deutschländer, T., and Webs, M. (2004). *Testreferenzjahre von Deutschland für mittlere und extreme Witterungsverhältnisse TRY*. Selbstverlag des Deutschen Wetterdienstes.

Constantin, A., Fuetterer, J., Streblow, R., Mueller, D., Kontes, G., and Rovas, D. (2013). Simulation assisted implementation of a model based control parameter fine-tuning methodology for a nonresidential building with a complex energy system. In *Proceedings of BS2013 : 13th Conference of International Building Performance Simulation Association, Chambéry, France, August 26-28*.

Constantin, A., Streblow, R., and Müller, D. (2014). The Modelica HouseModels Library: Presentation and evaluation of a room model with the ASHRAE standard 140. In *Proceedings of the 10th Modelica Conference, Lund*.

Corberan, J. M., Finn, D. P., Montagud, C., Murphy, F., and Edwards, K. C. (2011). A quasi-steady state mathematical model of an integrated ground source heat pump for building space control. *Energy and Buildings*, 43:82–92.

Dassault Systems (2011). Dymola - multi-engineering modelling and simulation. http://www.3ds.com/products/catia/portfolio/dymola.

De Ridder, F., Diehl, M., Mulder, G., Desmedt, J., and Van Bael, J. (2011). An optimal control algorithm for borehole thermal energy storage systems. *Energy and Buildings*, 43:2918–2925.

DIN 4108-2-2011 (2011). Thermal protection and energy economy in buildings - part 2: Minimum requirements to thermal insulation.

DIN EN 15251 (2007). Eingangsparameter für das raumklima zur auslegung und bewertung der energieeffizienz von gebäuden – raumluftqualität, temperatur, licht und akustik.

DIN EN 15316 (2008). Heating systems in buildings - method for calculation of system energy requirements and system efficiencies.

DIN EN 16147-2011 (2011). Heat pumps with electrically driven compressors - testing and requirements for marking of domestic hot water units.

DIN EN ISO 7730 (2006). Ergonomie der thermischen Umgebung – Analytische Bestimmung und Interpretation der thermischen Behaglichkeit durch Berechnung des PMV- und des PPD-Indexes und Kriterien der lokalen thermischen Behaglichkeit.

DIN SPEC 4701-10-A1-2009 (2009). Energy efficiency of heating and ventilation systems in buildings - part 10: Heating, domestic hot water supply, ventilation; amendment A1.

DIN SPEC 4701-10-A1:2012 (2012). Energy efficiency of heating and ventilation systems in buildings - part 10: Heating, domestic hot water supply, ventilation; amendment A1.

DIN V 4701-10 (2003). Energy efficiency of heating and ventilation systems in buildings - part 10: Heating, domestic hot water, ventilation.

Djuric, N., Huang, G., and Novakovic, V. (2011). Data fusion heat pump performance estimation. *Energy and Buildings*, 43:621–630.

Druck, H. (2006). Multiport store - model for TRNSYS, Type 340. Technical report, Institut für Thermodynamik und Wärmetechnik (ITW), University of Stuttgart.

Dunbabin, P. and Wickins, C. (2012). Detailed analysis from the first phase of the energy saving trust's heat pump field trial. Technical report, Department of Energy and Climate Change, London, United Kingdom.

EES (2014). Engineering equation solver. Online. `http://www.fchart.com/ees/` [accessed May 14, 2014].

EHPA (2012). Outlook 2012 - preview - european heat pump statistics, the european heat pump association eeig (ehpa). Online. `http://www.ehpa.org/fileadmin/red/Heat_Pump_Statistics/Outlook2012_PREVIEW_01.pdf` [accessed May 7,2013].

EN 12831 (2003). Heating systems in buildings - Method for calculation of the design heat load.

EN 1434-1:2007 (2007). Heat meters - part 1: General requirements; german version en 1434-1:2007.

EN 14511 (2012). Air conditioners, liquid chilling packages and heat pumps with electrically driven compressors for space heating and cooling.

EN 255 (1997). Air conditioners, liquid chilling packages and heat pumps with electrically driven compressors - heating mode. withdrawn July 2004, succeded by EN 14511.

EN 62053-21 (2003). Electricity metering equipment (a.c.) - particular requirements - part 21: Static meters for active energy (classes 1 and 2) (IEC 62053-21:2003).

EnergyPlus (2014). Energyplus energy simulation software. Online. `http://apps1.eere.energy.gov/buildings/energyplus/` [accessed July 2, 2014].

Esen, H., Inalli, M., Sengur, A., and Esen, M. (2008). Artificial neural networks and adaptive neuro-fuzzy assessments for ground-coupled heat pump system. *Energy and Buildings*, 40:1074–1083.

Eskola, L., Jokisalo, J., and Siren, K. (2011). Seasonal performance of heat pumps in cold climate. In *The 12th International Conference on Air Distribution in Rooms, Roomvent 2011*.

Fanger, P. (1970). *Thermal comfort*. Danish Technical Press.

Fisher, D. E. and Rees, S. J. (2005). Modeling ground source heat pump systems in a building energy simulationn program (EnergyPlus). In *Building Simulation 2005*, pages 311–318.

Freitas, C. R. d. (1985). Assessment of human bioclimate based on thermal response. *International Journal of Biometeorology*, 29, no. 2 pp.:97–119.

Fütterer, J. (2010). Wirtschaftliche und energetische Bewertung der Wärmepumpenheizung in Bestandsgebäuden. Master's thesis, RWTH Aachen University, E.ON Energy Research Center, Institute for Energy Efficient Buildings and Indoor Climate. (unpublished diploma thesis, supervised by K. Huchtemann, D. Müller).

Gasser, L., Welling, B., and Hilfiker, K. (2008). Exergie-Analyse zur Effizienzsteigerung von Luft-Wasser-Wärmepumpen. Technical report, Hochschule Luzern, Technik und Architektur, Thermische Energiesysteme und Verfahrenstechnik.

Giannakis, G., Kontes, G., Kosmatopoulos, E., and Rovas, D. (2011). A model-assisted adaptive controller fine-tuning methodology for efficient energy use in buildings. In *19th Mediterranean Conference on Control and Automation, Corfu, Greece*.

Ginsburg, S. T. (1999). *Hierarchische Wärmepumpenregelung mit Fuzzy Control und Robust Control*. PhD thesis, Eidgenössische Technische Hochschule Zürich, Switzerland.

Glück, B. (1990). *Wärmeübertragung – Wärmeabgabe von Raumheizflächen und Rohren*. Verlag für Bauwesen, 2 edition.

Haase, T., Hoh, A., Matthes, P., Tschirner, T., and Müller, D. (2007). Integrated simulation of building structure and building services installations with Modelica. In *Proceedings of Roomvent 2007, Helsinki, Finnland*.

Hackel, S. and Pertzborn, A. (2011). Effective design and operation of hybrid ground-source heat pumps: Three case studies. *Energy and Buildings*, 43:3497–3504.

Haller, M. Y., Dott, R., Ruschenburg, J., Ochs, F., and Bony, J. (2013). The reference framework for system simulations of the iea shc task 44 / hpp annex 38, part a: General simulation boundary conditions. Technical report, Institut für Solartechnik SPF, Hochschule für Technik HSR, Rapperswil, Switzerland.

He, M., Rees, S., and Shao, L. (2009). Simulation of a domestic ground source heat pump system using a transient numerical borehole heat exchanger model. *Proc. of Eleventh International IBPSA Conference, Building Simulation*, 1:607–614.

Heimrath, R. and Haller, M. (2007). The reference heating system, the template solar system of task 32. Technical report, Institute of Thermal Engineering Graz University of Technology.

Helpin, V., Kummert, M., and Cauret, O. (2011). Experimental and simulation study of hybrid ground-source heat pump systems with unglazed solar collectors for french office buildings. In *Proceedings of Building Simulation 2011: 12th Conference of International Building Performance Simulation Association, Sydney, 14-16 November.*, pages 2957–2964.

Hoh, A., Haase, T., Matthes, P., Tschirner, T., and Müller, D. (2006). Using modelica for combined simulation of building structure and technical installations. In de Oliveira Fernandes, E., Gameiro da Silva, M., and Rosado Pinto, J., editors, *Proceedings of Healthy Buildings 2006, Lissabon, Portugal*, volume V, pages 51–54. June 4-8, Lisboa, Portugal.

Hoh, A., Haase, T., Tschirner, T., and Müller, D. (2005). A combined thermo-hydraulic approach to simulation of active building components. In The Modelica Association and the Department of Thermodynamics, Hamburg University of Technology, editor, *Proceedings of the 4$^{th}$ International Modelica Conference 2005, Hamburg*.

Hoogmartens, J. and Helsen, L. (2011). Influence of control parameters on the system performance of ground coupled heat pump systems: A simulation study. In *Proceedings of Building Simulation 2011: 12th Conference of International Building Performance Simulation Association, Sydney, 14-16 November.*, pages 262–269.

Hoogmartens, J., Helsen, L., Franck, G., and Van Passel, W. (2011). Monitoring the system performance factor of domestic heat pump systems in Flandres (Belgium). In *ISHVAC 2011: The 7th International Symposium on Heating, Ventilation and Air Conditioning, Shanghai, China*.

Hubacher, B. and Ehrbar, M. (2000). Verbesserung des Abtauens bei luftbeaufschlagten Verdampfern, Analyse gängiger Abtauverfahren. Technical report, NTB Interstaatliche Hochschule für Technik Buchs.

Hube, W. (2004). *Prädiktive Wärmeflussregelung solaroptimierter Wohngebäude mit neuartigen Verschattungs- und Speichersystemen*. PhD thesis, University of Kaiserslautern.

Huchtemann, K. and Müller, D. (2010). Simulation of bivalent heat pump systems. In *8th International Conference on System Simulation in Buildings, Liege, December 13-15, 2010*.

Huchtemann, K. and Müller, D. (2012). Evaluation of a field test with retrofit heat pumps. *Building and Environment*, 53:100–106.

Huchtemann, K. and Müller, D. (2009). Advanced simulation methods for heat pump systems. In *7th international Modelica Conference - Como, Italy*.

Huchtemann, K. and Müller, D. (2013). Simulation study on supply temperature optimization in domestic heat pump systems. *Building and Environment*, 59:327–335.

Huchtemann, K. and Müller, D. (2014). Combined simulation of a deep ground source heat exchanger and an office building. *Energy and Buildings*, 73:97–105.

IDA-ICE (2014). Ida ice (indoor climate and energy), equa solutions ag. Online. `http://www.equa.ch/` [accessed June 6, 2014].

IEA EBC Annex 60 (2014). IEA EBC Annex 60 - New generation computational tools for building and community energy systems based on the Modelica and functional mockup interface standards. online. [accessed May 14, 2014].

Javed, S. (2012). *Thermal Modelling and Evaluation of Borehole Heat Transfer*. PhD thesis, Building Services Engineering, Department of Energy and Environment, Chalmers University of Technology, Sweden.

Jin, H. (2002). *Parameter estimation based models of water source heat pumps*. PhD thesis, Graduate College of the Oklahoma State University.

Kähler, A. and Ohl, J. (2009). Heizenergieeinsparung mit Vorlauftemperaturadaption - Verfahren und Feldergebnisse. Online. `http://www.techem.de/Deutsch/PDFs/b_Fachwissen_und_Dialog/Vorlauftemperatur/` [accessed April 1, 2012].

Karlsson, F. (2007). *Capacitiy Control of Residential Heat Pump Heating Systems*. PhD thesis, Building Services Engineering, Department of Energy and Environment, Chalmers University of Technology, Göteborg, Sweden.

Kenjo, L., Caccavelli, D., and Inard, C. (2003). A model of a low flow solar domestic hot water system. In *Building Simulation 2003, Eighth International IBPSA Conference*.

Kermi (2010). Kermi Flachheizkoerper Technik I/2010.

Kähler, A. and Ohl, J. (2008). Heizenergieeinsparungen mit Vorlauftemperaturadaption - Verfahren und Feldergebnisse Teil 2. *HLH*, 59(8):26–30.

Kinab, E., Marchio, D., Riviére, P., and Zoughaib, A. (2010). Reversible heat pump model for seasonal performance optimization. *Energy and Buildings*, 2269 - 2280:12.

Klein, K., Huchtemann, K., and Müller, D. (2014). Numerical study on hybrid heat pump systems in existing buildings. *Energy and buildings*, 69:193–201.

Kleinbach, E. M. (1990). Performance study of one-dimensional models for stratified thermal storage tank. Master's thesis, University of Wisconsin-Madison.

Knapp, T. and Wagner, A. (2012). Strom-Lastverschiebung mit Wärmepumpe und prädiktiver Regelung. *HLH Lüftung/Klima - Heizung/Sanitär - Gebäudetechnik*, 63(1):43–47.

Kraft, A. (2002). *Einsparpotentiale bei der Energieversorgung von Wohngebäuden durch Informationstechnologien*. PhD thesis, Forschungszentrum Jülich. (engl.: Energy saving potentials in households through modern building automation technologies).

Küpper, H. D. (2010). Effiziente elektronische Überhitzungsregelung für Kälte- und Wärmepumpenanlagen. In *DKV-Tagung Magdeburg, 2010*.

Lemmon, E., McLinden, M., and Huber, M. (2002). *NIST Reference Fluid Thermodynamic and Transport Properties Database (REFPROP)*. U.S. Department of Commerce, Technology Administration, National Institute of Standards and Technology, Gaithersburg, Maryland 20899.

Liao, Z. and Dexter, A. L. (2004). The potential for energy saving in heating systems through improving boiler controls. *Energy and Buildings*, 36:261–271.

Lüdemann, B. (2001). *Auslegung, Energiebedarf und Komfort von Anlagen zur Heizung und Warmwasserbereitung im Niedrigenergiehaus bei Berücksichtigung des Nutzerverhaltens*. PhD thesis, Technische Universität Hamburg-Harburg.

Madani, H., Claesson, J., and Lundqvist, P. (2013). A descriptive and comparative analysis of three common control techniques for an on/off controlled ground source heat pump (GSHP) system. *Energy and Buildings*, 65:1–9.

Marx, R. and Spindler, K. (2011). Modellierung von Wärmepumpen anhand eines komponentenbasierten Modells unter Berücksichtigung transienter Betriebsweisen. In *DKV-Tagungsbericht 2011 Aachen, 16. – 18. November 2011, 38. Jahrgang*, Universität Stuttgart, Institut für Thermodynamik und Wärmetechnik Pfaffenwaldring 6, 70550 Stuttgart, Deutschland marx@itw.uni-stuttgart.de.

MathWorks (2012). Simulink - simulation and model-based design.

MATLAB (2014). The Mathworks: MATLAB - The language of technical computing. Online. `http://www.mathworks.de/products/matlab/` [accessed July 2, 2014].

Matthes, P., Haase, T., Hoh, A., Tschirner, T., and Müller, D. (2006). Coupled simulation of building structure and building services installations with Modelica. In The Modelica Association and the Department of Thermodynamics, Arsenal Research, editor, *Proceedings of the 5$^{th}$ International Modelica Conference 2006, Wien, Österreich*, pages 717–723.

Matthes, P., Hoh, A., and Müller, D. (2007). Energieeinsparpotential durch adaptive Vorlauftemperatur-Regelung. *HLH Lüftung/Klima - Heizung/Sanitär - Gebäudetechnik*, 11:29–35.

Mayer, E. (2001). Individual thermal comfort controlled by an "artificial skin"-sensor. Technical report, International Energy Agency - Energy Conservation on Buildings and Community Systems, Annex 35, Hybrid Ventilation in New and Retrofitted Office Buildings.

Merz, R. M. (2002). *Objektorientierte Modellierung thermischen Gebäudeverhaltens*. PhD thesis, Universität Kaiserslautern.

Miara, M. and Günther, D. (2011). Effizienz von Wärmepumpenanlagen: Ergebnisse aus Felduntersuchungen. In *DKV-Tagungsbericht 2011 Aachen, 16. – 18. November 2011, 38. Jahrgang*.

Miara, M., Russ, C., and Becker, R. (2007). Wärmepumpen im Feldtest. *KI*, 9:24–27.

Michelsen, C. and Madlener, R. (2012). Homeowners' preferences for adopting innovative residential heating systems: A discrete choice analysis for germany. *Energy Economics*, 34:1271–1283.

Miura, H. and Ogino, T. (2011). Development of a predictive model for power consumption of air-to-water heat pumps for residential house. In *Proceedings of Building Simulation 2011: 12th Conference of International Building Performance Simulation Association, Sydney, 14-16 November.*, pages 2761–2768.

Modelica Association (2013). Modelica portal – modelica and the modelica association. Online. `http://www.modelica.org` [accessed March 10, 2014].

Modelica Buildings (2014). Online model documentation of the Modelica Buildings Library. Online. `http://simulationresearch.lbl.gov/modelica/releases/latest/help/Buildings.html` [accessed March 10, 2014].

Mokhtar, M., Stables, M., Liu, X., and Howe, J. (2013). Intelligent multi-agent system for building heat distribution control with combined gas boilers and ground source heat pump. *Energy and Buildings*, 62:615–626.

Montagud, C., Corberán, J. M., Montero, ., and Urchueguía, J. F. (2011). Analysis of the energy performance of a ground source heat pump system after five years of operation. *Energy and Buildings, E*, 3618 - 3626:9.

Müller, D. and Badakhshani, A. (2010). Gekoppelte Gebäude- und Anlagensimulation mit Modelica. In *Proc. of BauSim Conference, Wien, Austria.*, Wien. Proc. of BauSim Conference.

Nabe, C. and Seefeldt, F. (2011). Potenziale der Wärmepumpe zum Lastmanagement im Strommarkt und zur Netzintegration erneuerbarer Energien. BMWi Vorhaben 50/10, Ecofys Germany, Prognos AG, beauftragt durch: Bundesministerium für Wirtschaft & Technologie.

Nadler, N. (1991). Die Wärmeleistung von Raumheizkörpern in expliziter Darstellung. *HLH Lüftung/Klima - Heizung/Sanitär - Gebäudetechnik*, 11:621–624.

Ney, A. (1990). *Mathematische Modellierung und numerische Simulation des stationären und instationären Betriebsverhaltens von Kompressions-Wärmepumpen und Kälteanlagen.* PhD thesis, Technische Universität Berlin.

Nordman, R. (2012). Sepemo-build, final report. Technical report, SP Technical Research Institute of Sweden.

Ochsner, K. (2008). *Geothermal Heat Pumps - A Guide for Planning & Installing*. Earthscan, London.

Olympia Zogou, A. S. (2007). Optimization of thermal performance of a building with ground source heat pump system. *Energy Conversation and Management*, 48:2853–2863.

Pahud, D. and Lachal, B. (2004). Mesure des performances thermiques d'une pompe à chaleur couplée sur des sondes géothermiques à lugano (ti). Technical report, Office fédéral de l'energie, Bern, Switzerland.

Pärisch, P., Warmuth, J., Kirchner, M., and Tepe, R. (2012). Durchfluss- und Temperaturabhängigkeit von Wärmepumpen. In *22. Solarthermisches Symposium, 9.11. Mai 2012, Kloster Banz, Bad Staffeldstein, OTTI e. V.* ISBN 978-3-941785-89-2.

Partenay, V., Riederera, P., Salque, T., and Wurtz, E. (2010). The influence of the borehole short-time response on ground source heat pump system efficiency. *Energy and Buildings*, 43:1280–1287.

Phillips, W. F. and Dave, R. N. (1982). Effects of stratification on the performance of liquid-based solar heating systems. *Solar Energy*, 29:111–120.

Platt, M., Exner, S., and Bracke, R. (2010). Analyse des deutschen Wärmepumpenmarktes. Technical report, GeothermieZentrum Bochum, Bochum University of Applied Sciences, Germany.

Prívara, S., Široký, J., Ferkl, L., and Cigler, J. (2011). Model predictive control of a building heating system: The first experience. *Energy and Buildings*, 43:564–572.

Quoilin, S., Desideri, A., Wronski, J., I., B., and Lemort, V. (2014). ThermoCycle: A Modelica library for the simulation of thermodynamic systems. In *Proceedings of the 10th International Modelica Conference, Lund, Sweden*.

Rad, F. M., Fung, A. S., and Leong, W. H. (2009). Combined solar thermal and ground source heat pump system. *Proc. of Eleventh International IBPSA Conference*, 1:2297–2305.

Recknagel, H., Ginsberg, O., Gehrenbeck, K., Sprenger, E., Hönmann, W., and Schramek, E.-R., editors (2009). *Taschenbuch für Heizung und Klimatechnik*. Oldenburger Industrieverlag GmbH, 74. auflage edition.

RES (2009). Directive 2009/28/EC of the european parliament and of the council on the promotion of the use of energy from renewable sources and amending and subsequently repealing directives 2001/77/ec and 2003/30/ec. [accessed May 7,2013].

Reulen, L. (2014). Handwerkerunterstütztes statisches hydraulisches Abgleichverfahren von Heizkörpersystemen mit Hilfe von batteriebetriebenen Heizkörperventilaktoren. Master's thesis, RWTH Aachen University, Lehrstuhl für Gebäude- und Raumklimatechnik. (non-published student work, supervised by K. Huchtemann, T. Badenhop, D. Müller).

Rewitz, K. (2010). Modellierung von U-Rohr-Erdwärmesonden in Modelica. Master's thesis, Institute for Energy-Efficient Buildings and Indoor Climate, E.ON Energy Research Center, RWTH Aachen University. (non-published student project work, supervised by K. Huchtemann, D. Müller).

Richter, C. (2008). *Proposal of New Object-Oriented Equation-Based Model Libraries for Thermodynamic Systems*. PhD thesis, Technische Universität Carolo-Wilhelmina zu Braunschweig.

Riederer, P., Partenay, V., and Raguideau, O. (2009). Dynamic test method for the determination of the global seasonal performance factor of heat pumps used for heating, cooling and domestic hot water preparation. *Proc. of Eleventh International IBPSA Conference, Building Simulation*, 1:752–759.

Rietschel (2005). *Heizungstechnik*. Fitzner.

Rink, R. E., Gourishankar, V., and Zaheeruddin, M. (1988). Optimal control of heat-pump/heat-storage systems with time-of-day energy price incentive. *Journal of optimization theory and applications*, 58(1):93–108.

Russ, C., Miara, M., and Becker, R. (2008). Feldmessung Wärmepumpen im Gebäudebestand. Technical report, Fraunhofer Institut für Solare Energiesysteme, Freiburg.

Safa, A. A., Fung, A. S., and Leong, W. H. (2011). The archetype sustainable house: Performance simulation of a variable capacity two-stage air source heat pump system. In *Proceedings of Building Simulation 2011: 12th Conference of International Building Performance Simulation Association, Sydney, 14-16 November.*, pages 1378–1383.

Salvalai, G. (2012). Implementation and validation of simplified heat pump model in IDA-ICE energy simulation environment. *Energy and Buildings*, 10:10.

Schmidt-Holzmann, P. (2010). Thermodynamische Modellierung und Simulation von Wärmepumpen-Arbeitsmittelkreisläufen. Master's thesis, Institute for Energy-Efficient Buildings and Indoor Climate, E.ON Energy Research Center, RWTH Aachen University. (non-published diploma thesis, supervised by K. Huchtemann, D. Müller).

Seifert, J., Kozak, W., and Richter, W. (2009). Modelling of hydraulic circuits for different heat pump systems in low energy building. *Proc. of Eleventh International IBPSA Conference, Building Simulation*, 1:354–360.

Self, S. J., Reddy, B. V., and Rosen, M. A. (2012). Geothermal heat pump systems: Status review and comparison with other heating options. *Applied Energy*, 8:8.

SIA 2024 (2006). Standard Nutzungsbedingungen für die Energie- und Gebäudetechnik.

SIMULINK (2014). The Mathworks: SIMULINK - Simulation and model-based design. Online. `http://www.mathworks.de/products/simulink/` [accessed July 2, 2014].

Song, Z.-P. (1999). Total energy system analysis of heating. *Energy*, 25:807–822.

Streblow, R. (2010). *Thermal Sensation and Comfort Model for Inhomogeneous Indoor Environments*. PhD thesis, RWTH Aachen University.

Streicher, W. (2004). Benutzerfreundliche Heizungssysteme für Niedrigenergie- und Passivhäuser. Technical report, Bundesministerium für Verkehr, Innovation und Technologie, Austria.

Thomas, B., Soleimani-Mohseni, M., and Fahlén, P. (2005). Feed-forward in temperature control of buildings. *Energy and Buildings*, 37:755–761.

Thron, U. (2001). *Vorausschauende selbstadaptierende Heizungsregelung für Solarhäuser*. PhD thesis, Fachbereich Maschinenbau der Universität Hannover.

TISC (2014). TLK Inter Software Connector Suite, TLK thermo GmbH, Braunschweig. Online. `http://www.tlk-thermo.com/de/softwareprodukte/tisc.html` [accessed June 3, 2014].

Tritschler, M. (1999). *Bewertung der Genauigkeit von Heizkostenverteilern*. PhD thesis, Universität Stuttgart.

TRNSYS (2014). A transient systems simulation program. online. [accessed May 14, 2014].

Trockel, J. (2011). Modeling and simulation of heat pump cycles. Master's thesis, Institute for Energy-Efficient Buildings and Indoor Climate, E.ON Energy Research Center, RWTH Aachen University. (non-published diploma thesis, supervised by G. Mader (Danfoss A/S), K. Huchtemann, D. Müller).

Uhlmann, M. and Bertsch, S. (2009). Dynamische Simulation einer Wärmepumpe. In *News aus der Wärmepumpen-Forschung: 15. Tagung des BFE-Forschungsprogramms "Wärmepumpen, Wärme-Kraft-Kopplung, Kälte", Burgdorf, Schwitzerland*.

Uhlmann, M. and Bertsch, S. (2010). Dynamischer Wärmepumpentest, Phasen 3 und 4. Technical report, Bundesamt für Energie BFE, Forschungsprogramm Wärmepumpen, WKK, Kälte, Bern, Switzerland.

VDI 2078 (1996). Berechnung der Kühllast klimatisierter Räume (VDI-Kühllastregeln).

VDI 4650-1 (2009). Calculation of heat pumps - simplified method for the calculation of the seasonal performance factor of heat pumps - electric heat pumps for space heating and domestic hot water.

Verhelst, C. (2012). *Model Predictive Control of Ground Coupled Heat Pump Systems for Office Buildings*. PhD thesis, KU Leuven.

Verhelst, C., Logist, F., Van Impe, J., and Helsen, L. (2012). Study of the optimal control problem formulation for modulating air-to-water heat pumps connected to a residential floor heating system. *Energy and Buildings*, 45:43–53.

Viessmann GmbH (2011). *Planungshandbuch Wärmepumpen*. solarcontact, Hannover.

Viskanta, R., Behnia, M., and Karaids, A. (1977). Interferometric observations of the temperature structure in water cooled or heated from above. *Advances in Water Resources*, 1(2):57–69.

Wemhöner, C. and Afjei, T. (2003). Seasonal performance calculation for residential heat pumps with combined space heating and hot water production. Technical report, Institute of Energy, University of Applied Sciences Basel.

Wetter, M. (2009). Modelica-based modelling and simulation to support research and development in building energy and control systems. *Journal of Building Performance Simulation*, 2(2):143–161.

Wetter, M. and Afjei, T. (1996). Trnsys type 401 - kompressionswärmepumpe inklusiv frost- und taktverluste. Technical report, Zentralschweizerisches Technikum Luzern - Ingenieruschule HTL, Switzerland.

Wolff, D., Teuber, P., Budde, J., and Jagnow, K. (2004). Felduntersuchung – Betriebsverhalten von Heizungsanlagen mit Gas-Brennwertkesseln. Technical report, FH Braunschweig-Wolfenbüttel, IfHK.

WPZ (2009). WPZ-Bulletin, Ausgabe 1-2009, Interstaatliche Hochschule für Technik NTB, Buchs Switzerland. Online. `http://www.ecotec-energiesparhaus.de/Daten/WPZ-Bulletin-mit-allen-Testergebnissen-Stand-2009.pdf` [accessed May 9, 2013].

WPZ - Wärmepumpen-Testzentrum (2012). Prüfresultate Sole/Wasser- und Wasser/Wasser-Wärmepumpen basierend auf der EN 14511 und EN 255. Technical report, Interstaatliche Hochschule für Technik Buchs.

WPZ - Wärmepumpen-Testzentrum (2011). Prüfresultate Luft / Wasser-Wärmepumpen basierend auf der EN 14511 und EN 255. Technical report, Interstaatliche Hochschule für Technik Buchs.

Wu, S. T. and Han, S. M. (1978). A liquid solar energy storage tank model - i. formulation of a mathematical model. In *Modeling, Simulation, Testing and Measurements for Solar Energy Systems*, pages 53–60. The American Society of Mechanical Engineers.

Zaheer-Uddin, M. (1993). Optimal, sub-optimal and adaptive control methods for the design of temperature controllers for intelligent buildings. *Building and Environment*, 28(3):311–322.

Zogg, M. (2000). Effizientere Wärmepumpenheizungen durch Optimieren des Gesamtsystems. In *Vorschau zur 7. UAW-Tagung des Bundesamtes für Energie (BFE) vom 9.Mai 2000*.

Zogg, M. (2009). Wärmepumpen. http://www.zogg-engineering.ch/Publi/WP_ETH_Zogg.pdf. last visit 2012/04/23.

**E.ON ERC Band 1**
**Streblow, R.**
Thermal Sensation and Comfort Model for Inhomogeneous Indoor Environments
1. Auflage 2011
ISBN 978-3-942789-00-4

**E.ON ERC Band 2**
**Naderi, A.**
Multi-phase, multi-species reactive transport modeling as a tool for system analysis in geological carbon dioxide storage
1. Auflage 2011
ISBN 978-3-942789-01-1

**E.ON ERC Band 3**
**Westner, G.**
Four Essays related to Energy Economic Aspects of Combined Heat and Power Generation
1. Auflage 2012
ISBN 978-3-942789-02-8

**E.ON ERC Band 4**
**Lohwasser, R.**
Impact of Carbon Capture and Storage (CCS) on the European Electricity Market
1. Auflage 2012
ISBN 978-3-942789-03-5

**E.ON ERC Band 5**
**Dick, C.**
Multi-Resonant Converters as Photovoltaic Module-Integrated Maximum Power Point Tracker
1. Auflage 2012
ISBN 978-3-942789-04-2

**E.ON ERC Band 6**
**Lenke, R.**
A Contribution to the Design of Isolated DC-DC Converters for Utility Applications
1. Auflage 2012
ISBN 978-3-942789-05-9

**E.ON ERC Band 7**
**Brännström, F.**
Einsatz hybrider RANS-LES-Turbulenzmodelle in der Fahrzeugklimatisierung
1. Auflage 2012
ISBN 978-3-942789-06-6

**E.ON ERC Band 8**
**Bragard, M.**
The Integrated Emitter Turn-Off Thyristor - An Innovative MOS-Gated High-Power Device
1. Auflage 2012
ISBN 978-3-942789-07-3

**E.ON ERC Band 9**
**Hoh, A.**
Exergiebasierte Bewertung gebäudetechnischer Anlagen
1. Auflage 2013
ISBN 978-3-942789-08-0

**E.ON ERC Band 10**
**Köllensperger, P.**
The Internally Commutated Thyristor - Concept, Design and Application
1. Auflage 2013
ISBN 978-3-942789-09-7

**E.ON ERC Band 11**
**Achtnicht, M.**
Essays on Consumer Choices Relevant to Climate Change: Stated Preference Evidence from Germany
1. Auflage 2013
ISBN 978-3-942789-10-3

**E.ON ERC Band 12**
**Panašková, J.**
Olfaktorische Bewertung von Emissionen aus Bauprodukten
1. Auflage 2013
ISBN 978-3-942789-11-0

**E.ON ERC Band 13**
**Vogt, C.**
Optimization of Geothermal Energy Reservoir Modeling using Advanced Numerical Tools for Stochastic Parameter Estimation and Quantifying Uncertainties
1. Auflage 2013
ISBN 978-3-942789-12-7

**E.ON ERC Band 14**
**Bengini, A.**
Latency exploitation for parallelization of power systems simulation
1. Auflage 2013
ISBN 978-3-942789-13-4

**E.ON ERC Band 15**
**Butschen, T.**
Dual-ICT – A Clever Way to Unite Conduction and Switching Optimized Properties in a Single Wafer
1. Auflage 2013
ISBN 978-3-942789-14-1

**E.ON ERC Band 16**
**Li, W.**
Fault Detection and Protection inMedium Voltage DC Shipboard Power Systems
1. Auflage 2013
ISBN 978-3-942789-15-8

**E.ON ERC Band 17**
**Shen, J.**
Modeling Methodologies for Analysis and Synthesis of Controls and Modulation Schemes for High-Power Converters with Low Pulse Ratios
1. Auflage 2014
ISBN 978-3-942789-16-5

**E.ON ERC Band 18**
**Flieger, B.**
Innenraummodellierung einer Fahrzeugkabine in der Programmiersprache Modelica
1. Auflage 2014
ISBN 978-3-942789-17-2

**E.ON ERC Band 19**
**Liu, J.**
Measurement System and Technique for Future Active Distribution Grids
1. Auflage 2014
ISBN 978-3-942789-18-9

**E.ON ERC Band 20**
**Kandzia, C.**
Experimentelle Untersuchung der Strömungsstrukturen in einer Mischlüftung
1. Auflage 2014
ISBN 978-3-942789-19-6

**E.ON ERC Band 21**
**Thomas, S.**
A Medium-Voltage Multi-Level DC/DC Converter with High Voltage Transformation Ratio
1. Auflage 2014
ISBN 978-3-942789-20-2

**E.ON ERC Band 22**
**Tang, J.**
Probabilistic Analysis and Stability Assessment for Power Systems with Integration of Wind Generation and Synchrophasor Measurement
1. Auflage 2014
ISBN 978-3-942789-21-9

**E.ON ERC Band 23**
**Sorda, G.**
The Diffusion of Selected Renewable Energy Technologies: Modeling, Economic Impacts, and Policy Implications
1. Auflage 2014
ISBN 978-3-942789-22-6

**E.ON ERC Band 24**
**Rosen, C.**
Design considerations and functional analysis of local reserve energy markets for distributed generation
1. Auflage 2014
ISBN 978-3-942789-23-3

**E.ON ERC Band 25**
**Ni, F.**
Applications of Arbitrary Polynomial Chaos in Electrical Systems
1. Auflage 2015
ISBN 978-3-942789-24-0

**E.ON ERC Band 26**
**Michelsen, C. C.**
The *Energiewende* in the German Residential Sector: Empirical Essays on Homeowners' Choices of Space Heating Technologies
1. Auflage 2015
ISBN 978-3-942789-25-7

**E.ON ERC Band 27**
**Rolfs, W. - FCN**
Decision-Making under Multi-Dimensional Price Uncertainty for Long-Lived Energy Investments
1. Auflage 2015
ISBN 978-3-942789-26-4

**E.ON ERC Band 28**
**Wang, J. - ACS**
Design of Novel Control algorithms of Power Converters for Distributed Generation
1. Auflage 2015
ISBN 978-3-942789-27-1

**E.ON ERC Band 29**
**Helmedag, A. - ACS**
System-Level Multi-Physics Power Hardware in the Loop Testing for Wind Energy Converters
1. Auflage 2015
ISBN 978-3-942789-28-8

**E.ON ERC Band 30**
**Togawa, K.**
Stochastics-based Methods Enabling Testing of Grid-related Algorithms through Simulation
1. Auflage 2015
ISBN 978-3-942789-29-5